

**Internal ribosome entry in the *myc* gene family**

by

**Catherine L. Jopling BSc (Bristol)**

**Thesis submitted for the degree of Doctor of Philosophy at the**

**University of Leicester**

**October 2001**

UMI Number: U143474

All rights reserved

INFORMATION TO ALL USERS

The quality of this reproduction is dependent upon the quality of the copy submitted.

In the unlikely event that the author did not send a complete manuscript and there are missing pages, these will be noted. Also, if material had to be removed, a note will indicate the deletion.



UMI U143474

Published by ProQuest LLC 2013. Copyright in the Dissertation held by the Author.  
Microform Edition © ProQuest LLC.

All rights reserved. This work is protected against  
unauthorized copying under Title 17, United States Code.



ProQuest LLC  
789 East Eisenhower Parkway  
P.O. Box 1346  
Ann Arbor, MI 48106-1346

## Abstract

The proto-oncogene *c-myc* is encoded by a transcript in which the 5' UTR contains a potent internal ribosome entry segment (IRES). The *N-myc* gene shows considerable homology to *c-myc* and also possesses a 5' UTR that is long and structured. Thus, the potential for internal ribosome entry within this UTR was examined. *N-myc* was found to contain an IRES that was of comparable activity to that of *c-myc* in non-neuronal cells, but was specifically activated relative to the *c-myc* IRES in neuronal cells in which the *N-myc* transcript is expressed. Furthermore, the activity of the *N-myc* IRES was specifically inhibited during neuronal differentiation, when *N-myc* expression is reduced. The *trans*-acting factor requirements for *N-myc* IRES function were examined and a candidate protein was found, although not characterised.

An IRES was also identified in the 5' UTR of the third well-studied member of the *myc* gene family, *L-myc*. An alternative form of the UTR exists in which an intron is retained, but it was not possible to draw any definite conclusions on the IRES activity of this UTR.

Translation of both *c-* and *N-myc* mRNAs can occur by both cap-dependent and IRES-dependent mechanisms, so the existence of IRESs within these transcripts was intriguing. *c-Myc* protein levels were analysed during apoptosis and were maintained, despite the apoptotic inhibition of protein synthesis and the short half-life of *c-Myc*. The activity of the *c-myc* IRES was maintained during apoptosis and was responsible for this effect. The *c-myc* IRES was also shown to lie downstream of the p38 mitogen-activated protein kinase signalling pathway. Finally, the activity of the *c-myc* IRES was examined during a number of other cell stresses, but no significant differences between IRES- and cap-dependent translation were detected.

## **Acknowledgements**

Firstly I would like to thank Anne Willis for constant support and encouragement, for many helpful ideas, for always finding something positive in my results and for sympathy, cake and chocolate when things became really bad. I couldn't have had a better supervisor.

I would like to thank everyone I've worked with for helpful scientific contributions and for making Lab 206 such a friendly place. They are Steve Chappell, Mark Coldwell, Matthew deSchoolmeester, Jo Evans, Simon Flint, Graham Fraser, John Le Quesne, Sally Mitchell, Becky Pickering, Keith Spriggs, Mark Stoneley and Tanya Subkhankulova. Particular thanks to Graham for his expert technical help, to Graham and Simon for all the singing and dancing, to John, Matthew and Jo for surviving in the same bay as me, and to everyone for keeping me in my place with constant teasing!

I've made a lot of good friends in Leicester and it would be impossible to list everyone here. However, I'd particularly like to mention Fiona Wilson and Jo Carter, and also John, Craig, Simon and Pete for much beer, curry and fun.

Finally, thanks to my parents and sister Helen and to my friends outside Leicester for support over the years.

## Table of contents

Abstract.....	i
Acknowledgements.....	ii
Table of contents.....	iii
List of figures.....	ix
Abbreviations.....	xii
<b>Chapter 1: Introduction</b> .....	<b>1</b>
1.1 The cap-dependent paradigm for eukaryotic translation .....	1
1.1.1 A summary of protein synthesis.....	1
1.1.2 Initiation of translation in prokaryotes and eukaryotes .....	1
1.1.3 The cap-binding complex .....	2
1.1.4 43S preinitiation complex recruitment .....	3
1.1.5 Scanning .....	3
1.1.6 60S ribosomal subunit joining .....	4
1.2 Control of translation initiation by modification and sequestration of factors.....	5
1.2.1 Principles of translational control .....	5
1.2.2 Regulation of eIF4E activity.....	5
1.2.3 The 4E-BPs.....	6
1.2.4 eIF2 phosphorylation.....	6
1.2.5 Regulation of other initiation factors.....	7
1.2.6 Situations in which cap-dependent initiation is inhibited.....	8
1.3 Control of translation initiation by UTR elements.....	10
1.3.1 The effect of secondary structure in the 5' UTR .....	10
1.3.2 The iron response element .....	11
1.3.3 5' TOPs .....	12
1.3.4 Upstream open reading frames (uORFs).....	12
1.3.5 Ribosomal shunting.....	13
1.3.6 Internal ribosome entry segments .....	14
1.4 The viral IRESs .....	14
1.4.1 The picornaviruses .....	14
1.4.2 The dicistronic vector assay.....	15
1.4.3 Picornaviral IRES structure and ribosome binding.....	15

1.4.4 Involvement of the canonical translation machinery in picornaviral IRES-driven translation .....	17
1.4.5 <i>Trans</i> -acting factor requirements of picornaviral IRESs.....	18
1.4.6 The flaviviral and pestiviral IRESs .....	19
1.4.7 The insect picorna-like viral IRESs .....	20
1.5 Cellular IRESs .....	21
1.5.1 Cellular genes that contain IRESs.....	21
1.5.2 Structural and sequence features of cellular IRESs .....	22
1.5.3 Requirements of cellular IRESs.....	24
1.5.4 Situations in which cellular IRESs are used .....	25
1.5.5 Association of cellular IRESs with disease .....	27
1.6 The <i>myc</i> family .....	28
1.6.1 The <i>c-myc</i> gene and its role in cancer .....	28
1.6.2 The role of <i>c-myc</i> in cell growth and differentiation.....	28
1.6.3 <i>c-myc</i> and apoptosis.....	29
1.6.4 <i>c-Myc</i> protein.....	30
1.6.5 <i>c-Myc</i> target genes .....	31
1.6.6 Regulation of <i>c-myc</i> expression .....	32
1.6.7 Other <i>myc</i> genes .....	33
1.6.8 <i>N-myc</i> .....	33
1.6.9 <i>L-myc</i> .....	35
<b>Chapter 2: Materials and methods .....</b>	<b>37</b>
2.1 General Reagents .....	37
2.2 Tissue Culture Techniques .....	37
2.2.1 Tissue culture media and supplements .....	37
2.2.2 Maintenance of cell lines .....	38
2.2.3 Maintenance of ES cells .....	39
2.2.4 Calcium phosphate-mediated DNA transfection .....	39
2.2.5 FuGENE 6-mediated DNA transfection.....	39
2.2.6 DEAE-Dextran-mediated transfection .....	40
2.2.7 Cationic liposome-mediated RNA transfection .....	40
2.2.8 Induction of apoptosis and physiological stress.....	40

2.3 Bacterial Techniques .....	41
2.3.1 Bacterial media and supplements.....	41
2.3.2 Preparation of competent cells.....	41
2.3.3 Transformation of competent cells.....	42
2.4 Molecular Biological Techniques .....	42
2.4.1 Buffers and solutions.....	42
2.4.2 Plasmids used.....	42
2.4.3 Determination of nucleic acid concentration .....	43
2.4.4 Ethanol precipitation of nucleic acids .....	43
2.4.5 Phenol/chloroform extraction .....	43
2.4.6 Agarose gel electrophoresis .....	43
2.4.7 Gel isolation of DNA fragments .....	44
2.4.8 Purification of DNA using Qiaquick columns.....	44
2.4.9 Oligonucleotides .....	44
2.4.10 Polymerase chain reaction (PCR) .....	44
2.4.11 RT-PCR .....	44
2.4.12 PCR mutagenesis.....	46
2.4.13 Restriction enzyme digestion.....	46
2.4.14 Filling in recessed 3' ends .....	46
2.4.15 Alkaline phosphatase treatment of DNA.....	47
2.4.16 Phosphorylation of nucleic acids using T4 polynucleotide kinase .....	47
2.4.17 Ligations .....	47
2.4.18 Small scale preparation of plasmid DNA .....	47
2.4.19 Large scale preparation of plasmid DNA .....	48
2.4.20 Caesium chloride gradient purification of plasmid DNA.....	49
2.4.21 Large scale preparation of DNA by Qiagen column.....	49
2.4.22 Double stranded DNA sequencing.....	49
2.4.23 Radiolabelled DNA markers.....	50
2.5 RNA Techniques.....	50
2.5.1 Buffers and solutions.....	50
2.5.2 Isolation of total cellular RNA.....	51
2.5.3 Purification of poly(A) <sup>+</sup> mRNA from total cellular RNA.....	51

2.5.4 Reverse transcription of total cellular RNA .....	51
2.5.5 <i>In vitro</i> run-off transcription .....	51
2.5.6 RNase protection .....	53
2.5.7 Denaturing RNA agarose gel electrophoresis and Northern blotting .....	54
2.5.8 Synthesis of a radiolabelled DNA probe and hybridisation to immobilised RNA .....	54
2.5.9 Electrophoretic mobility shift assays (EMSAs).....	55
2.6 Biochemical Techniques .....	55
2.6.1 Buffers and Solutions .....	55
2.6.2 <i>In vitro</i> translation reactions .....	56
2.6.3 Preparation of total cell extract .....	56
2.6.4 Determination of protein concentration by Bradford assay.....	56
2.6.5 Preparation of cell lysates from transfected cells.....	56
2.6.6 Luciferase assays.....	57
2.6.7 $\beta$ -Galactosidase assays .....	57
2.6.8 SDS-polyacrylamide gel electrophoresis (SDS-PAGE).....	57
2.6.9 Coomassie staining of SDS-polyacrylamide gels .....	58
2.6.10 Transfer of proteins on to nitrocellulose membranes .....	58
2.6.11 Western blotting/immunodetection .....	58
2.6.12 Stripping and re-probing of western blots .....	59
2.6.13 Pulse labelling .....	59
2.6.15 p38MAPKinase assays .....	60
2.6.16 UV-crosslinking reactions .....	60
<b>Chapter 3: Internal ribosome entry in the N-<i>myc</i> 5' UTR .....</b>	<b>61</b>
3.1 Introduction.....	61
3.2 RT-PCR of the N- <i>myc</i> 5' UTR .....	61
3.3 Effect of the N- <i>myc</i> 5' UTR in a dicistronic context.....	62
3.4 The N- <i>myc</i> 5' UTR does not enhance downstream cistron activity by stimulation of ribosomal readthrough or reinitiation .....	64
3.5 Transfection of pRNF leads to the production of full length dicistronic RNA molecules.....	64
3.6 Activity of the N- <i>myc</i> IRES in a monocistronic context.....	66

3.7 Deletion analysis of the N- <i>myc</i> IRES.....	66
3.8 Mapping of the ribosome entry site .....	68
3.9 Discussion.....	70
<b>Chapter 4: Internal ribosome entry in the L-<i>myc</i> 5' UTR.....</b>	<b>72</b>
4.1 Introduction.....	72
4.2 RT-PCR and cloning of the L- <i>myc</i> 5' UTR .....	72
4.3 Effect of the L- <i>myc</i> 5' UTRs on downstream cistron expression in dicistronic RNA .....	73
4.4 Activity of the L- <i>myc</i> 5' UTRs in the presence of a hairpin structure upstream of <i>Renilla</i> luciferase .....	74
4.5 Analysis of transcripts produced on transfection of pRLsF and pRLIF.....	75
4.6 Effect of the L- <i>myc</i> 5' UTRs on translation in a monocistronic context.....	77
4.7 Discussion.....	78
<b>Chapter 5: Involvement of <i>trans</i>-acting factors in <i>myc</i> IRES function.....</b>	<b>80</b>
5.1 Introduction.....	80
5.2 N- <i>myc</i> IRES activity in different cell lines.....	80
5.3 Relative activity of the c- and N- <i>myc</i> IRESs .....	81
5.4 Activity of N- <i>myc</i> IRES deletion mutants in neuronal cells.....	81
5.5 N- <i>myc</i> IRES activity in differentiated neuronal cells.....	82
5.5 Comparison of human and murine <i>myc</i> IRES activity.....	83
5.7 N- <i>myc</i> IRES activity in supplemented reticulocyte lysate .....	84
5.8 IRES activity in <i>in vitro</i> transcribed RNA introduced into cell cytoplasm.....	84
5.9 Effects of known IRES <i>trans</i> -acting factors on N- <i>myc</i> IRES activity in the context of cultured cells.....	85
5.10 Analysis of binding of known <i>trans</i> -acting factors to the N- <i>myc</i> IRES.....	87
5.11 N- <i>myc</i> IRES binding to factors in cell extracts.....	87
5.12 Analysis of N- <i>myc</i> IRES interaction with hnRNPA1 .....	89
5.13 Discussion.....	90
<b>Chapter 6: Analysis of IRES function.....</b>	<b>92</b>
6.1 Introduction.....	92
6.2 c-Myc protein expression during apoptosis induced by TRAIL and staurosporine .....	92

6.3 c-Myc protein stability during apoptosis.....	93
6.4 c-myc IRES activity during apoptosis .....	93
6.5 Involvement of the p38MAPKinase signalling pathway in the maintenance of c-Myc protein levels.....	94
6.6 c-myc IRES activity in the presence of SB203580 .....	95
6.7 Cotransfection of pRMF with MKK6 expression vectors.....	95
6.8 c-myc IRES activity during heat shock .....	96
6.9 c-myc IRES activity during G <sub>0</sub> -G <sub>1</sub> transition .....	97
6.10 c-myc IRES activity during osmotic stress .....	98
6.11 N-myc IRES activity during TRAIL-induced apoptosis .....	99
6.12 Discussion.....	99
<b>Chapter 7: Discussion</b> .....	102
7.1 A comparison of cellular IRESs .....	102
7.2 A comparison of <i>myc</i> IRES structure.....	102
7.3 Protein factor requirements of the <i>myc</i> IRESs.....	104
7.4 <i>myc</i> IRES function .....	106
<b>References</b> .....	108

## List of figures

Figure	Preceding page
1.1 40S ribosomal subunit recruitment by the eIF4F complex.....	2
1.2 Cap-dependent translation initiation.....	3
1.3 Effects of eIF4E and 4E-BP phosphorylation on cap-dependent translation initiation...	6
1.4 Effect of eIF2 $\alpha$ phosphorylation on translation initiation.....	7
1.5 The apoptotic pathway.....	8
1.6 Translational control by the iron response element.....	11
1.7 Alternative strategies of ribosome recruitment.....	14
1.8 The dicistronic vector assay for IRES activity.....	15
1.9 Structure of a typical type II IRES.....	15
1.10 <i>myc</i> gene structure.....	28
1.11 Structure of the Myc and Max proteins.....	30
3.1 Sequence of the N- <i>myc</i> 5' UTR.....	61
3.2 RT-PCR of the N- <i>myc</i> 5' UTR.....	61
3.3 Construction of the vector pRNF.....	62
3.4 Effect of the N- <i>myc</i> 5' UTR on translation <i>in vitro</i> .....	63
3.5 <i>c-myc</i> , N- <i>myc</i> and EMCV IRES activity in HeLa cells.....	63
3.6 Effect of placing a stable RNA hairpin upstream of <i>Renilla</i> luciferase.....	64
3.7 Activity of the N- <i>myc</i> 5' UTR in the context of a dicistronic hairpin vector.....	64
3.8 Possible methods of production of monocistronic transcripts.....	65
3.9 Northern blot analysis of transcripts from pRNF-transfected cells.....	65
3.10 Construction of the vector pSKRNaseN.....	65
3.11 Expected products of RNase protection.....	65
3.12 RNase protection analysis of RNA from pRNF-transfected cells.....	65
3.13 Construction of the vector pGNL.....	66
3.14 N- <i>myc</i> IRES activity in a monocistronic context.....	66
3.15 Construction of an N- <i>myc</i> 5' UTR deletion series.....	67
3.16 IRES activity of N- <i>myc</i> 5' UTR deletion mutants.....	67
3.17 IRES activity of a fragment of the N- <i>myc</i> 5' UTR in which only the extreme 3' end is deleted.....	67
3.18 Sequence of the N- <i>myc</i> 5' UTR and the 5' end of the N- <i>myc</i> coding region.....	68

3.19 IRES activity of a construct bearing part of the coding region of N- <i>myc</i> .....	68
3.20 Positioning of out of frame AUG mutations in the N- <i>myc</i> IRES.....	68
3.21 Result of transfection of an N- <i>myc</i> IRES construct in which an upstream AUG has been mutated to UUG.....	68
3.22 Result of transfection of N- <i>myc</i> IRES mutants with out of frame AUG codons.....	69
3.23 Result of transfection of additional N- <i>myc</i> IRES mutants with out of frame AUG codons.....	69
4.1 Sequence of the L- <i>myc</i> 5' UTR.....	72
4.2 Construction of the vector pRLsF.....	72
4.3 Construction of the vector pRLIF.....	72
4.4 The effect of the L- <i>myc</i> 5' UTR in a dicistronic context in reticulocyte lysate.....	73
4.5 Transfection of dicistronic L- <i>myc</i> 5' UTR constructs into HeLa cells.....	73
4.6 Effect of the L- <i>myc</i> 5' UTRs on downstream cistron activity in a range of cell lines..	74
4.7 Effect of an upstream hairpin structure on dicistronic L- <i>myc</i> plasmid transfection.....	74
4.8 Northern analysis of transcripts in cells transfected with pRLsF and pRLIF.....	75
4.9 RNase protection analysis of RNA from pRLsF-transfected cells.....	76
4.10 RNase protection analysis of RNA from pRLIF-transfected cells.....	76
4.11 Possible mechanisms for the production of truncated RNA molecules in pRLIF- transfected cells.....	77
4.12 Results of transfection of monocistronic L- <i>myc</i> 5' UTR constructs.....	77
5.1 N- <i>myc</i> IRES activity in a range of cell lines.....	80
5.2 Relative activities of the c- <i>myc</i> and N- <i>myc</i> IRESs in various cell lines.....	81
5.3 IRES activity of N- <i>myc</i> 5' UTR deletion mutants in various cell lines.....	82
5.4 Differentiation of NT2 cells.....	82
5.5 N- <i>myc</i> IRES activity in differentiated neuronal cells.....	82
5.6 c- <i>myc</i> IRES activity in differentiated neuronal cells.....	82
5.7 Sequence alignment of <i>myc</i> 5' UTRs.....	83
5.8 Comparison of the activities of the human and murine c- <i>myc</i> IRESs.....	83
5.9 Comparison of the activities of the human and murine N- <i>myc</i> IRESs.....	83
5.10 Activity of the N- <i>myc</i> IRES in reticulocyte lysate supplemented with protein factors.....	84
5.11 Construction of the vector pSP64RNLPa.....	85

5.12 IRES activity on transfection of RNA into the cytoplasm of cells.....	85
5.13 Effect of cotransfection of expression vectors encoding various <i>trans</i> -acting factors on N- <i>myc</i> IRES activity.....	86
5.14 IRES activity in unr knockout cells.....	86
5.15 Construction of the vector pSKNL.....	87
5.16 EMSA of binding of known IRES <i>trans</i> -acting factors to the N- <i>myc</i> IRES.....	87
5.17 EMSA of protein binding by the N- <i>myc</i> IRES in cell extracts.....	87
5.18 UV cross-linking of HeLa total cell extract to N- <i>myc</i> IRES RNA.....	88
5.19 UV cross-linking of NT2 total cell extract to N- <i>myc</i> IRES RNA.....	88
5.20 EMSA of hnRNPA1 binding to N- <i>myc</i> , c- <i>myc</i> and GAPDH RNAs.....	89
5.21 EMSA of N- <i>myc</i> RNA with cell extract and hnRNPA1 antibody.....	90
6.1 c-Myc protein levels during apoptosis.....	93
6.2 Pulse chase analysis of c-Myc protein half life.....	93
6.3 c- <i>myc</i> IRES activity during TRAIL-induced apoptosis.....	93
6.4 Cell signalling pathways involved in translation.....	94
6.5 p38MAPKinase activity in apoptotic cells.....	94
6.6 Effects of SB203580 on c-Myc levels during apoptosis.....	95
6.7 c- <i>myc</i> IRES activity during apoptosis in the presence of SB203580.....	95
6.8 Cotransfection of pRMF with MKK6 expression vectors.....	96
6.9 c- <i>myc</i> IRES activity during heat shock.....	96
6.10 c- <i>myc</i> IRES activity during G <sub>0</sub> -G <sub>1</sub> transition.....	98
6.11 c- <i>myc</i> IRES activity during osmotic stress.....	98
6.12 N- <i>myc</i> IRES activity during TRAIL-induced apoptosis.....	99

## Abbreviations

Apaf-1	apoptotic protease-activating factor 1
ATP	adenosine 5'-triphosphate
BAG-1	Bcl-2-associated athanogene-1
bp	base pairs
BSA	bovine serum albumin
CIAP	calf intestinal alkaline phosphatase
cpm	counts per minute
CrPV	cricket paralysis virus
CSFV	classic swine fever virus
CTP	cytidine 5'-triphosphate
dATP	deoxyadenosine 5'-triphosphate
dCTP	deoxycytidine 5'-triphosphate
ddNTP	dideoxynucleotide
dGTP	deoxyguanosine 5'-triphosphate
DMSO	dimethyl sulphoxide
DNA	deoxyribonucleic acid
DTT	dithiothreitol
dTTP	deoxythymidine 5'-triphosphate
<i>E. coli</i>	<i>Escherichia coli</i>
EDTA	ethylenediaminetetra-acetate
eIF	eukaryotic initiation factor
EMCV	encephalomyocarditis virus
EMSA	electrophoretic mobility shift assay
FCS	foetal calf serum
FGF2	fibroblast growth factor 2
FMDV	foot and mouth disease virus
GDP	guanosine diphosphate
GTP	guanosine 5'-triphosphate
JNK	c-JUN NH <sub>2</sub> -terminal kinase

h	hours
HAV	hepatitis A virus
HCl	hydrochloric acid
HCV	hepatitis C virus
HEPES	4-(2-hydroxyethyl)-1-piperazine-ethanesulphonic acid
hnRNP	heterogeneous nuclear ribonucleoprotein
HRV	human rhinovirus
IRES	internal ribosome entry segment
kb	kilobases
kcal	kilocalories
LB	Luria-Bertani broth
MAPK	mitogen-activated protein kinase
met	methionine
met-tRNA <sub>1</sub>	initiator methionyl-tRNA
min	minutes
mRNA	messenger ribonucleic acid
nt	nucleotides
ODC	ornithine decarboxylase
ORF	open reading frame
PABP	poly(A) binding protein
PAGE	polyacrylamide gel electrophoresis
PBS	phosphate buffered saline
PCBP1/2	poly(rC) binding protein 1/2
PCR	polymerase chain reaction
PDGF2	platelet derived growth factor 2
PIPES	piperazine-N,N'-bis[2-ethanesulphonic acid]
<i>Pfu</i>	<i>Pyrococcus furiosus</i>
PTB	polypyrimidine tract binding protein
RNA	ribonucleic acid
RNase	ribonuclease

RNAsin	ribonucleic acid hydrolase inhibitor
RT-PCR	reverse transcription-polymerase chain reaction
SDS	sodium dodecyl sulphate
TAE	tris acetate EDTA
TBE	tris borate EDTA
TE	tris EDTA
4-thioUTP	4-thiouridine 5'-triphosphate
TMEV	Theiler's murine encephalomyelitis virus
TNF	tumor necrosis factor
TRAIL	TNF-related apoptosis-inducing ligand
tRNA	transfer ribonucleic acid
unr	upstream of N- <i>ras</i>
uORF	upstream open reading frame
UTP`	uridine 5'-triphosphate
UTR	untranslated region
UV	ultraviolet
VEGF	vascular endothelial growth factor

## Chapter 1

### Introduction

#### 1.1 The cap-dependent paradigm for eukaryotic translation

##### 1.1.1 A summary of protein synthesis

Protein synthesis in both prokaryotic and eukaryotic cells is divided into three stages; initiation, elongation and termination. The initiation phase involves the binding of the small ribosomal subunit, in combination with initiator methionyl-tRNA (Met-tRNA<sub>i</sub>) and various protein factors, to a messenger RNA (mRNA) molecule. The correct AUG initiation codon is then located and the large ribosomal subunit is recruited to form a complex competent to carry out peptide synthesis. During the subsequent elongation phase, the ribosome scans along the mRNA, recruiting the cognate aminoacyl-tRNA for each codon and directing peptide bond formation, such that a peptide chain is synthesised. Finally, a termination codon is encountered and the ribosome and peptide are released.

##### 1.1.2 Initiation of translation in prokaryotes and eukaryotes

The most important stage of this process in terms of control and complexity is initiation. In prokaryotes this is mediated by base pairing between the Shine-Dalgarno sequence, upstream of the initiation codon, and sequences within the 16S ribosomal RNA (rRNA) (Hershey and Merrick, 2000). In eukaryotic cells, however, initiation is a considerably more complex process. Following transcription in the nucleus, introns are removed from eukaryotic pre-mRNA by splicing. A modified guanosine nucleotide known as the cap structure is linked to the 5' end of the mRNA, such that the 5' terminal sequence is m<sup>7</sup>GpppN (Shatkin, 1976), and the 3' end is subjected to polyadenylation. The presence of both cap and poly(A) structures results in a synergistic stimulation of translation (Michel et al., 2000). RNA export into the cytoplasm then occurs in the form of a messenger ribonucleoprotein (mRNP) complex, from which the mRNA is mobilised into polysomes during translation initiation (Hershey and Merrick, 2000). Recruitment of the small (40S) ribosomal subunit is mediated by the cap, and is succeeded by ribosomal scanning until an initiation codon in the correct context is encountered.

### 1.1.3 The cap-binding complex

A complex array of eukaryotic initiation factors (eIFs) directs the process of translation initiation. The cap structure is bound specifically by eIF4E, which is part of the complex of factors known as eIF4F. The central core of eIF4F is eIF4G, a 1560 amino acid protein that possesses multiple binding sites for other components of the translational machinery (figure 1.1A), and thus provides a bridging function (Hentze, 1997). Recently, a homologue of eIF4G that shows equivalent function has been identified and termed eIF4GII, while the original protein is now known as eIF4GI (Gradi et al., 1998). Both proteins possess a single eIF4E-binding site in the N-terminus. The eIF4F complex also contains eIF4A, which binds to eIF4G at two sites, one in the central region and one close to the C-terminus (figure 1.1A). eIF4A is an ATP-dependent bidirectional RNA helicase and a member of the DEAD-box helicase family, and exists in two functional isoforms, eIF4AI and eIF4AII, whereas a third homologue, eIF4AIII, inhibits translation (Li et al., 1999). The helicase activity of eIF4A is stimulated by the factors eIF4B and eIF4H, although these do not associate directly with eIF4G and are not considered part of eIF4F (Rogers Jr. et al., 1999).

In addition to the core members of the eIF4F complex, eIF4G associates with several other proteins (figure 1.1A). The kinase Mnk1 (discussed in section 1.2.2) binds to the C-terminal of eIF4G (Pyronnet et al., 1999). Near the N-terminal of eIF4G a binding site is found for the poly(A) binding protein (PABP) (Le et al., 1997). This binding allows an indirect interaction between the cap and poly(A) tail to occur, and hence circularisation of the transcript (Wells et al., 1998), and also increases the affinity of eIF4F for the cap, possibly by inducing a conformational change (Wei et al., 1998). A recent study has shown that eIF4B also interacts with PABP, providing a further contribution to the 5' end-3' end communication (Bushell et al., 2001). Finally, the central region of eIF4G is able to interact with eIF3, a multi-subunit protein that in turn binds directly to the 40S ribosomal subunit (Bommer et al., 1991). Thus, the 40S ribosome is recruited to capped RNA via the cap-4E, 4E-4G, 4G-3, and 3-40S interactions (figure 1.1B). It remains unclear whether eIF4G is initially bound to eIF4E, and is then able to recruit the eIF3-40S complex to the cap, or eIF4G, eIF3 and the 40S subunit exist in complex and are recruited to the eIF4E-cap complex together (Sachs et al., 1997).

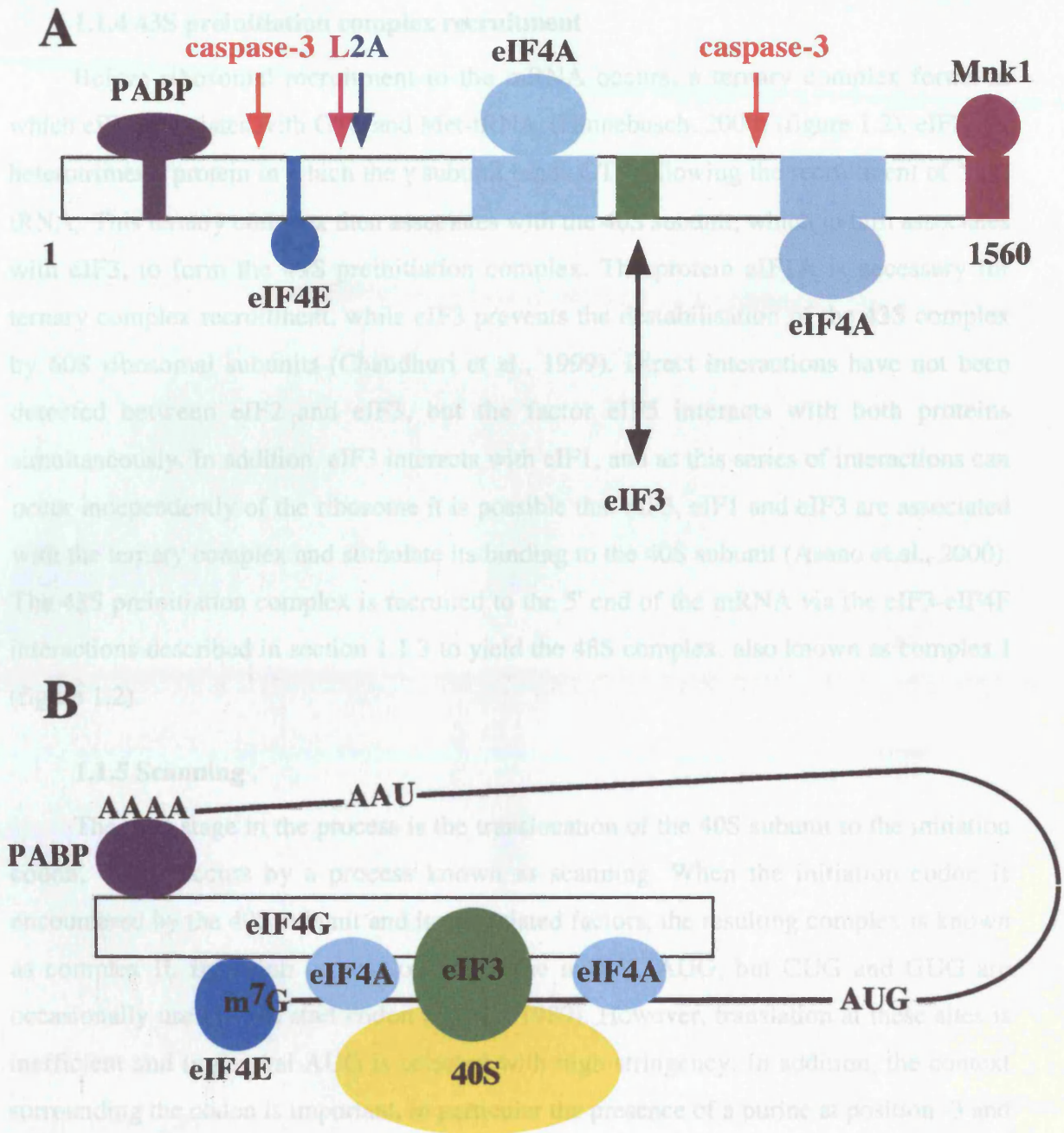


**Figure 1.1 40S ribosomal subunit recruitment by the eIF4F complex.** (A) The binding sites of protein factors on eIF4G. Sites of cleavage by the viral 2A and L proteases and caspase-3 are indicated by arrows. (B) Recruitment of a 40S ribosomal subunit to a capped mRNA molecule via cap-4E-4G-3-40S interactions. The interaction between eIF4G and PABP leads to circularisation of capped and polyadenylated mRNAs.

### 1.1.4 43S preinitiation complex recruitment

Before ribosomal recruitment to the mRNA occurs, a ternary complex forms in which eIF2 associates with GTP and Met-tRNA<sub>i</sub> (Hinnebusch, 2000) (figure 1.2). eIF2 is a heterotrimeric protein in which the  $\gamma$  subunit binds GTP, allowing the recruitment of Met-tRNA<sub>i</sub>. This ternary complex then associates with the 40S subunit, which in turn associates with eIF3, to form the 43S preinitiation complex. The protein eIF1A is necessary for ternary complex recruitment, while eIF3 prevents the destabilisation of the 43S complex by 60S ribosomal subunits (Chaudhuri et al., 1999). Direct interactions have not been detected between eIF2 and eIF3, but the factor eIF5 interacts with both proteins simultaneously. In addition, eIF3 interacts with eIF1, and as this series of interactions can occur independently of the ribosome it is possible that eIF5, eIF1 and eIF3 are associated with the ternary complex and stimulate its binding to the 40S subunit (Asano et al., 2000). The 43S preinitiation complex is recruited to the 5' end of the mRNA via the eIF3-eIF4F interactions described in section 1.1.3 to yield the 48S complex, also known as complex I (figure 1.2).

### 1.1.5 Scanning

The next stage in the process is the translocation of the 40S subunit to the initiation codon, which occurs by a process known as scanning. When the initiation codon is encountered by the 40S subunit and its associated factors, the resulting complex is known as complex II. Initiation usually occurs at the most 5' AUG, but CUG and GUG are occasionally used as the start codon (Kozak, 1989). However, translation at these sites is inefficient and in general AUG is selected with high stringency. In addition, the context surrounding the codon is important, in particular the presence of a purine at position -3 and a guanosine at +4 (where the A of AUG is defined as +1) (Kozak, 1987). AUG codons in poor context may be bypassed or used at low efficiency, with the majority of ribosomes initiating translation at a codon with better context downstream, a process known as leaky scanning (Kozak, 1989).

Ribosomal scanning proceeds in a 5'-3' direction, and secondary structure encountered in the 5' untranslated region (UTR) is unwound by the helicase activity of eIF4A, a process that requires ATP hydrolysis (Lorsch and Herschlag, 1998). The requirement for eIF4A in translation initiation is greatest for mRNAs that possess a high

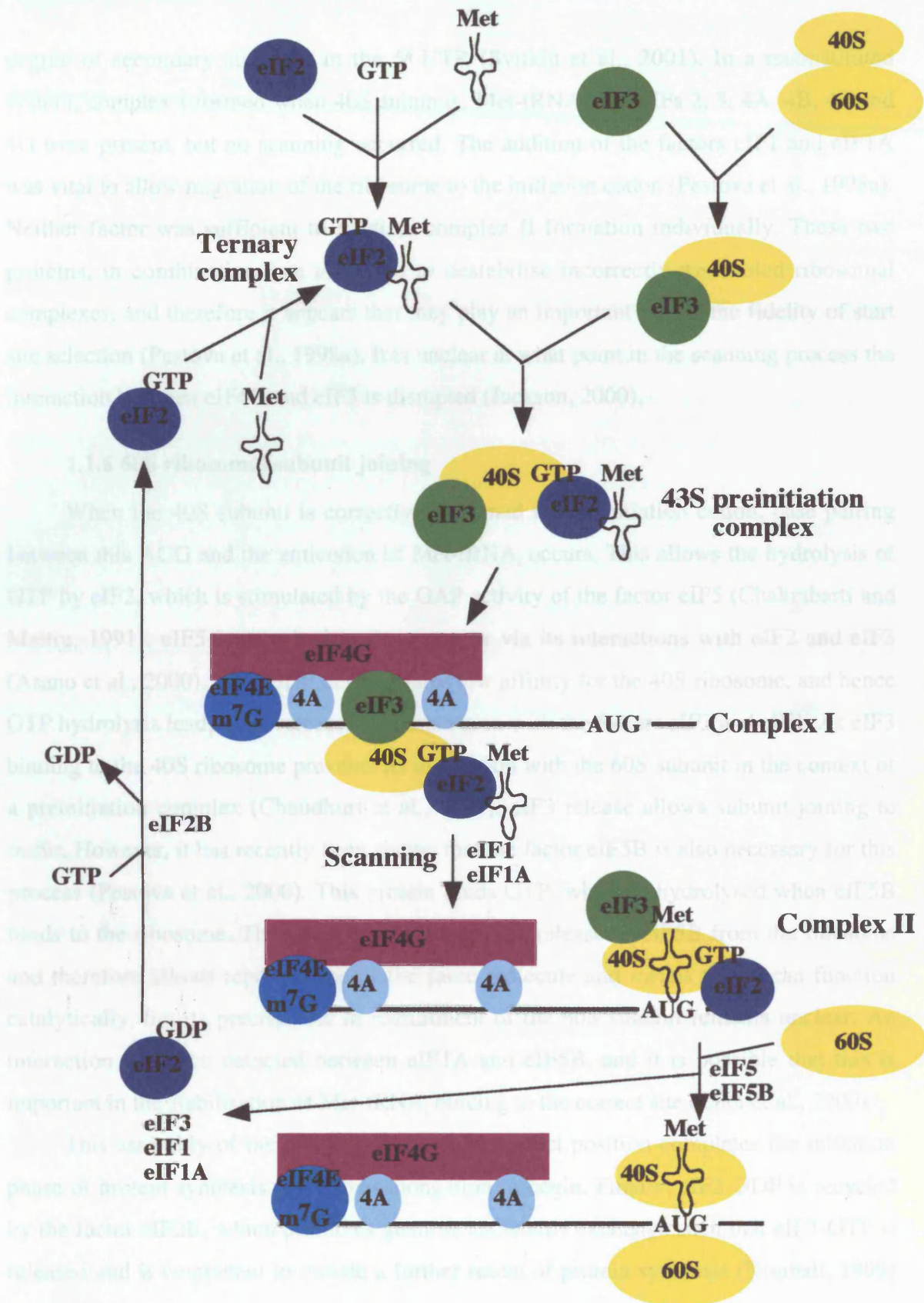


Figure 1.2 Cap-dependent translation initiation.

degree of secondary structure in the 5' UTR (Svitkin et al., 2001). In a reconstituted system, complex I formed when 40S subunits, Met-tRNA<sub>i</sub>, and eIFs 2, 3, 4A, 4B, 4E and 4G were present, but no scanning occurred. The addition of the factors eIF1 and eIF1A was vital to allow migration of the ribosome to the initiation codon (Pestova et al., 1998a). Neither factor was sufficient to mediate complex II formation individually. These two proteins, in combination, are also able to destabilise incorrectly assembled ribosomal complexes, and therefore it appears that they play an important role in the fidelity of start site selection (Pestova et al., 1998a). It is unclear at what point in the scanning process the interaction between eIF4G and eIF3 is disrupted (Jackson, 2000).

### 1.1.6 60S ribosomal subunit joining

When the 40S subunit is correctly positioned at the initiation codon, base pairing between this AUG and the anticodon of Met-tRNA<sub>i</sub> occurs. This allows the hydrolysis of GTP by eIF2, which is stimulated by the GAP activity of the factor eIF5 (Chakrabarti and Maitra, 1991). eIF5 is recruited to the complex via its interactions with eIF2 and eIF3 (Asano et al., 2000). eIF2-GDP demonstrates low affinity for the 40S ribosome, and hence GTP hydrolysis leads to its release, in combination with the factors eIF3 and eIF1. As eIF3 binding to the 40S ribosome prevents its interaction with the 60S subunit in the context of a preinitiation complex (Chaudhuri et al., 1999), eIF3 release allows subunit joining to occur. However, it has recently been shown that the factor eIF5B is also necessary for this process (Pestova et al., 2000). This protein binds GTP, which is hydrolysed when eIF5B binds to the ribosome. This hydrolysis mediates the release of eIF5B from the ribosome and therefore allows repeated use of the same molecule and means that it can function catalytically, but its precise role in recruitment of the 60S subunit remains unclear. An interaction has been detected between eIF1A and eIF5B, and it is possible that this is important in the stabilisation of Met-tRNA<sub>i</sub> binding to the correct site (Choi et al., 2000).

This assembly of the 80S ribosome at the correct position completes the initiation phase of protein synthesis and allows elongation to begin. Finally, eIF2-GDP is recycled by the factor eIF2B, which promotes guanine nucleotide exchange such that eIF2-GTP is released and is competent to initiate a further round of protein synthesis (Kimball, 1999) (figure 1.2).

## **1.2 Control of translation initiation by modification and sequestration of factors**

### **1.2.1 Principles of translational control**

Control of translation provides an important method for the regulation of gene expression, as it allows rapid changes in protein level using pre-existing mRNAs, without the need for transcription to occur. The methods used for translational control are generally reversible, and it is of great importance in situations where transcriptional control is lacking, such as in oocytes, and where the spatial control of gene expression is required, such as during embryonic patterning in *Drosophila* (Mathews et al., 2000). The cytoplasmic regulation of poly(A) tail length is important in these situations (Gray and Wickens, 1998), but will not be discussed in detail. The vast majority of translational control occurs at the level of initiation, as this is the rate-limiting step in this pathway, and as it would be inefficient to allow initiation to occur and then to impede translation at a later stage. Control may be global, as will be discussed in this section, or a feature of specific mRNAs, which will be considered later. Phosphorylation as a result of physiological stimuli is an important feature of the control of global protein synthesis.

### **1.2.2 Regulation of eIF4E activity**

A particularly important site for the control of translation initiation is eIF4E. Cap-binding is significant as the first step in the initiation pathway, and early studies indicated that eIF4E abundance was low relative to other components of the translation machinery in certain eukaryotic cell types (Duncan et al., 1987; Hiremath et al., 1985). However, a subsequent study indicated that eIF4E is present in reticulocyte lysate at higher concentration than previously assumed and is not limiting for protein synthesis (Rau et al., 1996). Despite this, the importance of eIF4E control in cell growth can be seen from the fact that it is overexpressed in a number of transformed cell lines (Miyagi et al., 1995). The transcription of eIF4E is stimulated during growth induced by c-Myc (Rosenwald et al., 1993), but phosphorylation of eIF4E protein is of more importance in translational control as it is rapid and reversible. Phosphorylation of eIF4E occurs in response to stimuli such as hormone treatment, growth factors and mitogens (Gingras et al., 1999b) and increases its affinity for the cap, such that cap-dependent initiation is enhanced (Minich et

al., 1994) (figure 1.3). In contrast, adenovirus and influenza virus infection result in a decrease in eIF4E phosphorylation, which contributes to the shutoff of host cell translation induced by these viruses (Feigenblum and Schneider, 1993; Huang and Schneider, 1991). The MAP kinase-interacting protein kinase-1 (Mnk1) is responsible for eIF4E phosphorylation (Waskiewicz et al., 1999) and lies downstream of both the extracellular signal-regulated kinase (ERK) and p38 mitogen-activated protein kinase (p38MAPK) signalling pathways (Fukunaga and Hunter, 1997). Mnk1 does not bind directly to eIF4E, but is recruited to the cap-binding complex via its interaction with the C-terminal of eIF4G (Pyronnet et al., 1999). The related kinase Mnk2 has recently been shown to bind to the same site on eIF4G and to phosphorylate eIF4E, but shows high basal activity under serum starvation, when Mnk1 is inactive (Scheper et al., 2001). It is possible that this kinase functions to retain a low level of eIF4E phosphorylation even in situations in which translation initiation is repressed.

### **1.2.3 The 4E-BPs**

The cap-binding activity of eIF4E is modulated by a family of proteins termed the 4E-binding proteins, or 4E-BPs. The homologous proteins 4E-BP1 and 4E-BP2 were the first to be identified (Pause et al., 1994a), but subsequently a third member of the family, 4E-BP3, was discovered (Poulin et al., 1998). All three proteins show the same function, in that they bind the domain of eIF4E that is normally bound by eIF4G. As binding of the 4E-BPs and eIF4G is mutually exclusive, the eIF4E-4E-BP interaction inhibits assembly of the cap-binding complex and subsequent cap-dependent initiation (Haghighat et al., 1995; Rau et al., 1996). The 4E-BPs are regulated by hyperphosphorylation in response to stimulation of cells by serum, growth factors or hormones. Such phosphorylation induces dissociation from eIF4E and a relief of translational inhibition (Pause et al., 1994a) (figure 1.3). The kinase FKBP12-rapamycin associated protein/ mammalian target of rapamycin (FRAP/mTOR) phosphorylates 4E-BP1 directly at two sites (Gingras et al., 1999a), and the 4E-BPs are also targets of the Akt/ protein kinase B (PKB) signalling pathway (Dufner et al., 1999).

### **1.2.4 eIF2 phosphorylation**

The  $\alpha$  subunit of the heterotrimeric protein eIF2 is subject to phosphorylation, which is of great importance in the control of protein synthesis. During recycling of eIF2-GDP to

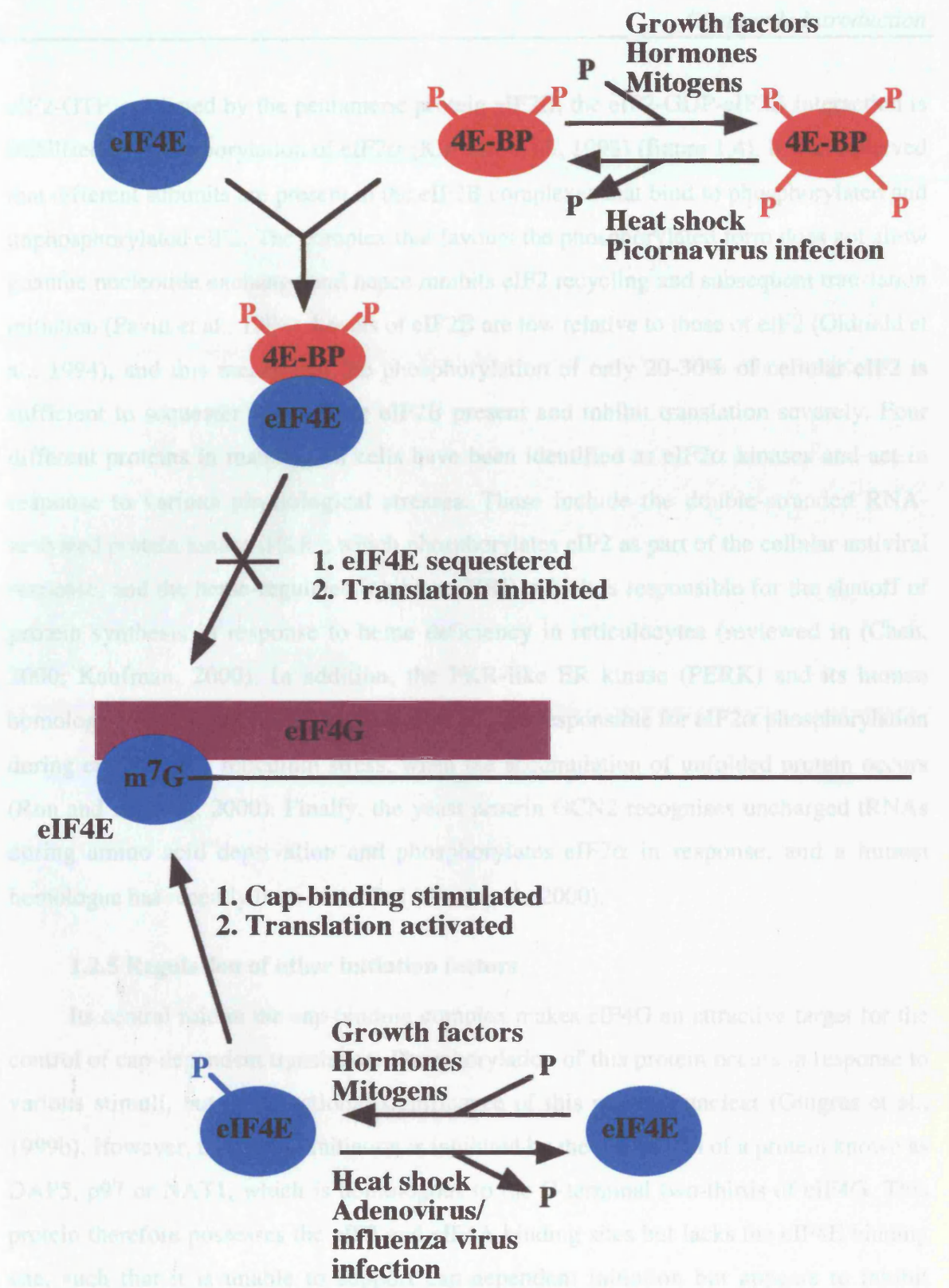


**Figure 1.3 Effects of eIF4E and 4E-BP phosphorylation on cap-dependent translation initiation.** Phosphorylation of eIF4E in response to physiological stimuli increases its affinity for the cap, leading to a stimulation of translation. The 4E-BPs bind to eIF4E when in a hypophosphorylated state and prevent its interaction with eIF4G, thereby inhibiting eIF4F formation and subsequent translation.

eIF2-GTP, mediated by the pentameric protein eIF2B, the eIF2-GDP-eIF2B interaction is stabilised by phosphorylation of eIF2 $\alpha$  (Kimball et al., 1998) (figure 1.4). It was observed that different subunits are present in the eIF2B complexes that bind to phosphorylated and unphosphorylated eIF2. The complex that favours the phosphorylated form does not allow guanine nucleotide exchange and hence inhibits eIF2 recycling and subsequent translation initiation (Pavitt et al., 1998). Levels of eIF2B are low relative to those of eIF2 (Oldfield et al., 1994), and this means that the phosphorylation of only 20-30% of cellular eIF2 is sufficient to sequester most of the eIF2B present and inhibit translation severely. Four different proteins in mammalian cells have been identified as eIF2 $\alpha$  kinases and act in response to various physiological stresses. These include the double-stranded RNA-activated protein kinase (PKR), which phosphorylates eIF2 as part of the cellular antiviral response, and the heme-regulated inhibitor (HRI), which is responsible for the shutoff of protein synthesis in response to heme deficiency in reticulocytes (reviewed in (Chen, 2000; Kaufman, 2000)). In addition, the PKR-like ER kinase (PERK) and its human homologue, the pancreatic eIF2 $\alpha$  kinase (PEK), are responsible for eIF2 $\alpha$  phosphorylation during endoplasmic reticulum stress, when the accumulation of unfolded protein occurs (Ron and Harding, 2000). Finally, the yeast protein GCN2 recognises uncharged tRNAs during amino acid deprivation and phosphorylates eIF2 $\alpha$  in response, and a human homologue has recently been identified (Sood et al., 2000).

### **1.2.5 Regulation of other initiation factors**

Its central role in the cap-binding complex makes eIF4G an attractive target for the control of cap-dependent translation. Phosphorylation of this protein occurs in response to various stimuli, but the functional significance of this remains unclear (Gingras et al., 1999b). However, translation initiation is inhibited by the expression of a protein known as DAP5, p97 or NAT1, which is homologous to the C-terminal two-thirds of eIF4G. This protein therefore possesses the eIF3 and eIF4A binding sites but lacks the eIF4E binding site, such that it is unable to support cap-dependent initiation but appears to inhibit translation by the sequestration of eIF3 and eIF4A (Imataka et al., 1997). In addition, cleavage of eIF4G occurs during picornaviral infection (discussed in section 1.4.1) and during apoptosis (section 1.2.6) and results in the inhibition of cap-dependent translation.

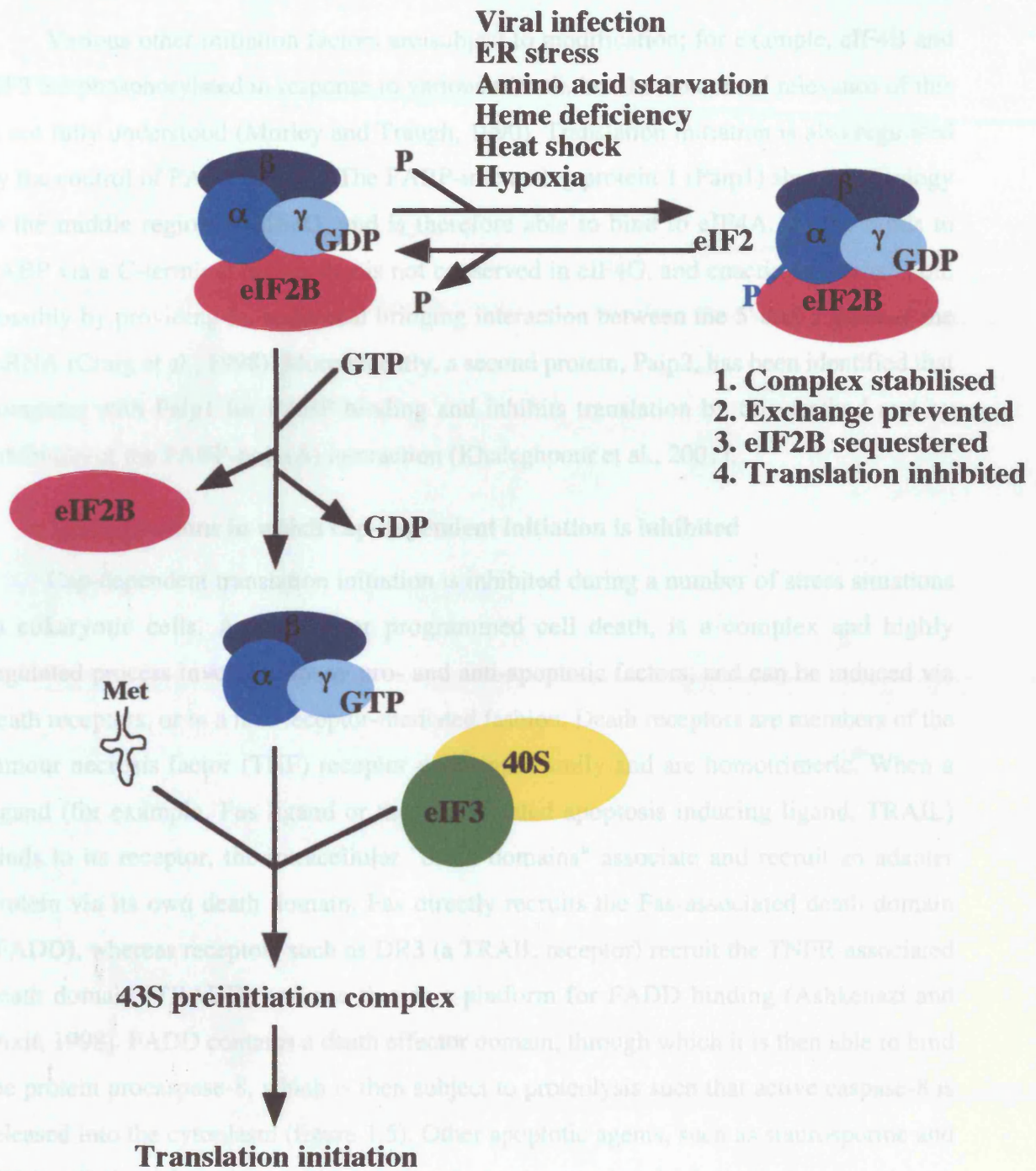


**Figure 1.4 Effect of eIF2 $\alpha$  phosphorylation on translation initiation.** The phosphorylation of the  $\alpha$  subunit of eIF2 in response to various cellular stresses prevents guanine nucleotide exchange by stabilisation of the eIF2-GDP-eIF2B complex. As eIF2-GTP is required to initiate translation, this phosphorylation leads to inhibition of protein synthesis.

Various other initiation factors are subject to modification; for example, eIF4B and eIF3 are phosphorylated in response to various stimuli, but the functional relevance of this is not fully understood (Morley and Traugh, 1990). Translation initiation is also regulated by the control of PABP activity. The PABP-interacting protein 1 (Paip1) shows homology to the middle region of eIF4G, and is therefore able to bind to eIF4A. It also binds to PABP via a C-terminal region that is not conserved in eIF4G, and coactivates translation, possibly by providing an additional bridging interaction between the 5' and 3' ends of the mRNA (Craig et al., 1998). More recently, a second protein, Paip2, has been identified that competes with Paip1 for PABP binding and inhibits translation by this method and by inhibition of the PABP-poly(A) interaction (Khaleghpour et al., 2001).

### **1.2.6 Situations in which cap-dependent initiation is inhibited**

Cap-dependent translation initiation is inhibited during a number of stress situations in eukaryotic cells. Apoptosis, or programmed cell death, is a complex and highly regulated process involving many pro- and anti-apoptotic factors, and can be induced via death receptors, or in a non-receptor-mediated fashion. Death receptors are members of the tumour necrosis factor (TNF) receptor gene superfamily and are homotrimeric. When a ligand (for example, Fas ligand or the TNF-related apoptosis inducing ligand, TRAIL) binds to its receptor, the intracellular "death domains" associate and recruit an adapter protein via its own death domain. Fas directly recruits the Fas-associated death domain (FADD), whereas receptors such as DR3 (a TRAIL receptor) recruit the TNFR-associated death domain (TRADD) and use this as a platform for FADD binding (Ashkenazi and Dixit, 1998). FADD contains a death effector domain, through which it is then able to bind the protein procaspase-8, which is then subject to proteolysis such that active caspase-8 is released into the cytoplasm (figure 1.5). Other apoptotic agents, such as staurosporine and UV irradiation, do not act via receptors. Instead, mitochondrial disruption is induced, resulting in the release of cytochrome *c*. Cytochrome *c* then associates with Apaf-1 and procaspase-9 to form an "apoptosome", from which active caspase-9 is released and induces downstream apoptotic events (Green and Reed, 1998) (figure 1.5).

The caspases are a family of cysteine proteases that are stored in the cell as inactive precursors. They are activated by proteolytic processing, leading to the release of large and small subunits that associate as an active heterodimer. The active caspases then cleave

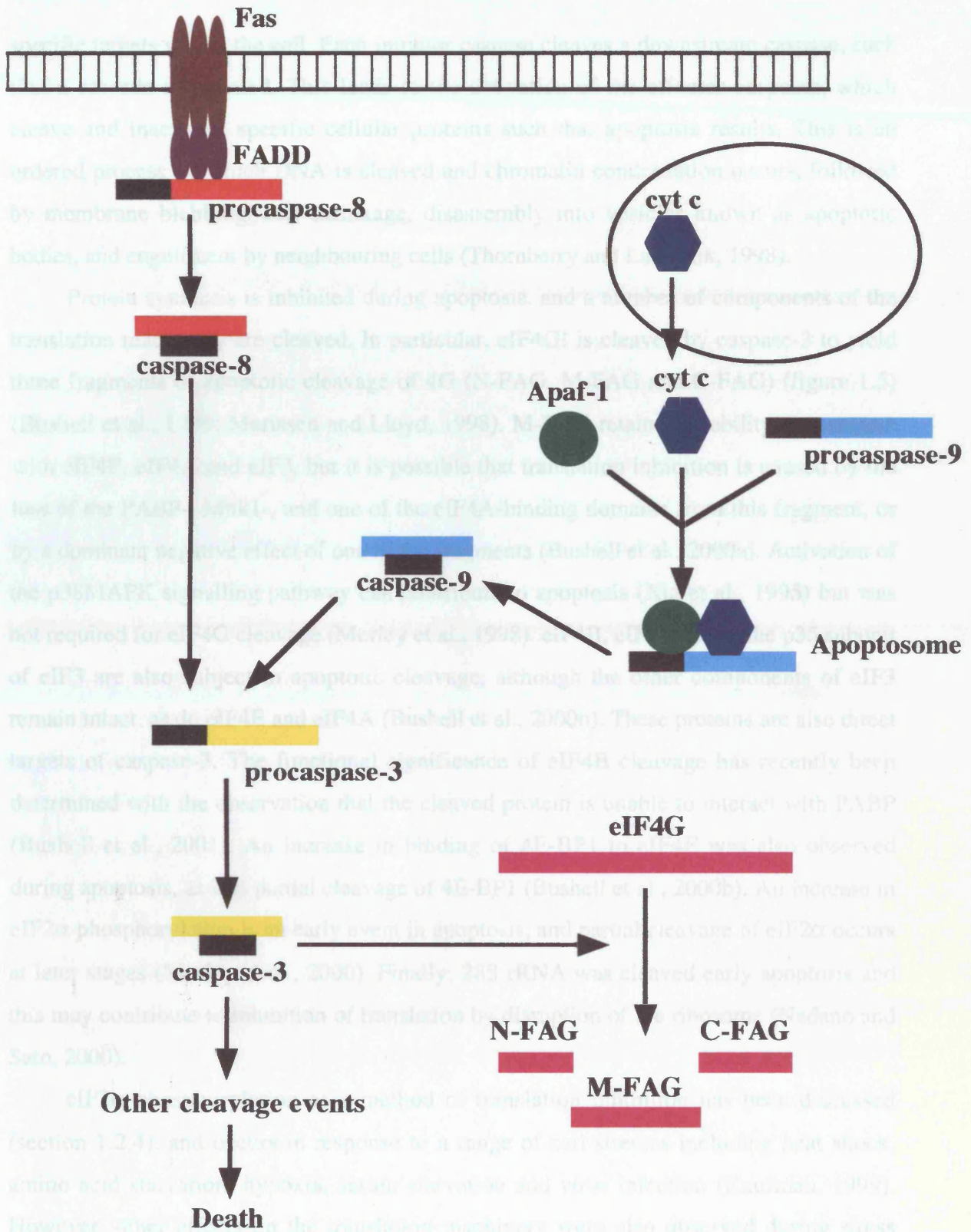


**Figure 1.5 The apoptotic pathway.** Major events of Fas-dependent and non-receptor-mediated apoptosis, leading to cleavage of eIF4G by caspase-3.

specific targets within the cell. Each initiator caspase cleaves a downstream caspase, such that a cascade is initiated. This leads to the activation of the effector caspases, which cleave and inactivate specific cellular proteins such that apoptosis results. This is an ordered process by which DNA is cleaved and chromatin condensation occurs, followed by membrane blebbing, cell shrinkage, disassembly into vesicles known as apoptotic bodies, and engulfment by neighbouring cells (Thornberry and Lazebnik, 1998).

Protein synthesis is inhibited during apoptosis, and a number of components of the translation machinery are cleaved. In particular, eIF4GI is cleaved by caspase-3 to yield three fragments of apoptotic cleavage of 4G (N-FAG, M-FAG and C-FAG) (figure 1.5) (Bushell et al., 1999; Marissen and Lloyd, 1998). M-FAG retains the ability to associate with eIF4E, eIF4A and eIF3, but it is possible that translation inhibition is caused by the loss of the PABP-, Mnk1-, and one of the eIF4A-binding domains from this fragment, or by a dominant negative effect of one of the fragments (Bushell et al., 2000a). Activation of the p38MAPK signalling pathway can contribute to apoptosis (Xia et al., 1995) but was not required for eIF4G cleavage (Morley et al., 1998). eIF4B, eIF4GII, and the p35 subunit of eIF3 are also subject to apoptotic cleavage, although the other components of eIF3 remain intact, as do eIF4E and eIF4A (Bushell et al., 2000b). These proteins are also direct targets of caspase-3. The functional significance of eIF4B cleavage has recently been determined with the observation that the cleaved protein is unable to interact with PABP (Bushell et al., 2001). An increase in binding of 4E-BP1 to eIF4E was also observed during apoptosis, as was partial cleavage of 4E-BP1 (Bushell et al., 2000b). An increase in eIF2 $\alpha$  phosphorylation is an early event in apoptosis, and partial cleavage of eIF2 $\alpha$  occurs at later stages (Morley et al., 2000). Finally, 28S rRNA was cleaved early apoptosis and this may contribute to inhibition of translation by disruption of the ribosome (Nadano and Sato, 2000).

eIF2 $\alpha$  phosphorylation as a method of translation inhibition has been discussed (section 1.2.4), and occurs in response to a range of cell stresses including heat shock, amino acid starvation, hypoxia, serum starvation and virus infection (Kaufman, 1999). However, other effects on the translation machinery were also observed during stress situations. Heat shock induces the dephosphorylation of eIF4E and hence a reduction in the cap-binding activity of eIF4F (Duncan et al., 1987; Lamphear and Panniers, 1991). Furthermore, dephosphorylation of 4E-BP1 occurs and results in increased sequestration

of eIF4E (Feigenblum and Schneider, 1996). This is not sufficient for the inhibition of protein synthesis observed under these conditions, but a recent study has shown the importance of the induction of heat shock protein 27 (Hsp27) in translation. Hsp27 sequesters eIF4G and causes the dissociation of the cap-binding complex (Cuesta et al., 2000).

In addition to stress situations, the level of translation initiation varies according to the growth status of the cell. During mitosis cap-dependent initiation is inhibited relative to interphase cells, and it was shown that eIF4E association with the cap is reduced during mitosis and is likely to contribute to this inhibition (Bonneau and Sonenberg, 1987). Recent observations indicate that mitosis induces hypophosphorylation of 4E-BP1, such that eIF4E is sequestered from the eIF4F complex. The phosphorylation level of eIF4E is also reduced, possibly because its separation from eIF4G results in its removal from the vicinity of the Mnk1 kinase. An additional result of mitosis is to increase the phosphorylation of eIF4GII, and this may contribute to the dissociation of eIF4E from eIF4G (Pyronnet et al., 2001). The phosphorylation state of 4E-BP1, and therefore the level of sequestration of eIF4E, correlates with translational activity throughout the cell cycle. It is hypophosphorylated during G<sub>2</sub>/M phase, but becomes hyperphosphorylated on G<sub>1</sub> entry and remains in this state throughout S phase (Pyronnet et al., 2001).

### **1.3 Control of translation initiation by UTR elements**

#### **1.3.1 The effect of secondary structure in the 5' UTR**

The 5' UTRs of cellular mRNAs are highly variable in their length and the degree of secondary structure possessed, and these features have a considerable effect on the efficiency of translation initiation. Secondary structure within a 5' UTR is able to inhibit translation, and the effect of such structure is dependent on its position relative to the cap. A stem-loop structure of -30kcal/mol free energy caused a major inhibition in translation when placed 12 nucleotides downstream of the cap, but when the same structure was placed 52 nucleotides from the cap it had no effect (Gray and Hentze, 1994b). This is due to the fact that secondary structure adjacent to the cap prevents binding of the 43S preinitiation complex to the mRNA. When a more stable stem-loop, of -61kcal/mol, was inserted 71 nucleotides downstream of the cap structure, translation initiation was blocked,

and "stalled" 43S complexes were detected on the 5' side of the structure (Gray and Hentze, 1994b). In the presence of secondary structure distal to the cap, 43S complexes are able to bind and the helicase action of eIF4A during subsequent scanning is sufficient to unwind a moderate degree of secondary structure. However, higher energy secondary structure is resilient to unwinding by eIF4A and results in an inhibition of scanning.

Transcripts that possess highly structured 5' UTRs are poorly translated under normal physiological conditions, and this is likely to be due to competition with other cellular mRNAs for limiting amounts of the eIF4F complex. An example of this is the *bcr/abl* gene fusion, which results from a chromosomal translocation. It possesses a long, structured 5' UTR that inhibits translation in certain cell lines (Muller and Witte, 1989). Overexpression of eIF4E stimulated the translation of mRNAs that possess structured 5' UTRs (Koromilas et al., 1992), and it appears that such transcripts are particularly sensitive to increases in global protein synthesis. Interestingly, transcripts encoding proto-oncogenes and growth factors tend to contain structured 5' UTRs (Kozak, 1991), allowing repression of their translation under normal circumstances and preventing excessive cell growth.

### 1.3.2 The iron response element

Expression of a number of proteins involved in iron storage and utilisation, including ferritin and erythroid 5-aminolevulinate synthase (eALAS), is translationally regulated by the presence of a structural motif known as the iron response element (IRE) in the 5' UTR (Hentze et al., 1987) (figure 1.6). Production of these proteins is switched on in response to iron, and repressed when cellular iron levels are low. This translational control is coordinated by the binding of the iron regulatory proteins (IRP-1 and IRP-2) to the IRE, a stem-loop structure that is generally located close to the cap. This interaction prevents binding of the 43S pre-initiation complex to the mRNA (Gray and Hentze, 1994a), and hence translation initiation, although the eIF4F complex is able to associate with the cap (Muckenthaler et al., 1998). Removal of the IRE to a position further from the cap results in a reduction in IRP-dependent regulation (Goossen and Hentze, 1992). The IRPs bind to IREs with high affinity under conditions of iron starvation, but dissociate or are degraded when iron is present.

## 13.3.5' TOPs

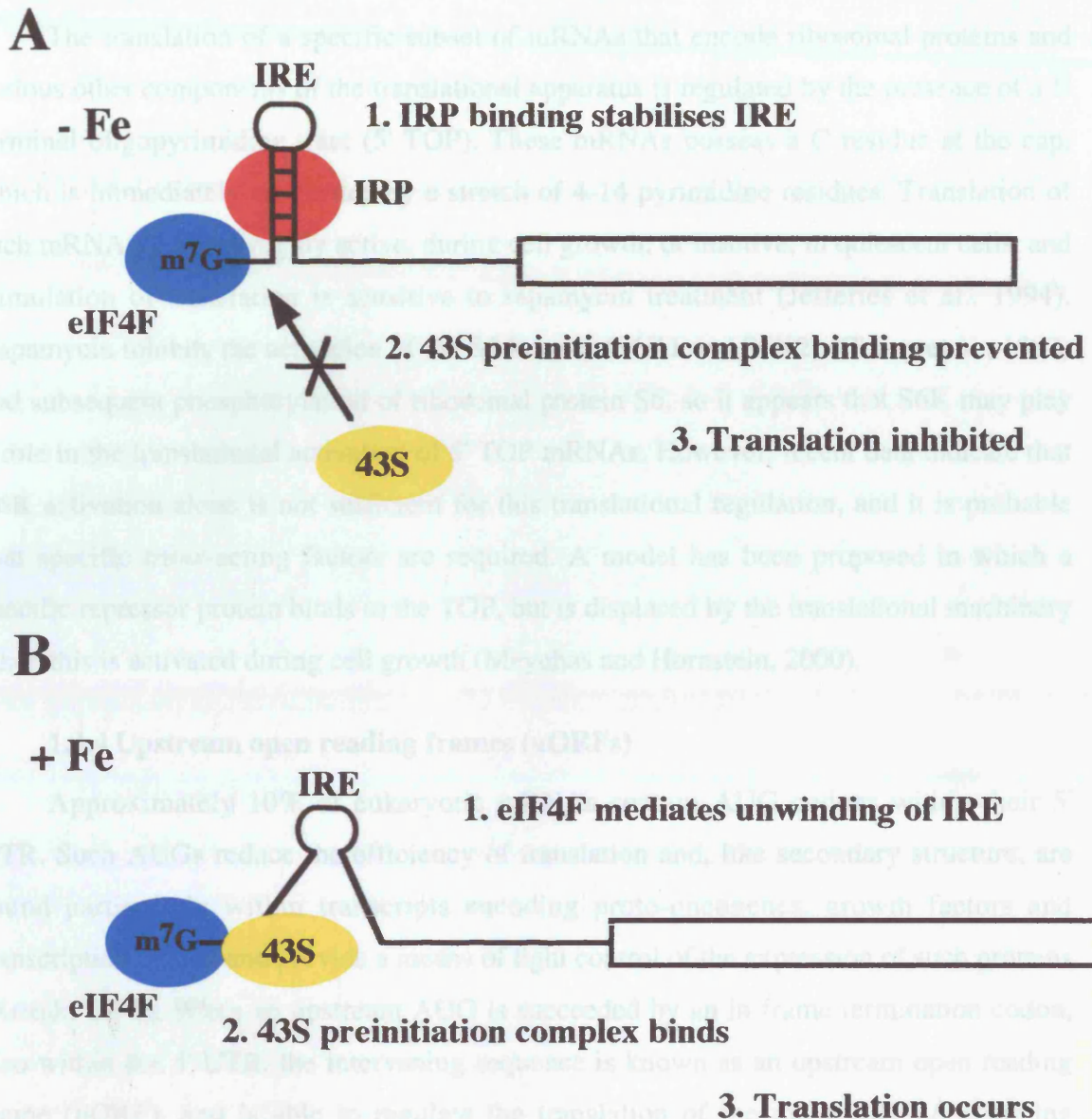


**Figure 1.6 Translational control by the iron response element.** Translation of a gene containing an IRE in its 5' UTR in the absence (A) and presence (B) of iron.

### 1.3.3 5' TOPs

The translation of a specific subset of mRNAs that encode ribosomal proteins and various other components of the translational apparatus is regulated by the presence of a 5' terminal oligopyrimidine tract (5' TOP). These mRNAs possess a C residue at the cap, which is immediately succeeded by a stretch of 4-14 pyrimidine residues. Translation of such mRNAs is either highly active, during cell growth, or inactive, in quiescent cells, and stimulation of translation is sensitive to rapamycin treatment (Jefferies et al., 1994). Rapamycin inhibits the activation of the S6 kinases (S6K1 and S6K2) (Chung et al., 1992) and subsequent phosphorylation of ribosomal protein S6, so it appears that S6K may play a role in the translational activation of 5' TOP mRNAs. However, recent data indicate that S6K activation alone is not sufficient for this translational regulation, and it is probable that specific *trans*-acting factors are required. A model has been proposed in which a specific repressor protein binds to the TOP, but is displaced by the translational machinery when this is activated during cell growth (Meyuhas and Hornstein, 2000).

### 1.3.4 Upstream open reading frames (uORFs)

Approximately 10% of eukaryotic mRNAs contain AUG codons within their 5' UTR. Such AUGs reduce the efficiency of translation and, like secondary structure, are found particularly within transcripts encoding proto-oncogenes, growth factors and transcription factors and provide a means of tight control of the expression of such proteins (Kozak, 1991). When an upstream AUG is succeeded by an in frame termination codon, also within the 5' UTR, the intervening sequence is known as an upstream open reading frame (uORF), and is able to regulate the translation of the main ORF. A scanning ribosome would be expected to initiate translation at the first AUG encountered, so uORFs are generally translated, although with varying efficiency depending on the context of the AUG codon. Following termination of uORF translation, some ribosomes remain associated with the message and continue to translate the main ORF, whereas the majority dissociate and have to reacquire the transcript to carry out further translation (Morris and Geballe, 2000). The efficiency with which such reinitiation occurs is dependent on the length and sequence of the spacer region between the uORF and the initiation codon of the main ORF (Child et al., 1999). In general, increasing the length of the spacer leads to

increased efficiency of reinitiation, possibly because this provides sufficient time for recharging of the ribosome with a new ternary complex.

A number of examples exist of genes regulated by uORFs. The best-studied example is the yeast GCN4 gene, translation of which is enhanced during amino acid starvation when general protein synthesis is repressed. This gene possesses four uORFs, and the effect on translation of the main ORF depends on which uORFs are utilised. Ribosomes enter at the cap, scan to uORF1, and continue to scan following translation of uORF1. If the ribosomes then acquire the ability to reinitiate by the time they reach uORF3 or uORF4, they will resume translation. Translation of these two uORFs is highly inhibitory to translation of the main ORF, probably due to the sequence surrounding the termination codon. However, during starvation eIF2 $\alpha$  phosphorylation occurs and the availability of the eIF2-GTP-Met-tRNA<sub>i</sub> ternary complex is limited. Under these conditions, the majority of ribosomes do not acquire reinitiation potential until they reach the initiation codon for the main ORF, thereby bypassing the inhibitory uORFs and allowing efficient translation of GCN4 (Morris and Geballe, 2000).

### 1.3.5 Ribosomal shunting

Ribosomal shunting is a variant of cap-dependent initiation that was first discovered in cauliflower mosaic virus (CaMV) (Futterer et al., 1993), but also occurs in related plant pararetroviruses, the late adenovirus mRNAs, and the Sendai virus P/C mRNA. Translation occurs by cap-dependent binding of the 40S subunit and scanning of the 5' end of the 5' UTR, but ribosomes are then able to jump over the remainder of the UTR, land close to the initiation codon, and begin translation. A single transcript can be translated by both scanning and shunting ribosomes at the same time, and the extent to which shunting is used is variable. The insertion of a stem-loop towards the 3' end of the late adenovirus tripartite leader (5' UTR) such that scanning, but not shunting, was blocked, indicated that approximately 50% of translation occurs via shunting early in infection. This is increased to almost 100% by late infection, when eIF4F activity is reduced (Yueh and Schneider, 1996).

The signals dictating shunting appear to vary according to the identity of the transcript. In the plant pararetroviruses, shunting is triggered by the presence of a short uORF and the stem-loop structure that succeeds it (Hemmings-Mieszczak and Hohn,

1999) (figure 1.7A). The adenovirus tripartite leader contains three regions of complementarity to 18S ribosomal RNA (rRNA), the deletion of which leads to a severe inhibition of shunting (Yueh and Schneider, 2000). Interestingly, the 5' UTRs of the human heat shock protein 70 (hsp70) and *c-fos* mRNAs also show complementarity to 18S rRNA, and are partially translated by shunting (Yueh and Schneider, 2000). Following heat shock, scanning of these mRNAs was completely inhibited but shunting was unaffected. Shunting can therefore provide a means of allowing translation of cellular mRNAs under conditions in which normal cap-dependent scanning is inhibited.

### **1.3.6 Internal ribosome entry segments**

All the variants of normal translation initiation discussed above remain dependent on the presence of a 5' terminal cap structure. However, in a range of viral and cellular mRNAs, a structured element within the 5' UTR, termed an internal ribosome entry segment (IRES), is able to recruit 40S ribosomal subunits independently of a cap (figure 1.7B). IRES-dependent translation will be discussed in detail below.

## **1.4 The viral IRESs**

### **1.4.1 The picornaviruses**

The first IRESs to be identified were in the 5' UTRs of poliovirus (Pelletier and Sonenberg, 1988) and encephalomyocarditis virus (EMCV) (Jang et al., 1988) RNAs. These are both members of the picornavirus family, and subsequently IRESs have been found in the 5' UTRs of all picornaviruses examined. This family comprises a large number of viruses, subdivided into six genera, all of which possess a positive-stranded RNA genome. Picornaviral mRNA is uncapped, and instead has a 5' terminus of pUp (Nomoto et al., 1977). Picornaviral 5' UTRs are long (610-1200 nucleotides) and are predicted to assume complex secondary structures, and also contain multiple upstream AUGs (Agol, 1991). Many picornaviruses encode a protease, such as the entero- and rhinoviral 2A proteases and the foot-and-mouth disease virus (FMDV) Lb protease, that cleaves various components of the eIF4F complex. In particular, cleavage of eIF4G occurs such that the eIF4E-binding domain in the N-terminal is separated from the remainder of the protein (Kirchweger et al., 1994; Lamphear et al., 1993). This leads to the inhibition of

host cell translation. Cap-dependent translation is further inhibited during EMCV and influenza infection by the dephosphorylation of 4E-BP1 (Ingras et al., 1996). Given these dual strategies, it would be impossible for efficient protein synthesis to occur by the cap-dependent method.

#### 14.2 The dicistronic vector strategy

The first example of a dicistronic vector is the F107A of poliovirus and EMCV, and in all cases subsequent dicistronic vectors were established by the use of dicistronic vectors (Perletti and Peliccioli, 1996). In the F107A vector, the second ORF is cap-dependent and downstream of a uORF. In the EMCV vector, the second ORF is cap-dependent and leads to efficient protein synthesis, but the majority of ribosomes dissociate from the mRNA when the uORF is encountered. A small proportion of ribosomes is able to translate the second ORF following readthrough or reinitiation, but synthesis of this reporter protein is much less efficient than the first protein. To test for an IRES, the sequence of interest is inserted between the cistrons (figure 1.8B). If an IRES is present, cap-dependent translation of the upstream cistron will be similar to that seen in the control, but ribosomes will also be recruited to the transcript upstream of the second cistron, such that its product is synthesized with high efficiency. The system shown as an example in figure 1.8, pRF, is based on the studies described below. It is important to carry out control experiments to ensure that expression of the second cistron is independent of the first cistron.

14.3 Protein synthesis

Deletion analysis in poliovirus and EMCV has demonstrated that IRESs are typically about 450 nucleotides in length (Wang and Baltimore, 1983). Examination of structure and function has necessitated the division of these IRESs into two groups (Jackson et al., 1990). The enterovirus and flavivirus IRESs are defined as type I IRESs, whereas the poliovirus and hepatitis C virus IRESs are defined as type II IRESs, where

**B**

1. Binding of protein factors to IRES

2. Direct recruitment of 43S preinitiation complex upstream of ORF

3. Translation

ORF

**A**

#### 1. Cap-dependent binding of 43S preinitiation complex

eIF4F

m<sup>7</sup>G

43S

43S

43S

uORF

#### 4. Translation

ORF

#### 2. Scanning

#### 3. Shunting

**Figure 1.7 Alternative strategies of ribosome recruitment.** (A) Ribosomal shunting directed by the CaMV 5' UTR. (B) Internal ribosome entry.

host cell translation. Cap-dependent translation is further inhibited during EMCV and poliovirus infection by the dephosphorylation of 4E-BP1 (Gingras et al., 1996). Given these characteristics, it would be impossible for efficient picornaviral translation to occur by the cap-dependent method.

#### **1.4.2 The dicistronic vector assay**

The presence of an IRES in the 5' UTRs of poliovirus and EMCV, and in all genes subsequently shown to contain IRESs, was established by the use of dicistronic vectors (Pelletier and Sonenberg, 1988). The control vector contains two reporter genes downstream of a single promoter, with a short spacer region between, such that dicistronic mRNAs are transcribed (figure 1.8A). Translation of the first cistron is cap-dependent and leads to efficient production of the reporter protein, but the majority of ribosomes dissociate from the mRNA when the termination codon is encountered. A small proportion of ribosomes is able to translate the second cistron following readthrough or reinitiation, but synthesis of this reporter protein is much lower than of the first protein. To test for an IRES, the sequence of interest is inserted between the cistrons (figure 1.8B). If an IRES is present, cap-dependent translation of the upstream cistron will be similar to that seen in the control vector, but ribosomes will also be recruited to the transcript upstream of the second cistron, such that its product is also synthesised with high efficiency. The vector shown as an example in figure 1.8, pRF, was used in the studies described herein. It is important to carry out control experiments to determine that expression of the second cistron is independent of the first cistron, and that the transcripts expressed are truly dicistronic.

#### **1.4.3 Picornaviral IRES structure and ribosome binding**

Deletion analysis of picornaviral 5' UTRs has demonstrated that the IRES is typically about 450 nucleotides in length and is located towards the 3' end of the UTR. Examination of structure and function has necessitated the division of these IRESs into two groups (Jackson et al., 1990). The entero- and rhinovirus IRESs are defined as type I IRESs, whereas the cardio- and aphthovirus IRESs are considered to be type II. The hepatitis A virus (HAV) IRES does not fit into either group, and so has a separate classification. Within each group, conservation of primary sequence between IRESs is limited to short motifs, but considerable conservation of secondary structure is seen. An example of the secondary structure of a type II IRES is shown in figure 1.9. However, few

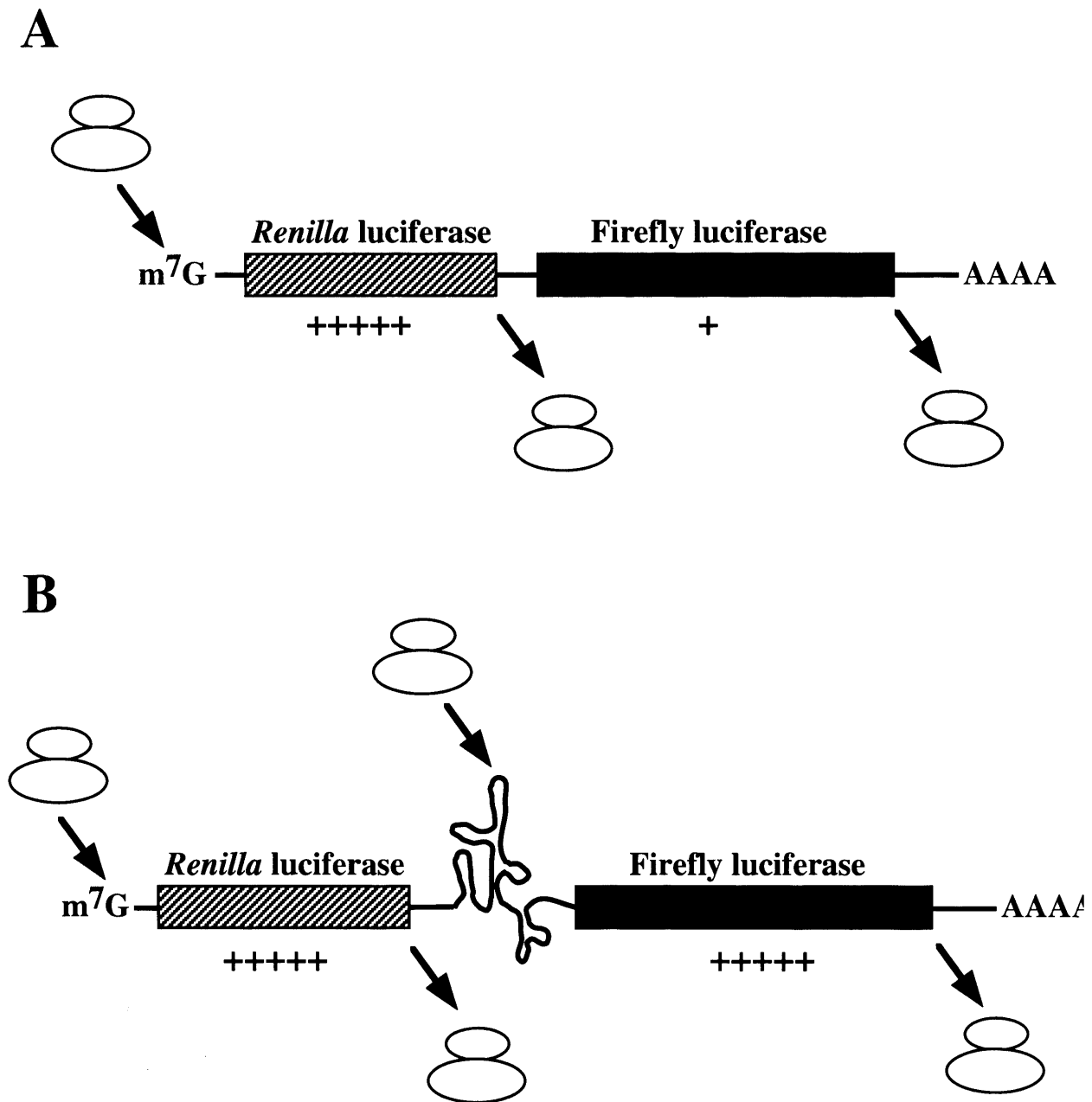


**Figure 1.8 The dicistronic vector assay for IRES activity.** (A) RNA synthesised from the dicistronic vector pRF. Ribosomes enter only at the cap, such that *Renilla* luciferase expression (indicated by plus signs) is high. The majority of ribosomes terminate translation at the 3' end of the *Renilla* luciferase cistron, although a small proportion remain associated with the transcript, or reinitiate translation, such that a small amount of firefly luciferase is produced. (B) RNA synthesised from the vector pRxF, in which an IRES is inserted between the cistrons. *Renilla* luciferase is translated as in (A), but ribosomes are also recruited upstream of the firefly luciferase cistron by the IRES such that high levels of firefly luciferase are also synthesised.

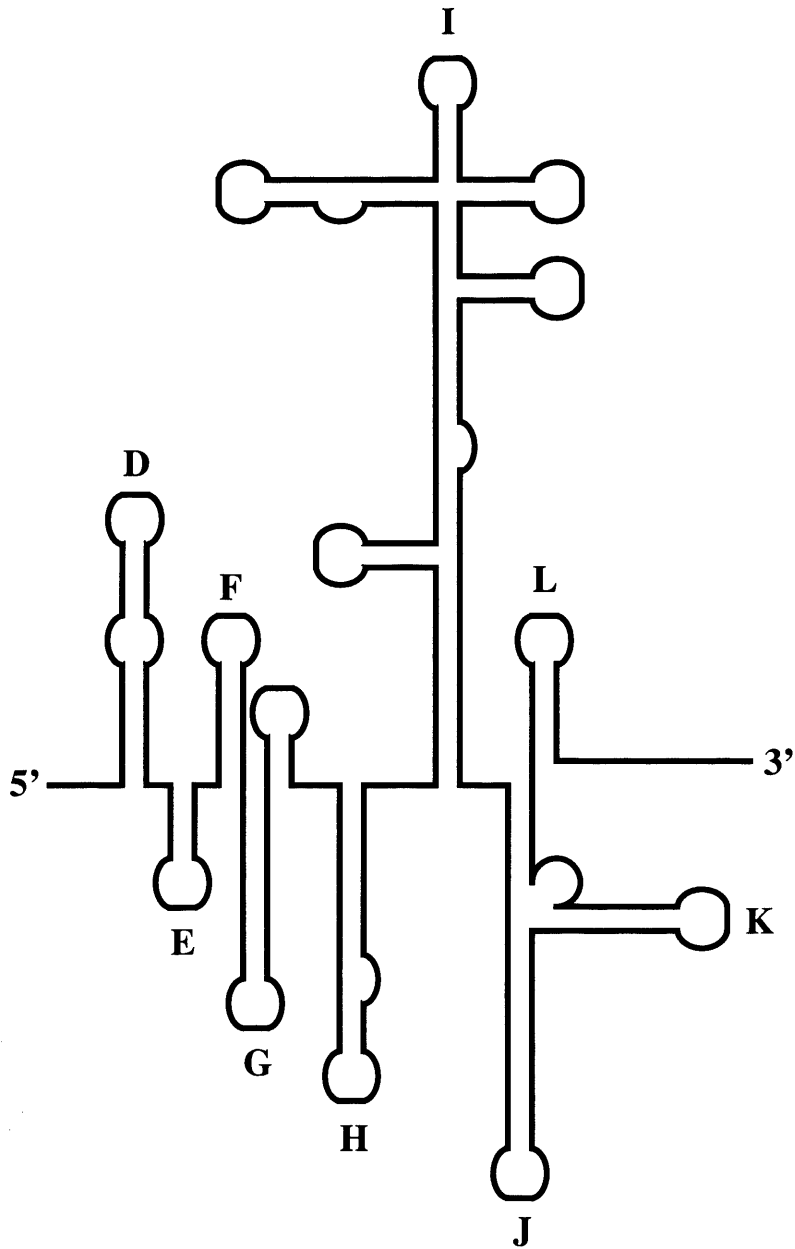


**Figure 1.9 Structure of a typical type II IRES.** The structure and domains of the EMCV IRES are shown as an example of the type II picornaviral IRESs.

similarities have been observed between the groups. Structure mapping indicates that the regions of sequence homology tend to be found in unpaired RNA loops (Jackson et al., 1990). A particularly important sequence motif is the GNRA tetraloop, which is found in both classes of picornaviral IRES, although randomisation of the sequence demonstrates that sequences corresponding to RNRA allow efficient IRES function (Robertson et al., 1999). This leads to a model in which the secondary structure serves as a scaffold to orientate sequence motifs in the correct position for recognition by components of the translational machinery, thereby allowing ribosome recruitment.

A feature shared by all picornaviral IRESs examined is a conserved region of about 25 nucleotides at the 3' boundary of the IRES that comprises a stretch of about 10 pyrimidine residues, a G-poor sequence, and an AUG codon. Ribosome entry occurs at this AUG, as can be seen in the case of the EMCV IRES by the fact that an AUG codon a short distance upstream is never used for initiation, but is used efficiently if the IRES is truncated such that translation is cap-dependent (Kaminski et al., 1990). This indicates that the IRES is able to bypass upstream AUGs and direct the ribosome specifically to its initiation codon. This method, in which ribosome entry occurs at the authentic initiation codon, is also used by the other type II IRESs. However, type I IRESs such as poliovirus and human rhinovirus (HRV) show different behaviour and do not use the AUG codon at which the ribosome enters for initiation (Borman and Jackson, 1992). Instead, ribosome entry is probably followed by scanning to the authentic initiation codon, which is 154nt downstream in poliovirus (Pestova et al., 1994). The foot and mouth disease virus (FMDV) IRES is an exception to the type II IRES rule in that it possesses two functional initiation sites; one at the site of ribosome entry, and the other 84nt downstream (Belsham, 1992). The sequence context of the AUG at which the ribosome enters has some bearing on whether it is used as an initiation codon (Pestova et al., 1994). However, the construction of chimaeric IRESs has indicated that the identity of the main body of the IRES is the major feature that dictates whether initiation occurs on landing or following scanning (Ohlmann and Jackson, 1999).

#### 1.4.4 Involvement of the canonical translation machinery in picornaviral IRES-driven translation

It has proved possible to assemble correctly positioned initiation complexes on EMCV IRES RNA *in vitro* using purified eIF4F, eIF3, eIF2, Met-tRNA<sub>i</sub>, ATP, GTP and 40S ribosomal subunits (Pestova et al., 1996a). eIF4B enhanced this assembly, as did the polypyrimidine tract binding protein (PTB) (discussed in section 1.4.5), although this protein was not essential. The central third of eIF4G bound directly to the J-K domain of the EMCV IRES (figure 1.9), and this portion of the protein, together with eIF4A, was sufficient to replace eIF4F in IRES function (Pestova et al., 1996b). Direct binding of eIF4G to eIF4A was necessary for this function (Lomakin et al., 2000). Thus, all components of the canonical translation machinery, with the exception of eIF4E and full-length eIF4G, are necessary for this IRES to initiate translation. This has led to a model in which eIF4F binding to the J-K domain, close to the 3' end of the IRES, is followed by unwinding of downstream IRES structure by eIF4A such that the 43S preinitiation complex, recruited via the eIF4G-eIF3 interaction, is able to bind (Pestova et al., 1996b).

As yet, no reconstitution experiments have been carried out on type I IRESs, but the activity of the poliovirus IRES is strongly inhibited by a dominant negative form of eIF4A (Pause et al., 1994b), which suggests that the eIF4G-eIF4A complex is required for its function. Viral protease activity stimulates the activity of the type I IRESs, but has no effect on type II IRES function (Ziegler et al., 1995), indicating that the eIF4E-eIF4G interaction is not required by any of these IRESs. The HAV IRES is an exception to these rules in that it is inhibited by the picornaviral proteases and requires full-length eIF4G in complex with eIF4E to function (Ali et al., 2001; Borman and Kean, 1997).

Picornaviral RNA molecules are polyadenylated, and in a physiological HeLa translation extract and a ribosome-depleted reticulocyte lysate system the poly(A) tail stimulates translation from all classes of picornaviral IRES (Bergamini et al., 2000; Michel et al., 2001). This stimulation requires interaction between PABP and eIF4G and was negated by the action of the HRV 2A protease (Michel et al., 2001). Thus, it is likely that the poly(A) tail is only relevant to IRES activity in the very early stages of picornaviral infection before protease activity occurs, except in the cases of EMCV and HAV, which do not encode proteases.

### 1.4.5 *Trans*-acting factor requirements of picornaviral IRESs

Although the type II viral IRESs are able to function efficiently in reticulocyte lysate systems, translation mediated by the type I IRESs is inefficient in such extracts unless supplemented with HeLa cell cytoplasmic extracts (Borman et al., 1995). This led to the hypothesis that polioviral and HRV IRES activity was dependent on *trans*-acting protein factors that are present in HeLa cell extract, but absent in reticulocyte lysate. Fractionation of cell extract revealed that two separate activities are necessary for HRV IRES function. One of these proteins was the polypyrimidine tract binding protein (PTB) (Hunt and Jackson, 1999), previously identified as a negative regulator of alternative splicing (Lin and Patton, 1995). The second activity corresponded to a complex of the proteins unr (encoded by a gene upstream of *N-ras*) and the unr-interacting protein (unrip or p38) (Hunt et al., 1999). Recombinant unr and PTB in combination led to a synergistic stimulation of HRV IRES-driven translation, but unrip had no significant effect, possibly due to incorrect folding of the recombinant protein (Hunt et al., 1999). The poliovirus IRES was activated by PTB but not by unr (Hunt et al., 1999). However, poliovirus IRES-mediated translation shows a requirement for the poly(rC) binding protein 2 (PCBP2), although not for the related protein PCBP1 (Blyn et al., 1997). Subsequently, PCBP2 binding to both type I and type II picornaviral IRESs has been detected, but is only required for translation directed by type I IRESs (Walter et al., 1999). It should be noted that PTB, unr and PCBP2 all contain multiple RNA-binding motifs, and therefore are capable of contacting IRESs at multiple sites concurrently. Finally, poliovirus IRES activity is stimulated by the La autoantigen, a protein with a range of functions in RNA metabolism (Meerovitch et al., 1993). The concentrations required were higher than those in HeLa cell extracts, so the physiological significance of this is unclear.

Reconstitution experiments carried out using the type II IRESs from FMDV and Theiler's murine encephalomyelitis virus (TMEV) indicate that the same set of canonical initiation factors is necessary for correct 48S initiation complex assembly as on EMCV (Pilipenko et al., 2000). In both cases this complex formation was considerably more dependent on PTB than 48S assembly on the EMCV IRES. However, 48S complex formation on the FMDV IRES was not possible in the presence of these purified factors alone, although the IRES functioned efficiently in reticulocyte lysate. Fractionation of reticulocyte lysate led to the identification of the additional factor required by the FMDV

IRES, a protein named IRES *trans*-acting factor 45 (ITAF<sub>45</sub>), that does not belong to any known families of RNA-binding proteins (Pilipenko et al., 2000). PTB and ITAF<sub>45</sub> bound to nonoverlapping sites on the FMDV IRES and induced localised changes in secondary structure. ITAF<sub>45</sub> was not required by the TMEV IRES. Thus, although all three type II IRESs examined show the same requirement for components of the canonical translation machinery, the *trans*-acting factor requirements are different in each case. It has been postulated that this differential requirement is due to small structural differences in the IRESs, such that *trans*-acting factors are required in some cases to remodel incorrectly folded IRESs into a functional conformation (Pilipenko et al., 2000). This theory is supported by the observation that the EMCV IRES can be rendered highly dependent on PTB by a structural mutation in the J-K domain (Kaminski and Jackson, 1998).

#### 1.4.6 The flaviviral and pestiviral IRESs

Internal ribosome entry is not solely a feature of the picornaviruses. IRESs have been identified in the 5' UTRs of a number of other viruses and show significant functional differences to the viral IRESs described above. Of particular interest are the IRESs found in the 5' UTRs of the flavivirus hepatitis C virus (HCV) (Tsukiyama-Kohara et al., 1992) and pestiviruses such as the classical swine fever virus (CSFV) (Rijnbrand et al., 1997). The HCV IRES comprises almost the entire 342nt 5' UTR, and early reports suggested that parts of the coding region were also necessary for IRES activity (Reynolds et al., 1995). However, a recent study shows that the requirement is merely for an unstructured region of RNA downstream of the initiation codon, and is not dependent on RNA sequence (Rijnbrand et al., 2001). Structural homology is seen between the HCV and pestivirus IRESs, with a complex pseudoknot upstream of the initiation codon that is of particular importance for IRES function (Rijnbrand et al., 1997; Wang et al., 1995). This structure is different to that of both groups of picornaviral IRES, and the picornaviral IRESs are approximately 100nt longer.

The mechanism of internal initiation used by these viruses also differs considerably to that used by the picornaviruses. Reconstitution experiments carried out using the HCV and CSFV IRESs demonstrated that 40S ribosomal subunits were able to bind close to the pseudoknot in the absence of any initiation factors (Pestova et al., 1998b). Recruitment of the 40S ribosome requires interactions with a complex series of structural domains that

provide high affinity binding (Kieft et al., 2001). A correctly positioned 48S initiation complex assembled when 40S subunits, eIF2, Met-tRNA<sub>i</sub>, and GTP were present, and this was enhanced by eIF3. Further experiments indicated that eIF3 binds specifically to the IRES and is essential for later 80S ribosome assembly, but even at this stage there is no requirement for any components of eIF4F (Pestova et al., 1998b). However, HCV IRES activity is stimulated by PTB, presumably as a result of stabilisation of secondary structure (Gosert et al., 2000).

Very recently, cryo-electron microscopy (cryo-EM) studies have allowed direct visualisation of HCV IRES RNA bound to a 40S ribosomal subunit, and provide further proof of the multiple interactions between this IRES and the ribosome (Spahn et al., 2001). These exciting experiments also show that a conformational change is induced in the 40S subunit by IRES binding, implying that the HCV IRES is able to actively manipulate the ribosome into the desired orientation. Further cryo-EM studies have allowed visualisation of PTB binding to the HCV IRES and show the structural distinctions between the HCV and FMDV IRESs (Beales et al., 2001).

#### **1.4.7 The insect picorna-like viral IRESs**

The insect picorna-like viruses, such as cricket paralysis virus (CrPV), are naturally dicistronic and contain IRESs both in the 5' UTR, directing translation of the upstream cistron, and in the intergenic region (IGR), such that translation of the downstream cistron is allowed (Sasaki and Nakashima, 1999; Wilson et al., 2000b). As was observed with HCV, 40S ribosomal subunits are able to assemble on the CrPV IGR-IRES in the absence of any initiation factors (Wilson et al., 2000a). However, the mechanism of function used by the IGR-IRES is even more remarkable than that of the HCV IRES. Incubation of IRES RNA with 40S and 60S ribosomal subunits was sufficient to allow assembly of 80S monosomes, and no initiation factors were necessary for this process. A series of conclusive experiments demonstrated that competent initiation complexes form on the IRES in the absence of eIF2, Met-tRNA<sub>i</sub> or GTP hydrolysis. Moreover, the N-terminal residue of the protein product is alanine and is encoded by the codon GCU. This N-terminal is not a result of peptide cleavage, and the codon encoding it is positioned in the A site of the arrested ribosome. Tertiary interactions occur between the codon in the P site and upstream IRES sequence, and it appears that this can substitute for tRNA binding to

the P site and allow a pseudotranslocation event to occur after Ala-tRNA binds to the A site (Wilson et al., 2000a). It seems that this methionine-independent initiation is a general mechanism used by the insect picorna-like virus IRESs, although different N-terminal amino acids are used (Sasaki and Nakashima, 2000).

## 1.5 Cellular IRESs

### 1.5.1 Cellular genes that contain IRESs

The first observation that internal ribosome entry was also used by cellular mRNAs was made using the transcript encoding the immunoglobulin heavy-chain binding protein (BiP) (Macejak and Sarnow, 1991). Subsequently, IRESs have been detected in an increasing number of cellular transcripts (summarised in table 1.1). It is difficult to predict what proportion of cellular genes use internal ribosome entry as a method of translation. Transcripts that contain long, structured 5' UTRs, sometimes containing upstream AUGs, are likely candidates, and a high degree of UTR sequence conservation between species indicates a probable function for the UTR. The *mt* IRES, for example, is 95% identical in human and murine genes (Stoneley et al., 2001). However, such features merely provide an indication that an IRES may exist, and the experiments described in section 1.4.2 are necessary to establish that this is truly the case. Microarray analysis of polysome-associated mRNAs in poliovirus-infected cells provided an elegant means of identifying transcripts that are actively translated under these conditions, when eIF4G is cleaved (Johannes et al., 1999). Approximately 3% of cellular transcripts were associated with the translation machinery at a late stage of poliovirus infection, and are likely to contain IRESs, although once again dicistronic vector assays are necessary to prove this.

Interestingly, the proteins encoded by genes that contain IRESs tend to function in the control of cell growth and death, and are frequently proto-oncogenes. Examples include *c-myc*, the expression of which is important in cell cycle progression and apoptosis (Stoneley et al., 1998) (see sections 1.6.2 and 1.6.3) and growth factors such as fibroblast growth factor-2 (FGF-2) (Vagner et al., 1995) and vascular endothelial growth factor (VEGF) (Akiri et al., 1998). Pro-apoptotic proteins that are translated by internal ribosome entry include the apoptotic protease activating factor (Apaf-1) (Coldwell et al., 2000), whereas an IRES is also found in the transcript encoding the Bcl-2-associated athanogene-

Transcription factors	Antennapedia Ultrabithorax <i>c-myc</i> MYT2 NRF AML1/RUNX1 Nkx6.1 Gtx Chicken <i>c-jun</i>
Growth factors and protein kinases	FGF-2 PDGF/ <i>c-sis</i> VEGF Pim-1 Cyr61 p58 <sup>PITSLRE</sup>
Pro- and anti-apoptotic proteins	Apaf-1 XIAP DAP5 BAG-1
Factors associated with translation	eIF4G La
Factors associated with metabolism and transport	Kv1.4 ODC Nuclear form of Notch2 Cat-1 Nerve-specific connexin-32
Dendritic proteins	ARC CamKII Dendrin MAP2 RC3
Other proteins	BiP Mnt

**Table 1.1 Cellular IRESs.** The cellular genes in which IRESs have been identified to date, and the function of the proteins encoded.

1 (BAG-1) (Coldwell et al., 2001), an anti-apoptotic factor. Therefore, it appears that internal ribosome entry is used, at least in part, as a method of regulating the growth status of the cell.

### 1.5.2 Structural and sequence features of cellular IRESs

In contrast to the viral IRESs, no common sequence or structural motifs have been detected between cellular IRESs, although these sequences tend to be long and GC-rich

and have a high degree of predicted secondary structure. A suggestion was made that a "Y-shaped motif" was a common structural feature (Le and Maizel Jr, 1997), but this was based merely on computer folding predictions for a few cellular IRESs, and no experimental evidence has been provided of its existence or role in IRES function. The only experimentally derived cellular IRES structure that has been published is for the *c-myc* IRES (Le Quesne et al., 2001). This structure consists of two stem-loop domains, of which domain 1 is considerably more complex and contains an overlapping double pseudoknot. The domains are capped by loops that conform to the sequences GNRA and AUUU, often detected in viral IRES loop regions. Mutation analysis indicated that the pseudoknot was inhibitory to IRES function, possibly by impeding ribosome binding. The mutation of other structural features diminished IRES activity, but none was sufficient to abolish it. This implies that the *c-myc* IRES is a modular entity in which domains with partial IRES activity are able to collaborate to recruit ribosomes more efficiently. This is in contrast to observations regarding viral IRES function.

A further example of a modular cellular IRES is that of the transcript encoding the Gtx homeodomain protein. The 5' UTR of this gene is 196nt long, but deletion analysis indicated that a 9nt fragment of the UTR possesses IRES activity, and multiple copies of this segment lead to a synergistic stimulation of this activity (Chappell et al., 2000a). Clearly, such a short segment of RNA would be unable to assume the complex secondary structure previously associated with IRES activity. Instead, its activity appears to be due to its exact complementarity to a region of 18S rRNA, and previous studies have shown that it is possible to photochemically cross-link Gtx 5' UTR RNA to the 40S ribosomal subunit (Hu et al., 1999). A selection system in which short segments of RNA were randomised and tested for IRES activity led to the identification of two sequences that were able to promote internal ribosome entry, were more efficient when multiple copies were present, and showed complementarity to 18S rRNA (Owens et al., 2001). Although this presents an interesting and novel mechanism of ribosome recruitment, it is unlikely that this method is used by the majority of cellular IRESs. Despite the lack of similarity to viral IRES structures, most cellular IRESs are long and GC-rich with a complex predicted secondary structure, and are likely to recruit ribosomes in a manner analogous to that of the viral IRESs. Complementarity to 18S rRNA appears to be a specialised mechanism, and as yet the extent to which it is used is unclear.

### 1.5.3 Requirements of cellular IRESs

The requirements of cellular IRESs are much less clearly defined than those of their viral counterparts; as yet, no attempt has been made to reconstitute initiation complexes from purified components, and the initiation factors necessary for IRES activity are not known. Some cellular IRESs, such as those of ornithine decarboxylase (ODC) (Pyronnet et al., 2000) and the transcription factor AML1/RUNX1 (Pozner et al., 2000), are able to direct translation when *in vitro*-transcribed dicistronic RNA is used to programme reticulocyte lysate systems. However, the majority of cellular IRESs are inactive *in vitro*. The *c-myc* and Apaf-1 IRESs direct internal ribosome entry to a variable extent in transfected cell lines of different derivation (Coldwell et al., 2000; Stoneley et al., 2000b). Moreover, the activity of the FGF-2 and *c-myc* IRESs, but not the EMCV IRES, was shown to be highly tissue-specific in the context of transgenic mice (Creancier et al., 2001; Creancier et al., 2000). This implies a requirement for a precise set of cellular proteins that display varying expression in different tissues.

Attempts have been made to identify *trans*-acting factors involved in cellular IRES function. The *c-myc* IRES presents a particularly complex scenario, as it is unable to function when dicistronic RNA is introduced directly into the cytoplasm of HeLa cells. Therefore, it appears that the IRES must go through a "nuclear event"; perhaps a covalent modification of the RNA, or perhaps association with a specific protein factor in the nucleus or at the nuclear membrane (Stoneley et al., 2000b). However, there has been more success in the identification of *trans*-acting factors associated with other IRESs. In a number of cases it appears that factors that stimulate viral IRESs also have a role in cellular IRES activity. For example, the Apaf-1 IRES is more active in cell lines that contain high levels of unr and PTB, and these proteins in combination are able to stimulate the activity of this IRES both *in vitro* and in transfected cells. Interestingly, unr binds directly to Apaf-1 IRES RNA, but PTB is only able to bind in the presence of unr (Mitchell et al., 2001). It is likely that unr functions as a chaperone, allowing the IRES to assume the correct tertiary structure for PTB binding. PTB also binds to the BiP IRES, but in this case its binding is inhibitory to IRES activity (Kim et al., 2000b), indicating that this protein does not always stimulate IRES function.

The La autoantigen is another factor that appears to function in both viral and cellular IRES-driven translation. La binds specifically to the X-linked inhibitor of

apoptosis (XIAP) IRES RNA, while XIAP IRES activity was inhibited in reticulocyte lysate and cultured cells by the addition of, or cotransfection with, a dominant negative form of La protein (Holcik and Korneluk, 2000). The La protein itself is encoded by alternative transcripts with different lengths of 5' UTR, La1 and La1', both of which contain IRESs (Carter and Sarnow, 2000). The death-associated protein 5 (DAP5), discussed in section 1.2.5, possesses an IRES, and recombinant DAP5 protein is able to stimulate translation from this IRES (Sella et al., 1999). It is likely that this stimulation is due to the homology of DAP5 to eIF4G, as it is able to bind eIF3 and eIF4A and hence could provide the eIF4G functions necessary for cap-independent translation. Finally, the splicing factor hnRNP C binds to the IRES in the gene *c-sis*, which encodes the B chain of platelet-derived growth factor (PDGF) (Sella et al., 1999). However, binding does not necessarily imply that a protein is required for IRES function, and no such role has yet been demonstrated. Much work is still to be done in determining the proteins factors and mechanisms used by cellular IRESs.

#### **1.5.4 Situations in which cellular IRESs are used**

The existence of the viral IRESs serves a clear purpose in allowing translation of viral gene products at the same time as inhibiting the cellular translation machinery. However, there is not such a clear rationale for the existence of IRESs in cellular transcripts. Translation of many IRES-containing genes, such as *c-myc*, can occur by both cap- and IRES-dependent methods in the context of the same 5' UTR (Stoneley et al., 2000b). It therefore appears likely that cellular IRESs exist in order to maintain production of certain essential proteins in situations in which cap-dependent initiation is inhibited, and that translation of the same mRNA may be cap-dependent at other times. There are numerous such situations (discussed in section 1.2.6) and mounting evidence indicates that various cellular IRESs are used under these conditions.

During apoptosis various initiation factors, including eIF4G, are cleaved by caspases such that cap-dependent initiation is inhibited (section 1.2.6). The DAP5 IRES continued to function during apoptosis induced by Fas ligand (Henis-Korenblit et al., 2000). DAP5 is itself subject to caspase cleavage and the p86 form that results was particularly effective at stimulating its own translation. It is therefore possible that DAP5 is required for residual translation late in apoptosis, and an IRES is used to maintain its expression for these

purposes (Henis-Korenblit et al., 2000). Another protein with a role in apoptosis that can be translated via an IRES is XIAP. XIAP is important for cell survival following  $\gamma$ -irradiation, and its expression was upregulated following radiation in one of four cell lines tested.  $\gamma$ -irradiation led to a stimulation of XIAP IRES activity in this cell line, but not in the other three lines, presumably due to differences in cellular environment (Holcik et al., 2000).

An example of the same gene using cap-dependent and IRES-dependent translation for different purposes is that of the two PITSLRE protein kinases (p110<sup>PITSLRE</sup> and p58<sup>PITSLRE</sup>), which are synthesised from the same transcript. Translation of p110<sup>PITSLRE</sup> is cap-dependent and it is expressed throughout the cell cycle. p58<sup>PITSLRE</sup> is translated from a downstream in-frame AUG codon, and translation occurs via an IRES in the coding region of p110<sup>PITSLRE</sup>. This form of the protein is specifically expressed during G<sub>2</sub>/M phases, and it was shown that the IRES was specifically activated at G<sub>2</sub>/M (Cornelis et al., 2000). A second IRES that is active during mitosis was discovered in ornithine decarboxylase (ODC), an enzyme involved in polyamine biosynthesis. The amount of ODC mRNA remains constant throughout the cell cycle, but levels of protein peak at G<sub>1</sub>/S phase, when global protein synthesis is activated. A second peak in expression at G<sub>2</sub>/M occurred during the inhibition of the cellular translational machinery and was caused by activation of the ODC IRES (Pyronnet et al., 2000). This study also suggested that the *c-myc* IRES remains active during mitosis, but this was in disagreement with other findings (T. Subkhankulova, personal communication).

Differentiation is a further cellular process in which certain IRESs have been implicated. Megakaryocytes are a major site of PDGF synthesis, and the PDGF2/*c-sis* IRES was activated during megakaryocytic differentiation (Bernstein et al., 1997). The transcription factor AML1/RUNX1 is expressed mainly in the haematopoietic system. AML1 transcripts possess alternative 5' UTRs, of which the longer P-UTR contains an IRES. Activity of this IRES was stimulated during megakaryocytic differentiation, but inhibited during erythroid differentiation (Pozner et al., 2000). Transgenic studies showed that the FGF-2 IRES was highly active in embryonic brain tissue, and this activity was maintained in the adult brain (Creancier et al., 2000). The activity of the FGF-2 IRES was low in other adult tissues, and the *c-myc* IRES was active in most embryonic tissues in

transgenic mice, but inactive in adults (Creancier et al., 2001). Therefore, it appears that in most situations IRES activity is downregulated during development.

Very recently, two further instances of IRES utilisation during conditions in which cap-dependent translation is inhibited have emerged. Levels of the cationic amino acid transporter, Cat-1, are considerably increased during amino acid starvation, such that increased transport of arginine and lysine into cells occurs. The cat-1 gene contains an IRES that was activated during amino acid starvation in transfected cells, when a decrease in protein synthesis was induced by eIF2 $\alpha$  phosphorylation. The activity of the BiP IRES was unaffected by these conditions, indicating that this activation was specific to the cat-1 IRES (Fernandez et al., 2001). Finally, activity of the BAG-1 IRES was maintained during heat shock. This allowed continued production of the p36 isoform of this protein, which has a role in the protein refolding response (Coldwell et al., 2001).

In conclusion, it appears that cellular IRESs are active during a wide variety of situations in which cap-dependent initiation is inhibited, and it is probable that many more instances will be discovered. The current data indicate that this behaviour is very specific, and IRESs are used under different conditions to maintain expression of particular proteins that are required in these circumstances.

### **1.5.5 Association of cellular IRESs with disease**

C-Myc is a proto-oncogene and its overexpression is associated with a number of cancers (section 1.6.1). In multiple myeloma (MM) a point mutation in the *c-myc* 5' UTR was detected and led to increased binding of several unidentified protein factors (Paulin et al., 1998). Subsequent studies indicated that this mutation was present in 42% of bone marrow samples from MM patients, but in none of the healthy bone marrow samples analysed. The mutant IRES was more active than the wild type version in a range of cell lines, and this stimulation was greatest in an MM derived cell line (Chappell et al., 2000b). A further example of a cellular IRES mutation contributing to a disease is in Charcot-Marie-Tooth Disease. A mutation in the 5' UTR of the nerve-specific connexin-32 mRNA was detected in a family with this disease and caused a complete inactivation of the IRES (Hudder and Werner, 2000).

## 1.6 The *myc* family

### 1.6.1 The *c-myc* gene and its role in cancer

*c-myc* is a proto-oncogene that was first isolated from chicken cells as the cellular homologue of *v-myc* (Vennstrom et al., 1982). Subsequently, the *c-myc* gene has been isolated from various mammalian species, including humans, and found to consist of three exons (Saito et al., 1983). Transcription initiation occurs from four different promoters (figure 1.10A), of which P2 is the most frequently used (Bentley and Groudine, 1986). Deregulated expression of *c-myc* is associated with a number of different tumours. In Burkitt's lymphoma, this deregulation occurs by chromosomal translocation such that the *c-myc* coding region is downstream of one of the immunoglobulin promoter/enhancer regions. Amplification of the *c-myc* gene is also associated with various other tumours including small cell lung carcinoma, breast carcinoma and colon carcinoma (Henriksson and Luscher, 1996; Nesbit et al., 1999). In addition to alterations in gene expression, point mutations in the *c-myc* coding region have been detected in Burkitt's lymphoma and result in mutant c-Myc protein, although the role of this protein in tumorigenesis is unclear (Nesbit et al., 1999). A large proportion of transgenic mice in which the *c-myc* gene was juxtaposed to the immunoglobulin enhancer developed B-cell lymphomas after a latency period, indicating that although overexpression of *c-myc* predisposes towards tumorigenesis it must be accompanied by other genetic changes (Adams et al., 1985). *In vitro* studies support this finding, in that the *c-myc* gene is sufficient to immortalise cultured cells but must cooperate with another oncogene, such as *ras*, to induce transformation (Land et al., 1983).

### 1.6.2 The role of *c-myc* in cell growth and differentiation

The importance of regulated *c-myc* expression is related to its central role in cell fate. *c-myc* mRNA levels are very low in quiescent cells. However, stimulation of cells with growth factors or serum leads to a rapid induction of *c-myc* expression as G<sub>0</sub>-G<sub>1</sub> transition occurs. Following this increase, *c-myc* mRNA levels are reduced, but are maintained at a low level throughout the cell cycle (Dean et al., 1986; Rabbitts et al., 1985). Cells that constitutively express *c-myc* show a reduced G<sub>1</sub> phase, whereas *c-myc* null cells remain in both G<sub>1</sub> and G<sub>2</sub> phases for prolonged periods (Karn et al., 1989; Matejak et al., 1997). Experiments in *Drosophila* indicate that overexpression of *myc* increases cell size and

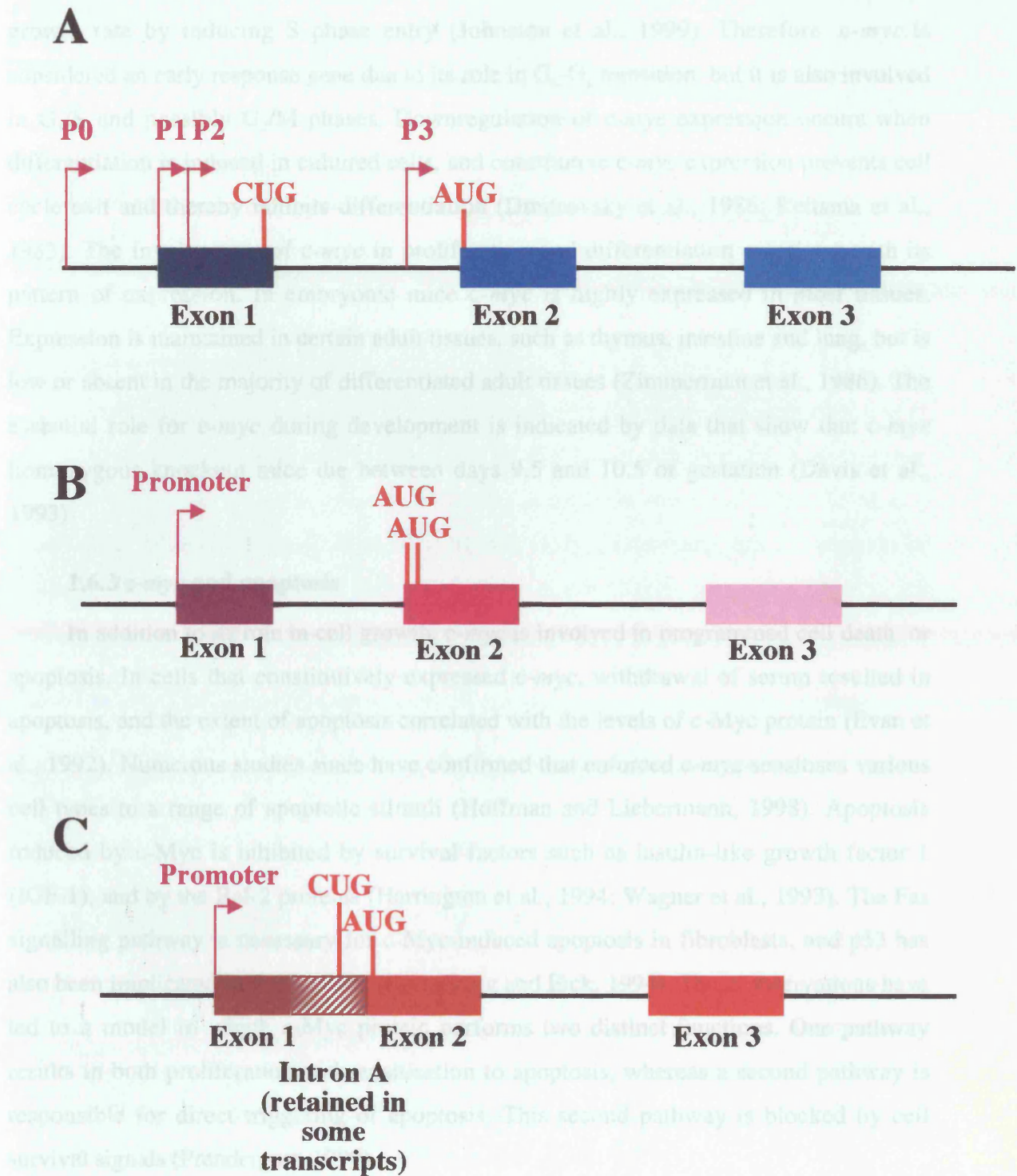


**Figure 1.10 *myc* gene structure.** The exon-intron structures, promoters, and translation initiation codons of the (A) *c-myc*, (B) *N-myc* and (C) *L-myc* genes are shown. *L-myc* is subject to alternative splicing such that intron 1 is retained in a proportion of mature transcripts. Portions of intron 2 are retained in some *L-myc* transcripts, but this is not shown.

growth rate by inducing S phase entry (Johnston et al., 1999). Therefore, *c-myc* is considered an early response gene due to its role in G<sub>0</sub>-G<sub>1</sub> transition, but it is also involved in G<sub>1</sub>/S and possibly G<sub>2</sub>/M phases. Downregulation of *c-myc* expression occurs when differentiation is induced in cultured cells, and constitutive *c-myc* expression prevents cell cycle exit and thereby inhibits differentiation (Dmitrovsky et al., 1986; Reitsma et al., 1983). The involvement of *c-myc* in proliferation and differentiation correlates with its pattern of expression. In embryonic mice *c-myc* is highly expressed in most tissues. Expression is maintained in certain adult tissues, such as thymus, intestine and lung, but is low or absent in the majority of differentiated adult tissues (Zimmerman et al., 1986). The essential role for *c-myc* during development is indicated by data that show that *c-myc* homozygous knockout mice die between days 9.5 and 10.5 of gestation (Davis et al., 1993).

### 1.6.3 *c-myc* and apoptosis

In addition to its role in cell growth, *c-myc* is involved in programmed cell death, or apoptosis. In cells that constitutively expressed *c-myc*, withdrawal of serum resulted in apoptosis, and the extent of apoptosis correlated with the levels of c-Myc protein (Evan et al., 1992). Numerous studies since have confirmed that enforced *c-myc* sensitises various cell types to a range of apoptotic stimuli (Hoffman and Liebermann, 1998). Apoptosis induced by c-Myc is inhibited by survival factors such as insulin-like growth factor 1 (IGF-1), and by the Bcl-2 proteins (Harrington et al., 1994; Wagner et al., 1993). The Fas signalling pathway is necessary for c-Myc-induced apoptosis in fibroblasts, and p53 has also been implicated in this process (Hermeking and Eick, 1994). These observations have led to a model in which c-Myc protein performs two distinct functions. One pathway results in both proliferation and sensitisation to apoptosis, whereas a second pathway is responsible for direct triggering of apoptosis. This second pathway is blocked by cell survival signals (Prendergast, 1999).

Recently, new insights have emerged into c-Myc-mediated apoptosis as it was shown that c-Myc triggered cytochrome *c* release from mitochondria under low serum conditions (Juin et al., 1999). This release occurred before apoptotic morphological changes and was therefore an early event, and was inhibited by the survival factor IGF-1. Accumulation of cytosolic cytochrome *c* was necessary for c-Myc-induced apoptosis, and

was not dependent on p53 or Fas signalling. However, cytosolic cytochrome *c* was only sufficient to sensitise cells to apoptosis and not to induce the process. It is likely that Fas signalling, or p53 activation, would then provide a suitable trigger to induce cell death (Jain et al., 1999). Cytochrome *c* release is induced by translocation of the protein Bax to the mitochondrial membrane, where it creates or alters the function of a membrane pore, and a recent study has shown that c-Myc is necessary for activation of Bax following translocation to the mitochondria (Soucie et al., 2001).

#### 1.6.4 c-Myc protein

Translation of the *c-myc* gene is initiated from an AUG codon towards the 5' end of exon 2 to yield a 64kDa protein (c-Myc 2). A second minor initiation site is an in frame CUG codon near the 3' end of exon 1 and results in a 67kDa version of c-Myc (c-Myc 1) (Hann et al., 1988) (figure 1.10A). A third form of c-Myc, known as c-Myc S, is produced by translation from an internal codon and is 45kDa in size (Spotts et al., 1997). c-Myc is a nuclear protein, and complete localisation is directed by nuclear localisation signal 1 (NLS1), although a second NLS also exists (Dang and Lee, 1988) (figure 1.11A). Phosphorylation of c-Myc is directed by casein kinase II (CKII) in two regions and by a number of kinases in the transactivation domain, but the functional significance of this is unclear (Henriksson and Luscher, 1996).

The N-terminal 143 amino acids of c-Myc contain a transactivation domain (Kato et al., 1990) (figure 1.11A). Two regions within this domain, termed myc homology boxes (MBI and MBII), are highly conserved between Myc proteins. They are important for transactivation, transcriptional repression and transformation by c-Myc, and also direct degradation of Myc via the proteasome (Flinn et al., 1998). A basic region towards the C-terminal of c-Myc allows the protein to directly contact DNA in the promoters of target genes (figure 1.11A). Its recognition sites are the canonical E-box sequence CACGTG and noncanonical variants of this sequence (Prendergast and Ziff, 1991).

A helix-loop-helix leucine zipper (HLH/LZ) motif is present at the C terminal (figure 1.11A) and directs dimerisation of proteins, but c-Myc does not homodimerise. Instead, it forms heterodimers with the protein Max, which shows homology to the C-terminal region of c-Myc but does not possess a transactivation domain (figure 1.11B). Myc/Max heterodimers bind DNA and allow c-Myc to perform its transcription factor

functions (Kato et al., 1993). The importance of Max can be seen from the embryonic lethality of a homozygous Max knockout (Shen-Li et al., 2000). Unlike c-Myc, Max is ubiquitously expressed and stable, so is present in excess. DNA binding by Myc is regulated through a complex network of proteins that possess a bHLH/LZ domain. Max is able to heterodimerise and to bind the Mad-family members (Mad1, Max1, Mad2 and Mad3) and the proteins Myb (Myb1 and Myb2) and Max (Bandino and

### Transactivation domain

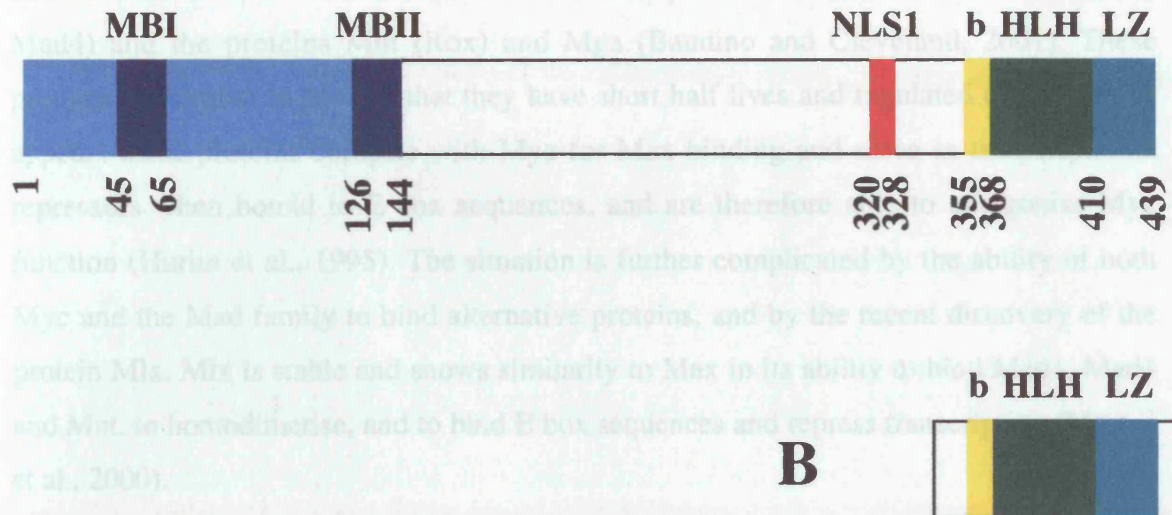


**Figure 1.11 Structure of the Myc and Max proteins.** The domain structure of (A) the Myc proteins and (B) Max is shown. Abbreviations are as follows: MB, Myc homology box. NLS, nuclear localisation signal. b, basic region. HLH, helix-loop-helix. LZ, leucine zipper.

Simultaneous exposure to cells to cyclophosphamide prevents new protein synthesis such that only the expression of direct target genes is affected. However, there are disadvantages to this system and other methods have also been used, such as analysis of binding of c-Myc to a candidate promoter. Expression patterns in c-Myc null cells have also been studied although this allows identification of both direct and indirect targets (Cole and McMahon, 1999).

The various target genes that have been identified provide an insight into the multiple cellular events mediated by c-Myc. Its role in cell cycle progression is supported by its ability to transactivate cyclin E, and probably *cdk2A*, directly, and to repress the

functions (Kato et al., 1992). The importance of Max can be seen from the embryonic lethality of a homozygous Max knockout (Shen-Li et al., 2000). Unlike c-Myc, Max is ubiquitously expressed and stable, so is present in excess. DNA binding by Myc is regulated through a complex network of proteins that possess a bHLH/LZ domain. Max is able to homodimerise and to bind the Mad family members (Mad1, Mxi1, Mad3 and Mad4) and the proteins Mnt (Rox) and Mga (Baudino and Cleveland, 2001). These proteins are similar to Myc in that they have short half lives and regulated expression. It appears these proteins compete with Myc for Max binding and serve as transcriptional repressors when bound to E box sequences, and are therefore able to antagonise Myc function (Hurlin et al., 1995). The situation is further complicated by the ability of both Myc and the Mad family to bind alternative proteins, and by the recent discovery of the protein Mlx. Mlx is stable and shows similarity to Max in its ability to bind Mad1, Mad4 and Mnt, to homodimerise, and to bind E box sequences and repress transcription (Meroni et al., 2000).

### 1.6.5 c-Myc target genes

Identification of the genes directly regulated by c-Myc has proved challenging. It appears that c-Myc is able to transactivate growth-related genes through E boxes, and to transcriptionally repress differentiation-related genes, and that both these functions are necessary for c-Myc-mediated transformation (Dang, 1999). The Myc-ER system is the most accurate method of determining direct c-Myc target genes (Eilers et al., 1991). Myc is fused to the estrogen receptor (ER) and is retained in the cytoplasm until stimulation with its ligand, when it translocates to the nucleus and activates Myc target genes. Simultaneous exposure of cells to cycloheximide prevents new protein synthesis such that only the expression of direct target genes is affected. However, there are disadvantages to this system and other methods have also been used, such as analysis of binding of c-Myc to a candidate promoter. Expression patterns in c-Myc null cells have also been studied, although this allows identification of both direct and indirect targets (Cole and McMahon, 1999).

The various target genes that have been identified provide an insight into the multiple cellular events mediated by c-Myc. Its role in cell cycle progression is supported by its ability to transactivate cyclin E, and probably *cdc25A*, directly, and to repress the

expression of the p27 cyclin-dependent kinase (CDK) inhibitor (Dang, 1999). c-Myc is also able to repress the induction of the growth arrest genes *gadd34*, *gadd45*, and *gadd153* that occurs in response to DNA damage (Amundson et al., 1998). Transactivation of the ornithine decarboxylase (ODC) gene by c-Myc contributes to the DNA metabolism required at G<sub>1</sub>/S phase transition (Bello-Fernandez et al., 1993). A further method by which c-Myc contributes to cell growth is via the activation of various targets involved in translation. These include nucleolin and BN51, which are involved in ribosome biogenesis, eIF4E, and several ribosomal proteins (Greasley et al., 2000; Kim et al., 2000a). Target genes involved in apoptosis are less well characterised. However, a recent study has indicated that the protein caveolin-1 can suppress c-Myc-mediated apoptosis, but its expression is downregulated at the level of transcription by c-Myc (Timme et al., 2000). The E2F transcription factors are targets of c-Myc that allow it to stimulate S phase entry or apoptosis by the activation of different family members (Leone et al., 2001). Finally, microarray analysis has allowed the identification of a number of new c-Myc targets, including eIF4G, and is likely to provide the basis for future elucidation of c-Myc function (Coller et al., 1999; Nesbit et al., 2000).

### 1.6.6 Regulation of *c-myc* expression

The central role of *c-myc* in cell growth and death means that its expression is tightly controlled. The Ras/Raf/MEK/ERK signalling pathway is required for the induction of *c-myc* transcription in response to growth factors, but is not sufficient, indicating that other pathways also contribute to this transcriptional regulation (Cheng et al., 1999). Both *c-myc* mRNA and protein are subject to rapid turnover in cells and further regulation of expression occurs at the levels of mRNA and protein stability (Dani et al., 1984). Heat shock was shown to induce a five- to eight-fold increase in the half-life of c-Myc protein (Lüscher and Eisenman, 1988). *c-myc* transcripts originating from the P0, P1 and P2 promoters possess long, GC-rich 5' UTRs that would be expected to impede cap-dependent translation. A role for translational control in the regulation of *c-myc* expression was first postulated after studies of chromosomal translocations in tumours with deregulated expression revealed that the non-coding exon 1 is frequently lost (Saito et al., 1983).

Activation of the FRAP/mTOR signalling pathway results in a selective stimulation of *c-myc* translation following the dissociation of 4E-BP1 from eIF4E (West et al., 1998).

This is likely to be due to a relief in the inhibition posed to cap-dependent initiation by the highly structured 5' UTR when the levels of active eIF4F increase. A more direct role was identified for the *c-myc* 5' UTR in regulation of translation when it was discovered that it contains a highly active IRES, the characteristics of which are discussed in section 1.5 (Stoneley et al., 1998). Recently, it has been suggested that transcripts originating from the P0 promoter contain an additional IRES that directs translation of a uORF to produce MYCHEX1, a protein of unknown function (Nanbru et al., 2001). An role for the poly(A) tail in the regulation of *c-myc* translation became apparent following treatment with cordycepin, such that short-tailed mRNAs were produced. This caused a decrease in *c-myc* mRNA levels but had no effect on c-Myc protein levels (Ioannidis et al., 1999).

### 1.6.7 Other *myc* genes

Four homologues of the *c-myc* gene have been detected. N- and L-*myc* have been extensively characterised and are discussed in detail below, whereas little is known about s- and B-*myc*. The rat and murine B-*myc* genes have been cloned and show highest expression in the adult brain. B-*myc* contains a single exon that shows homology to *c-myc* exon 2, and encodes a protein similar to the N-terminal region of c-Myc (Asker et al., 1995). B-Myc protein does not possess a region corresponding to the bHLH/LZ domain of c-Myc, and therefore is unable to dimerise or bind DNA. Like c-Myc, B-Myc is a rapidly degraded nuclear phosphoprotein, but it acts as an inhibitor of cellular proliferation, possibly by antagonising c-Myc function (Gregory et al., 2000). The s-*myc* gene was isolated from rat tissue and contains a single exon with homology to the second and third exons of *c-myc* (Sugiyama et al., 1989), but no s-Myc protein has been identified and it is likely that s-*myc* is a pseudogene (Henriksson and Luscher, 1996).

### 1.6.8 N-*myc*

N-*myc* was first identified as a gene with homology to *c-myc* that was amplified in a human neuroblastoma (Schwab et al., 1983). Subsequently, a close association between N-*myc* amplification and neuroblastoma has been established, with greater amplification correlating with an advanced disease state and a poor prognosis (Brodeur et al., 1984). N-*myc* overexpression has also been detected in small cell lung carcinomas, and occasionally in other tumours such as retinoblastomas and breast carcinomas (Nesbit et al., 1999). N-*myc* is able to mediate transformation of cultured cells in a manner analogous to

that of *c-myc* (Schwab et al., 1985). Sequence analysis of the *N-myc* gene revealed considerable similarity to *c-myc*, with a three exon structure of which exon 1 is long, GC-rich and non-coding (Kohl et al., 1986) (figure 1.10B). There are differences between the two genes in terms of length of introns and 3' UTRs, but exons 2 and 3 are very similar in size (Stanton et al., 1986). *N-myc* translation initiation occurs from two alternative AUG codons, both of which are located towards the 5' end of exon 2 (Makela et al., 1989). Translation of *N-myc* yields a protein with 32% identical amino acids to those of *c-Myc*, but many differences are conservative and the regions of identity tend to cluster in domains important for function (Stanton et al., 1986).

The most significant difference between the *N-* and *c-myc* genes is in their pattern of expression. Whereas *c-myc* mRNA and protein are widely distributed during embryogenesis, *N-myc* expression is more restricted. Levels of *N-myc* mRNA were greatest in the embryonic brain, kidney and intestine, and were very low in other tissues. In adult tissues the expression of *N-myc* was switched off (Zimmerman et al., 1986). More detailed analysis of *N-myc* expression during murine embryogenesis indicated a complex variation in mRNA levels according to tissue and developmental stage, with particularly high expression at day 9.5 (Kato et al., 1991). These data imply that an important function of the *N-Myc* protein is in early development. This was confirmed by studies using *N-myc* homozygous knockout mice, which die at day 11.5 and show severe defects, particularly in the nervous system, genitourinary system, lung and gut (Stanton et al., 1992). This study also indicated that *c-* and *N-myc* are rarely coexpressed, and when expressed in the same organ are present in different cell types. It is therefore likely that expression of these two genes is vital for the proliferation of different components of the embryo.

The function of *N-Myc* protein has been studied less extensively than that of *c-Myc*. However, it was inferred from sequence homology that the two proteins were likely to act in a similar manner, and it has subsequently been shown that *N-Myc* forms heterodimers with Max and preferentially binds to the CACGTG motif bound by *c-Myc* (Ma et al., 1993). However, *c-* and *N-Myc* show different specificity of binding to variants of the E box sequence (Prochownik and Van Antwerp, 1993). *N-Myc* expression increased the levels of the *c-Myc* targets  $\alpha$ -prothymosin and ODC, and resulted in accelerated S phase entry (Lutz et al., 1996). The role of *c-Myc* in cell death is also echoed by *N-Myc*, which is able to induce apoptosis in collaboration with interferon  $\gamma$  (IFN $\gamma$ ) (Lutz et al., 1998). *N-*

Myc and c-Myc both induced apoptosis after withdrawal of the survival factor interleukin 3 (IL-3), but showed a different response to cytotoxic drugs, as c-Myc expression sensitised cells to apoptosis induced by these drugs whereas N-Myc expression resulted in drug resistance (Nesbit et al., 1998). A serial analysis of gene expression (SAGE) screen used to identify genes upregulated in N-*myc*-expressing cells revealed a number of target genes involved in ribosome biogenesis and translation. The same process was carried out using c-*myc*-expressing cells, and indicated that 40% of these genes were also targets of c-Myc (Boon et al., 2001). Therefore, although the functions of c- and N-Myc are extremely similar, there are distinctions in their targets. However, a recent transgenic study showed that the N-*myc* coding region under the control of the c-*myc* promoter in c-*myc* null mice allows normal development to occur (Malynn et al., 2000).

N-*myc* expression is subject to regulation by a number of mechanisms. A transcriptional enhancer upstream of the N-*myc* gene was particularly effective in neuroblastoma cells (Imamura et al., 1992). Evidence of post-transcriptional regulation has also been obtained with the observation that the neuronal-specific protein HuD binds to N-*myc* pre-mRNA and is involved in mRNA processing and stability (Chagnovich et al., 1996; Lazarova et al., 1999). Furthermore, a tissue specific element within intron 1 confers post-transcriptional regulation on N-*myc* or heterologous pre-mRNAs, but the mechanism for this regulation is not known (Sivak et al., 1999).

### 1.6.9 L-*myc*

The third well-characterised member of the *myc* family, L-*myc*, is also a proto-oncogene and was detected due to its amplification in a number of small cell lung carcinomas (Nau et al., 1985). However, the expression of L-*myc* is less strongly associated with cancer than that of c- or N-*myc*, and it mediates transformation *in vitro* to a lesser extent than these genes (Birrer et al., 1988). The L-*myc* gene consists of three exons, of which exons 2 and 3 contain the coding region and show homology to the equivalent exons in c- and N-*myc* (Legouy et al., 1987). In contrast to c- and N-*myc*, L-*myc* pre-mRNA molecules are subject to alternative splicing, resulting in a complex array of transcripts. Transcription initiation occurs at a single promoter, but intron 1 is retained in a proportion of mature transcripts so that two different forms of the 5' UTR exist (Kaye et al., 1988) (figure 1.10C). Exon 1 is long and GC-rich, so would be expected to assume a

complex secondary structure, but transcripts in which intron 1 is retained possess longer 5' UTRs that would be even more inhibitory to cap-dependent translation. Some *L-myc* transcripts retain variable portions of intron 2 and terminate at polyadenylation signals within this intron. As these mRNA molecules do not contain exon 3, they do not encode functional L-Myc protein (Kaye et al., 1988).

Translation initiation on both unspliced and spliced *L-myc* transcripts occurs from an AUG codon at the 5' end of exon 2. A second, minor site of initiation is a CUG codon in intron 1 and is therefore only used in the unspliced mRNA molecules (Dosaka-Akita et al., 1991). L-Myc protein structure is similar to that of c- and N-Myc, and L-Myc also dimerises with Max and binds E box sequences, although binding properties to divergent sequences were distinct from the other family members (Ma et al., 1993; Prochownik and Van Antwerp, 1993).

*L-myc* expression is highly restricted in a manner analogous to that of *N-myc*. It is expressed during embryogenesis in the nervous system, kidney and lung, and expression is maintained in the adult lung although not in other adult tissues (Zimmerman et al., 1986). However, *L-myc* homozygous knockout mice were viable, showed no obvious developmental defects, and exhibited normal physiology (Hatton et al., 1996). Therefore it appears that whereas c- and N-Myc proteins are essential for development, L-Myc is dispensable. The effect of *L-myc* expression on cell growth showed differences to that of *c-myc*, as constitutive expression of *L-myc* during lens maturation directly affected differentiation, whereas *c-myc* inhibited proliferative arrest but did not affect differentiation (Morgenbesser et al., 1995). L-Myc shows apoptotic behaviour that is similar to that of N-Myc, but distinct from that of c-Myc, in that it promotes apoptosis in response to IL-3 withdrawal but confers resistance to cytotoxic drugs (Nesbit et al., 1998).

When a complex expression library was screened for genes able to restore proliferation to *c-myc* null cells, the only gene detected was *N-myc* (Nikiforov et al., 2000). This supports the previous observation that *N-myc* can functionally replace *c-myc*, but suggests that *L-myc* cannot do so. This provides further evidence that, although L-Myc shows considerable similarity to the other Myc proteins, it is less potent in its function and is not essential to cells.

## **Chapter 2**

### **Materials and methods**

#### **2.1 General Reagents**

Unless otherwise stated all chemical reagents were of analytical grade and were obtained from BDH laboratory supplies (Lutterworth, Leicestershire), Fisher Scientific (Loughborough, Leicestershire), ICN Flow Ltd (Thame, Oxfordshire), Sigma Chemical Company Ltd (Poole, Dorset) or Oxoid (Unipath, Basingstoke, Hampshire). Products for molecular biological techniques were routinely purchased from Calbiochem (c/o CN Biosciences UK, Beeston, Nottingham), Gibco-BRL (Paisley, Scotland), MBI Fermentas (c/o Helena Biosciences, Sunderland, Tyne and Wear), New England Biolabs (NEB) (c/o CP Labs, Bishops Cleeve, Hertfordshire), Pharmacia Biotech (Milton Keynes, Buckinghamshire), Promega (Southampton), QIAGEN (Crawley, West Sussex), Roche UK Ltd (Lewes, East Sussex) and Stratagene Ltd (Cambridge). Radiolabelled chemicals were purchased from Amersham International (Little Chalfont, Buckinghamshire) and NEN Dupont (Hounslow).

#### **2.2 Tissue Culture Techniques**

##### **2.2.1 Tissue culture media and supplements**

DMEM medium: Dulbecco's modified eagle medium, without sodium pyruvate (Gibco-BRL).

F-12 medium: Ham's F-12 nutrient mixture medium (Gibco-BRL)

MEM medium: Minimal essential medium (Sigma)

RPMI 1640 medium: Rose Park Memorial Institute 1640 medium, with L-glutamine (Gibco-BRL).

Media were supplemented with foetal calf serum (FCS) (Helena Biosciences), horse serum (Gibco-BRL), L-glutamine (Sigma) and non-essential amino acids (NEAA) (Sigma) as indicated in table 2.1.

Cell line	Origin	Growth medium
<b>Balb/c 3T3</b>	Murine embryonic fibroblast	DMEM + 10% FCS
<b>CHO-T</b>	Chinese hamster ovary T-cells	F-12 + 10% FCS
<b>COS 7</b>	Monkey epithelial cells immortalised with SV40 DNA	DMEM + 10% FCS
<b>HEK 293</b>	Human embryonic kidney	DMEM + Glutamax + 10% FCS
<b>HeLa</b>	Human cervical carcinoma	DMEM + 10% FCS
<b>HL60</b>	Human promyelocytic leukaemia	RPMI +15% FCS
<b>IMR32</b>	Human neuroblastoma	DMEM + 10% FCS
<b>MCF7</b>	Human breast carcinoma	DMEM + Glutamax + 10% FCS
<b>MEL</b>	Murine erythroleukaemia	RPMI + 15% FCS
<b>N2a</b>	Murine neuroblastoma	MEM + 10% FCS + 2mM L-glutamine +1% NEAA
<b>NB2a</b>	Murine neuroblastoma	DMEM + 5% FCS + 5% horse serum + 2mM L-glutamine
<b>NIE-115</b>	Murine neuroblastoma	DMEM + 10% FCS + 2mM L-glutamine
<b>NT2</b>	Human teratocarcinoma	DMEM/F-12 (1:1) + 10% FCS + 2mM L-glutamine
<b>PC-12</b>	Rat neuroblastoma	DMEM + 5% FCS + 5% horse serum + 2mM L-glutamine
<b>SH-SY5Y</b>	Human neuroblastoma	DMEM +Glutamax/F-12 (1:1) + 10% FCS

**Table 2.1** Name and tissue origin of cell lines used. Cells were grown in the medium indicated as detailed in section 2.2.2.

### 2.2.2 Maintenance of cell lines

The cell lines in table 2.1 were cultured in the growth medium indicated in sterile plasticware (TPP, c/o Helena Biosciences). Adherent cell lines were grown to confluence in 75cm<sup>2</sup> flasks and treated with 1x trypsin/0.5mM EDTA (Gibco BRL). Approximately 1x10<sup>6</sup> cells were diluted into fresh medium and replated into a new flask. Cells grown in suspension were maintained at concentrations of 5x10<sup>5</sup>-1x10<sup>6</sup> cells/ml. All cells were grown at 37°C in a humidified atmosphere containing 5% CO<sub>2</sub>.

### 2.2.3 Maintenance of ES cells

The ES cell lines L (unr +/+), A (unr -/-) and B (unr -/-) were cultured in DMEM + Glutamax supplemented with 15% FCS, 0.00125% monothioglycerol, and 5.6µl/ml LiF, and the medium was changed daily. Cells were grown at 37°C in a humidified atmosphere containing 5% CO<sub>2</sub> on a layer of feeder cells. Following trypsin treatment, cells were applied to a gelatinised plate for 1 hour such that feeder cells entered the gelatin. ES cells remained in the supernatant and were separated and grown on gelatinised 6-well plates for transfection.

### 2.2.4 Calcium phosphate-mediated DNA transfection

Calcium phosphate-mediated DNA transfection of mammalian cells were performed essentially as described in (Jordan et al., 1996) with minor modifications. Approximately 24 hours before transfection,  $1 \times 10^5$  cells were seeded onto a 6-well plate in 2ml of complete medium. A solution of 10µl of 2.5M CaCl<sub>2</sub> and 1-1.5µg of plasmid DNA was diluted with sterile deionised water to a final volume of 100µl. An equal volume of 2x HEPES buffered saline (50mM HEPES, pH7.05, 1.5mM Na<sub>2</sub>HPO<sub>4</sub>, 140mM NaCl) was added to this solution whilst bubbling air through the mixture. The calcium phosphate-DNA co-precipitate was allowed to form for 5 min and was then added to the medium covering the cells in a dropwise manner. After exposing the cells to the precipitate for 15-20 hours at 37°C, the medium was removed and the cells were washed twice with phosphate buffered saline (PBS) (4.3mM Na<sub>2</sub>HPO<sub>4</sub>, 1.5mM KH<sub>2</sub>PO<sub>4</sub>, 137mM NaCl, 2.7mM KCl, pH 7.4). Subsequently, fresh medium was added and the cells were grown for a further 24 hours before harvesting.

### 2.2.5 FuGENE 6-mediated DNA transfection

Cells were seeded as for calcium phosphate-mediated transfection. 3µl of FuGENE 6 transfection reagent (Roche) was added directly to 100µl of serum-free DMEM and incubated at room temperature for 5 min. This mixture was added in a dropwise manner to a solution containing 1-1.5µg of plasmid DNA and incubated at room temperature for a further 15 min, then added to the medium covering the cells. Cells were grown for a further 48 hours before harvesting.

### 2.2.6 DEAE-Dextran-mediated transfection

Approximately 24 hours before transfection,  $1 \times 10^6$  COS 7 cells were seeded onto a 10cm plate in 10ml of complete medium. The medium was aspirated and replaced with serum-free DMEM and the cells were returned to 37°C. A mixture of 3.2ml of serum-free DMEM, 0.8ml of 0.25M Tris-HCl, pH7.5 and 0.5ml of 10mg/ml Dextran was assembled. 1-10µg of plasmid DNA was added to this and the medium was aspirated from the cells and replaced with the mixture. The cells were incubated at 37°C for 20 min. Chloroquine was added to the mixture covering the cells to a final concentration of 40µg/ml, and the cells were incubated at 37°C for 3-4 hours. The medium was aspirated and the cells were washed twice with PBS. Fresh complete medium was added and the cells were harvested after growing for a further 48 hours.

### 2.2.7 Cationic liposome-mediated RNA transfection

Cationic liposome-mediated RNA transfection of mammalian cells was performed as described by (Dwarki et al., 1993). Capped and polyadenylated transcripts were synthesised using *in vitro* run-off transcription (section 2.5.5) on an *Eco*RI-linearised pSP64R(x)LpA template. Approximately  $2 \times 10^5$  HeLa cells were seeded onto a 6-well plate in 2ml of complete medium. The cells were transfected as they approached confluence. The medium was aspirated and replaced with Opti-MEM I reduced serum medium (Gibco-BRL), and the cells were returned to 37°C. 12.5µg of lipofectin (Gibco-BRL) was added to 1ml of Opti-MEM I medium and incubated at room temperature for 20 min. 5µg of RNA was added directly to the media-lipid mixture and the solution was mixed. After a further incubation of 10 min at room temperature the Opti-MEM I medium was removed from the cells and replaced with the media-lipid-RNA solution. Finally, the cells were returned to the 37°C incubator and harvested after 8 hours.

### 2.2.8 Induction of apoptosis and physiological stress

His-tagged TRAIL was synthesised from the plasmid pET28b (a gift of Dr Marion MacFarlane, University of Leicester). Apoptosis was induced by the application of 0.25µg/ml TRAIL or 1µM staurosporine in fresh medium to HeLa cells. To inhibit p38MAPK activity, SB203580 was applied to cells at a concentration of 50µM 1 hour prior to TRAIL treatment.

Heat shock was induced by removing the medium from cells and replacing it with fresh medium pre-warmed to 44°C in a waterbath. Cells were then placed in a 44°C oven for 30 minutes, then returned to 37°C.

To send cells into G<sub>0</sub> phase, the medium was removed and replaced with serum-free medium after washing three times with PBS. Cells were grown in this medium for 24 hours, after which G<sub>0</sub>-G<sub>1</sub> transition was induced by replacement with fresh complete medium.

Osmotic shock was induced by the addition of 0.3M sorbitol in complete medium to cells, which were then grown at 37°C for 30 minutes. This medium was then removed, the cells were washed three times with PBS, and fresh complete medium was added before returning the cells to 37°C.

## 2.3 Bacterial Techniques

### 2.3.1 Bacterial media and supplements

**LB medium:** 10g Bacto-tryptone, 5g bacto-yeast extract, 10g NaCl dissolved in 1l of deionised water.

**LB agar plates:** 1l LB medium supplemented with 15g of agar.

**Ampicillin:** a stock solution of 50 mg/ml of the sodium salt of ampicillin was prepared using sterile deionised water and used at a final concentration of 50µg/ml.

### Bacterial strains

The *Escherichia coli* strains JM109 (Yanisch-Perron et al., 1985) and DH5α (Hanahan, 1983) were used in bacterial manipulations.

### 2.3.2 Preparation of competent cells

A single colony from an LB agar plate was inoculated into 2.5ml of LB medium and incubated overnight at 37°C with shaking. The entire overnight culture was inoculated into 250ml of LB medium supplemented with 20mM MgSO<sub>4</sub> and incubated at 37°C until the A<sub>595</sub> reached 0.4-0.6. Cells were pelleted by centrifugation at 4,500x g for 5 min at 4°C using a GSA rotor (Sorvall). The pellet was gently resuspended in 100ml of ice-cold filter sterile TFB1 (30mM KAc, 10mM CaCl<sub>2</sub>, 50mM MnCl<sub>2</sub>, 100mM RbCl, 15% glycerol, adjusted to pH 5.8 with 1M acetic acid). After incubating on ice for 5 min, the cells were

centrifuged at 4,500x g for 5 min at 4°C. The pellet was resuspended in 10 ml of ice-cold filter sterile TFB2 (1 mM MOPS, 75mM CaCl<sub>2</sub>, 10mM RbCl, 15% glycerol, adjusted to pH 6.5 with 1M KOH) and incubated on ice for 1 hour. Finally, the cells were rapidly frozen in an isopropanol/dry ice bath in 200µl aliquots and stored at -70°C.

### 2.3.3 Transformation of competent cells

Ligation products or plasmid DNA (10ng) were added to 50µl of competent cells and incubated on ice for 20 min. After heating the mixture at 42°C for 1 min, 150µl of LB medium was added. Subsequently, the cells were incubated with shaking at 37°C for 45 min. The sample was then spread onto a pre-warmed LB agar plate containing ampicillin and incubated at 37°C for 16-20 hours.

## 2.4 Molecular Biological Techniques

### 2.4.1 Buffers and solutions

**TE:** 10mM Tris-HCl pH8.0, 1mM EDTA

**1xTAE:** 40mM Tris, 40mM acetic acid, 1mM EDTA, pH 8.0

**1x TBE:** 89mM Tris, 89mM boric acid, 2.5mM EDTA, pH 8.0

**5x TBE loading buffer:** 50% v/v glycerol, 200mM Tris, 200mM acetic acid, 5mM EDTA, 0.1% Bromophenol lue, 0.1% Xylene cyanol FF

**DNA formamide loading dyes:** 100% deionised formamide, 0.1%(w/v) Xylene cyanol FF, 0.1%(w/v) Bromophenol blue, 1mM EDTA

### 2.4.2 Plasmids used

pGL3', pGML, pRF, pRMF, pRemcvF,phpRMF, pSP64RLpA, pSP64RMLpA, pSP64RhrvLpA (all described in (Stoneley et al., 2000b)

pSKL, pSKML (Stoneley, 1998)

pSKGAP:E/H (Paulin, 1997)

pBluescript II SK (+) (Stratagene)

pcDNA3 (Invitrogen)

pcDAP5, pceIF4G, pcITAF45, pcLa, pcPCBP1, pcPCBP2, pcPTB, pcunr (synthesised by Joanne Evans)

MKK6WT, MKK6GLU (a gift of Dr Martin Dickens, University of Leicester)

pJ7lacZ (a gift of Dr David Heery, University of Leicester)

#### **2.4.3 Determination of nucleic acid concentration**

The concentration of DNA, RNA or oligonucleotides was determined by measuring the optical density of a solution at 260nm.

#### **2.4.4 Ethanol precipitation of nucleic acids**

Nucleic acids were precipitated by the addition of 0.1 volume of 3M sodium acetate, pH5.2 and 2.5 volumes of absolute ethanol. The sample was incubated at  $-20^{\circ}\text{C}$  for 15-30 min, following which the nucleic acid was pelleted by centrifugation at 12,000x g for 10 min. Excess salt was removed from the pellet by washing with 70% ethanol, then the nucleic acid was dried briefly and resuspended in either TE or sterile deionised water.

#### **2.4.5 Phenol/chloroform extraction**

Solutions of nucleic acid were separated from contaminating proteins by the addition of an equal volume of phenol:chloroform:isoamyl alcohol (25:24:1). After vigorous mixing, the phases were separated by centrifugation at 12,000x g for 5 min. The upper aqueous phase was removed to a separate tube, to which an equal volume of chloroform:isoamyl alcohol (24:1) was added. Following extraction and separation of the phases, the aqueous layer was transferred to a new tube and the nucleic acid was precipitated.

#### **2.4.6 Agarose gel electrophoresis**

Fragments of DNA or RNA were fractionated according to their molecular weight by electrophoresis through agarose gels. Agarose was melted in 1x TBE buffer and cooled, after which 2 $\mu\text{l}$  of 10mg/ml ethidium bromide was added to the agarose solution and the gel was cast in a suitable support. The set gel was submerged in 1x TBE buffer in a horizontal electrophoresis tank. Samples were mixed with 0.2 volume of 5x TBE loading buffer and separated in the gel at up to 8V/cm. After electrophoresis, the nucleic acid was visualised on a UV transilluminator.

#### **2.4.7 Gel isolation of DNA fragments**

DNA fragments were separated by agarose gel electrophoresis as described, except the gel was prepared and submerged in 1x TAE. Agarose containing the required fragment was excised from the gel.

#### **2.4.8 Purification of DNA using Qiaquick columns**

The Qiaquick gel extraction kit (Qiagen) was used to isolate DNA from agarose gel fragments or to purify DNA fragments. The manufacturer's protocols were followed and the DNA was eluted from the column in 30µl of sterile deionised water.

#### **2.4.9 Oligonucleotides**

Oligonucleotides were purchased from the Protein and Nucleic Acid Chemistry Laboratory (University of Leicester), Gibco BRL or Sigma Chemical Company. After ethanol precipitation where necessary, oligonucleotides were resuspended in sterile deionised water. Details of the oligonucleotides employed are given in Table 2.2.

#### **2.4.10 Polymerase chain reaction (PCR)**

Standard PCR reactions were performed in a final volume of 50µl containing 1x *Pfu* reaction buffer (Stratagene), 1M Betaine, 5% DMSO, 2ng of template DNA, 200ng of both the upstream and downstream primers, 400µM of each dNTP and 2.5 units of *PfuTurbo* DNA polymerase (Stratagene). Reactions were performed in a Techne Genius Thermal Cycler. DNA was initially denatured by heating at 94°C for 3 min, after which the samples were heated at 94°C for 30 s (denaturation), primer  $T_m$  -5°C for 30-150 s (annealing) and 72°C for 60-90 s (extension), respectively, for 25-35 cycles, followed by a final extension at 72°C for 7 min.

#### **2.4.11 RT-PCR**

To amplify DNA using single-stranded DNA obtained from total cellular RNA by reverse transcription (RT) as detailed in section as a template, 10µl of the RT reaction was used in a standard PCR reaction. The concentrations of reaction components were adjusted to take account of those already present.

The highly GC-rich *N-myc* 5' UTR was amplified using the *C. therm.* Polymerase One-Step RT-PCR System (Roche). The reaction was performed in 50µl total volume

containing 1x *C. therm* reaction buffer, 1M Betaine, 5%DMSO, 5mM DTT, 20 units of RNasin (Promega), 400 $\mu$ M dNTPs, 300ng of each primer, 100pg of poly(A)<sup>+</sup> RNA and 2 $\mu$ l of *C. therm* polymerase mixture. Reverse transcription was carried out at 65°C for 30 min and was immediately followed by a standard PCR as detailed in section 2.4.10.

Oligonucleotide name	Sequence
AUG1F	GGGGCTCCTGGGAAATGGGTTGGAGCCGAG
AUG1R	CTCGGCTCCAACCCATTTCCCAGGAGCCCC
AUG2F	TAGCCATCCGAGGATGGCCCCGCCCCCGG
AUG2R	CGGGGGGGCGGGGCCATCCTCGGATGGCTA
AUG3F	GTCGGCGGGAGTGATGGAGGTCGGCGCCGG
AUG3R	CCGGCGCCGACCTCCATCACTCCCGCCGAC
AUG4F	AACGGGGCGGAAAGATGGCCTCAGTCGCCG
AUG4R	CGGCGACTGAGGCCATCTTTCGCCCCGTT
AUG5F	CGAGCCGATGCCGAGATGGTCCACGTCCAC
AUG5R	GTGGACGTGGACCATCTCGGCATCGGCTCG
BRNaseF	GTGGATCCGCAAGAAGATGCAGATG
CJNF	AGGAATTCGTCTGGACGCGCTGGGTGGATGCGGG
H3LUC3'	ATAAGCTTGCATATCTTTCATAGCCTT
LF2	TGGAATTCAATGCGCCTGCAGCTCGCGCTCCC
LG2	GTCCATGGCCGTTCCGTGCGGGAGGGAAGG
LR2	GTCCATGGCCGCTCCCTCGCTCCAGCCGCC
LUC3'	GCGTATCTTTCATAGCCTT
MmycF	CTACTAGTCGCTGTAGTAATTCCAGCG
MmycR	CATGCCATGGTCGTGGCTGTCTGC
NF1	ATCTGTCTGTACGCGCTGGGTGGATGCGGG
NFA	GCGGAATTCCTGTAGCCATCCGAG
NFB	GCCGAATTCTCCCCTGCAGTCGGC
NFC	CCCGAATTCAAAACGAACGGGGCG
NGR	AGGGCTGTAGCGAGTCAAACCTGCAGGTCTG
NmycUTRR	TTTCCATGGTGGACGTGGAGCAGC
NRA	TGGCCATGGTCTGTGCGCGCTTGC
NRB	TGCCCATGGTCCGGAGGCGATTCT
NRC	GTCCATGGAATACGGGGGGTGCT
NRD	CTCGCCATGGGCTCGCCTCCCGGC
NRE	TGGCCATGGAGCAGCTCGGCATCG
NREXT	TCCGCCATGGAGCAGGGCTGTAGCGAGTCA
NRUUG	TCTTCCATGGTGGGACGTGGAGCAGCTCGGCAAC
NSPEF	CTGGAAGTCTGGACGCGCTGG
RNaseF	GCAAGAAGATGCACCTGATG

**Table 2.2** Sequences of oligonucleotides employed.

#### 2.4.12 PCR mutagenesis

Mutagenic PCR was carried out in a 50 $\mu$ l total volume containing 1x *Pfu* reaction buffer, 200 $\mu$ M of each dNTP, 250ng wild-type template DNA, 125ng of each mutagenic primer and 2.5 units of *PfuTurbo* DNA polymerase. The reaction was heated to 95°C for 30s, then incubated at 95°C for 30 s, (primer  $T_m$ -5)°C for 2 min and 68°C for 11 min for 18 cycles, followed by cooling on ice. A 5 $\mu$ l sample was subjected to agarose gel electrophoresis to confirm the integrity of the reaction products before treating the remainder of the reaction mixture with 1 $\mu$ l of T4 DNA ligase for 2-4 h at room temperature. This was inactivated by heating at 65°C for 10 min, then template DNA was digested by treatment with 10 units of *Dpn* I for 1-2 h. 5 $\mu$ l of the reaction products were then used to transform competent *E. coli*.

Alternatively, two mutagenic half reactions were carried out, amplifying the regions of the N-*myc* 5' UTR 5' and 3' of the mutation using the primer pairs CJNF/ mutant reverse primer, and mutant forward primer/ NmycUTRR. The resultant products were gel isolated and 1 $\mu$ l of a 1/500 dilution of both was used as the template in a third PCR reaction using the primers CJNF and NmycUTRR. The mutant N-*myc* 5' UTR obtained by this reaction was digested with *Eco* RI and *Nco* I and inserted into the vector pRF.

#### 2.4.13 Restriction enzyme digestion

DNA was digested with restriction enzymes in a total volume of 10-50 $\mu$ l under the conditions recommended by the suppliers. Reactions were incubated at the appropriate temperature for 1-2 hours.

#### 2.4.14 Filling in recessed 3' ends

The large (Klenow) fragment of *E. coli* DNA polymerase I was used to fill in the recessed 3' ends of DNA fragments. The reaction was performed in a final volume of 25 $\mu$ l, containing 80 $\mu$ M of each dNTP, a maximum of 2 $\mu$ g of DNA and 1x Fill-in buffer (Amersham) or 1x restriction enzyme buffer supplemented with 100 $\mu$ g/ml of BSA. 1-5 units of Klenow DNA polymerase were added and the reaction was incubated at 30°C for 15 min, then stopped by heating at 65°C for 10 min.

#### **2.4.15 Alkaline phosphatase treatment of DNA**

Linearised plasmids were treated with calf intestinal alkaline phosphatase (CIAP) to remove a phosphate group from the 5' ends and prevent self-ligation. Following restriction digestion, the restriction enzyme was inactivated by heating the reaction at 65°C for 10 min. Dephosphorylation was performed in a final volume of 50µl in 1x restriction enzyme buffer, using 1 unit of CIAP. The reaction was incubated for 30 min at 37°C for DNA fragments with overhanging 5' ends, and incubated at 37°C for 15 min followed by 56°C for 15 min for DNA fragments with blunt ends. Another unit of enzyme was then added and the incubation was repeated. The reaction was terminated by heating at 75°C for 10 min and the DNA was purified. For those restriction enzymes that are resistant to heat-inactivation, the DNA was purified following digestion and resuspended in 50µl of 1X CIAP reaction buffer (MBI Fermentas). The reactions were then performed as described above.

#### **2.4.16 Phosphorylation of nucleic acids using T4 polynucleotide kinase**

Blunt-ended DNA fragments that were used in ligations were first treated with T4 polynucleotide kinase (T4 PNK) to add a 5' terminal phosphate group. Restriction enzymes were inactivated by heating at 65°C for 10 min prior to treatment. Reactions were performed in a final volume of 50µl containing 1x restriction enzyme buffer, 100µM ATP and 10 units of T4 PNK and incubated at 37°C for 30 min. The kinase reaction was terminated by heating at 75°C for 10 min.

#### **2.4.17 Ligations**

Ligations were performed in a total volume of 10µl. Vector DNA (50ng) was mixed in a 1:3 molar ratio with insert DNA in a reaction containing 1x T4 DNA ligase buffer (MBI Fermentas) and 2.5 units of T4 DNA ligase. The reaction was incubated at 16°C for 2-16 hours, after which 5µl of the ligation reaction was used to transform competent *E.coli*.

#### **2.4.18 Small scale preparation of plasmid DNA**

A single colony of *E.coli* was inoculated into 5ml of LB media containing ampicillin and incubated at 37°C for 12-16 hours with shaking. Approximately 1.5ml of the culture

was decanted into a labelled tube and the bacteria were pelleted by centrifugation at 12,000x g for 1 min. The pellet was resuspended in 100µl of ice-cold solution I (25mM Tris-HCl, 10mM EDTA, 50mM Glucose, pH 8.0). After a 5 min incubation on ice, 200µl of solution II (1% SDS, 0.2M NaOH) was added and the solutions were mixed gently. The sample was incubated on ice for 5 min, following which 150µl of solution III (5M potassium acetate pH4.8) was added. After briefly mixing the solutions, the sample was incubated on ice for a further 5 min. The precipitated matter was pelleted by centrifugation at 12,000x g for 5 min and the supernatant was removed to a fresh tube. Plasmid DNA was precipitated from this solution by the addition of 0.6 volumes of isopropanol, followed by centrifugation and ethanol washing as described in section. The pellet was dried and resuspended in 30µl of 1x TE buffer. Diagnostic restriction digests were performed using 5µl of this solution.

#### **2.4.19 Large scale preparation of plasmid DNA**

To prepare milligram quantities of plasmid DNA, an overnight culture of *E. coli* containing the plasmid was inoculated into 250mls of LB media supplemented with ampicillin. The culture was grown for 12-16 hours in a 37°C shaking incubator. Cells were harvested by centrifugation at 5,000x g for 10 min at 4°C. The pellet was resuspended in 6ml of ice-cold solution I and incubated on ice for 5 min. 12ml of solution II was then added and the sample was incubated on ice for 5 min. This solution was neutralised with 9ml of 7.5M NH<sub>4</sub>Ac, pH7.6 and incubated for a further 10 min on ice prior to centrifugation at 10,000x g for 10 min at 4°C and the supernatant was removed to a fresh tube. Isopropanol (0.6 volumes) was added and the solution was incubated at room temperature for 10 min, then subjected to centrifugation (10,000x g) for 10 min at room temperature. The plasmid DNA in the pellet was resuspended thoroughly in 2M NH<sub>4</sub>Ac, pH7.4. The insoluble matter was pelleted as before and the supernatant removed to a fresh tube. After the addition of 1 volume of isopropanol, the solution was incubated at room temperature for 10 min and the plasmid DNA was pelleted by centrifugation. The pellet was resuspended in 1ml of sterile deionised water and contaminating RNA was removed by the addition of 100µg of RNase A and incubation at 37°C for 30 min. 0.5 volume of 7.5M NH<sub>4</sub>Ac, pH7.6 was added and the solution was incubated at room temperature for 5 min. The precipitated proteins were pelleted by centrifugation and the supernatant was

removed to a fresh tube. Finally, the plasmid DNA was precipitated using 1 volume of isopropanol, pelleted by centrifugation and washed with 70% ethanol. The resulting pellet was resuspended in a volume of 0.5-1ml of TE.

#### **2.4.20 Caesium chloride gradient purification of plasmid DNA**

To prepare DNA suitable for transfection, further purification was carried out on a CsCl<sub>2</sub> gradient. Plasmid DNA was resuspended in 2ml of TE, into which 2.5g of CsCl<sub>2</sub> were subsequently dissolved. This solution was transferred to a 3.5ml polyallomer tube and supplemented with 1mg of ethidium bromide. If necessary, additional TE was added to give a final volume of 3.5ml. The tube was sealed and subjected to centrifugation in a Sorvall Ti270 rotor at 100,000 rpm for 16 hours at 20°C. The supercoiled plasmid DNA was removed from the gradient using a syringe and separated from the ethidium bromide by repeated extraction with an equal volume of CsCl<sub>2</sub>-saturated isopropanol (ITC). The aqueous solution was diluted with 2 volumes of deionised water and the plasmid DNA was precipitated by the addition of an equal volume of isopropanol and 0.1 volume of 3M NaAc, pH5.2. After centrifugation at 12,000x g for 10 min the pellet was resuspended in 0.5ml of deionised water and plasmid DNA was ethanol precipitated as described previously. The final pellet was resuspended in 0.25-1ml of 1x TE.

#### **2.4.21 Large scale preparation of DNA by Qiagen column**

Alternatively, DNA suitable for transfection was obtained from a 100ml overnight culture of *E. coli* by the Qiagen midiprep procedure, according to the manufacturer's protocols.

#### **2.4.22 Double stranded DNA sequencing**

Plasmid DNA was isolated using the small scale method and contaminating RNA was digested with 1µg of RNase A at 37°C for 30 min. The DNA was then ethanol precipitated and resuspended in 10µl of sterile deionised water and denatured by incubating with 0.1 volumes of 2mM NaOH, 2mM EDTA, pH8.0 at 37°C for 15 min. The solution was then neutralised with 0.1 volumes of 7.5M NH<sub>4</sub>Ac, pH7.4, and 1 volume of isopropanol was added. Following incubation at room temperature for 10 min, the single stranded DNA was pelleted by centrifugation at 12,000x g for 10 min and air-dried. The pellet was resuspended in 10µl of a 5ng/µl solution of sequencing primer and 2µl of

annealing buffer (280mM Tris-HCl, pH7.5, 100mM MgCl<sub>2</sub>, 350mM NaCl). This solution was heated at 65°C for 2 min, then incubated at room temperature for 10 min and on ice for 5 min to achieve primer annealing. Samples were labelled at 20°C for 5 min, in a reaction containing 0.4µl [ $\alpha$ -<sup>35</sup>S] dATP (12.5mCi/ml), 3µl of labelling mix A (2µM dGTP, 2µM dCTP, 2µM dTTP), and 1 unit of T7 DNA polymerase. Labelling was terminated by the addition of 2.5µl of each termination mix (150µM dNTPs, 10mM MgCl<sub>2</sub>, 40mM Tris-HCl, pH 7.5, 50mM NaCl, 15µM ddNTP G, A, T, or C) and incubation at 37°C for 5 min. Finally, the reaction was stopped by adding 4µl of DNA formamide loading dyes. The labelled DNA fragments were fractionated on a 6% polyacrylamide/7M urea gel, following which the gel was dried for 1 hour at 80°C and exposed to x-ray film (Fuji) for 16-48 hours.

#### 2.4.23 Radiolabelled DNA markers

1 µg of pBR322 DNA was digested with 5 units of *Hpa*II for 20 min in a volume of 10 µl and the reaction was stopped by heating at 90°C for 2 min. The DNA fragments were radiolabelled using the Klenow fragment of *E. coli* DNA polymerase I in a reaction volume of 15µl containing 1x restriction buffer, 100 µg/ml of BSA, 1mM dCTP, 10µCi of [ $\alpha$ -<sup>32</sup>P] dCTP (800 Ci/mmol) and 5 units of Klenow DNA polymerase. The reaction was incubated at 30°C for 15 min and stopped by the addition of RNA formamide loading buffer.

## 2.5 RNA Techniques

### 2.5.1 Buffers and solutions

**RNA formamide loading buffer:** 80% deionised formamide, 10mM EDTA, 0.1% SDS, 0.1% Xylene cyanol FF, 0.1% Bromophenol blue

**RNA formaldehyde loading buffer:** 50% glycerol, 1mM EDTA, 0.4% Bromophenol blue, 0.4% Xylene cyanol FF

All solutions used for RNA were subjected to purification through a 0.2µm filter prior to use, unless purchased sterile.

### **2.5.2 Isolation of total cellular RNA**

Total cellular RNA was isolated using TRI Reagent (Sigma).  $5-10 \times 10^6$  suspension cells were pelleted by centrifugation at  $1000 \times g$  for 5 min, washed with PBS and lysed by resuspension in 1ml of TRI Reagent and incubation at  $20^\circ\text{C}$  for 5 min. Adherent cells were washed with PBS and treated with 1ml of TRI Reagent *in situ* and lysates were removed with a cell scraper and transferred to a fresh tube.  $200 \mu\text{l}$  of chloroform was added to the lysate and the mixture was vigorously mixed using a vortex for at least 30 s, followed by centrifugation at  $12,000 \times g$  for 15 min. The upper aqueous phase was transferred to a fresh tube and an equal volume of isopropanol was added to this solution. The sample was incubated at room temperature for 10 min and the precipitated RNA was pelleted by centrifugation at  $12,000 \times g$  for 15 min and washed with 75% ethanol. After briefly drying the pellet, it was resuspended in  $100 \mu\text{l}$  of TE and stored at  $-80^\circ\text{C}$ .

### **2.5.3 Purification of poly(A)<sup>+</sup> mRNA from total cellular RNA**

Poly(A)<sup>+</sup> mRNA was purified from total cellular RNA using oligo[dT]<sub>25</sub> magnetic DynaBeads (DynaL Inc.). The manufacturer's protocols were followed, except that  $50 \mu\text{l}$  of oligo[dT]<sub>25</sub> beads were used to isolate poly(A)<sup>+</sup> RNA from  $50 \mu\text{g}$  of total RNA. Isolated RNA was stored at  $-80^\circ\text{C}$  and beads were reconditioned according to the manufacturer's instructions and stored at  $4^\circ\text{C}$ .

### **2.5.4 Reverse transcription of total cellular RNA**

Cellular RNA was isolated by the method described previously and  $1 \mu\text{g}$  was combined with  $0.5 \mu\text{g}$  of random hexanucleotides in a total volume of  $15 \mu\text{l}$  in filter sterile deionised water. The sample was heated at  $70^\circ\text{C}$  for 5 min and then incubated on ice for 5 min. The reaction volume was made up to  $25 \mu\text{l}$  containing 1x Superscript reaction buffer (Gibco-BRL), 0.4mM dNTPs, 40 units of RNasin and 30 units of Superscript reverse transcriptase (Gibco-BRL). This solution was incubated at  $37^\circ\text{C}$  for 1 hour to allow reverse transcription to occur. The enzyme was inactivated by heating at  $95^\circ\text{C}$  for 5min. The sample was either used immediately to amplify a DNA fragment or stored at  $-20^\circ\text{C}$ .

### **2.5.5 *In vitro* run-off transcription**

$10 \mu\text{g}$  of vector DNA was linearised by restriction digestion using a site downstream of the sequence of interest. Subsequently, the protein was removed by phenol/chloroform

extraction and, following ethanol precipitation, the DNA was resuspended in 10 $\mu$ l of filter sterile deionised water. To synthesise uncapped transcripts, a reaction was assembled containing 1x Transcription buffer (MBI Fermentas), 10mM DTT, 20 units of RNasin, 0.5mM of each NTP, 1 $\mu$ g of DNA template, and 20 units of T7, T3, or SP6 RNA polymerase in a final volume of 50 $\mu$ l. After incubation at 37°C for 1 hour, a further 10 units of RNA polymerase were added and the sample was incubated at 37°C for 30 min. The DNA template was then digested with 10 units of RNase-free DNase I for 15 min at 37°C. Immediately after digestion, the RNA was phenol/chloroform extracted and unincorporated nucleotides were removed by passing the solution through a Sephadex G-50 column. The RNA was precipitated by the addition of 0.5 volume of 7.5M NH<sub>4</sub>Ac and 2.5 volumes of ethanol. After incubation at -70°C for 30min, the RNA was pelleted by centrifugation and washed with 75% ethanol. The pellet was resuspended in 30 $\mu$ l of 1x TE and 1 $\mu$ l of the RNA was subjected to agarose gel electrophoresis to ensure the product was not degraded.

Capped transcripts were synthesised in an identical reaction to which 1mM m<sup>7</sup>G(5')ppp(5')G was also added. The RNA was synthesised and isolated as described above.

Radiolabelled transcripts for use in RNase protection assays were synthesised in a 10 $\mu$ l reaction volume containing 1x transcription buffer, 4mM KOH, 20 units of Rnasin, 50 $\mu$ Ci of [ $\alpha$ -<sup>32</sup>P]UTP (800Ci/mmol), 0.67mM ATP, CTP and GTP, 10 $\mu$ M unlabelled UTP, 1 $\mu$ g of template DNA and 20 units of T7 RNA polymerase. After incubation for 1 hour at 37°C, the template DNA was removed and the RNA purified as described previously, then resuspended in 10 $\mu$ l of RNA formamide loading buffer after precipitation. Transcripts were heated at 85°C for 5 min, fractionated on a 4% polyacrylamide/7M urea gel and detected by exposure to x-ray film for 30 s. A slice of polyacrylamide containing only full length transcripts was excised from the gel, and RNA was extracted by incubation with 0.5ml of extraction buffer (0.5M NH<sub>4</sub>Ac, 1mM EDTA, 0.2% SDS) for 16 hours at 4°C. Radiolabelled RNA was precipitated from the supernatant using 0.1 volume of NH<sub>4</sub>Ac and 2.5 volumes of ethanol, pelleted by centrifugation, washed with 75% ethanol and resuspended in 50 $\mu$ l of deionised water.

For the radiolabelled transcripts used in UV crosslinking assays, the reaction took place in a 20 $\mu$ l volume containing 1x transcription buffer, 1mM ATP and GTP, 0.75mM

UTP, 0.25mM 4-thioUTP, 50 $\mu$ Ci of [ $\alpha$ -<sup>32</sup>P] CTP (400Ci/mmol), 20 units of RNasin, 1 $\mu$ g of template DNA and 20 units of T7 RNA polymerase. The RNA was synthesised and isolated in the same manner as unlabelled RNA.

For electrophoretic mobility shift assays, radiolabelled transcripts were synthesised in the same manner as for UV cross-linking except that the 50 $\mu$ l reaction contained 1x transcription buffer, 0.5mM ATP, GTP and UTP, 0.1mM CTP, 50 $\mu$ Ci of [ $\alpha$ -<sup>32</sup>P] CTP (400Ci/mmol), 20 units of RNasin, 1 $\mu$ g of template RNA and 20 units of T7 RNA polymerase.

Radiolabelled transcript concentrations were determined by Cerenkov scintillation counting.

### 2.5.6 RNase protection

RNA samples were combined with  $2.5 \times 10^5$  cpm of radiolabelled riboprobe and precipitated with 0.1 volume of 3M NaAc, pH4.6 and 2.5 volumes of ethanol for 30min at -20°C. The RNA was pelleted by centrifugation, washed with 75% ethanol, and briefly dried, after which it was resuspended in 30 $\mu$ l of hybridisation buffer (80% deionised formamide, 40mM PIPES, pH6.4, 0.4M NaCl, 1mM EDTA). The samples were heated at 85°C for 5 min and then incubated at 50°C for 16 hours to allow annealing to occur. 300 $\mu$ l of RNase digestion buffer (10mM Tris-HCl, pH 7.5, 5mM EDTA, 200mM sodium acetate) was then added and single stranded RNA was digested for 90 min at 37°C with RNase ONE™ (Promega) at a concentration of 1 unit/ $\mu$ g of RNA. The reaction was terminated by the addition of 10 $\mu$ l of 20%(w/v) SDS and proteins were digested with 2.5 $\mu$ l of 20mg/ml proteinase K at 37°C for 15 min. The sample was extracted once with phenol/chloroform and the aqueous phase was removed to a separate tube containing 10 $\mu$ g of carrier tRNA. The sample was incubated with 825 $\mu$ l of 100% ethanol at -20°C for 30 min and RNA was pelleted by centrifugation and washed with 75% ethanol. The pellet was dried briefly and resuspended in 10 $\mu$ l of RNA formamide loading buffer. RNA was denatured by heating at 85°C for 5 min and fractionated by electrophoresis through a 4% polyacrylamide/7M urea gel. Finally, radiolabelled RNA fragments were detected by analysis of the dried gel using a Molecular Dynamics phosphorimager.

### 2.5.7 Denaturing RNA agarose gel electrophoresis and Northern blotting

Samples of RNA were denatured by incubation in 1x gel buffer (20mM MOPS, pH7.0, 5mM NaAc, and 1mM EDTA), 6.5% formaldehyde, and 50% deionised formamide at 55°C for 15 min in a volume of 20µl. 4µl of loading buffer was added to each sample prior to fractionation by electrophoresis through a 1% agarose gel containing 1x gel buffer and 6% formaldehyde. The gel was submerged in 1x gel buffer and run at 120V for 2-3 hours. After electrophoresis was complete, the portion of gel containing the RNA markers (Gibco-BRL) was removed, stained with ethidium bromide (5µg/ml) for 10 min and destained for 10 min using 1x gel buffer. The markers were visualised using a UV transilluminator and photographed for later reference. The remainder of the gel was washed in deionised water before being soaked in 0.05 M NaOH for 20 min. After rinsing with deionised water, the gel was incubated in 20x SSC (3M NaCl, 0.3M tri-sodium citrate) for 30 min. The RNA was transferred from the gel to Zetaprobe membrane (Biorad, Hemel Hempstead, Hertfordshire, UK) using capillary blotting for 16 hours and was fixed to the membrane by baking at 80°C for 2 hours before hybridisation.

### 2.5.8 Synthesis of a radiolabelled DNA probe and hybridisation to immobilised RNA

The plasmid pGL3' was digested with *Nco*I and *Ava*I and the 1058 bp luciferase-encoding fragment was isolated from an agarose gel (section 2.4.7). To prepare a random-primed radiolabelled DNA probe, 30ng of the DNA fragment was heated at 95°C for 5 min in 11µl of sterile deionised water. The reaction volume was then made up to 20µl, containing 1x labelling buffer (Promega), 0.25mM BSA, 0.4mM dATP, dGTP and dTTP, 20µCi of [ $\alpha$ -<sup>32</sup>P]dCTP (3000 Ci/mmol) and 5 units of Klenow DNA polymerase and incubated at 37°C for 1-2 hours. Unincorporated nucleotides were removed by passing the probe through a Sephadex G-50 column.

The RNA bound to the filter was pre-hybridised with 10ml of Church-Gilbert buffer (180mM Na<sub>2</sub>HPO<sub>4</sub>, 70mM NaH<sub>2</sub>PO<sub>4</sub>, 7% SDS) supplemented with 0.2mg/ml denatured Salmon sperm DNA and 50µg/ml bakers yeast tRNA (Sigma) for 1 hour at 65°C. The random-primed radiolabelled DNA probe was denatured by heating at 95°C for 5 min and added directly to the pre-hybridisation buffer, followed by hybridisation at 65°C for 16-24 hours. After this the filter was washed once for 20 min at 65°C with Church-Gilbert buffer

followed by 2-4 washes for 20 min with Church Wash buffer 1 (14.4mM Na<sub>2</sub>HPO<sub>4</sub>, 5.6mM NaH<sub>2</sub>PO<sub>4</sub>, 1mM EDTA, 5% SDS). Further washes using Church Wash buffer 2 (14.4mM Na<sub>2</sub>HPO<sub>4</sub>, 5.6mM NaH<sub>2</sub>PO<sub>4</sub>, 1mM EDTA, 1% SDS) were performed if the background counts on the filter remained high after the initial washes. Excess moisture was removed from the filter and radiolabelled probe was detected by phosphorimager analysis.

### 2.5.9 Electrophoretic mobility shift assays (EMSAs)

2.5x10<sup>4</sup> cpm of radiolabelled RNA was combined with protein or cell extract in a total volume of 20µl, containing 1x transcription buffer, 1mM ATP and 20 units of RNasin. The reaction was incubated at 21°C for 10 min, after which 1x TBE loading buffer was added and the entire reaction was applied to a 5% polyacrylamide, 0.5x TBE gel in a Bio-Rad Protean II system in 0.5x TBE. For *N-myc* 5' UTR transcripts, gels were run until two successive dye fronts had run off the gel and a third dye front had run halfway down the gel. Radiolabelled RNA was visualised using a phosphorimager.

## 2.6 Biochemical Techniques

### 2.6.1 Buffers and Solutions

**1x SDS sample buffer:** 50mM Tris pH 6.8, 10% glycerol, 4% SDS, 0.1% bromophenol blue, 10% β-mercaptoethanol, 1mM EDTA

**SDS-PAGE resolving buffer:** 1.5M Tris, 0.24% TEMED, 1% SDS pH 8.8

**SDS-PAGE stacking buffer:** 0.25M Tris, 0.12% TEMED, 0.2% SDS pH 6.8

**1x SDS running buffer:** 25mM Tris, 192mM glycine, 0.1% SDS pH 8.3

**TBST (Tris buffered saline, Tween):** 10mM Tris pH 8.0, 0.9% NaCl, 0.1% Tween

**Coomassie staining solution:** 0.1% Coomassie brilliant blue R-250 dissolved in 5:1:5 methanol:acetic acid:water

**Destaining solution:** 5:1:5 methanol:acetic acid:water

**Protease inhibitors:** 19µg/ml Aprotinin, 1µg/ml Leupeptin, 1µg/ml TLCK, 20µg/ml PMSF, pepstatin

### **2.6.2 *In vitro* translation reactions**

*In vitro* translation reactions were performed using the Flexi<sup>®</sup> rabbit reticulocyte lysate system (Promega) with minor modifications to the manufacturer's recommendations. Each reaction contained 8.25µl of reticulocyte lysates, 0.6mM MgOAc, 20 units of RNasin, 2µl of 1mM complete amino acid mixture and between 20 and 100ng of RNA substrate in a final volume of 12.5µl. 2µg of a supplementary protein was added where necessary.

### **2.6.3 Preparation of total cell extract**

6-9 x 10<sup>7</sup> cells were pelleted by centrifugation at 1000 rpm for 5 min, washed in PBS and pelleted again. The pellet was resuspended in 600µl of polysome buffer (300mM KCl, 5mM MgCl<sub>2</sub>, 10mM HEPES pH7.4, 0.5% NP-40) and incubated on ice for 1 hour. Nuclei were sheared by sonication, and cell debris was pelleted by centrifugation at 13000 rpm for 10 min at 4°C. The supernatant was removed to fresh tubes and stored in aliquots at -80°C.

### **2.6.4 Determination of protein concentration by Bradford assay**

Cell extracts were diluted 1:10 and 1:20 in sterile deionised water, while stock BSA (2mg/ml) was diluted to concentrations of 0.1-1.5mg/ml. Bradford reagent (Pierce and Warriner) was added according to the manufacturer's instructions, and the absorbance at 595nm was measured. Protein concentration was determined using a standard curve.

### **2.6.5 Preparation of cell lysates from transfected cells**

After transfection, the medium was aspirated and the adherent cells were washed twice with PBS. Cells were lysed by the addition of 200µl of 1x Reporter lysis buffer (Promega) or 1x Passive lysis buffer (Promega) and lysates were removed from wells with a cell scraper, then transferred to a tube. For cells in which apoptosis had been induced, detached cells were harvested from the aspirated medium by centrifugation and combined with the cell lysate from the same well. Lysates were subjected to one freeze-thaw cycle at -20°C and the insoluble matter was pelleted by centrifugation. The supernatant was removed to a fresh tube.

### 2.6.6 Luciferase assays

The activity of firefly luciferase in lysates prepared from cells transfected with monocistronic reporter vectors was measured using a luciferase reporter assay system (Promega). Lysates were prepared using 1x Reporter lysis buffer and 5 $\mu$ l of lysate was added to 25 $\mu$ l of luciferase assay reagent. Light emission was measured over 10 s using an Optocomp I luminometer (MGM Instruments).

The activity of both firefly and *Renilla* luciferase in lysates of cells transfected with dicistronic luciferase plasmids was measured using a Dual-luciferase reporter assay system (Promega). 5 $\mu$ l of lysate prepared using Passive lysis buffer was used for each assay. Assays were performed according to the manufacturer's protocols, except that only 25 $\mu$ l of each reagent was used. Light emission was measured as described previously.

### 2.6.7 $\beta$ -Galactosidase assays

The activity of  $\beta$ -galactosidase in lysates prepared from cells transfected with pJ7lacZ was measured using a Galacto-Light Plus assay system (Tropix). 5 $\mu$ l of cell lysate was added to 25 $\mu$ l of Galacton Plus reaction buffer (Galacton-Plus substrate diluted 1:100 with Reaction Buffer diluent) and incubated at room temperature for 1 hour. 37.5 $\mu$ l of Light Emission Accelerator II was then added and enzyme activity was determined by immediately measuring the light emission from the reaction in a luminometer, as previously described. Cotransfection with pJ7lacZ was used to allow normalisation of luciferase values such that variations in transfection efficiency were accounted for, but a direct measure of transfection efficiency was not made.

### 2.6.8 SDS-polyacrylamide gel electrophoresis (SDS-PAGE)

Protein extracts were denatured by the addition of 1x SDS sample buffer containing protease inhibitors and heated at 95°C for 5 min prior to loading. SDS-polyacrylamide gels were prepared as detailed in Table 2.3 and polymerised by the addition of ammonium persulphate (APS) solution. Gels were run in a Bio-Rad Protean II system in SDS running buffer, according to standard procedures. Typically, vertical gels were run at a constant voltage of 150V (minigels) or 40mA (large gels) until the Bromophenol blue dye front reached the bottom of the gel.

<b>% gel</b>	<b>Water</b>	<b>Resolving/stacking buffer</b>	<b>30%:0.8% acylamide: bisacrylamide solution</b>
7.5	2.52ml	1.25ml	1.25ml
10	2.1ml	1.25ml	1.67ml
Stacking gel	0.9ml	1.25ml	0.33ml

**Table 2.3** Composition of SDS-PAGE gels.

### 2.6.9 Coomassie staining of SDS-polyacrylamide gels

Gels were stained in a Coomassie staining solution for 30min at room temperature and subsequently destained in destaining solution for 3-5 hours. Gels were then incubated in deionised water for 30min to remove acetic acid before drying.

### 2.6.10 Transfer of proteins on to nitrocellulose membranes

Cell extracts separated by SDS-PAGE were transferred on to nitrocellulose (Schleicher and Schuell, Dassel, Germany) by semi-dry blotting in transfer buffer (50mM Tris, 192mM glycine, 20% methanol) for between 30 and 90 min at 10V. Protein transfer was visualised temporarily by staining with Ponceau-S solution (0.5% w/v in 5% w/v trichloroacetic acid [TCA]).

### 2.6.11 Western blotting/immunodetection

Proteins immobilized on to nitrocellulose after SDS-PAGE were detected immunologically. Nitrocellulose membranes were incubated in a 5% dried milk solution in TBST for 1 hour at room temperature to block non-specific binding sites. Membranes were then incubated in 5-10ml of primary antibody diluted appropriately in 5% milk TBST for 12-16 hours at 4°C with constant agitation. After three 10 min washes in TBST, the membranes were incubated with horseradish peroxidase-conjugated secondary antibodies to mouse IgG (Dako A/S, Denmark) or rabbit IgG (Sigma), diluted 1:2000 and 1:10,000 respectively in 5% milk TBST, for 1 hour at room temperature with constant agitation. Three 10 min washes in TBST solution were carried out and protein-antibody complexes were detected using an enhanced chemiluminescence (ECL) technique. For this, 1ml Luminol solution (50mg Luminol (5-amino-2,3-dihydro-1,4-phthalazinedione) in 0.1M Tris-HCl pH8.6), 10µl Enhancer (11 mg para-coumaric acid in 10 ml DMSO) and 3.1µl 3% hydrogen peroxide were mixed and incubated on the membrane for 60 s.

Chemiluminescence was visualised by exposing the membrane to X-ray film for periods of between 10 s and 30 min.

### **2.6.12 Stripping and re-probing of western blots**

Nitrocellulose membranes were stripped of existing protein-antibody interactions by incubation in a solution of 100mM  $\beta$ -mercaptoethanol, 2% SDS and 62.5mM Tris-HCl pH 6.7 for 10 min at 50°C. Membranes were then washed in TBST and re-probed with a different primary antibody as described above.

### **2.6.13 Pulse labelling**

$2 \times 10^6$  cells, with or without pre-treatment with TRAIL for 3 hours, were starved in methionine-free medium for 1 hour and then labeled for 30 min with 250 $\mu$ Ci of [<sup>35</sup>S] methionine (1175Ci/mmol) in 1ml of methionine-free medium. Fresh complete medium was then added to the cells and samples were harvested at predetermined times by washing with 1x PBS and scraping into 1.5ml of antibody buffer (10mM Tris-HCl pH7.5, 50mM NaCl, 0.5% NP-40, 0.5% sodium deoxycholate, 0.5% SDS, 10mM iodoacetamide) containing protease inhibitors. Apoptotic cells were harvested by centrifugation and combined with adherent cells in antibody buffer, and cells were disrupted by passage through a 21-gauge needle. Samples were pre-cleared by incubation with mouse immunoglobulin G and protein A/G agarose (Santa Cruz Biotechnology, Inc) at 4°C for 1 hour, with rotation. After centrifugation at 4000rpm for 5 min at 4°C, the supernatants were removed to fresh tubes and incubated with agarose-conjugated Myc monoclonal antibody C-33 (Santa Cruz Biotechnology, Inc) for 12-16 hours at 4°C, with rotation. The immunoprecipitates were collected by centrifugation at 4000rpm for 5 min at 4°C, and were washed three times with 1ml RIPA buffer (50mM Tris-HCl pH 7.5, 150mM NaCl, 1% Triton X-100, 0.5% sodium deoxycholate, 0.1% SDS). The pellets were resuspended in 30 $\mu$ l of 1x SDS-PAGE sample buffer, heated at 95°C for 5 min, and the agarose beads removed by centrifugation at 13 000rpm for 5 min. The supernatants were subjected to SDS-PAGE using 7.5% polyacrylamide gels, and radiolabeled proteins were visualised using a phosphorimager.

### 2.6.15 p38MAPKinase assays

$2 \times 10^5$  cells, with or without preincubation with SB203580 for 1 hour, were treated with TRAIL and harvested at predetermined times by washing with ice-cold 1x PBS and scraping into 250 $\mu$ l of Triton lysis buffer containing protease inhibitors (20mM HEPES pH 7.5, 137mM NaCl, 25mM  $\beta$ -glycerophosphate, 2mM NaPP<sub>i</sub>, 2mM EDTA, 10% glycerol, 1% Triton X-100, 2mM benzamidine, 0.5mM DTT, 1mM Na<sub>3</sub>VO<sub>4</sub>). Apoptotic cells were harvested from the aspirated medium by centrifugation and combined with the scraped lysates. After centrifugation at 13000 rpm for 5 min at 4°C, the supernatants were removed to fresh tubes and incubated with 5 $\mu$ l of anti-p38 antibody (Santa Cruz Biotechnology, Inc.) and 4 $\mu$ g of protein A-sepharose at 4°C for 3 hours with rotation. The immunoprecipitates were harvested by centrifugation at 3000rpm for 30 seconds at 4°C, and washed three times with Triton lysis buffer and once with kinase assay buffer (25mM HEPES pH7.4, 25mM  $\beta$ -glycerophosphate, 25mM MgCl<sub>2</sub>, 0.5mM Na<sub>3</sub>VO<sub>4</sub>, 0.5mM EDTA, 0.5mM DTT). Pellets were resuspended in 30 $\mu$ l of kinase assay buffer and incubated with 5 $\mu$ g of glutathione S-transferase-ATF2 (1-109) and 2.5 $\mu$ Ci [ $\gamma$ -<sup>32</sup>P] ATP (50Ci/mmol) for 30 min at 30°C. Incorporation of radiolabel into glutathione S-transferase-ATF2 was determined by phosphorimager analysis following electrophoresis on a 10% polyacrylamide gel.

### 2.6.16 UV-crosslinking reactions

Samples containing 25 $\mu$ g of cell extract were incubated with 4-thioUTP-containing radiolabelled transcripts (5x10<sup>5</sup> cpm) in the absence or presence of unlabelled competitor RNAs for 10 min at 30°C. The reaction was performed in a final volume of 30 $\mu$ l in 1x Transcription buffer containing 1mM ATP. Heparin (0.05 $\mu$ g/ $\mu$ l) was added to the samples, followed by a further incubation for 10 min at 30°C. The reaction mixes were then irradiated at 312nm using a UV source (UVP) at a distance of 3 cm for 30 min at 0°C. After irradiation, unbound RNA was digested with 0.2mg/ml pancreatic RNase A (Sigma) and RNase T1 (Ambion) for 1 hour at room temperature. An equal volume of 2x SDS sample buffer was added to each sample. The crosslinked RNA-protein complexes separated on a 10% SDS polyacrylamide gel and visualised using a phosphorimager following fixation in destaining solution and drying.

## Chapter 3

### Internal ribosome entry in the N-myc 5' UTR

#### 3.1 Introduction

The proto-oncogene N-*myc* contains a long and highly GC-rich 5' UTR (Kohl et al., 1986), and it has been suggested that this UTR could assume a complex secondary structure and play a role in translational control (Stanton et al., 1986). The N-*myc* 5' UTR demonstrates little sequence similarity to that of *c-myc* (Ibson and Rabbitts, 1988), although in both cases the predominant initiation codon occurs in exon 2 and exon 1 is non-coding (Hann et al., 1988; Makela et al., 1989) (figure 1.10A and B). In addition, the GC content of the two UTRs is almost identical (*c-myc*, 64.6%, N-*myc*, 65.5%). The presence of a highly active IRES in the *c-myc* 5' UTR (Stoneley et al., 1998), together with the fact that both *c-* and N-Myc proteins are similar in structure and function and both show tightly regulated expression, implied that N-*myc* expression might also be controlled by internal ribosome entry. Many of the cellular IRESs identified to date have been found in proto-oncogenes (Willis, 1999), and this is probably related to the importance of tight control in the expression of their protein products. It was therefore decided to obtain the N-*myc* 5' UTR and test its IRES activity using standard dicistronic assays (described in section 1.4.2).

#### 3.2 RT-PCR of the N-myc 5' UTR

To obtain cDNA corresponding to the N-*myc* 5' UTR, an RT-PCR reaction was carried out using the oligonucleotide primers NF1 and NGR (table 2.2). Poly(A)<sup>+</sup> RNA isolated from the human neuroblastoma cell line SH-SY5Y, in which N-*myc* RNA is expressed (Sadee et al., 1987), was used as a template. A single PCR product of 376bp was detected (figure 3.2, lane 6). However, the published sequence data predicted that a fragment 686bp in length would be obtained using these primers (Ibson and Rabbitts, 1988) (figure 3.1, sequence shown in red and blue). This implied that the product was the result of non-specific primer annealing during the PCR, but as this was the only fragment obtained it was subjected to DNA sequencing.

Analysis of the sequence indicated that it was derived from the N-*myc* 5' UTR and corresponded exactly to the published sequence, with the exception of a region of 310nt

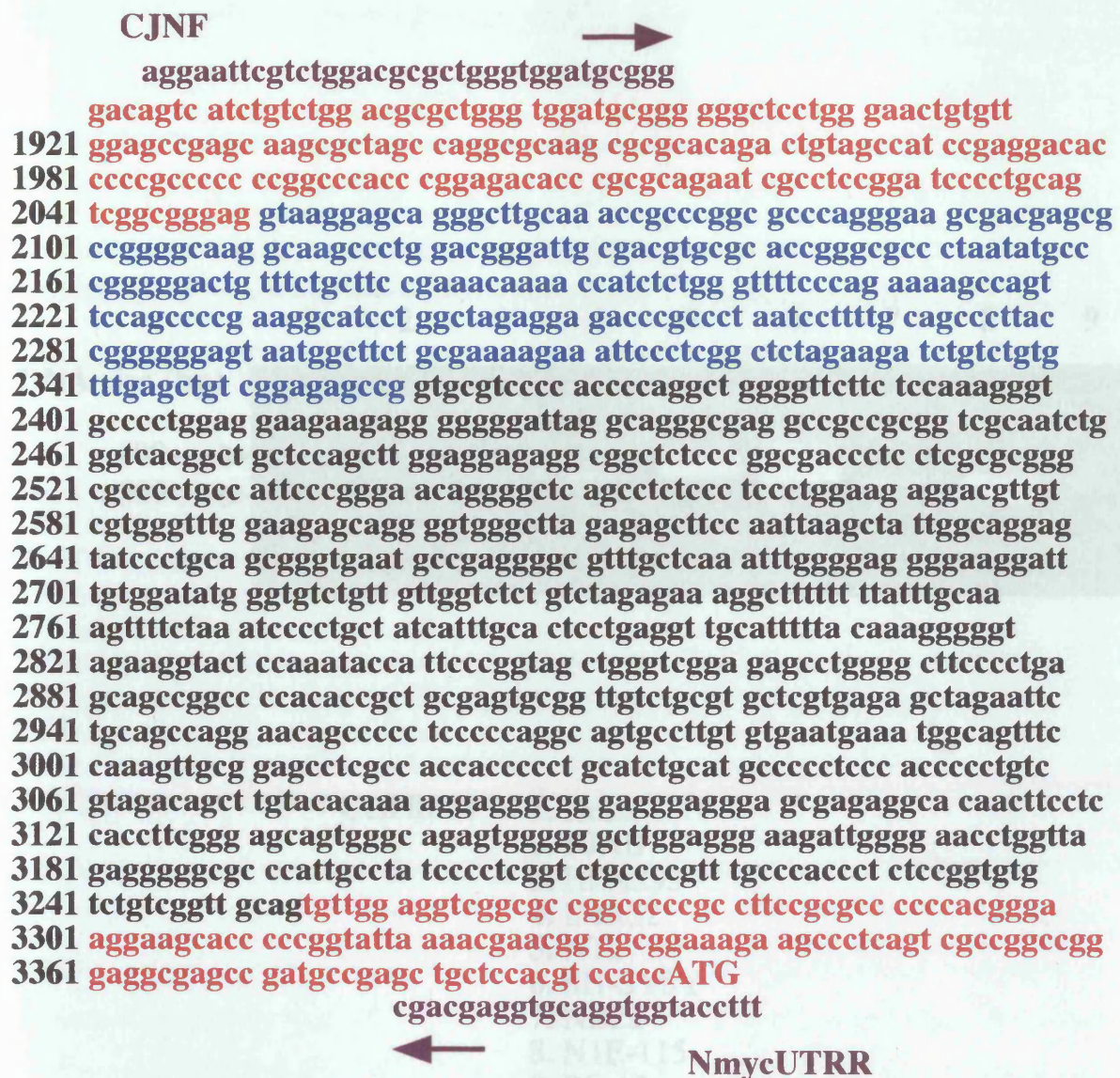
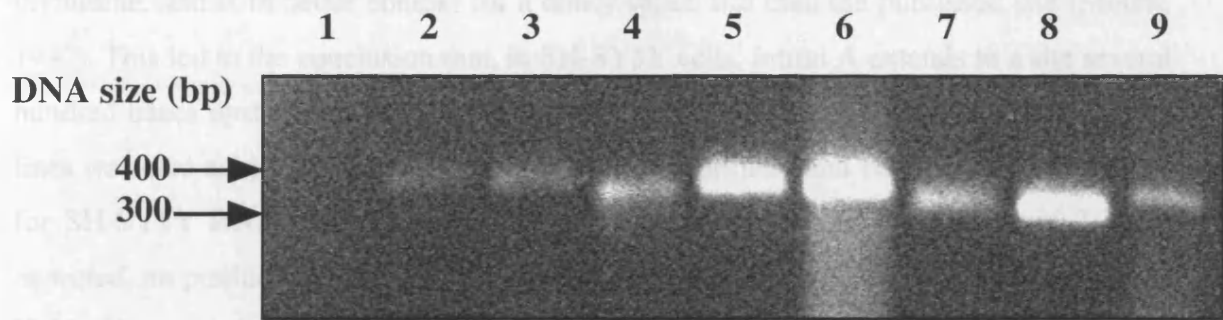


Figure 3.1 Sequence of the N-myc 5' UTR. The DNA sequence encoding the N-myc 5' UTR is shown. The database sequence of intron A is coloured black, whereas the data obtained by RT-PCR indicate that intron A also encompasses the area shown in blue. The 5' UTR is shown in red, and the primers used to obtain it are indicated in purple.



Further evidence in support of this hypothesis can be seen by comparison of different species. The 5' UTRs of murine (Katchi et al., 1988) and rat (Segiyama et al., 1991) c-myc bear considerable homology to that of human transcripts (74.2 and 77.7% identical, respectively). An alignment of the human and murine UTRs is shown in figure 5.7. The murine UTR contains an exon 1 splice site in a similar position to that of the PCR products obtained from human cells. Sequence similarity is great enough to allow the use of the human primers to amplify the mouse and rat *N-myc* 5' UTRs as were used for the human sequences. The results of RT-PCR using RNA from the murine cell lines NB2a and N1E-115 and the rat line PC-12 are shown in figure 3.2, lanes 7-9, and confirm that the products obtained are very similar in size.

It is reasonable to conclude that the human A donor splice site of the *N-myc* gene is in an active position in the 5' UTR of the *N-myc* gene. This has been confirmed by RT-PCR analysis of the 5' UTR of the *N-myc* gene in various cell lines. The results of RT-PCR using poly(A)<sup>+</sup> RNA from various cell lines are shown in figure 3.2. Lanes 1-6 represent samples from human cell lines, lanes 7 and 8 from murine cell lines, and lane 9 from a rat cell line.

### 3.3 Effect of the *N-myc* 5' UTR in a dicistronic context

The dicistronic vector pRF (figure 3.3) was used to determine whether the *N-myc* 5' UTR confers an IRES. A second PCR was carried out using the RT-PCR product

that was absent in the PCR product. In figure 3.1 the sequence obtained by PCR is represented in red, and the missing region in blue. This region lies immediately upstream of the donor splice site of intron A. It was noted with interest that the point at which the truncation in the PCR product begins is succeeded immediately by the bases guanine and thymidine, and is in better context for a donor splice site than the published site (Mount, 1982). This led to the conclusion that, in SH-SY5Y cells, intron A extends to a site several hundred bases upstream of its published boundary. RNA from several other human cell lines was also subjected to RT-PCR using the same primers and conditions as were used for SH-SY5Y RNA. The products obtained are shown in lanes 1-5 of figure 3.2. As expected, no product was visible when RNA was extracted from the non-neuronal cell line HeLa. However, in the *N-myc* expressing cell lines BJAB, HEK293, IMR32 and NT2, a unique product of the same size as that obtained from SH-SY5Y cells was amplified. This implies that the donor splice site of *N-myc* intron A has been incorrectly assigned.

Further evidence in support of this hypothesis can be seen by comparison of different species. The 5' UTRs of *N-myc* transcripts from murine (Kato et al., 1988) and rat (Sugiyama et al., 1991) cells bear considerable homology to that of human transcripts (74.2 and 77.7% identical, respectively). A sequence alignment of the human and murine UTRs is shown in figure 5.7. The murine and rat UTRs have exon 1/intron A boundaries in a similar position to that of the PCR products obtained from human cells. Sequence similarity is great enough to allow the use of the same primers to amplify the mouse and rat *N-myc* 5' UTRs as were used for the human sequence. The results of RT-PCR using RNA from the murine cell lines NB2a and N1E-115 and the rat line PC-12 are shown in figure 3.2, lanes 7-9, and confirm that the products obtained are very similar in size.

It is reasonable to conclude that the intron A donor splice site of the *N-myc* gene is in an upstream position in all the cell lines tested, with no evidence of any alternative splicing. As RNA was analysed from cells from a range of different human origins it is likely that this feature extends to all human *N-myc* transcripts, although no tissue samples have been examined.

### 3.3 Effect of the *N-myc* 5' UTR in a dicistronic context

The dicistronic vector pRF (figure 3.3) was used to determine whether the *N-myc* 5' UTR contains an IRES. A second PCR was carried out using the RT-PCR product

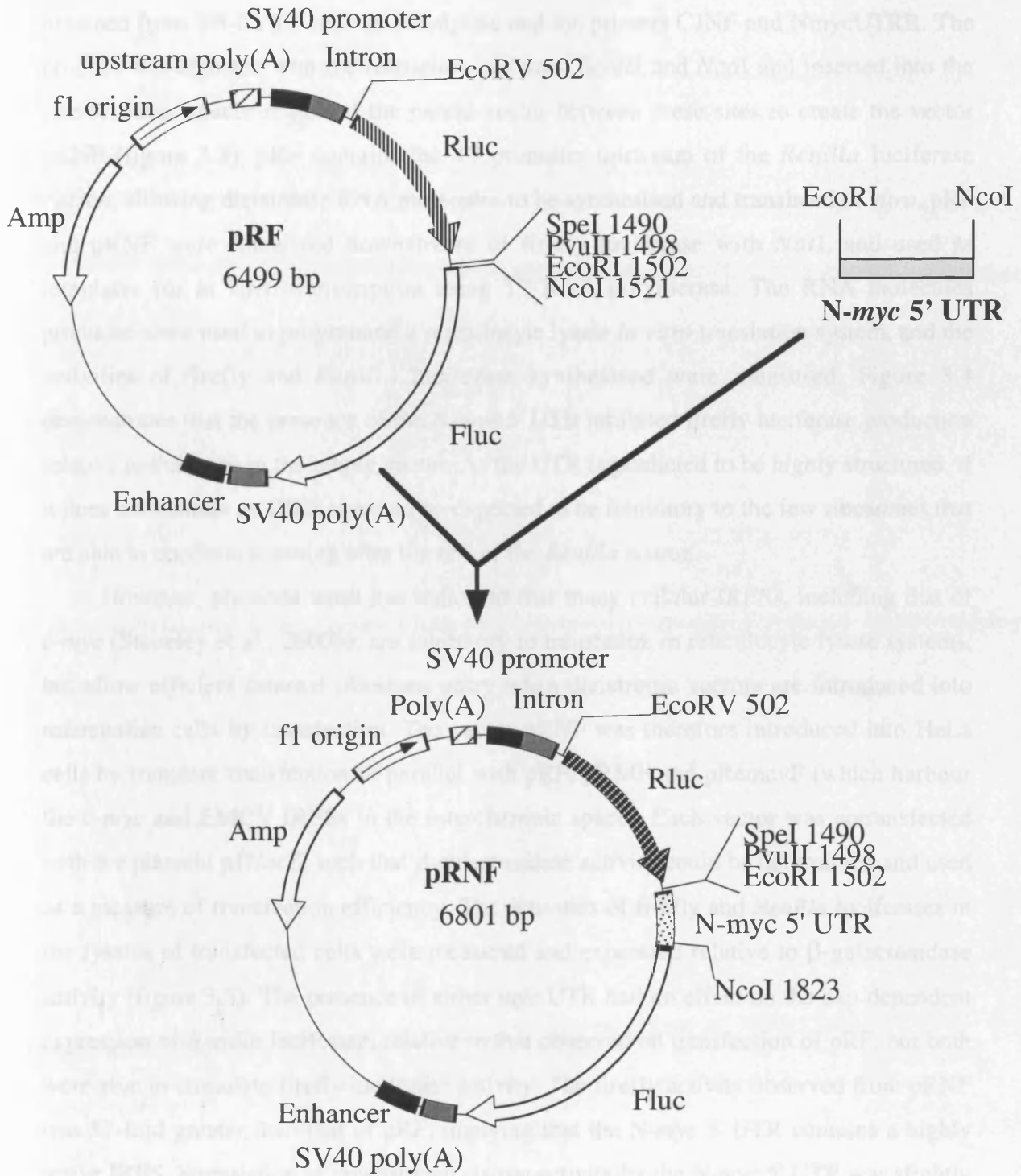


**Figure 3.3 Construction of the vector pRNF.** An RT-PCR product encoding the N-myc 5' UTR was digested with *EcoRI* and *NcoI* and inserted between these sites in the vector pRF after digestion and dephosphorylation of the vector.

obtained from SH-SY5Y cells as a template and the primers CJNF and NmycUTRR. The product was digested with the restriction enzymes *EcoRI* and *NcoI* and inserted into the intercistronic spacer region of the parent vector between these sites to create the vector pRNF (figure 3.3). pRF contains the T7 promoter upstream of the *Renilla* luciferase cistron, allowing dicistronic RNA molecules to be synthesised and translated *in vitro*. pRF and pRNF were linearised downstream of firefly luciferase with *NotI*, and used as templates for *in vitro* transcription using T7 RNA polymerase. The RNA molecules produced were used to programme a reticulocyte lysate *in vitro* translation system, and the activities of firefly and *Renilla* luciferase synthesised were measured. Figure 3.4 demonstrates that the presence of the N-myc 5' UTR inhibited firefly luciferase production relative to that seen in the empty vector. As the UTR is predicted to be highly structured, if it does not contain an IRES it would be expected to be inhibitory to the few ribosomes that are able to continue scanning after the end of the *Renilla* cistron.

However, previous work has indicated that many cellular IRESs, including that of *c-myc* (Stoneley et al., 2000b), are inhibitory to translation in reticulocyte lysate systems, but allow efficient internal ribosome entry when dicistronic vectors are introduced into mammalian cells by transfection. The vector pRNF was therefore introduced into HeLa cells by transient transfection in parallel with pRF, pRMF and pRemcvF (which harbour the *c-myc* and EMCV IRESs in the intercistronic space). Each vector was cotransfected with the plasmid pJ7lacZ, such that  $\beta$ -galactosidase activity could be determined and used as a measure of transfection efficiency. The activities of firefly and *Renilla* luciferases in the lysates of transfected cells were measured and expressed relative to  $\beta$ -galactosidase activity (figure 3.5). The presence of either *myc* UTR had no effect on the cap-dependent expression of *Renilla* luciferase, relative to that observed on transfection of pRF, but both were able to stimulate firefly luciferase activity. The firefly activity observed from pRNF was 87-fold greater than that of pRF, implying that the N-myc 5' UTR contains a highly active IRES. Stimulation of downstream cistron activity by the N-myc 5' UTR was slightly more efficient than by the *c-myc* 5' UTR, and threefold more efficient than that mediated by the highly active EMCV IRES.

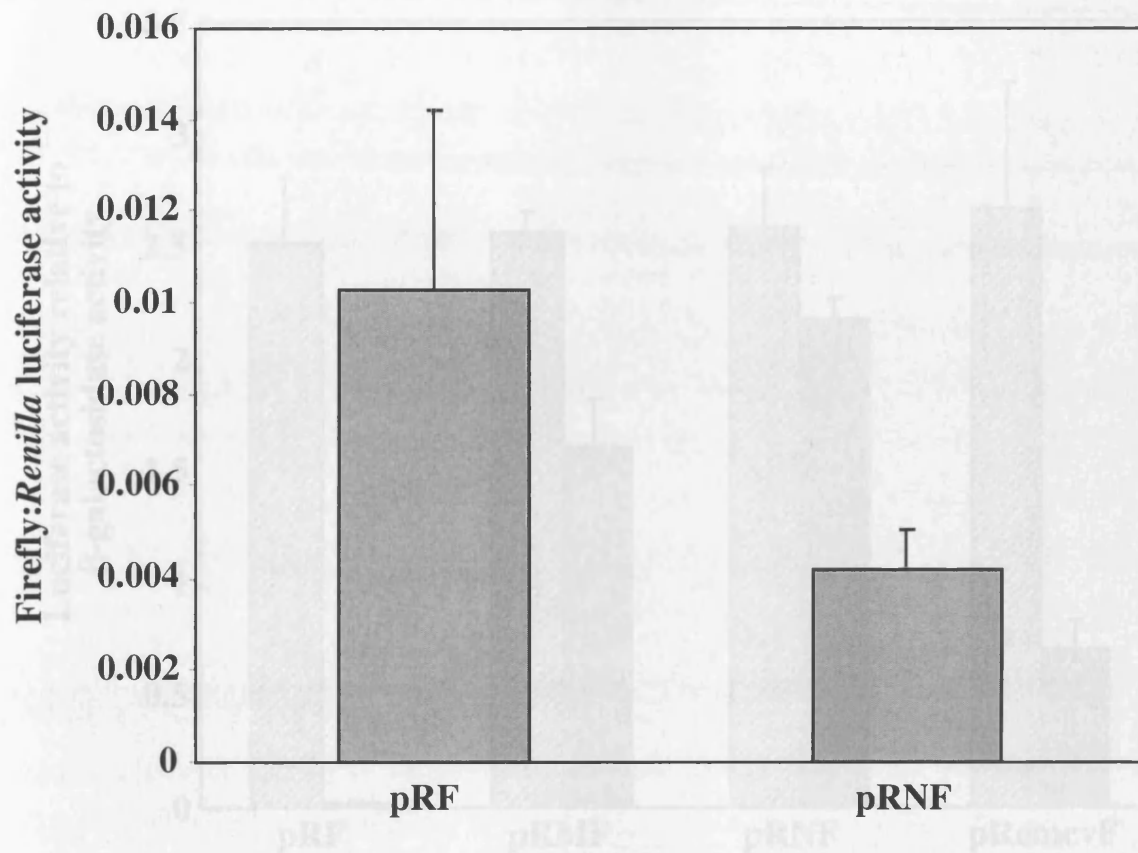


**Figure 3.4 Effect of the N-myc 5' UTR on translation *in vitro*.** Dicistronic RNA molecules produced by *in vitro* transcription using pRF and pRNF as templates were used to programme reticulocyte lysate. The level of firefly luciferase produced is shown relative to that of *Renilla* luciferase. Results represent an average of four independent experiments, and error bars represent standard deviations.

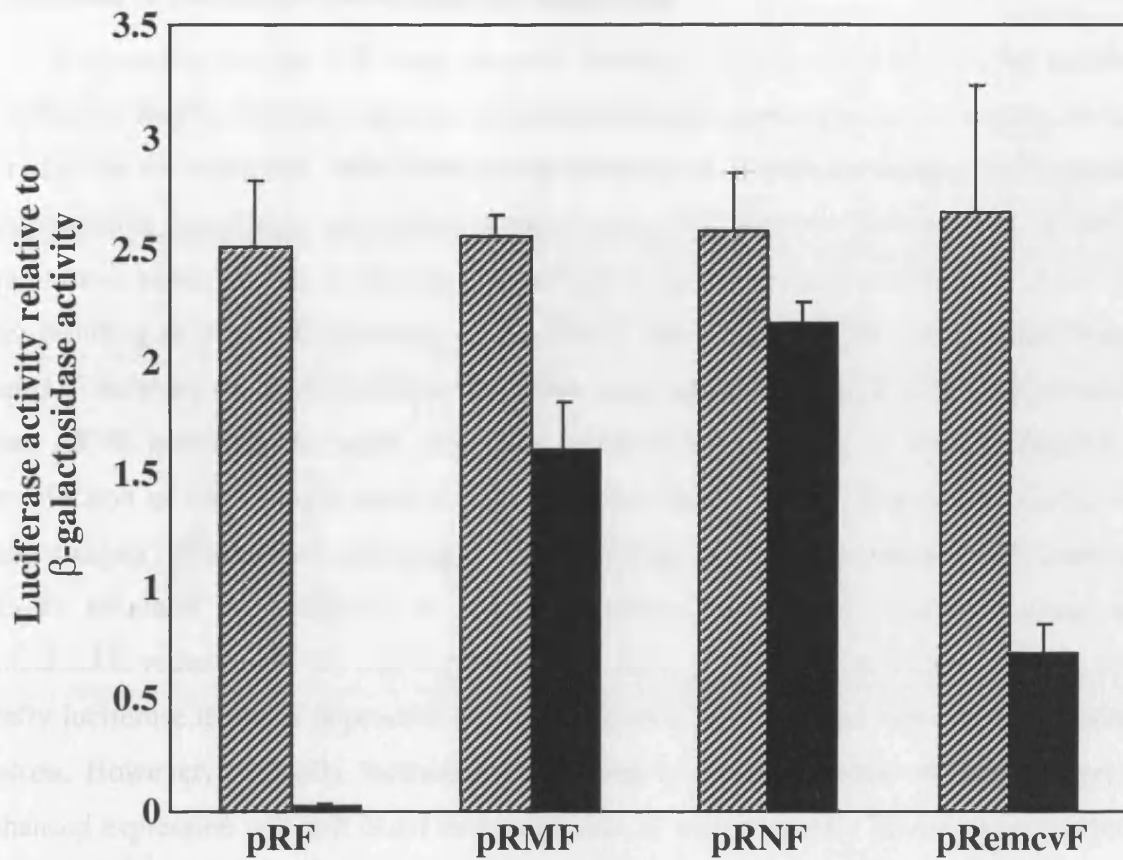


**Figure 3.5 *c-myc*, *N-myc* and EMCV IRES activity in HeLa cells.** The activities of *Renilla* (shaded) and firefly (black) luciferases were determined in HeLa cells after transfection with the constructs pRF, pRMF, pRNF and pRemcvF. Values obtained were normalised to the transfection control of  $\beta$ -galactosidase. Results are an average of three independent experiments and error bars represent standard deviations.

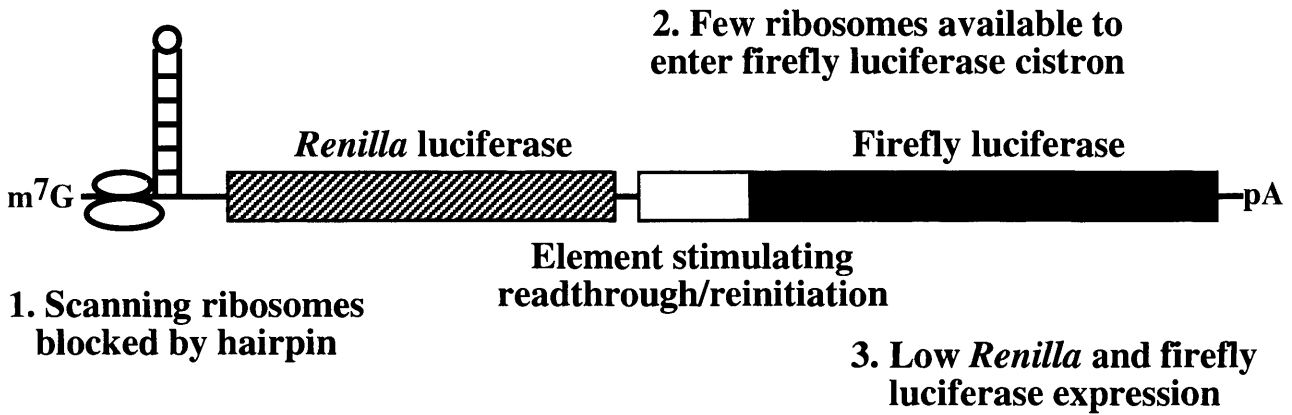
### **3.4 The N-myc 5' UTR does not enhance downstream cistron activity by stimulation of ribosomal readthrough or reinitiation**

It is possible that the UTR does not allow internal ribosome entry to occur but is able to stimulate firefly luciferase activity by allowing ribosomes to continue scanning, or to reinitiate on the transcript, after terminating synthesis of *Renilla* luciferase. To examine this possibility, translation was studied in the context of an upstream RNA hairpin. A 60bp palindromic sequence had previously been inserted into the vector pRMF at the *EcoRV* site, resulting in phpRMF (Stoneley et al., 1998). The *c-myc* 5' UTR was excised from phpRMF between the *SpeI* and *NcoI* restriction sites, and the N-myc 5' UTR was excised from pRNF between the same sites and inserted in its place to create phpRNF. Transfection of this plasmid leads to the production of dicistronic transcripts bearing a stable hairpin (-55kcal/mol) upstream of the *Renilla* luciferase cistron (figure 3.6). Such a hairpin structure is inhibitory to scanning ribosomes and will therefore cause a considerable reduction in the cap-dependent expression of *Renilla* luciferase, and also of firefly luciferase if this is dependent on ribosomes that have scanned through the *Renilla* cistron. However, if firefly luciferase expression is due to internal ribosome entry, enhanced expression will still occur in the presence of such a hairpin. Transfection studies using pRNF and phpRNF were carried out in NB2a cells, as the hairpin was found to be particularly efficient in these cells (figure 3.7). The presence of the hairpin reduced *Renilla* luciferase expression to 20% of that observed when pRNF was transfected, as expected. Firefly luciferase activity was marginally increased by the presence of the hairpin (to 125% of pRNF levels). This is likely to be due to the presence of limiting quantities of certain components of the translation machinery in transfected cells. In such a situation, the inhibition of *Renilla* luciferase translation in cells transfected with phpRNF would leave more factors available to synthesise firefly luciferase. A readthrough/reinitiation mechanism is therefore not responsible for the enhancement of downstream cistron expression observed in the presence of the N-myc 5' UTR.

### **3.5 Transfection of pRNF leads to the production of full length dicistronic RNA molecules**

An alternative explanation for the stimulation of downstream cistron expression in pRNF would be the presence of an RNA cleavage site or a cryptic promoter or splice site

**A**



**B**

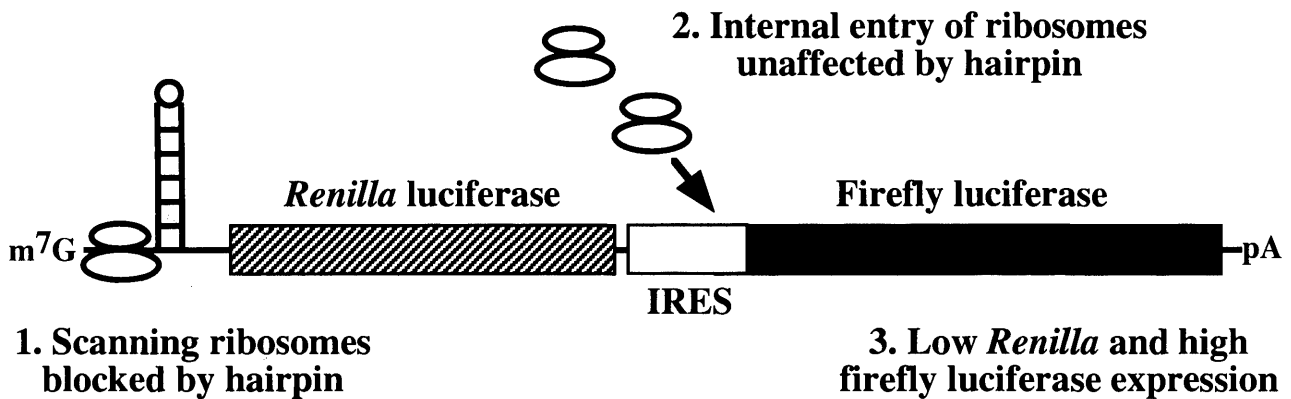


**Figure 3.6 Effect of placing a stable RNA hairpin upstream of *Renilla* luciferase.** (A) In the presence of a hairpin, few ribosomes are able to scan through the *Renilla* luciferase cistron and therefore few ribosomes are available for readthrough/reinitiation on the firefly luciferase cistron. This leads to low levels of expression from both reporters. (B) If an IRES is present between the cistrons, internal ribosome entry will be unaffected by the hairpin and firefly luciferase expression will remain high.

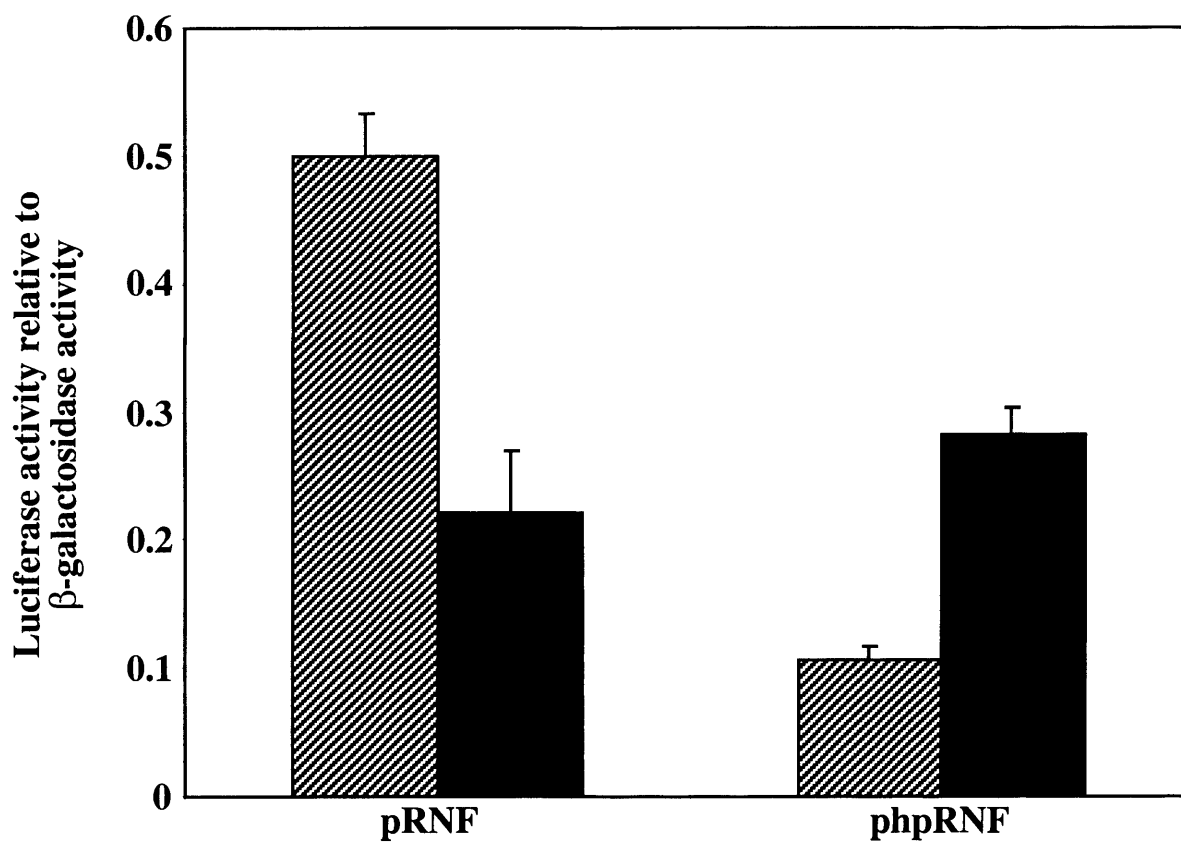
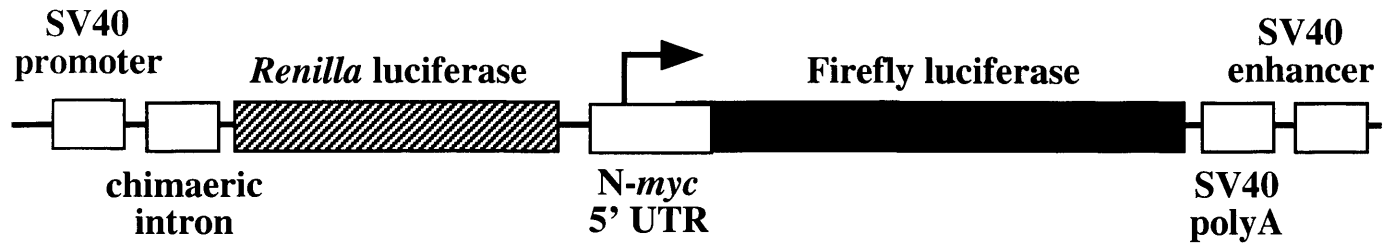


**Figure 3.7 Activity of the N-myc 5' UTR in the context of a dicistronic hairpin vector.** The vector phpRNF was introduced into NB2a cells by transfection, leading to the production of transcripts bearing a stable RNA hairpin upstream of the *Renilla* luciferase cistron. The activities of *Renilla* (shaded) and firefly (black) luciferases on transfection of this plasmid and pRNF were normalised to  $\beta$ -galactosidase activity. Results are an average of three independent experiments and error bars represent standard deviations.

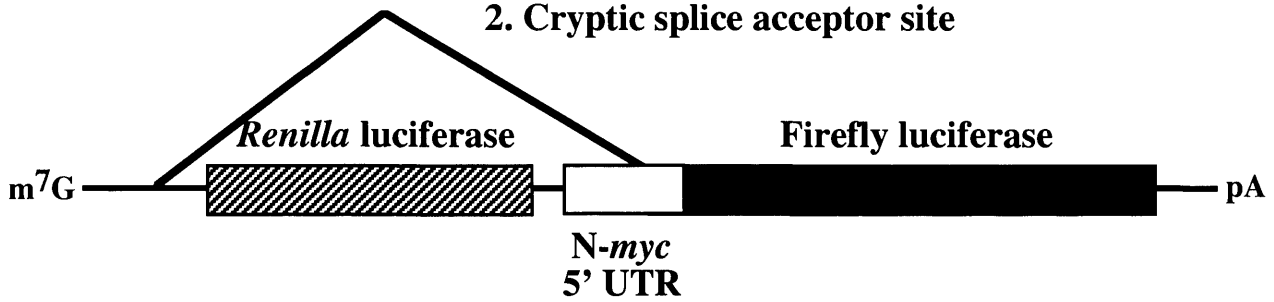
in the N-myc 5' UTR (figure 3.8). Such a mechanism would allow the production of monocistronic firefly luciferase RNA molecules when pRNF was transfected into cells. To examine the nature of the transcripts produced, Northern blot analysis was carried out on poly(A)<sup>+</sup> RNA isolated from pRNF-transfected COS 7 cells, as these cells give a particularly high efficiency of transfection. A radiolabelled DNA probe corresponding to a region of the firefly luciferase cistron between the *Nco*I and *Ava*I sites was generated by random primed DNA synthesis in the presence of <sup>32</sup>P-labelled dCTP, using Klenow polymerase (figure 3.9A). A band of the expected size for dicistronic pRNF RNA was detected, but a smaller band that might be expected to correspond to monocistronic transcripts was also visible (figure 3.9B). However, it is possible that the smaller band could be an artefact, as similar bands have been observed on Northern analysis of RNA derived from pRMF and pRBF (a vector that contains the BAG-1 IRES) (M. Stoneley and M.J. Coldwell, personal communication).

To examine further the identity of this band, RNase protection analysis was carried out. A region spanning the most 3' 76 nucleotides of the *Renilla* luciferase cistron, the intercistronic spacer and N-myc 5' UTR, and the most 5' 101 nucleotides of the firefly luciferase cistron was amplified from pRNF by PCR with the primers RNaseF and Hluc3'. This fragment was digested with *Hind*III and inserted into the vector pSK+Bluescript between the *Hind*III site and the *Bam*HI site, which was filled in with Klenow fragment to create a blunt end (figure 3.10). The resultant vector, pSKRNaseN, was linearised with *Not*I, allowing production of an antisense riboprobe by *in vitro* transcription from the T7 promoter. This radiolabelled transcript should hybridise to any RNA molecules bearing the firefly luciferase cistron (figure 3.11). Following digestion of single stranded RNA, the size of radiolabelled RNA molecules remaining indicates the length of transcript that was able to hybridise to the probe. Analysis was carried out using RNA from pRNF-transfected HeLa cells, with RNA from mock-transfected HeLa cells and yeast tRNA as controls (figure 3.12). The single band protected in lane 3 is of the expected size for full-length dicistronic pRNF RNA (546 nucleotides). No further bands of greater than 101nt in length are visible, therefore there is no RNA present that could represent monocistronic firefly luciferase transcripts. No products were detected in lanes 1 and 2, indicating that hybridisation was specific. This leads to the conclusion that the smaller band detected by

### 1. Cryptic promoter



### 2. Cryptic splice acceptor site



### 3. RNA cleavage site

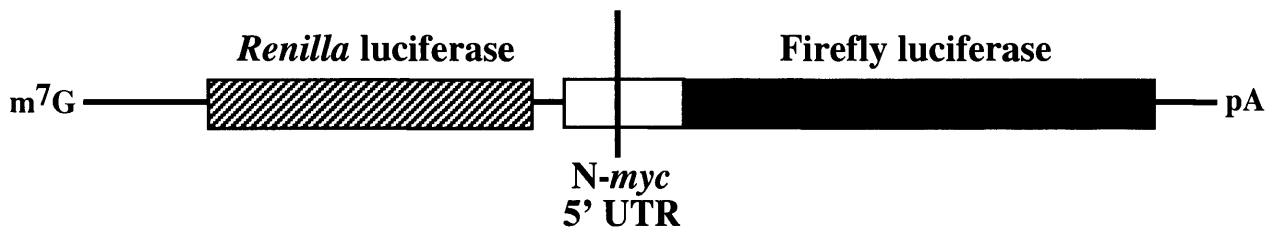


**Figure 3.8 Possible methods of production of monocistronic transcripts.** The presence of a cryptic promoter, a cryptic splice acceptor site or an RNA cleavage site within the N-*myc* 5' UTR would result in the production of monocistronic transcripts bearing the firefly luciferase cistron and a portion of the 5' UTR. In the first two instances the resultant transcript would be capped, and in all cases it would retain a poly(A) tail.

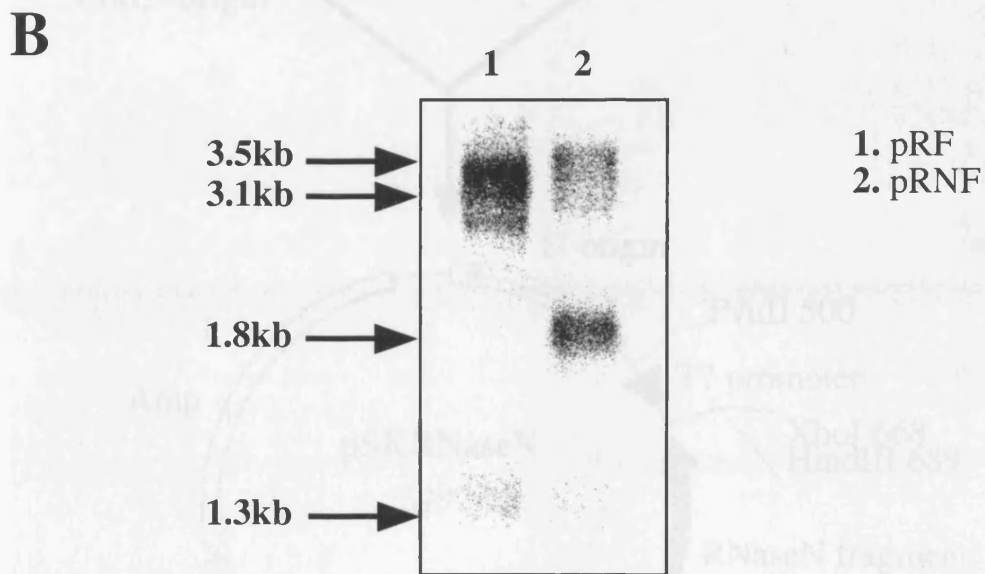
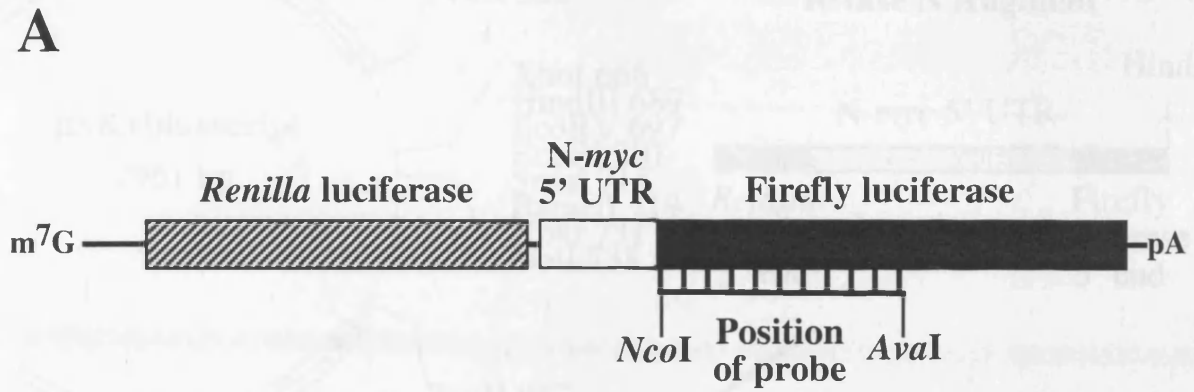


**Figure 3.9 Northern blot analysis of transcripts from pRNF-transfected cells.** COS 7 cells were transfected with pRF or pRNF and poly(A)<sup>+</sup> RNA was isolated and subjected to Northern blotting. (A) The membrane was probed with radiolabelled DNA derived from the firefly luciferase coding region. (B) Radiolabelled bands visualised after probing.

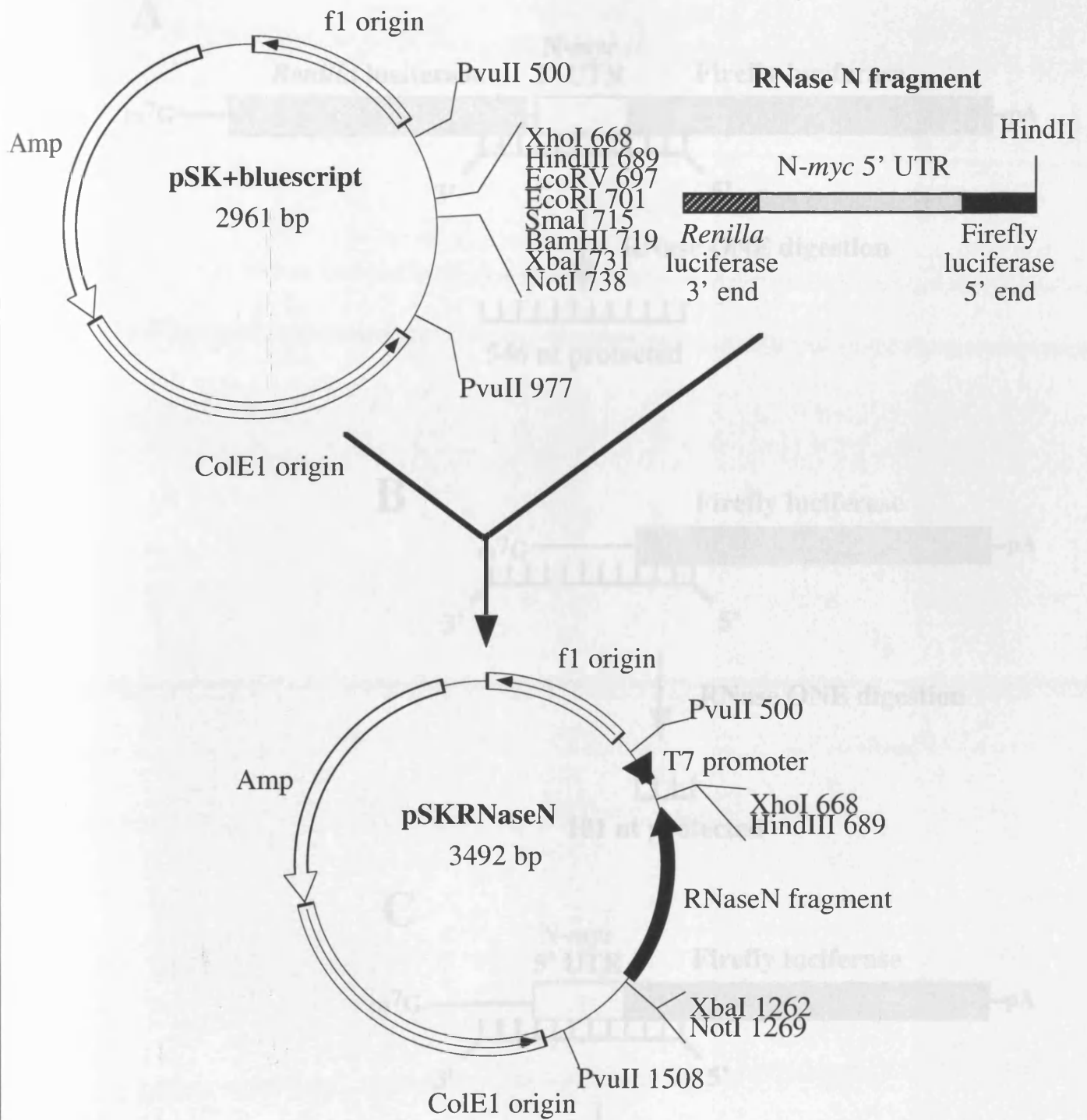


**Figure 3.10 Construction of the vector pSKRNaseN.** A fragment spanning the 3' end of the *Renilla luciferase* coding region, the N-myc 5' UTR and the 5' end of the firefly luciferase coding region was amplified from the vector pRNF by PCR, digested with *HindIII*, and inserted in the vector pSK+bluescript between the *HindIII* site and the filled-in *BamHI* site in an antisense fashion relative to the T7 promoter.



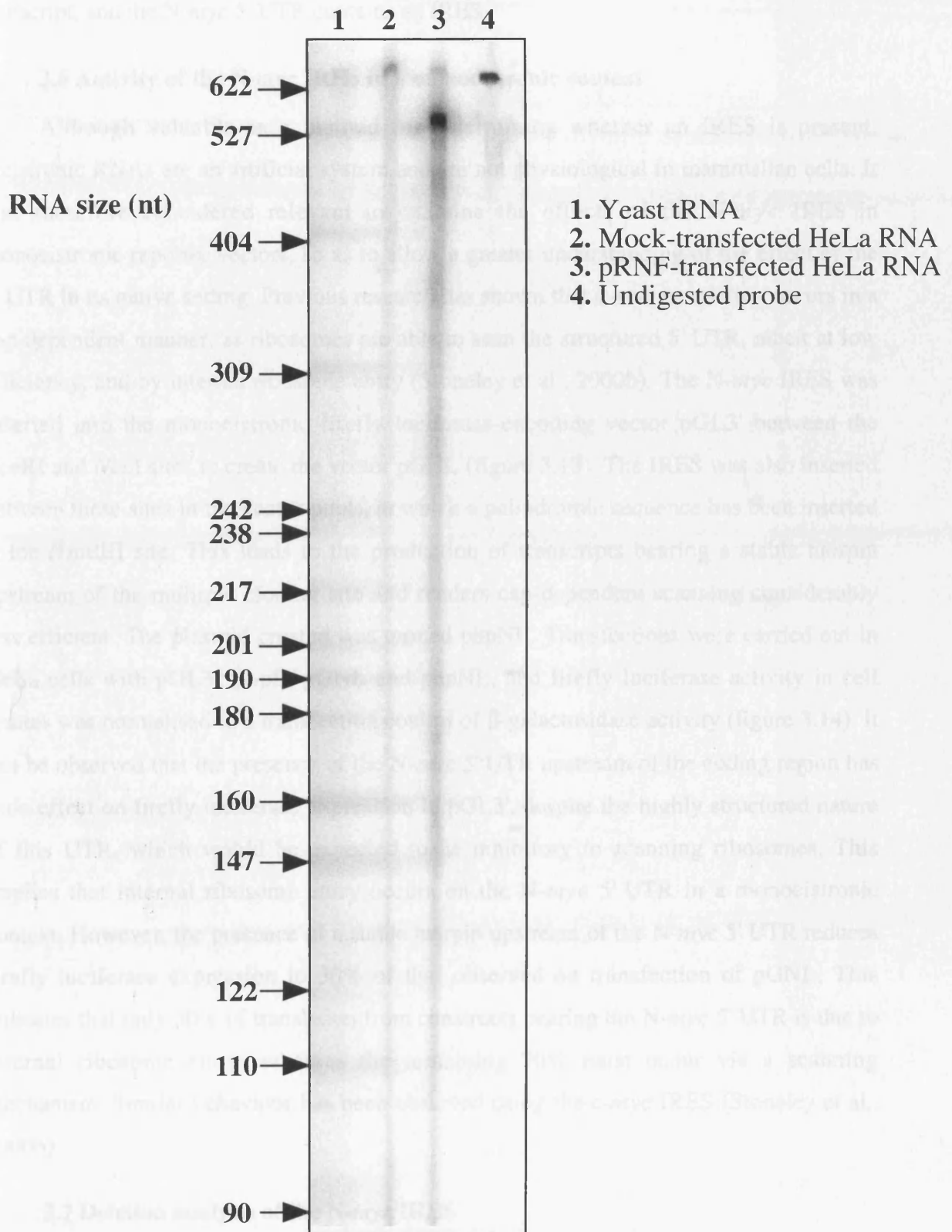


**Figure 3.12 RNase protection analysis of RNA from pRNF-transfected cells.** Poly(A)<sup>+</sup> selected RNA from HeLa cells transfected with pRNF or mock-transfected HeLa cells, or yeast tRNA, was hybridised to a radiolabelled antisense riboprobe, and single stranded RNA was digested using RNase ONE. The products were separated by electrophoresis on a 7M urea/4% polyacrylamide gel in parallel with radiolabelled pBR322/*Hpa*II markers.

Northern blotting did not correspond to a functional monocistronic firefly luciferase transcript, and the N-myc 5' UTR contains an IRES.

### 3.6 Activity of the N-myc IRES in a monocistronic context

Although valuable as a method for determining whether an IRES is present, dicistronic RNAs are an artificial system and are not physiological in mammalian cells. It was therefore considered relevant to examine the effects of the N-myc IRES in monocistronic reporter vectors, so as to allow a greater understanding of the effect of the 5' UTR in its native setting. Previous research has shown that c-myc translation occurs in a cap-dependent manner, as ribosomes are able to scan the structured 5' UTR, albeit at low efficiency, and by internal ribosome entry (Stoneley et al., 2000b). The N-myc IRES was inserted into the monocistronic firefly luciferase-encoding vector pGL3' between the *EcoRI* and *NcoI* sites to create the vector pGNL (figure 3.13). The IRES was also inserted between these sites in the vector phpL, in which a palindromic sequence has been inserted at the *HindIII* site. This leads to the production of transcripts bearing a stable hairpin upstream of the multiple cloning site and renders cap-dependent scanning considerably less efficient. The plasmid created was termed phpNL. Transfections were carried out in HeLa cells with pGL3', phpL, pGNL and phpNL, and firefly luciferase activity in cell lysates was normalised to a transfection control of  $\beta$ -galactosidase activity (figure 3.14). It can be observed that the presence of the N-myc 5' UTR upstream of the coding region has little effect on firefly luciferase expression in pGL3', despite the highly structured nature of this UTR, which would be expected to be inhibitory to scanning ribosomes. This implies that internal ribosome entry occurs on the N-myc 5' UTR in a monocistronic context. However, the presence of a stable hairpin upstream of the N-myc 5' UTR reduces firefly luciferase expression to 30% of that observed on transfection of pGNL. This indicates that only 30% of translation from constructs bearing the N-myc 5' UTR is due to internal ribosome entry, whereas the remaining 70% must occur via a scanning mechanism. Similar behaviour has been observed using the c-myc IRES (Stoneley et al., 2000b).

### 3.7 Deletion analysis of the N-myc IRES

To examine in detail which regions of the N-myc 5' UTR contribute to IRES activity, a series of deletion constructs was created. PCR amplification was carried out using

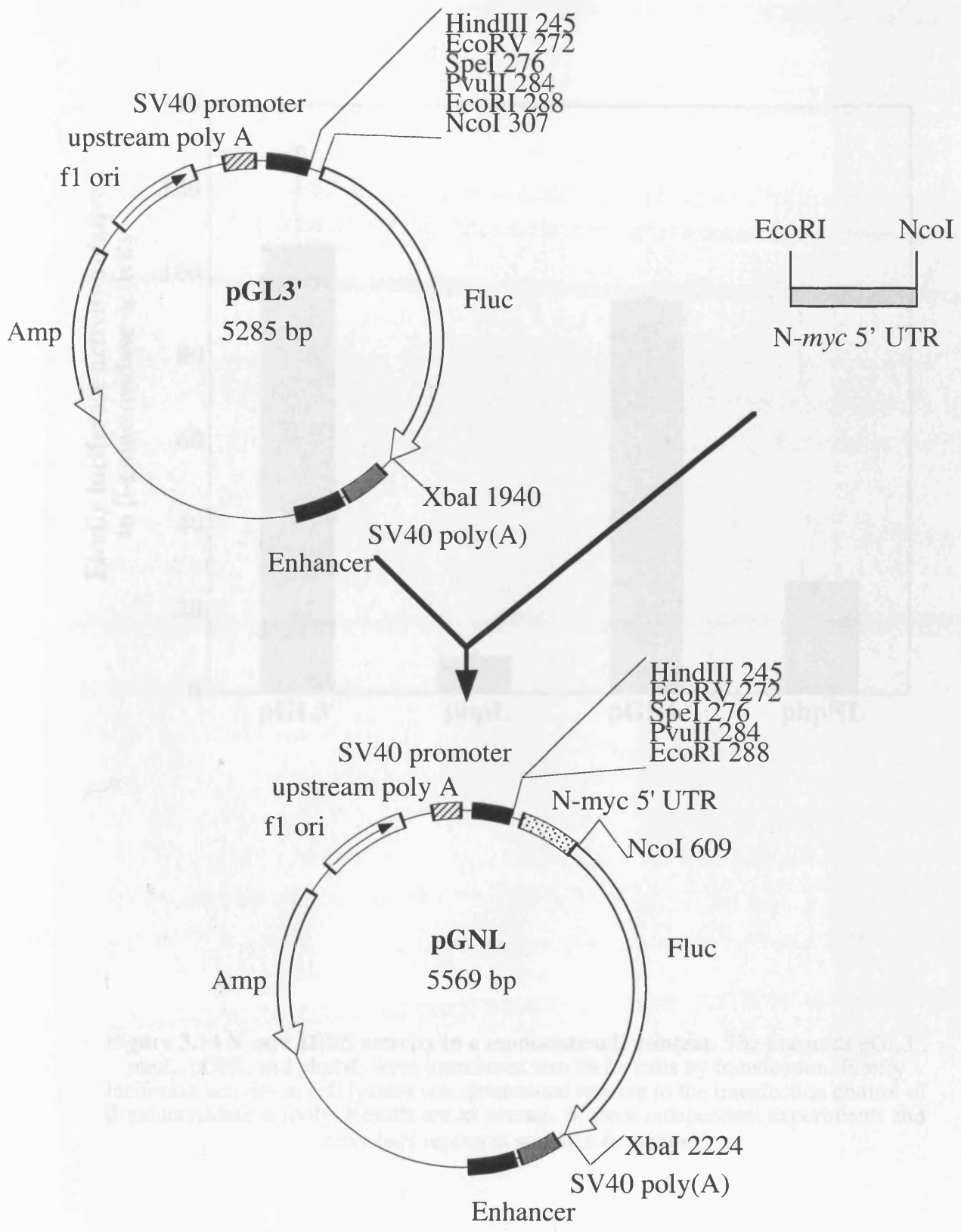


**Figure 3.13 Construction of the vector pGNL.** An RT-PCR product encoding the N-myc 5' UTR was digested with *EcoRI* and *NcoI*, and inserted between these sites in the vector pGL3' after digestion and dephosphorylation of the vector.

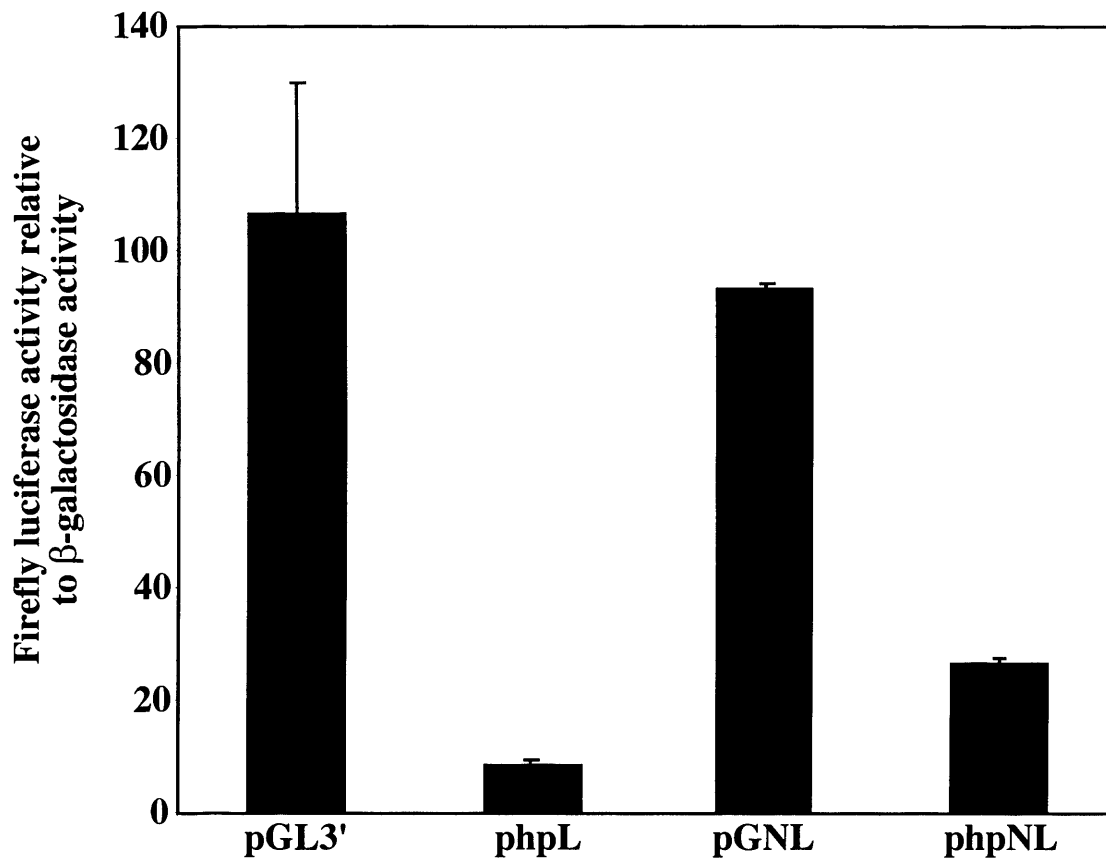


**Figure 3.14 *N-myc* IRES activity in a monocistronic context.** The plasmids pGL3', phpL, pGNL and phpNL were introduced into HeLa cells by transfection. Firefly luciferase activity in cell lysates was determined relative to the transfection control of  $\beta$ -galactosidase activity. Results are an average of three independent experiments and error bars represent standard deviations.

primers that hybridise in different places on the UTR, with wild type pRNF as a template. The resultant PCR products were digested with *EcoRI* and *NcoI* and inserted in pRF in the intercistronic space. The series of UTR fragments produced is shown in figure 3.15. These plasmids were then used to transfect HeLa cells in parallel with the wild type vector pRNF, and IRES activity was calculated by normalising firefly luciferase activity to that of *Renilla* luciferase (figure 3.16). Deletion of the most 5' 86 nucleotides reduced the IRES activity to 30% of wild type levels, indicating a significant role for this region, but no further reduction was observed on deletion of the next 70nt. When a further 85nt segment was removed, activity was reduced to only 7% of wild type levels. All deletions from the 3' end of the UTR had a drastic effect on IRES activity. Removal of 74nt reduced the activity to 20% of wild type levels, while successive deletions caused almost complete abolition of IRES activity. Constructs in which both the 5' and 3' ends were deleted also demonstrated very low IRES activity. This indicates that the entire UTR is necessary for the IRES to be fully active, but elements residing towards the 3' end are particularly crucial to its function. This is in contrast to the *c-myc* IRES, in which deletions from both ends of the UTR cause a gradual reduction in IRES activity, and the most 3' 56nt can be deleted with no effect on activity.

To further define the region of the 5' UTR necessary for full activity, a shorter 3' deletion was made by the PCR method used previously. Removal of the most 3' 24nt reduced IRES activity to 37% of wild type levels (figure 3.17), a surprisingly large effect for such a small proportion of the full UTR. This region does not contain any known *cis*-acting IRES motifs, the deletion of which would be expected to cause a significant reduction in activity.

Given the data presented above, it was considered possible that the 5' end of the N-myc coding region might play a role in IRES activity, as this could account for the presence of crucial elements so close to the 3' end of the 5' UTR. An involvement of part of the coding region in IRES activity has been observed in the HCV, CSFV and GB virus B IRESs (Rijnbrand et al., 2001). RT-PCR was therefore carried out on poly(A)<sup>+</sup> RNA from SH-SY5Y cells using the primers CJNF and NREXT, such that a region spanning the entire 5' UTR and 60nt of the coding region was amplified. This fragment was inserted into pRF between the *EcoRI* and *NcoI* sites. The reverse primer was designed such that the fragment would be inserted with the N-myc initiation codon in frame with the firefly

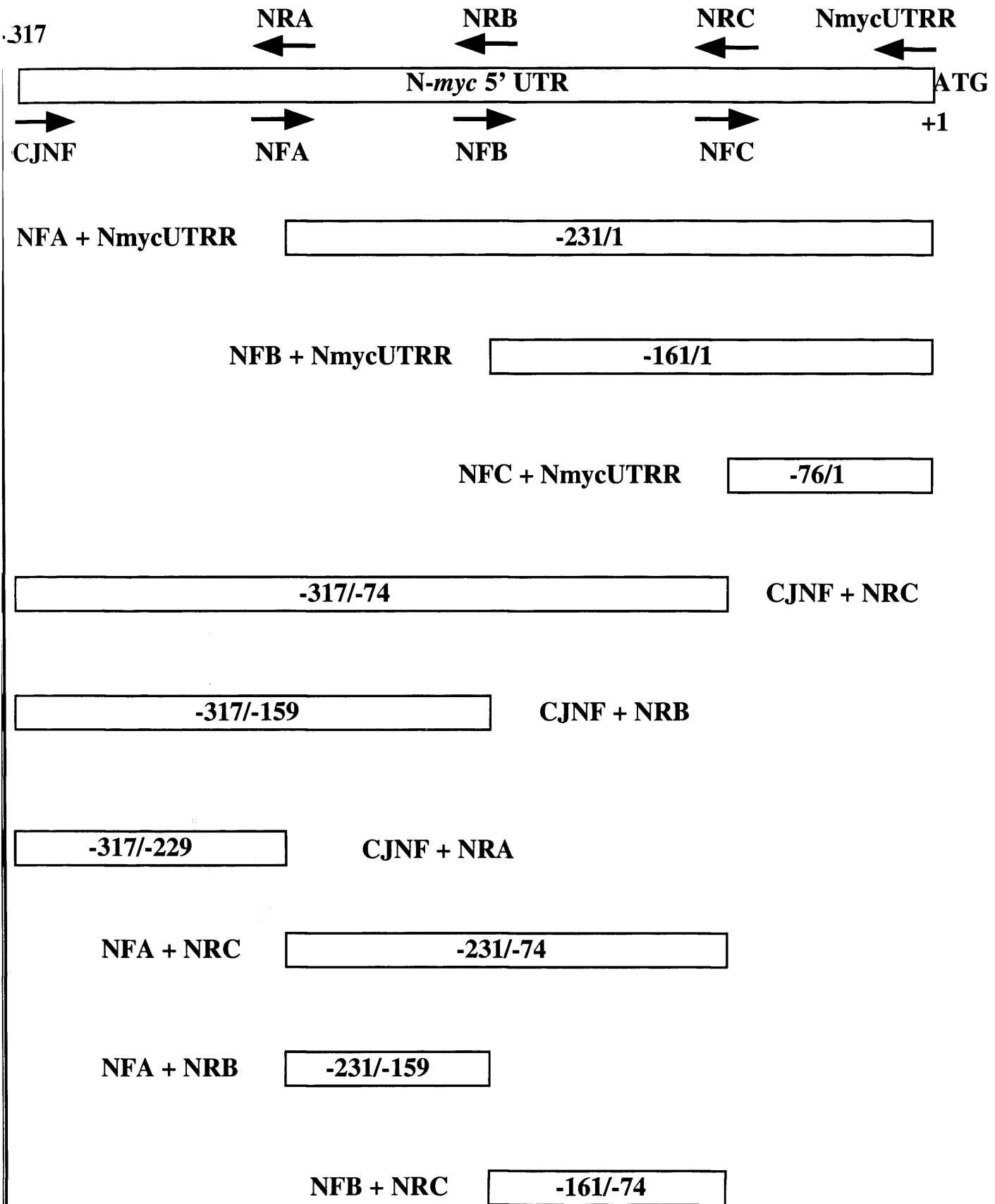


**Figure 3.15 Construction of an N-myc 5' UTR deletion series.** A series of fragments of the N-myc 5' UTR was created by PCR amplification from pRNF using the primers indicated. The products were digested with *Eco*RI and *Nco*I and inserted into pRF between these sites.

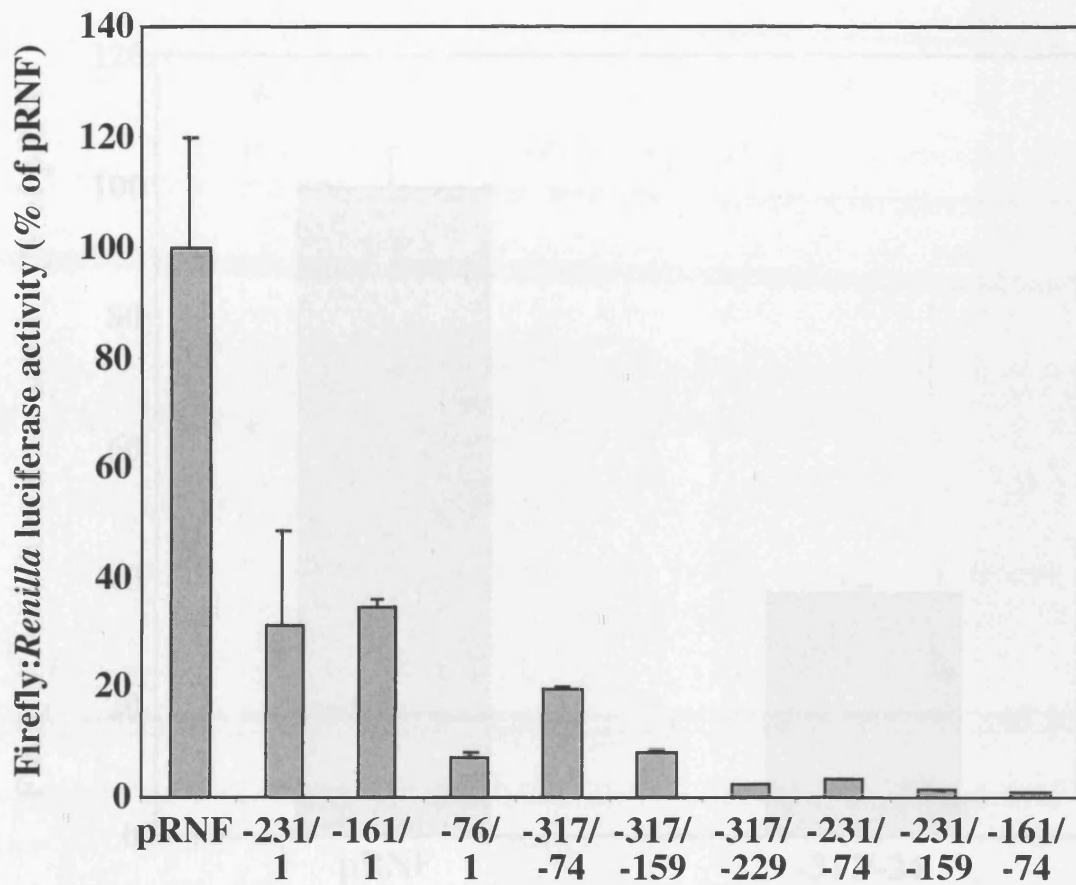


**Figure 3.16 IRES activity of N-myc 5' UTR deletion mutants.** The fragments of the N-myc 5' UTR indicated were inserted into the vector pRF and introduced into HeLa cells by transfection in parallel with the wildtype pRNF vector. IRES activity of the deletion mutants was calculated as a ratio of firefly:*Renilla* luciferase activity and expressed as a percentage of pRNF IRES activity. Results are an average of three independent experiments and error bars represent standard deviations.

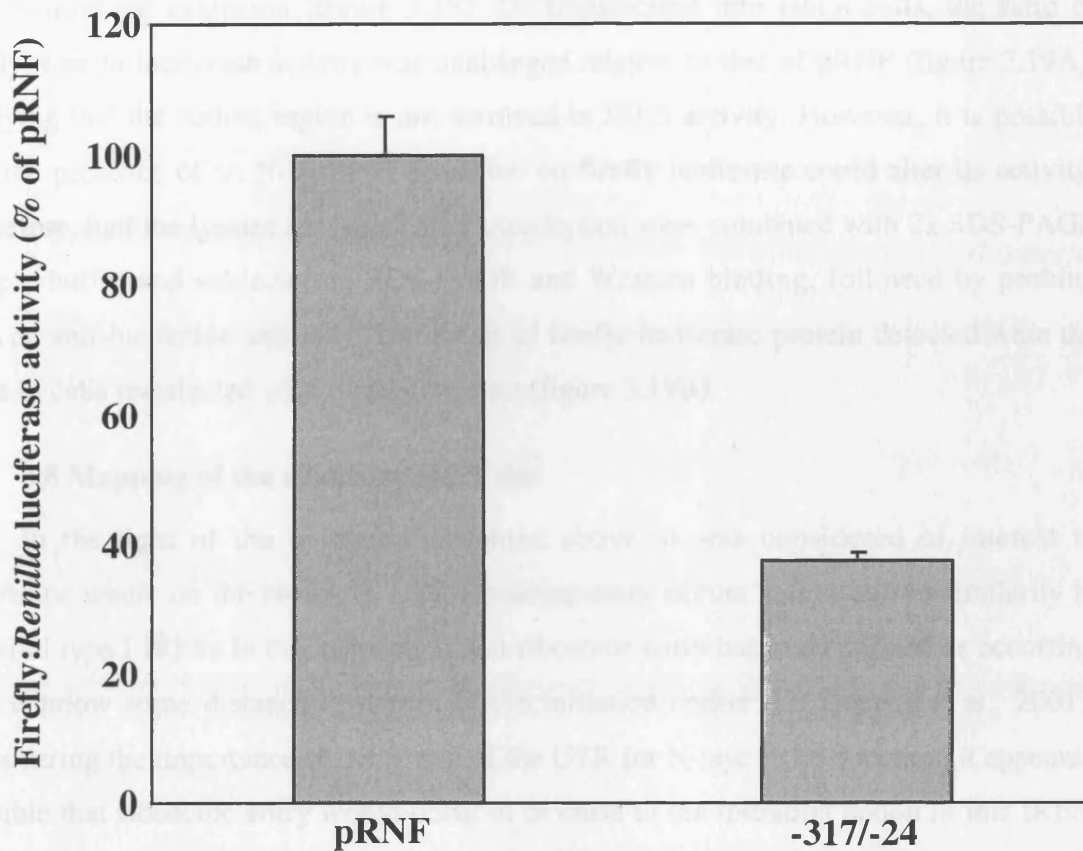


**Figure 3.17 IRES activity of a fragment of the *N-myc* 5' UTR in which only the extreme 3' end is deleted.** PCR amplification of the *N-myc* 5' UTR using the primers CJNF and NRD was used to create a mutant in which only the most 3' 24nt were deleted. This fragment was inserted into pRF between the *Eco*RI and *Nco*I sites and transfected into HeLa cells in parallel with pRNF. IRES activity is expressed by the ratio of firefly:*Renilla* luciferase as a percentage of pRNF values. Results are an average of three independent experiments and error bars represent standard deviations.

luciferase coding region, leading to the production of firefly luciferase with a 20 amino acid N-terminal extension (figure 3.18). On transfection into HeLa cells, the ratio of firefly:*Renilla* luciferase activity was unchanged relative to that of pRNF (figure 3.19A), implying that the coding region is not involved in IRES activity. However, it is possible that the presence of an N-terminal extension on firefly luciferase could alter its activity. Therefore, half the lysates harvested after transfection were combined with 2x SDS-PAGE sample buffer and subjected to SDS-PAGE and Western blotting, followed by probing with an anti-luciferase antibody. The levels of firefly luciferase protein detected were the same in cells transfected with either construct (figure 3.19B).

### 3.8 Mapping of the ribosome entry site

In the light of the evidence presented above, it was considered of interest to determine where on the N-myc 5' UTR ribosome entry occurs. *c-myc* shows similarity to the viral type I IRESs in this respect, in that ribosome entry has been defined as occurring in a window some distance upstream of the initiation codon (Le Quesne et al., 2001). Considering the importance of the 3' end of the UTR for N-myc IRES function, it appeared possible that ribosome entry would occur at or close to the initiation codon in this IRES. An in frame AUG codon resides 24 nt upstream of the initiation codon. As ribosome entry within viral IRESs has been found to occur at AUG codons (Jackson et al., 1995), this was a potential site for ribosome landing. Hence, this AUG was mutated to UUG (figure 3.20, blue), a codon from which translation is rarely initiated and which has not been found to be used for ribosome entry. This mutation had a small stimulatory effect (110%) on N-myc IRES activity on transfection into HeLa cells (figure 3.21), but this effect is not great enough to be significant and therefore this is unlikely to be the ribosome binding site. In addition, the -317/-24 deletion mutant retains this AUG as the firefly luciferase initiation codon. If ribosome entry occurred at this site this deletion would be expected to have no effect on activity.

A series of constructs was therefore generated by mutagenic PCR so as to create RNA molecules containing AUG codons within the UTR that are out of frame relative to the firefly luciferase initiation codon. If the ribosome acquires the message upstream of such an AUG and scans the remainder of the UTR, translation will initiate when this AUG is encountered. This will lead to the production of a nonsense protein as translation will be

CJNF



aggaattcgtctggacgcgctgggtggatgcggg

-317 gtctggacgc gctgggtgga tgcggggggc tcttggaac tgtgttgag

-267 ccgagcaagc gctagccagg cgcaagcgcg cacagactgt agccatccga

-217 ggacaccccc gcccccccg cccaccgga gacaccgcg cagaatgcc

-167 tccgatccc ctgcagtcgg cgggagtgtt ggaggtcggc gccggcccc

-117 gccttcgcg cccccacgg gaaggaagca cccccgtat taaaacgaac

-67 ggggcggaaa gaagccctca gtcgccggc gggaggcgag ccgatccga

-17 gctgtccac gtcacc**ATG** ccgggatga tctgcaagaa ccagacctc

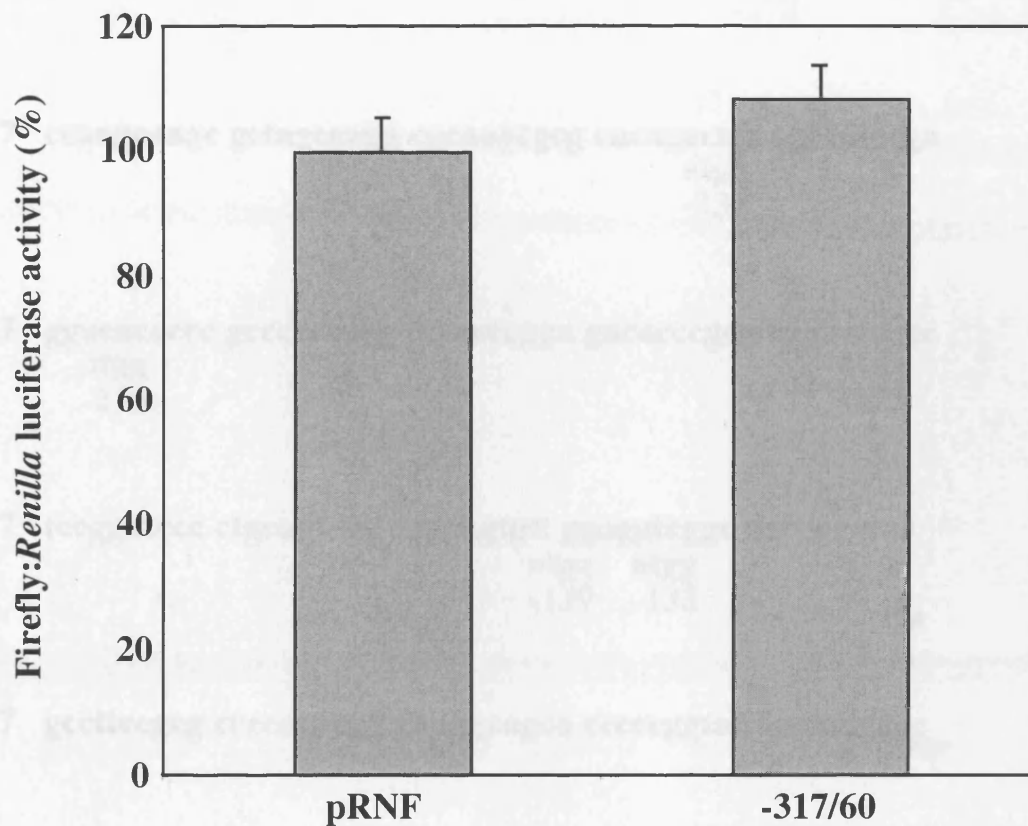
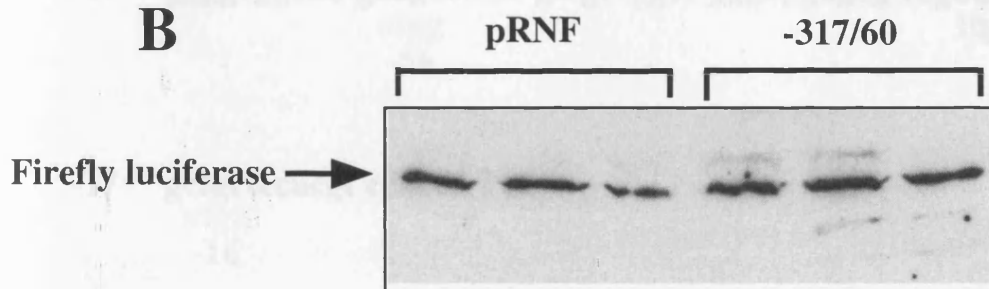
+34 gagttgact cgctacagcc ctgctcc**ATG**  
actgagcgatgctgggacgaggtaccgct



NREXT

**Figure 3.18 Sequence of the N-myc 5' UTR and the 5' end of the N-myc coding region.** A cDNA corresponding to the N-myc 5' UTR (black) attached to the first 60nt of its coding region (blue) was obtained by RT-PCR using the primers CJNF and NREXT (purple). The positions of the authentic initiation codon, and of the firefly luciferase initiation codon when this product was inserted into pRF, are shown in red.

Figure 3.18 IRES activity of a construct bearing part of the coding region of N-myc. A region spanning the N-myc 5' UTR and the first 60 nt of its coding region was amplified from SH-SY5Y RNA by RT-PCR using the primers CJNF and NREXT and inserted in the vector pRF between the EcoRI and NotI sites. (A) The IRES activity of this construct was determined by the ratio of firefly *Renilla luciferase* activity as a percentage of that of pRF in transfection into HeLa cells. Results are an average of three independent experiments and error bars represent standard deviations. (B) Triplicate cell lysates from the experiment assayed in (A) were also subjected to Western blotting and probed with an anti-firefly luciferase antibody. Equal loading of proteins was confirmed by Ponceau staining.

**A****B****Figure 3.19 IRES activity of a construct bearing part of the coding region of N-myc.**

A region spanning the N-myc 5' UTR and the first 60 nt of the coding region was amplified from SH-SY5Y RNA by RT-PCR using the primers CJNF and NREXT and inserted in the vector pRF between the *EcoRI* and *NcoI* sites. (A) The IRES activity of this construct was determined by the ratio of firefly:*Renilla* luciferase activity as a percentage of that of pRNF on transfection into HeLa cells. Results are an average of three independent experiments and error bars represent standard deviations. (B) Triplicate cell lysates from one experiment assayed in (A) were also subjected to Western blotting and probed with an anti-firefly luciferase antibody. Equal loading of proteins was confirmed by Ponceau staining

-317 gctcggacgc gctgggtgga tgcggggggc tctgggaac tgtgttgag  
 atgg  
 -278

-267 ccgagcaage gctagccagg cgcaagecgc cacagactgt agccatccga  
 atgg  
 -232

-217 ggacaccccc gcccccegg ccacccgga gacaccegc cagaatcgc  
 atgg  
 -215 atgg  
 -173

-167 tccggatecc ctgcagtcgg cgggagtgt ggaggtcgg gccggcccc  
 atgg atgg  
 -139 -133

-117 gccttcgcg cccccacgg gaaggaagca cccccgtat taaaacgaac

-67 ggggeggaaa gaagccctca gtcgccggcc gggaggcgag ccgatgccga  
 atgg  
 -56 ttg

-17 gctgctcacgt ccaccATG  
 atgg  
 -16

**Figure 3.20 Positioning of out of frame AUG mutations in the N-myc IRES.** DNA encoding the N-myc IRES in the vector pRNF was mutated to introduce the sequence ATGG at each of the positions shown in red. Later mutations are shown in purple. On transfection into cells, this would lead to the creation of transcripts bearing an out of frame AUG codon upstream of the firefly luciferase initiation codon. An additional mutation was created at position -24 as shown in blue, such that an in frame upstream AUG codon was altered to UUG.

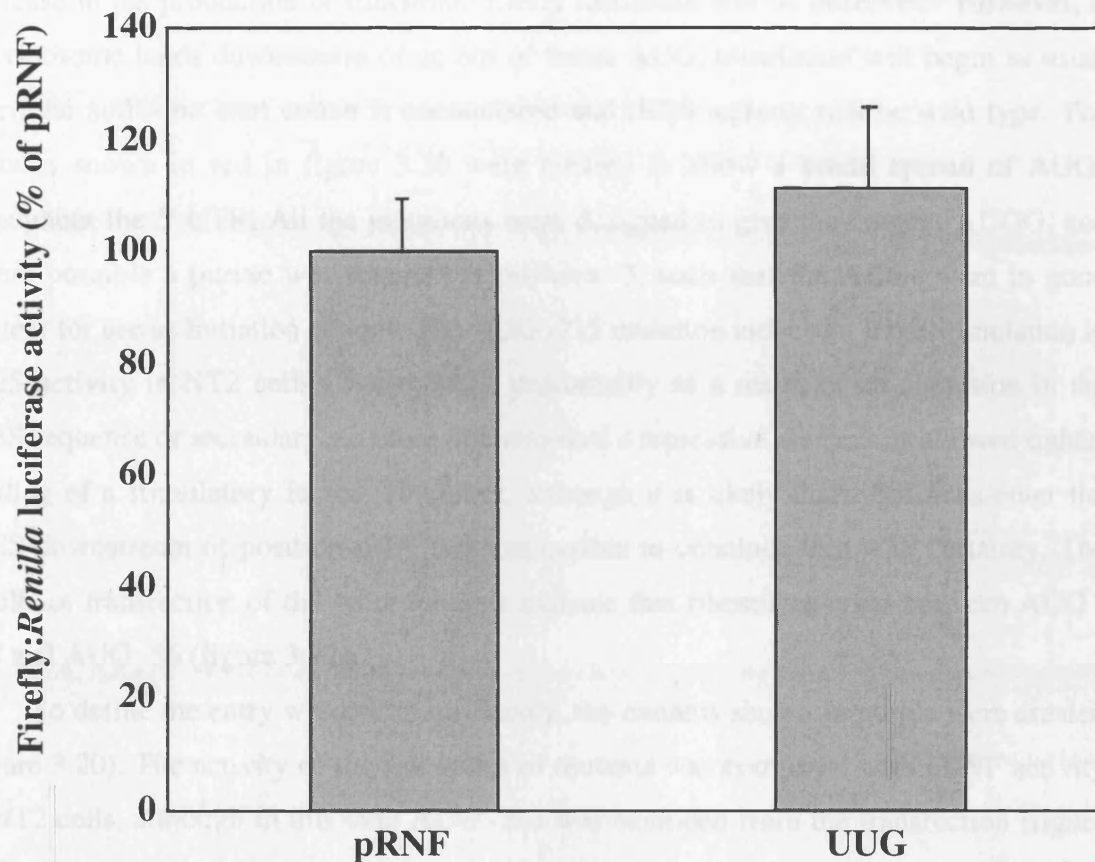


**Figure 3.21 Result of transfection of an N-myc IRES construct in which an upstream AUG has been mutated to UUG.** A mutant version of pRNF bearing a UUG codon at position -24, where an in frame AUG codon is found in the wild type IRES, was introduced into HeLa cells by transfection in parallel with wild type pRNF. IRES activity was determined as a ratio of firefly:*Renilla* luciferase activity and expressed as a percentage of pRNF values. Results are an average of three independent experiments and error bars represent standard deviations.

out of frame when the firefly luciferase coding region is encountered. Therefore, a decrease in the production of functional firefly luciferase will be observed. However, if the ribosome lands downstream of an out of frame AUG, translation will begin as usual when the authentic start codon is encountered and IRES activity will be wild type. The mutants shown in red in figure 3.20 were created to allow a broad spread of AUGs throughout the 5' UTR. All the mutations were designed to give the context AUGG, and where possible a purine was retained at position -3, such that the AUGs were in good context for use as initiation codons. The AUG -215 mutation induced a large stimulation in IRES activity in NT2 cells (figure 3.22), presumably as a result of an alteration in the IRES sequence or secondary structure that removed a repressive element or allowed tighter binding of a stimulatory factor. Therefore, although it is likely that ribosomes enter the IRES downstream of position -215, it is impossible to conclude this with certainty. The results of transfection of the other mutants indicate that ribosomes enter between AUG -278 and AUG -56 (figure 3.22).

To define the entry window more closely, the mutants shown in purple were created (figure 3.20). The activity of the full series of mutants was compared with pRNF activity in NT2 cells, although in this case AUG -215 was excluded from the transfection (figure 3.23). The slightly enhanced activity of AUG -238 supported the theory that AUG -215 lies upstream of the entry window, and this was confirmed by the fact that AUG -173 displayed wild type activity. AUG -139 and AUG -133 are both able to induce a partial reduction in functional firefly luciferase. This makes it difficult to define the ribosome entry window precisely, although it can be stated with a degree of certainty that it lies between positions -173 and -56. It is possible that ribosomes enter upstream of position -139, and AUGs -139 and -133 are in poor context for translation initiation so that they are only used by a small proportion of scanning ribosomes. Alternatively, it is possible that ribosomes acquire the message immediately upstream of this region and are not yet fully competent to initiate translation as they scan through it. A third possibility is that there are several sites of ribosome entry between -173 and -56, so that a subset of ribosomes enter upstream of -139. A final explanation is that the area around AUGs -139 and -133 is important for IRES function, and these mutations alter the sequence or structure such that IRES activity is reduced, although ribosomes enter downstream of this region. It is impossible to distinguish between these mechanisms on the basis of the data presented.

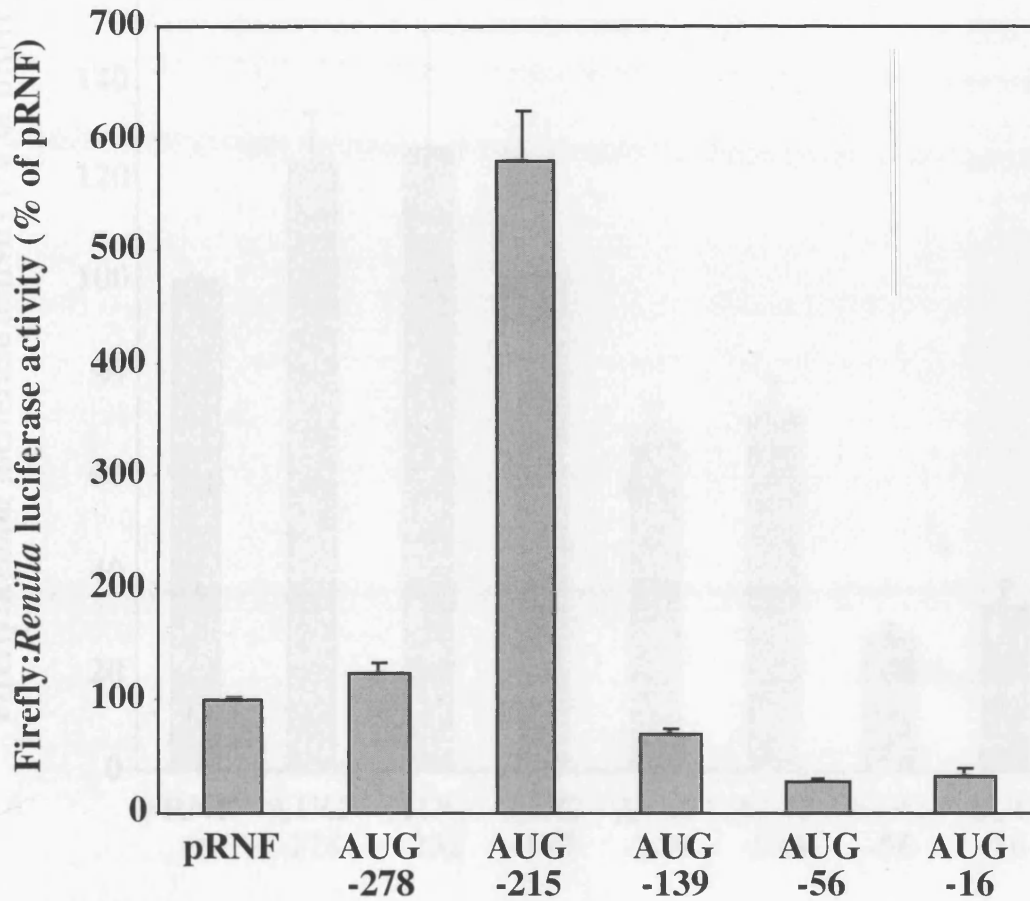


**Figure 3.22 Result of transfection of N-myc IRES mutants with out of frame AUG codons.** Mutant versions of pRNF bearing the out of frame initiation codons shown in red in figure 3.20 were introduced into NT2 cells by transfection in parallel with wild type pRNF. IRES activity was determined as a ratio of firefly:*Renilla* luciferase activity and expressed as a percentage of pRNF values. Results are an average of three independent experiments and error bars represent standard deviations.

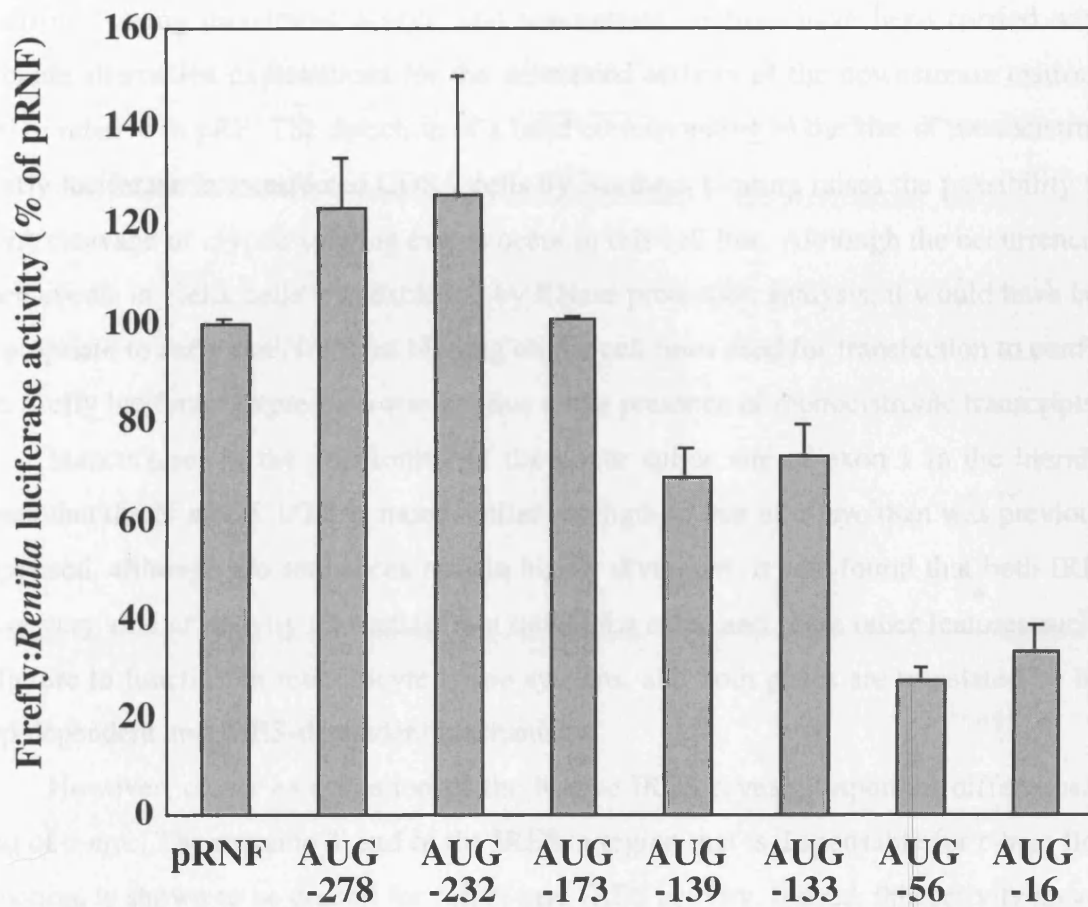


**Figure 3.23 Result of transfection of additional N-myc IRES mutants with out of frame AUG codons.** Mutant versions of pRNF bearing the out of frame initiation codons shown were introduced into NT2 cells by transfection in parallel with wild type pRNF.

IRES activity was determined as a ratio of firefly:*Renilla* luciferase activity and expressed as a percentage of pRNF values. Results are an average of three independent experiments and error bars represent standard deviations.

### 3.9 Discussion

The initial hypothesis that the N-*myc* 5' UTR could contain an IRES has been confirmed using dicistronic assays, and appropriate controls have been carried out to exclude alternative explanations for the stimulated activity of the downstream cistron in pRNF relative to pRF. The detection of a band corresponding to the size of monocistronic firefly luciferase in transfected COS 7 cells by Northern blotting raises the possibility that RNA cleavage or cryptic splicing events occur in this cell line. Although the occurrence of such events in HeLa cells was excluded by RNase protection analysis, it would have been appropriate to carry out Northern blotting on the cell lines used for transfection to confirm the firefly luciferase expression was not due to the presence of monocistronic transcripts.

Inaccuracies in the positioning of the donor splice site of exon 1 in the literature mean that the N-*myc* 5' UTR is more similar in length to that of c-*myc* than was previously supposed, although the sequences remain highly divergent. It was found that both IRESs have very similar activity on transfection into HeLa cells, and share other features such as a failure to function in reticulocyte lysate systems, and both genes are translated by both cap-dependent and IRES-dependent mechanisms.

However, closer examination of the N-*myc* IRES reveals important differences to that of c-*myc*. The extreme 3' end of the IRES, a region that is dispensable for c-*myc* IRES function, is shown to be crucial for full N-*myc* IRES activity. Indeed, this activity appears to be considerably more dependent on the presence of the entire 5' UTR than that of the c-*myc* IRES. The N-*myc* IRES is 81nt shorter than that of c-*myc*, and perhaps represents a minimal IRES from which extraneous sequence has been excluded. Another significant difference was observed in the positioning of the ribosome entry window within the IRES. In c-*myc* this is between positions -219 and -202 (Le Quesne et al., 2001), upstream of the complex structural element of a double pseudoknot. In N-*myc* it has proved difficult to define the entry window precisely, although it has been reduced to a 117nt region. It is possible that ribosome binding occurs at multiple positions within this window, which is unprecedented in previously studied IRESs. However, further mutations will be needed to prove that this is the case, or to map the region of entry more precisely. Ideally it would be necessary to formulate a structural model for the N-*myc* IRES and relate this to the position of the ribosome binding site.

It is possible that the common features of c- and N-Myc proteins have presented a false illusion that the IRESs should operate by the same mechanism. The similar length and activity of the two IRESs does not necessarily mean that they have anything else in common. An interesting feature of both, however, is that their activity is considerably greater than that of most other cellular IRESs identified to date and, indeed, of highly active viral IRESs such as EMCV. The similarity in size probably relates to the common evolutionary background of both genes, but perhaps more recent developments have allowed each IRES to assume its own optimum method of operation, resulting in elements of similar efficiency but different mechanism.

## Chapter 4

### Internal ribosome entry in the *L-myc* 5' UTR

#### 4.1 Introduction

The *L-myc* gene shares the same three exon, two intron structure as *c-* and *N-myc*, and also has its major initiation codon positioned towards the 5' end of exon 2 such that exon 1 is entirely non-coding (figure 1.10C). Unlike the other *myc* genes, the *L-myc* transcript is subject to alternative splicing. One of the sites where this occurs is within the 5' UTR, as intron A may be spliced or unspliced, such that two distinct forms of the UTR are made. These show little sequence similarity to the *c-* or *N-myc* 5' UTRs, but are long and possess a high degree of predicted secondary structure. The shorter isoform is 217nt in length and consists of 80.6% Gs and Cs, whereas the unspliced version is 581nt long and 77.5% GC in content. As *L-myc* is a proto-oncogene with tightly regulated expression, like the other members of the *myc* family, this led to the hypothesis that the *L-myc* 5' UTRs might contain internal ribosome entry segments.

#### 4.2 RT-PCR and cloning of the *L-myc* 5' UTR

Two isoforms of the *L-myc* 5' UTR exist, as intron A (shown in blue in figure 4.1) is spliced out in some transcripts but retained in others (Kaye et al., 1988). The exon sequences, present in both forms of the UTR, are shown in black in figure 4.1. Total RNA from HL60 cells was used as a template for RT-PCR using the primers LF2 (purple, figure 4.1) and LR2 (turquoise, figure 4.1) to obtain the short isoform of the UTR. LR2 hybridises to regions of exon 1 and exon 2 and will therefore only amplify cDNA in which intron A is not present. The reverse primer LG2 is complementary to the region spanning the intron A/ exon 2 boundary (purple, figure 4.1) and was used in combination with LF2 in a separate RT-PCR reaction, also using HL60 RNA, to obtain the long isoform of the UTR. Both PCR products were digested with the restriction enzymes *EcoRI* and *NcoI* and inserted into the intercistronic region of pRF between these sites (figures 4.2 and 4.3). The plasmids created were designated pRLsF (containing the short isoform) and pRLlF (containing the long isoform).



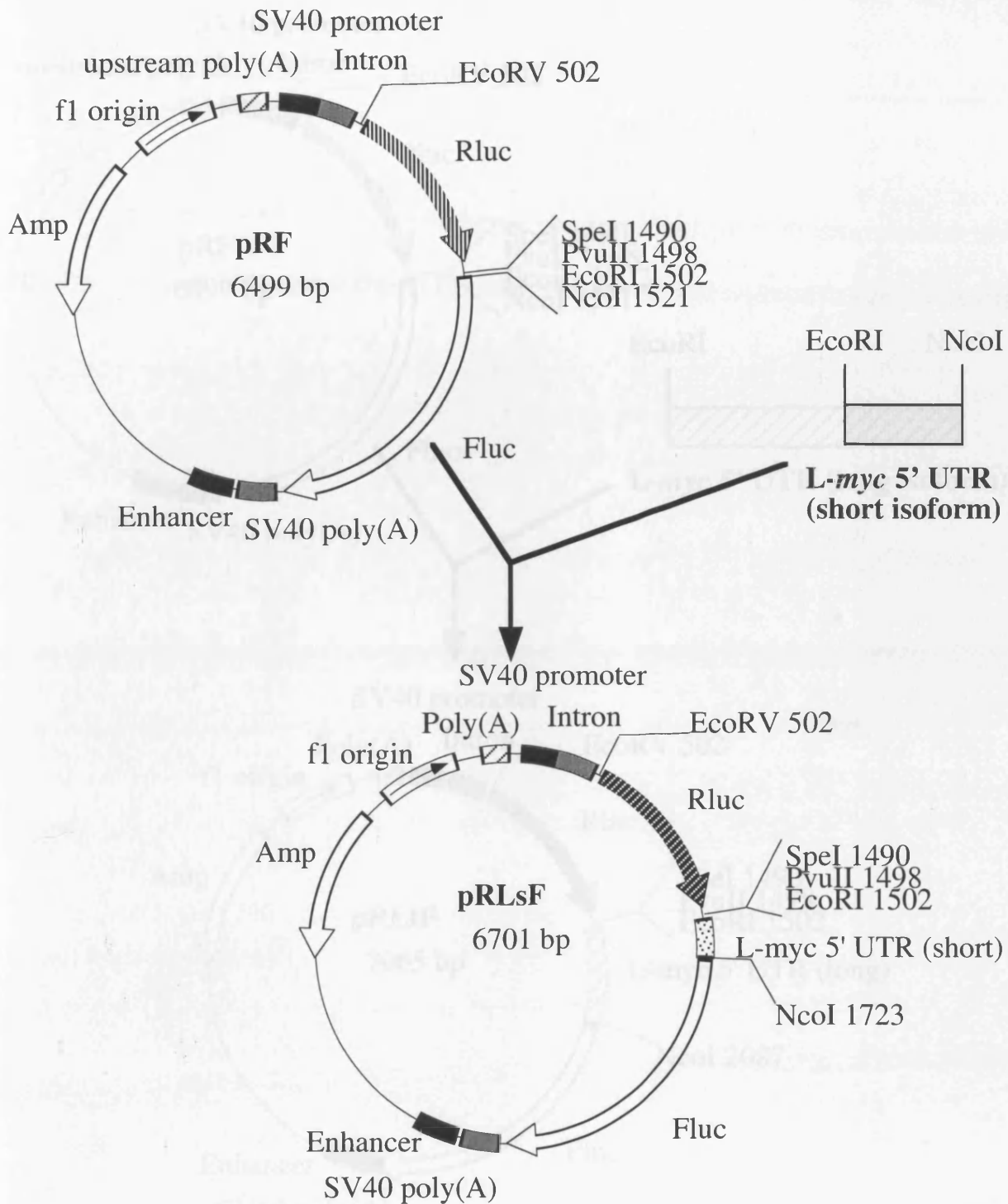


**Figure 4.2 Construction of the vector pRLsF.** The short isoform of the *L-myc* 5' UTR, in which the intron is spliced, was amplified by RT-PCR from HL60 RNA using the primers LF2 and LR2. The product of this reaction was digested with *EcoRI* and *NcoI* and inserted between these sites in pRF following digestion and dephosphorylation of the vector.

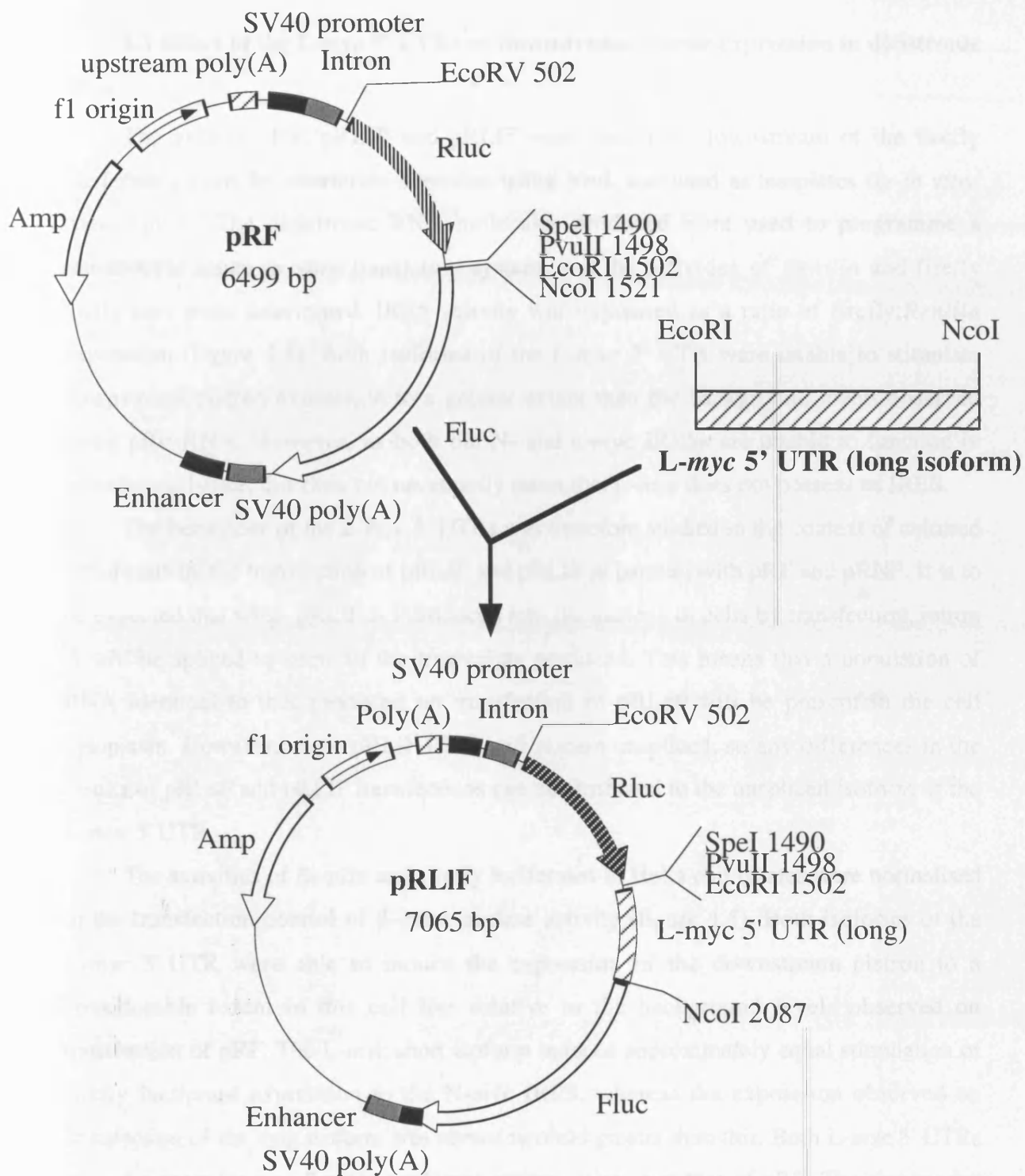


**Figure 4.3 Construction of the vector pRLIF.** The long isoform of the L-myc 5' UTR (containing intron 1) was amplified by RT-PCR from HL60 RNA using the primers LF2 and LG2. The product of this reaction was digested with *EcoRI* and *NcoI*, the plasmid pRF was digested with the same enzymes and dephosphorylated, and the fragment and vector were ligated together to create pRLIF.

### 4.3 Effect of the L-myc 5' UTRs on downstream cistron expression in dicistronic RNA

The vectors pRF, pRLsF and pRLIF were linearised downstream of the firefly luciferase cistron by restriction digestion using *NotI*, and used as templates for *in vitro* transcription. The dicistronic RNA molecules produced were used to programme a reticulocyte lysate *in vitro* translation system, and the activities of *Renilla* and firefly luciferases were determined. IRES activity was expressed as a ratio of firefly:*Renilla* expression (figure 4.4). Both isoforms of the L-myc 5' UTR were unable to stimulate downstream cistron expression to a greater extent than the background levels observed using pRF RNA. However, as both the N- and c-myc IRESs are unable to function in reticulocyte lysate, this does not necessarily mean that L-myc does not possess an IRES.

The behaviour of the L-myc 5' UTRs was therefore studied in the context of cultured HeLa cells by the transfection of pRLsF and pRLIF in parallel with pRF and pRNF. It is to be expected that when pRLIF is introduced into the nucleus of cells by transfection, intron A will be spliced in some of the transcripts produced. This means that a population of RNA identical to that produced on transfection of pRLsF will be present in the cell cytoplasm. However, some pRLIF RNA will remain unspliced, so any differences in the results of pRLsF and pRLIF transfections can be attributed to the unspliced isoform of the L-myc 5' UTR.

The activities of *Renilla* and firefly luciferases in HeLa cell lysates were normalised to the transfection control of  $\beta$ -galactosidase activity (figure 4.5). Both isoforms of the L-myc 5' UTR were able to induce the expression of the downstream cistron to a considerable extent in this cell line relative to the background levels observed on transfection of pRF. The L-myc short isoform induced approximately equal stimulation of firefly luciferase expression to the N-myc IRES, whereas the expression observed on transfection of the long isoform was almost twofold greater than this. Both L-myc 5' UTRs caused a repression of *Renilla* luciferase activity relative to that of pRF. The reasons for this are unclear, but a similar effect has been observed with the BAG-1 IRES in the same vector system (Coldwell et al., 2001), and may be due to competition between IRES-dependent and cap-dependent initiation for components of the translational machinery.

The vectors pRLsF and pRLIF were then introduced into several other cell lines by transfection. The activities of both luciferases were normalised to  $\beta$ -galactosidase activity,

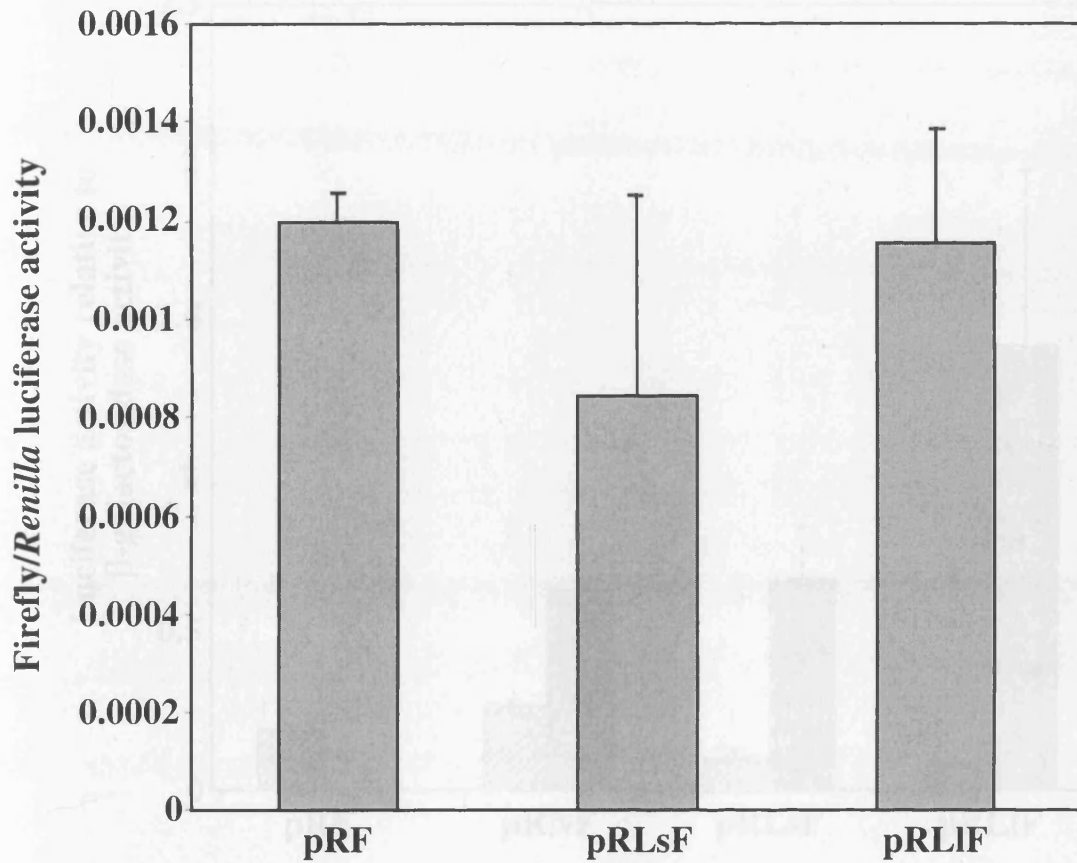


**Figure 4.4** The effect of the *L-myc* 5' UTR in a dicistronic context in reticulocyte lysate. Dicistronic RNA was synthesised by *in vitro* transcription using *NotI*-linearised pRF, pRLsF and pRLIF as templates. These RNA molecules were used to programme a reticulocyte lysate *in vitro* translation system, and the activity of firefly luciferase produced from each RNA is expressed relative to *Renilla* luciferase activity. Results are an average of three independent experiments and error bars represent standard deviations.

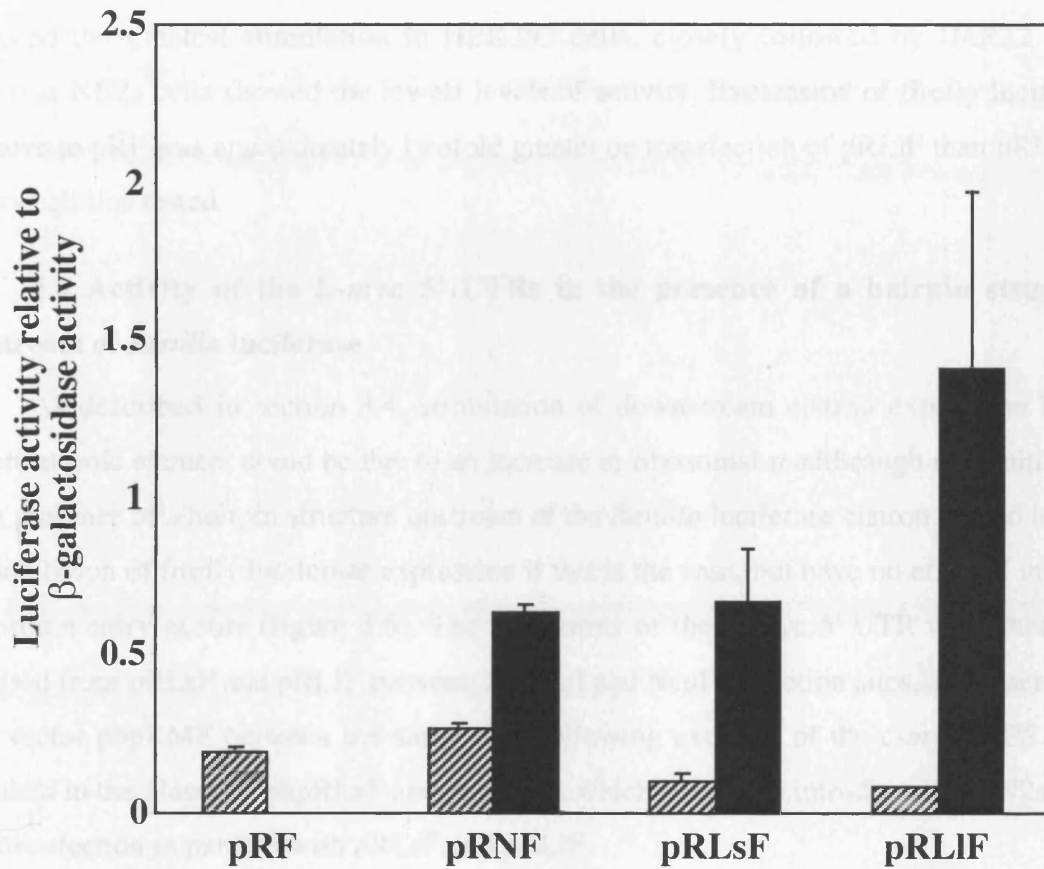


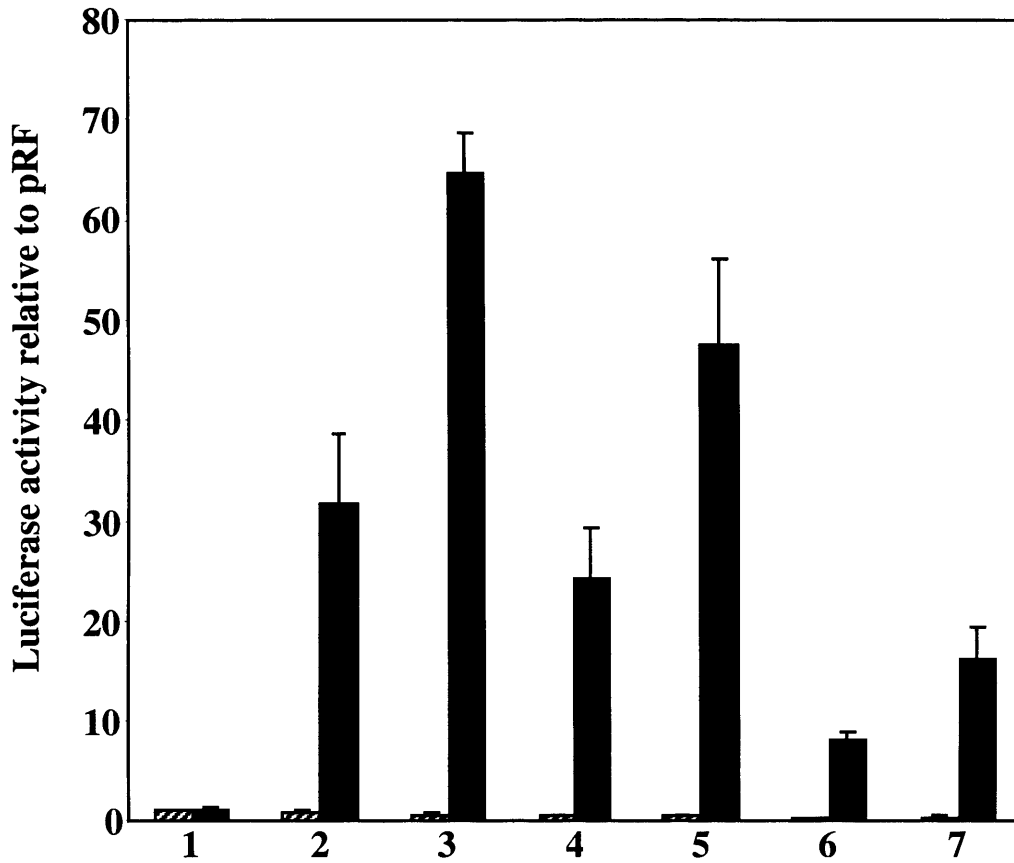
**Figure 4.5 Transfection of dicistronic *L-myc* 5' UTR constructs into HeLa cells.** The plasmids pRLsF and pRLIF were introduced into HeLa cells by transfection in parallel with pRF and pRNF. The activities of *Renilla* (shaded) and firefly (black) luciferase in the lysates were determined and expressed relative to the transfection control of  $\beta$ -galactosidase activity. Results are an average of three independent experiments and error bars represent standard deviations.

and expressed relative to the values obtained on transfection of pRF into the same cell line (figure 4.6). In every cell line tested, both L-myc 5' UTR isoforms were able to stimulate firefly luciferase activity relative to the readthrough observed from pRF. Both UTRs induced the greatest stimulation in HEK293 cells, closely followed by IMR32 cells, whereas NB2a cells showed the lowest levels of activity. Expression of firefly luciferase relative to pRF was approximately twofold greater on transfection of pRLIF than pRLsF in every cell line tested.

#### 4.4 Activity of the L-myc 5' UTRs in the presence of a hairpin structure upstream of *Renilla* luciferase

As described in section 3.4, stimulation of downstream cistron expression by an intercistronic element could be due to an increase in ribosomal readthrough or reinitiation. The presence of a hairpin structure upstream of the *Renilla* luciferase cistron should lead to an inhibition of firefly luciferase expression if this is the case, but have no effect if internal ribosome entry occurs (figure 3.6). The two forms of the L-myc 5' UTR were therefore excised from pRLsF and pRLIF between the *SpeI* and *NcoI* restriction sites, and inserted in the vector phpRMF between the same sites following excision of the *c-myc* IRES. This resulted in the plasmids phpRLsF and phpRLIF, which were then introduced into N2a cells by transfection in parallel with pRLsF and pRLIF.

The activities of *Renilla* and firefly luciferases in the cell lysates were determined and expressed relative to the transfection control of  $\beta$ -galactosidase activity (figure 4.7). Unfortunately, the hairpin was only strong enough to inhibit *Renilla* luciferase expression marginally in the context of either vector. The same phenomenon was observed when attempts were made to transfect other cell lines with these vectors. It is likely that the inhibition of *Renilla* luciferase translation observed when pRLsF and pRLIF were transfected means that a more structured hairpin would be necessary to achieve significant further inhibition. Firefly luciferase activity was slightly greater on transfection of phpRLsF than with pRLsF, which suggests that readthrough or reinitiation mechanisms are unlikely to play a role in the effect mediated by the short UTR isoform. Firefly luciferase expression from pRLIF was inhibited by the presence of an upstream hairpin, implying that the unspliced form of the UTR is unlikely to function as an IRES. However, the results obtained here are inconclusive.



**Plasmid and cell line**

1. pRF
2. pRLsF, HEK293
3. pRLIF, HEK293
4. pRLsF, IMR32
5. pRLIF, IMR32
6. pRLsF, NB2a
7. pRLIF, NB2a

**Figure 4.6 Effect of the *L-myc* 5' UTRs on downstream cistron activity in a range of cell lines.** The plasmids pRF, pRLsF and pRLIF were introduced into the cell lines indicated by transfection. The activities of *Renilla* (shaded) and firefly (black) luciferases in the cell lysates were assayed and normalised to the transfection control of  $\beta$ -galactosidase activity. The results obtained on transfection of pRLsF and pRLIF are expressed relative to the values obtained when pRF was introduced into the same cell line. Results are an average of three independent experiments and error bars represent standard deviations.

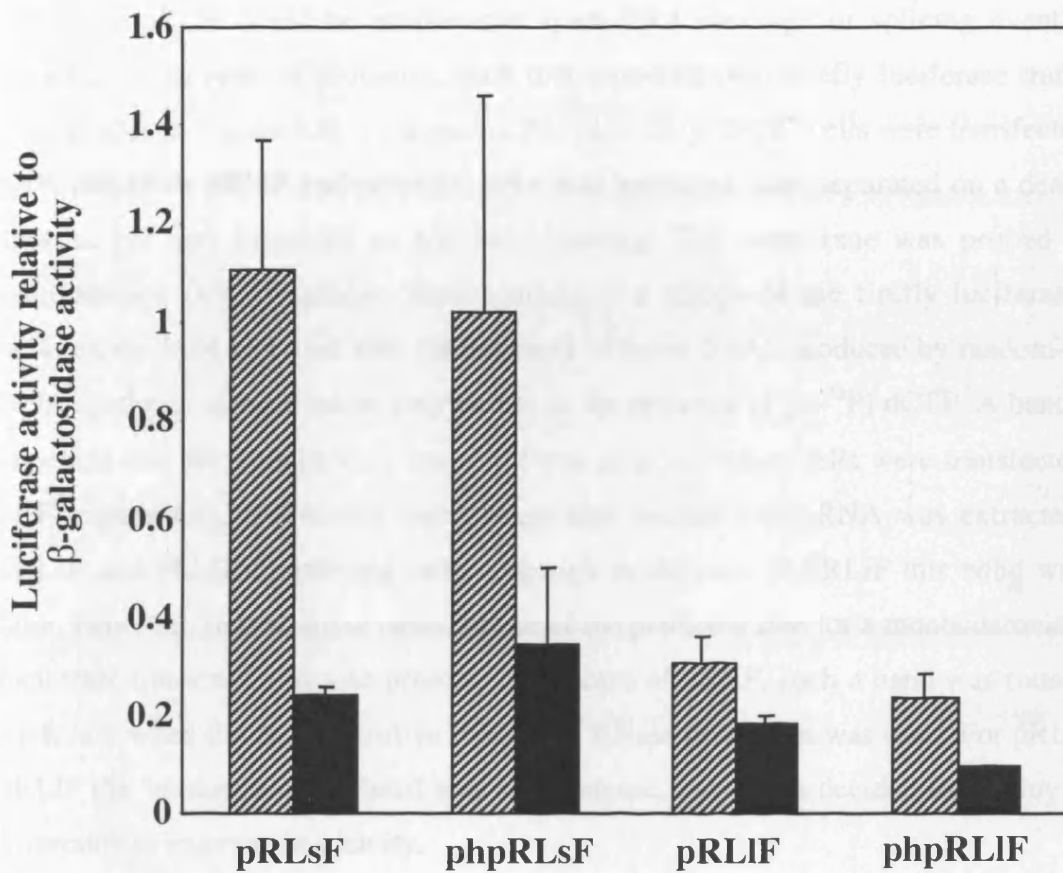


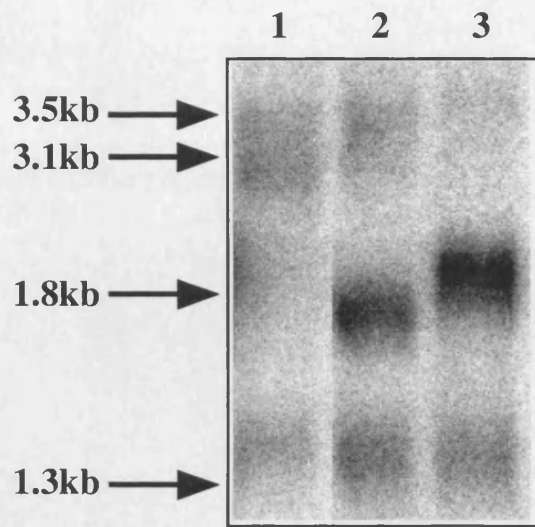
**Figure 4.7 Effect of an upstream hairpin structure on dicistronic *L-myc* plasmid transfections.** Both isoforms of the *L-myc* 5' UTR were inserted in the vector phpRF between the *SpeI* and *NcoI* sites, to create the vectors phpRLsF and phpRLIF. These plasmids were introduced into N2a cells by transfection in parallel with pRLsF and pRLIF. The activities of *Renilla* (shaded) and firefly (black) luciferase in the lysates are expressed relative to a transfection control of  $\beta$ -galactosidase activity. Results are an average of three independent experiments and error bars represent standard deviations.

#### 4.5 Analysis of transcripts produced on transfection of pRLsF and pRLIF

The fact that *Renilla* luciferase expression was low when cells were transfected with pRLsF or pRLIF could be attributable to an RNA cleavage or splicing event or the presence of an internal promoter, such that monocistronic firefly luciferase transcripts were produced (figure 3.8). To examine this possibility, COS7 cells were transfected with pRF, pRLsF or pRLIF and poly(A)<sup>+</sup> RNA was extracted, then separated on a denaturing agarose gel and subjected to Northern blotting. The membrane was probed with a radiolabelled DNA fragment corresponding to a region of the firefly luciferase gene between the *Nco*I and *Ava*I sites (as indicated in figure 3.9A), produced by random-primed DNA synthesis using Klenow polymerase in the presence of [ $\alpha$ -<sup>32</sup>P] dCTP. A band of the expected size for a dicistronic transcript was detected when cells were transfected with pRF (figure 4.8), and similar bands were also visible when RNA was extracted from pRLsF and pRLIF-transfected cells, although in the case of pRLIF this band was very faint. However, in both these cases a band of the predicted size for a monocistronic firefly luciferase transcript was also present. In the case of pRNF, such a band was found to be irrelevant when the more sensitive method of RNase protection was used. For pRLsF and pRLIF the "monocistronic" band was more intense, but it was decided to employ RNase protection to examine its identity.

PCR was carried out using the primers BRNaseF and Hluc3', with pRLsF and pRLIF as templates, and the products were inserted into the vector pSK+Bluescript between the *Bam*HI and *Hind*III sites (see figure 3.10) to produce the plasmids pSKRNaseLs and pSKRNaseLl. These plasmids were linearised with *Not*I and used as templates for *in vitro* transcription by T7 RNA polymerase to produce <sup>32</sup>P-labelled antisense riboprobes. As explained in section 3.5, these riboprobes are complementary to the most 3' 76nt of the *Renilla* luciferase cistron, the intercistronic region containing one of the *L-myc* 5' UTRs, and the most 5' 101nt of the firefly luciferase coding region. Poly(A)<sup>+</sup> RNA was extracted from COS7 cells following transfection with pRLsF or pRLIF, and allowed to hybridise to the appropriate riboprobe. The size of radiolabelled RNA protected following digestion of single-stranded RNA with RNaseONE indicates the size of firefly luciferase transcripts present in the cell (figure 3.11).

When an antisense riboprobe was synthesised from the plasmid pSKRNaseLs and allowed to hybridise to yeast tRNA or RNA from mock-transfected COS7 cells, no



1. pRF
2. pRLsF
3. pRLIF

**Figure 4.8 Northern analysis of transcripts in cells transfected with pRLsF and pRLIF.** The plasmids pRF, pRLsF and pRLIF were introduced into COS7 cells by transfection. Poly(A)<sup>+</sup> RNA was harvested from transfected cells and subjected to denaturing agarose gel electrophoresis and Northern blotting. The membrane was probed with a random-primed radiolabelled DNA probe corresponding to a region of the firefly luciferase cistron between the *Nco*I and *Ava*I sites (see figure 3.9A)

protected bands were observed (figure 4.9, lanes 1 and 2). The undigested riboprobe was 523nt in size (lane 4). When hybridised to RNA from COS7 cells that had been transfected with pRLsF, a single protected band of 451nt in length was observed (lane 3). This is the predicted size for a dicistronic transcript containing both *Renilla* and firefly luciferase coding regions with the spliced *L-myc* 5' UTR between. Although there is a certain level of background smearing in the remainder of lane 3, this does not contain any further protected bands and is likely to be due to degradation of the probe. This indicates that the only transcripts containing the entire firefly luciferase cistron in cells transfected with pRLsF are dicistronic. Although the data obtained from transfection of the dicistronic hairpin vector remain inconclusive, it appears highly probable that the spliced isoform of the *L-myc* 5' UTR contains an IRES. Once again, it has been shown that the small transcript detected by Northern blotting does not encode full length firefly luciferase. It is possible that monocistronic firefly luciferase transcripts with truncated 5' ends are present and are detected by the probe, but such transcripts would not be functionally relevant. RNase protection provides a more accurate and sensitive method of determining the nature of transcripts in the cell.

RNase protection was carried out using an antisense riboprobe made using pSKRNaseL1 as a template to detect the length of transcripts in cells that had been transfected with pRLIF. The probe was 887nt in length, but a slightly smaller band was also present when undigested probe was subjected to electrophoresis (figure 4.10, lane 4). As full length probe was purified by gel extraction before RNase protection was carried out, it is likely that this doublet is the result of a highly GC-rich RNA adopting alternative secondary structures with different gel mobility. When examining the results of this experiment, it was assumed that the riboprobe was entirely full length.

No bands were protected when this riboprobe was hybridised to yeast tRNA or RNA from mock-transfected COS7 cells (figure 4.10, lanes 1 and 2). When hybridised to RNA isolated from pRLIF-transfected COS7 cells, it was expected that a band of 810nt would be protected if full length dicistronic RNA was present. It is possible that this is the case and the position of the band is obscured by the presence of undigested probe (lane 3), but if so only small quantities of this RNA can be present. In contrast, an intense band was observed at approximately 480nt in lane 3. This band is diffuse, but this is likely to be a further indication of the alternative mobility observed with undigested probe in this gel.

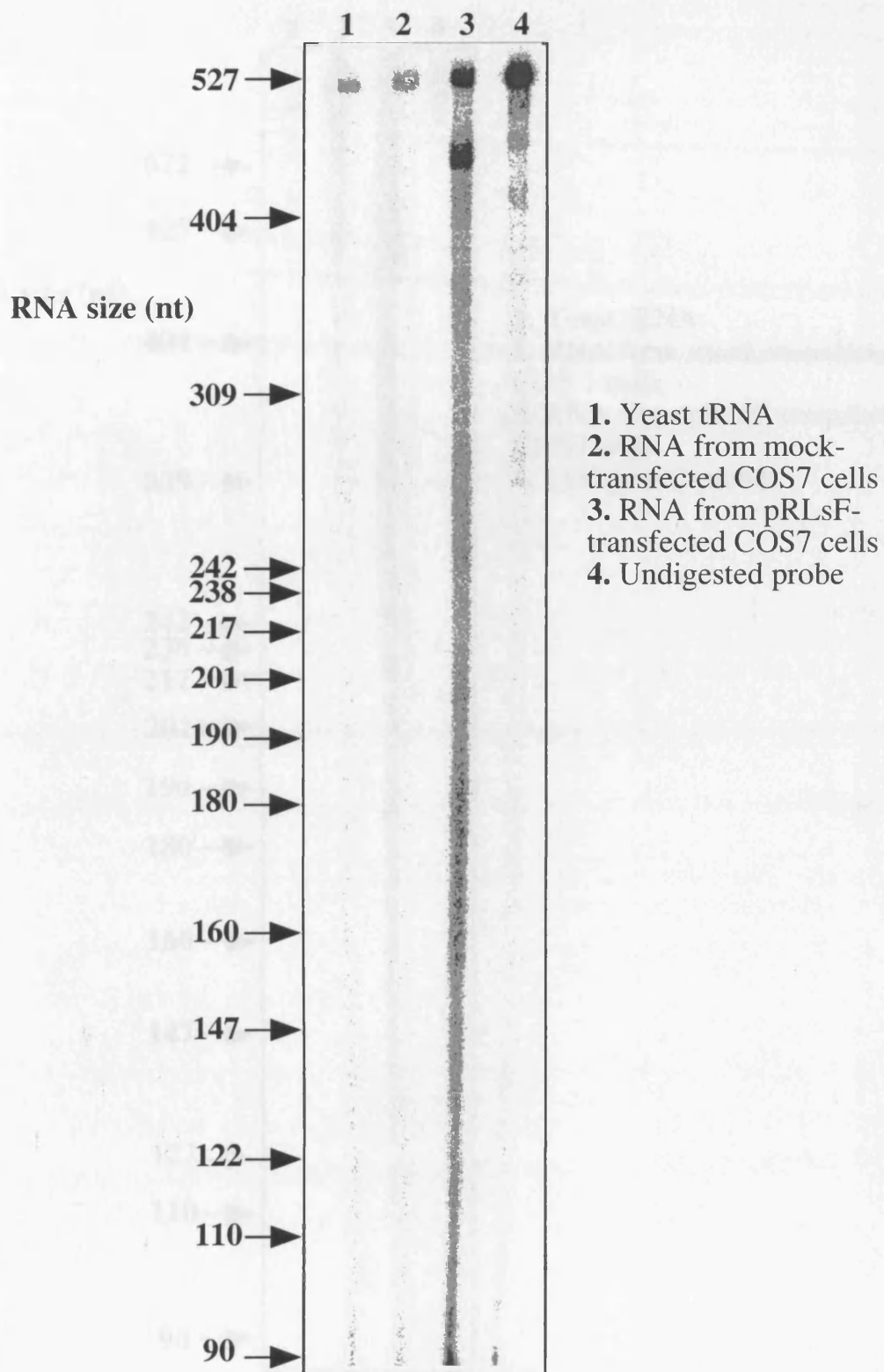


**Figure 4.9 RNase protection analysis of RNA from pRLsF-transfected cells.** Poly(A)<sup>+</sup> selected RNA from COS7 cells transfected with pRLsF, RNA from mock-transfected cells, and yeast tRNA were hybridised to a radiolabelled antisense riboprobe, and single stranded RNA was digested using RNase ONE. The products were separated by electrophoresis on a 7M urea/4% polyacrylamide gel in parallel with radiolabelled pBR322/*Hpa*II markers.

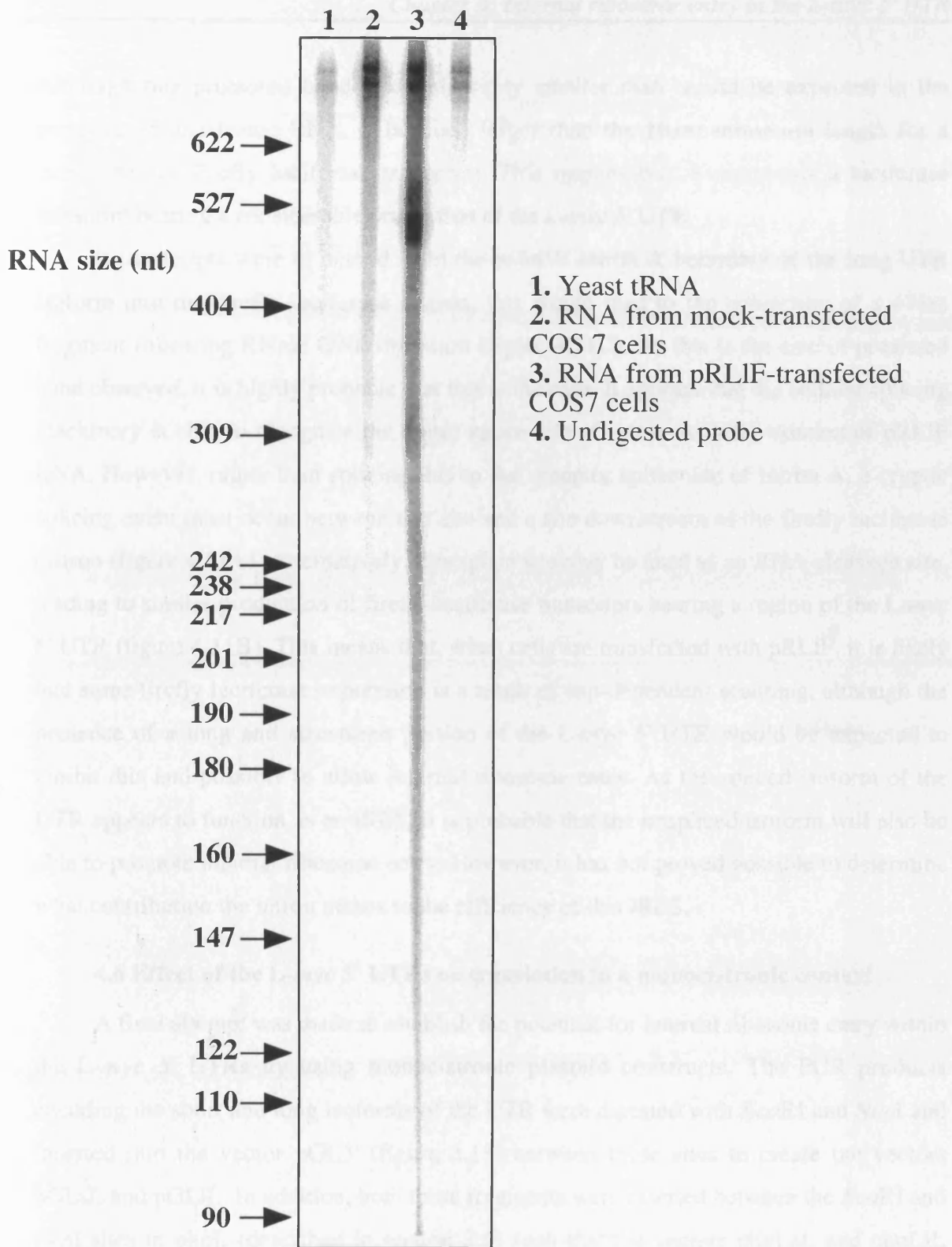


**Figure 4.10 RNase protection analysis of RNA from pRLIF-transfected cells.** Poly(A)<sup>+</sup> selected RNA from COS7 cells transfected with pRLIF, RNA from mock-transfected cells, and yeast tRNA were hybridised to a radiolabelled antisense riboprobe, and single stranded RNA was digested using RNase ONE. The products were separated by electrophoresis on a 7M urea/4% polyacrylamide gel in parallel with radiolabelled pBR322/*Hpa*II markers.

Although this protected band is considerably smaller than would be expected in the presence of dicistronic RNA, it is much larger than the 101nt minimum length for a monocistronic firefly luciferase transcript. This implies that it represents a luciferase transcript bearing a considerable proportion of the *L-myc* 5' UTR.

If transcripts were to extend from the exon 1/ intron A boundary of the long UTR isoform into the firefly luciferase cistron, this would lead to the protection of a 474nt fragment following RNase ONE digestion (figure 4.11C). As this is the size of protected band observed, it is highly probable that this is the case. It appears that the cellular splicing machinery is able to recognise the donor splice site of intron A in the context of pRLIF RNA. However, rather than splicing this to the acceptor splice site of intron A, a cryptic splicing event must occur between this site and a site downstream of the firefly luciferase cistron (figure 4.11A). Alternatively, this splice site may be used as an RNA cleavage site, leading to similar production of firefly luciferase transcripts bearing a region of the *L-myc* 5' UTR (figure 4.11B). This means that, when cells are transfected with pRLIF, it is likely that some firefly luciferase expression is a result of cap-dependent scanning, although the presence of a long and structured portion of the *L-myc* 5' UTR would be expected to inhibit this and possibly to allow internal ribosome entry. As the spliced isoform of the UTR appears to function as an IRES, it is probable that the unspliced isoform will also be able to promote internal ribosome entry. However, it has not proved possible to determine what contribution the intron makes to the efficiency of this IRES.

#### **4.6 Effect of the *L-myc* 5' UTRs on translation in a monocistronic context**

A final attempt was made to establish the potential for internal ribosome entry within the *L-myc* 5' UTRs by using monocistronic plasmid constructs. The PCR products encoding the short and long isoforms of the UTR were digested with *EcoRI* and *NcoI* and inserted into the vector pGL3' (figure 3.13) between these sites to create the vectors pGLsL and pGLlL. In addition, both these fragments were inserted between the *EcoRI* and *NcoI* sites in phpL (described in section 3.6) such that the vectors phpLsL and phpLlL were made. These four plasmids were introduced into NT2 cells by transfection in parallel with pGL3' and phpL. Firefly luciferase activities were determined and expressed relative to the transfection control of  $\beta$ -galactosidase activity (figure 4.12). Both isoforms of the *L-myc* 5' UTR inhibited translation such that it was approximately 30% of the levels

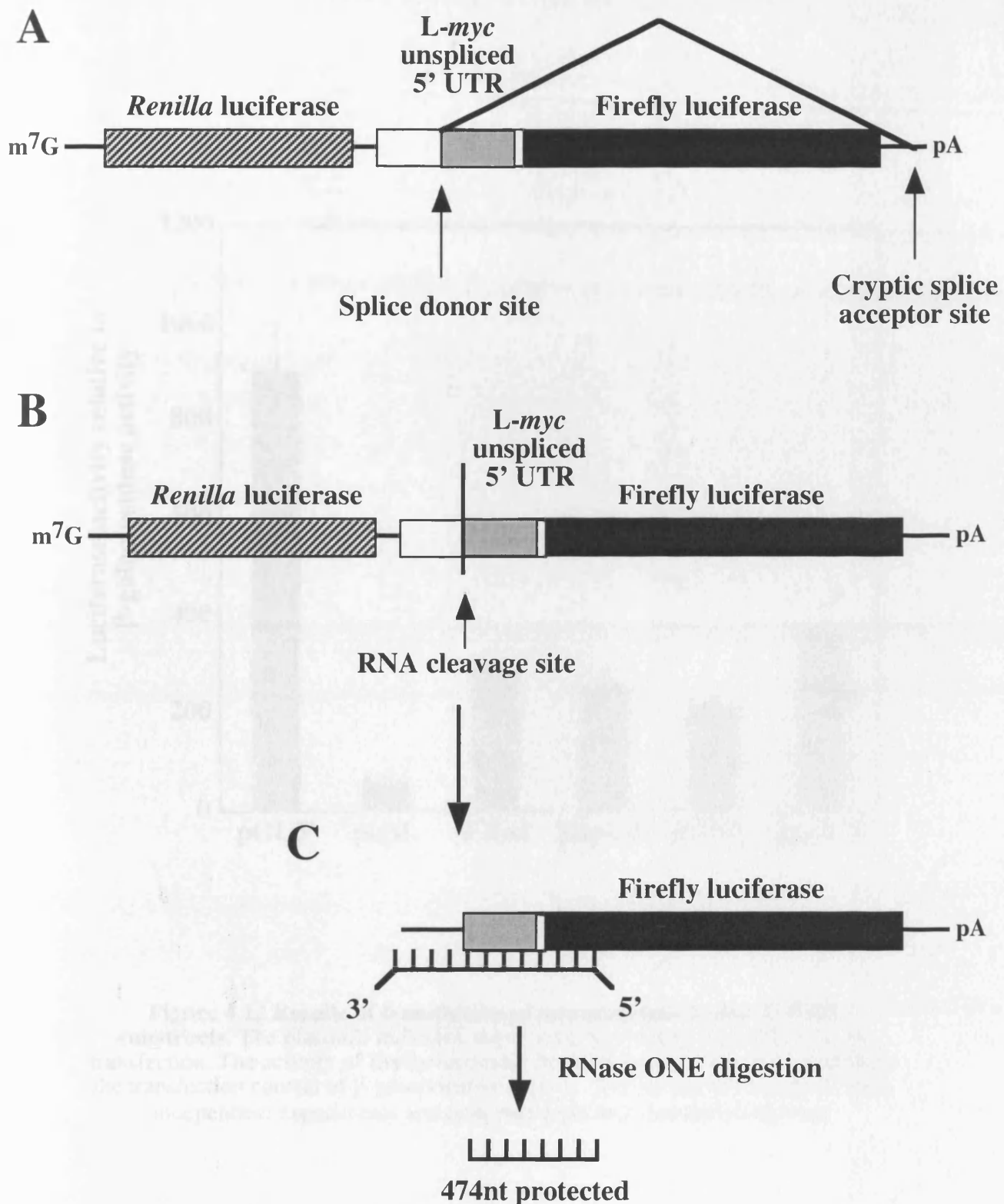


**Figure 4.11 Possible mechanisms for the production of truncated RNA molecules in pRLIF-transfected cells.** A 474nt fragment was detected following RNase protection analysis of RNA from pRLIF-transfected cells. This might result from (A) a cryptic splicing event between the splice donor site in the *L-myc* 5' UTR and an acceptor site downstream of firefly luciferase or (B) an RNA cleavage event at the splice donor site. (C) Hybridisation of an antisense riboprobe to an RNA molecule produced by such a mechanism. Intron A is indicated by shading and exon sequences are shown in white.

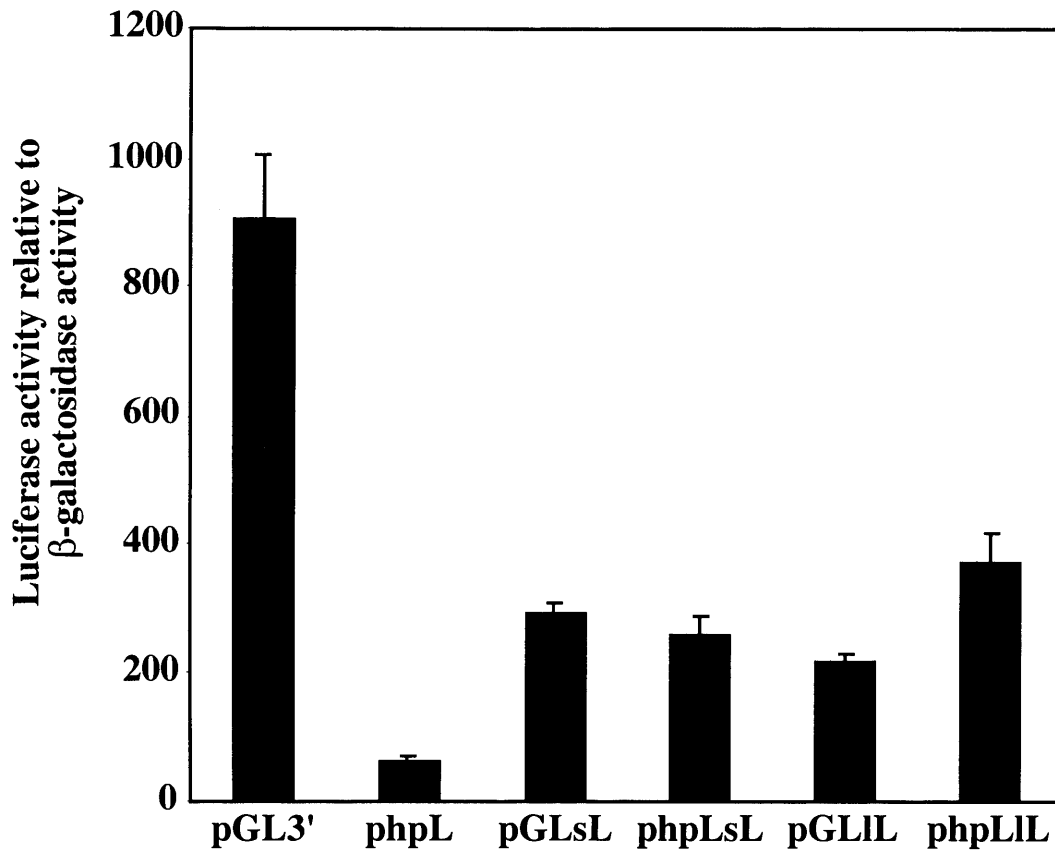


**Figure 4.12 Results of transfection of monocistronic *L-myc* 5' UTR constructs.** The plasmids indicated above were introduced into NT2 cells by transfection. The activity of firefly luciferase in cell lysates is expressed relative to the transfection control of  $\beta$ -galactosidase activity. Results are an average of three independent experiments and error bars represent standard deviations.

observed on transfection of pGL3' (compare pGL3', pGLsL and pGLIL). This is likely to be due to the impediment to scanning ribosomes posed by the highly structured UTRs, and the inhibition seen is greater with the long UTR isoform than with the short form.

The presence of a structured hairpin upstream of the multiple cloning site led to a severe inhibition of translation from pGL3', as was previously observed (compare phpL to pGL3'). However, when such a hairpin was inserted upstream of the spliced isoform of the *L-myc* 5' UTR, luciferase expression was almost unaffected (pGLsL and phpLsL). This provides further support to the hypothesis that this form of the UTR contains an IRES, as luciferase expression from phpLsL was considerably enhanced relative to that seen from phpL and is therefore IRES-dependent. Moreover, the fact that luciferase expression is almost identical on transfection of pGLsL or phpLsL implies that the inhibition of cap-dependent initiation has no effect on translation in the context of the spliced *L-myc* UTR. Therefore it appears that such translation is almost entirely IRES-dependent, in contrast to observations made with *c-* and *N-myc*.

The data obtained on transfection of phpLIL and pGLIL is more difficult to interpret, as the presence of a hairpin upstream of the 5' UTR caused an activation of luciferase expression. As previous results indicated that a cryptic splicing or RNA cleavage mechanism took place in the unspliced form of the UTR in the context of the dicistronic vector, it is possible that a similar mechanism also occurs in monocistronic vectors, but to a greater extent in phpLIL than in pGLIL. As pGLIL showed inhibited translation relative to pGL3', the luciferase transcripts must have contained a portion of the 5' UTR so that scanning was inhibited. Once again, though, it is impossible to draw any firm conclusions as to the mechanisms of translation initiation that occur in the context of the unspliced 5' UTR.

#### 4.7 Discussion

It now appears that all three members of the *myc* family possess internal ribosome entry segments. The complexity of splicing in the *L-myc* 5' UTR has led to difficulty in establishing the precise role of internal ribosome entry in its translation. However, three pieces of data, taken in combination, indicate that the spliced form of the UTR contains an IRES; (a) this UTR promotes downstream cistron expression when a dicistronic vector is transfected into mammalian cells, (b) full length dicistronic RNA is the only functional

luciferase transcript in these transfected cells, (c) in monocistronic vectors, the presence of a structured hairpin upstream of the UTR does not impede translation. As translation was equally efficient in cells that were transfected with monocistronic firefly luciferase constructs bearing this UTR with or without an upstream hairpin, translation of L-myc transcripts with the spliced form of the UTR must occur almost entirely by internal ribosome entry. This represents an interesting difference between the L-myc IRES and those found in c- and N-myc.

It remains unclear why *Renilla* luciferase expression is downregulated on transfection of dicistronic vectors containing the L-myc 5' UTR. This feature is probably responsible for the difficulties encountered in obtaining an effect on upstream cistron expression in the context of a hairpin. To confirm that the short isoform of L-myc contains an IRES, it would be desirable to create a vector with a more structured hairpin upstream of *Renilla* luciferase for further control experiments.

The data obtained with the unspliced isoform of the L-myc 5' UTR suggest that it may be able to promote internal ribosome entry, as firefly luciferase expression is high when the majority of this UTR lies upstream of the coding region, and would be expected to inhibit scanning. However, the results of RNase protection analysis indicate that most transcripts produced when pRLIF is transfected into cells are not dicistronic. The transfection of monocistronic constructs bearing the long UTR isoform also yields confusing results. It appears that the presence of partially used donor and acceptor splice sites in the dicistronic vector employed here leads to cryptic splicing or RNA cleavage, possibly by multiple mechanisms. Therefore, it is impossible to determine the extent of internal ribosome entry due to the nature of the transcripts produced.

As almost all the short isoform of the UTR is contained within exon 1, it is possible that it is able to promote internal ribosome entry even in the long form, where intron A is present downstream. However, in this case ribosomes would then have to scan through the long and structured intron sequence before encountering the initiation codon. Therefore, a significant level of internal ribosome entry can only be expected to occur in the unspliced UTR if the intron sequence itself functions as an IRES. A final point to consider is the lack of evidence as to the proportion of L-Myc protein synthesised from each transcript *in vivo*. It is possible that translation from RNA molecules containing the unspliced UTR is very inefficient.

## Chapter 5

### Involvement of *trans*-acting factors in *myc* IRES function

#### 5.1 Introduction

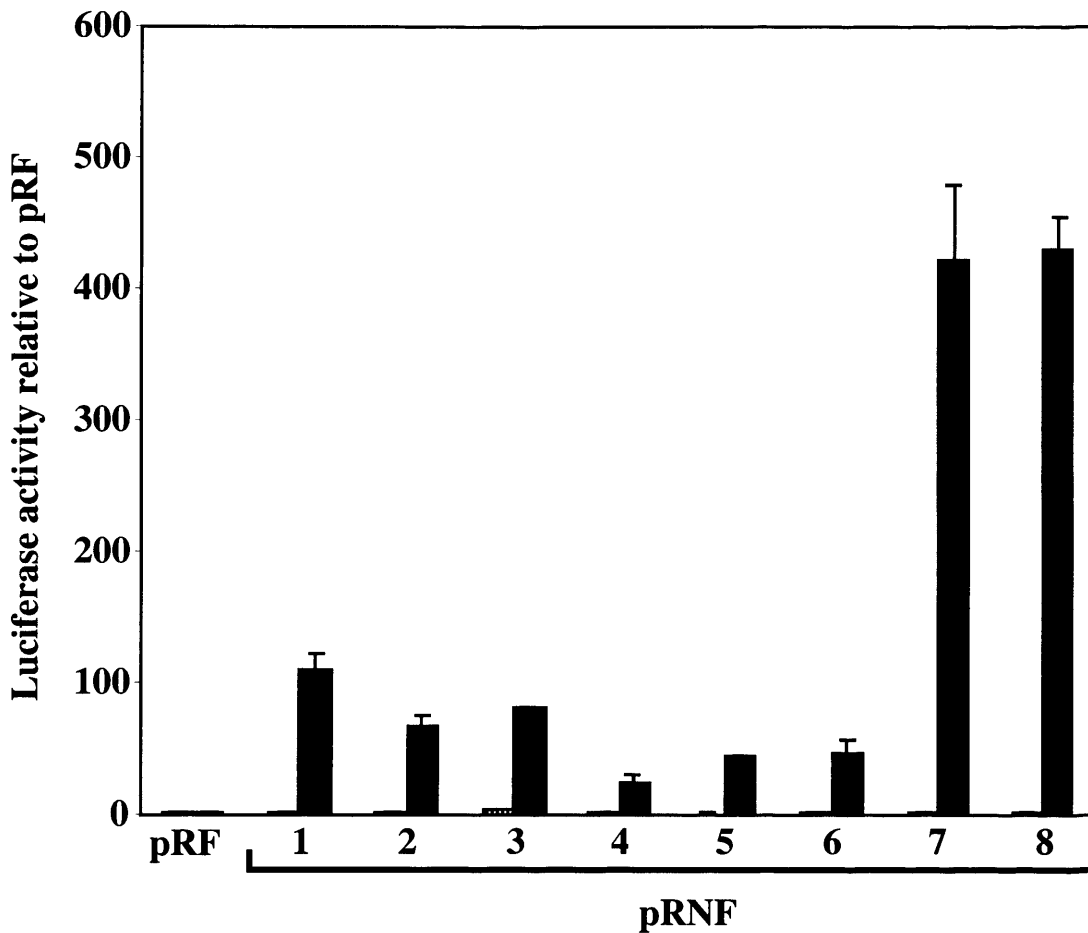
The data presented in chapter 3 indicate that the N-*myc* IRES is unable to function when *in vitro* transcribed dicistronic RNA is translated in a reticulocyte lysate system (figure 3.4). This feature is shared by various other cellular IRESs, including that of *c-myc*, and by the type I picornaviral IRESs such as those poliovirus and HRV. It therefore appears probable that *myc* IRES activity is dependent on certain *trans*-acting protein factors that are not present at sufficiently high levels in reticulocyte lysate. A number of factors have been identified as interacting with and stimulating activity from specific viral and cellular IRESs (discussed in section 1.4.5). Therefore, the behaviour of the N-*myc* IRES in the context of cultured cell transfection was analysed in more detail, and attempts were made to identify protein factors that interact with this IRES.

#### 5.2 N-*myc* IRES activity in different cell lines

It has already been demonstrated that the N-*myc* 5' UTR contains a highly active IRES when introduced into HeLa cells by transfection. However, HeLa cells do not express N-*myc* RNA, and do not necessarily provide the same translational environment as cells in which N-*myc* is expressed. The *c-myc* IRES is known to show very variable activity when introduced into different cell lines, presumably due to the concentrations of necessary protein factors (Stoneley et al., 2000b). It was therefore decided to examine the activity of the N-*myc* IRES in a range of different cell lines.

The vectors pRF and pRNF were introduced into the cell lines indicated in figure 5.1 by transfection. In all cases the activities of *Renilla* and firefly luciferases were determined in the cell lysates and normalised to a transfection control of  $\beta$ -galactosidase activity. The activities of both luciferases on transfection of pRNF were then expressed relative to those obtained when pRF was introduced into the same cell line (figure 5.1), so that the low levels of firefly luciferase activity caused by ribosomal readthrough in the empty vector can be accounted for.

N-*myc* IRES activity was seen to vary to a considerable extent between cell lines. It has already been shown in chapter 3 that this IRES is highly active in HeLa cells, but it



- Cell lines**
1. HeLa
  2. MCF7
  3. HEK293
  4. N1E-115
  5. N2a
  6. NB2a
  7. NT2
  8. SH-SY5Y

**Figure 5.1 N-myc IRES activity in a range of cell lines.** The vectors pRF and pRNF were introduced into the cell lines indicated above by transfection. In all cases the activities of *Renilla* (shaded) and firefly (black) luciferases in the lysates were determined relative to the transfection control of  $\beta$ -galactosidase activity. For each cell line the values obtained on transfection of pRNF are expressed relative to those obtained from pRF. Results are an average of three independent experiments and error bars represent standard deviations.

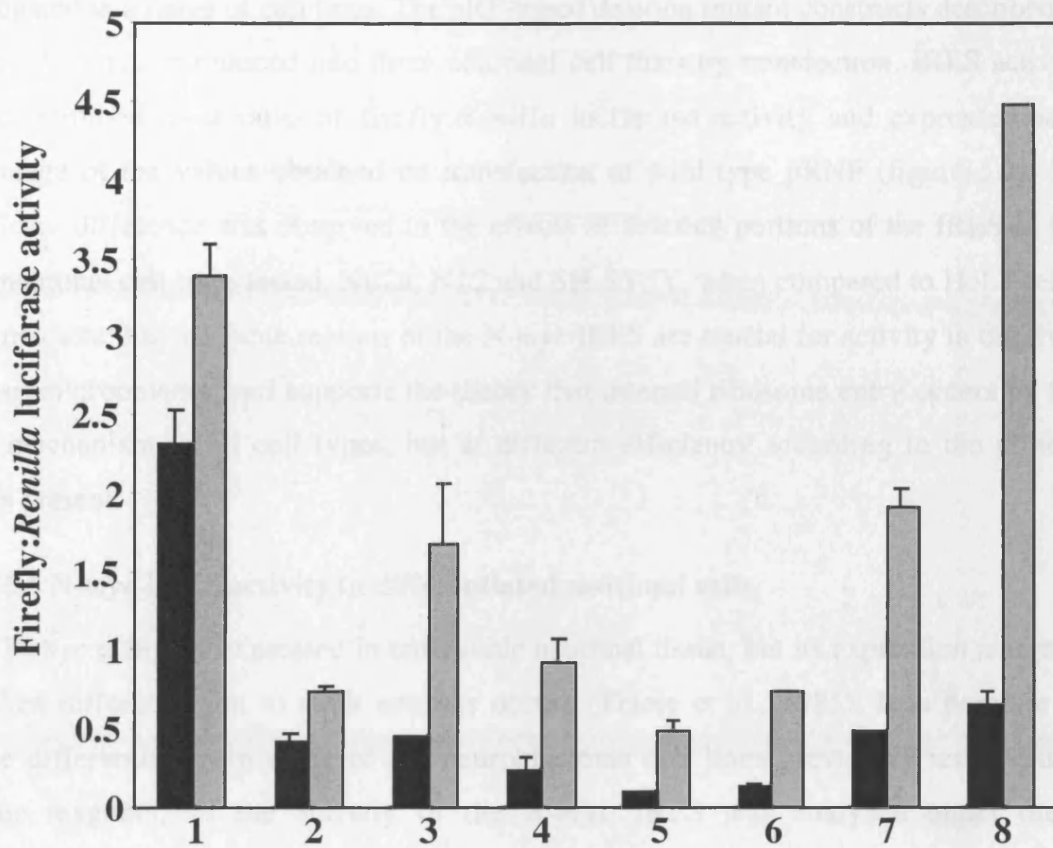
can be seen that activity in NT2 and SH-SY5Y cells is almost fourfold greater. Interestingly, both these cell lines express N-*myc*; SH-SY5Y cells are derived from a neuroblastoma, whereas NT2 cells are a committed neuronal precursor line derived from a teratocarcinoma. This suggests that the N-*myc* IRES might be more active in cells in which its RNA is expressed. However, the neuroblastoma cells N1E-115, N2a and NB2a, and the embryonic kidney line HEK293, all of which express N-*myc*, show lower IRES activity than HeLa cells, which do not. Even so, the IRES is active in all of these cell lines, indicating that it is able to function in a cellular environment in which N-*myc* RNA is expressed and translated and therefore is likely to be physiologically relevant. MCF7 cells, which are derived from a breast carcinoma and do not express N-*myc*, show IRES activity slightly lower than that of HeLa cells.

### 5.3 Relative activity of the c- and N-*myc* IRESs

In the light of the data presented above, it was considered relevant to compare the activity of the c- and N-*myc* IRESs in a variety of cell lines. The vectors pRMF and pRNF were therefore introduced into the same cell lines as were used in section 5.2, and the activity of both IRESs was determined as a ratio of firefly:*Renilla* luciferase activity. The results are shown in figure 5.2, where the ratio of N-*myc*:c-*myc* IRES activity has been quantified and is shown in the table. In HeLa cells the N-*myc* IRES is slightly more active than that of c-*myc* (as seen in figure 3.5), and the same is true for MCF7 cells. However, all the other cell lines show considerably enhanced N-*myc* IRES activity relative to that of c-*myc*, with a maximum of almost sevenfold difference seen in SH-SY5Y cells. As all these cell lines express N-*myc*, whereas HeLa and MCF7 cells do not, this implies that the translational environment of neuronal cells is more favourable to N-*myc* than c-*myc* IRES activity. This is likely to be due to stimulation of the N-*myc* IRES as opposed to inhibition of the c-*myc* IRES, as c-*myc* IRES activity is high in several of the neuronal cell lines tested. No correlation was observed between the relative activity of the N- and c-*myc* IRESs and the absolute activity of the N-*myc* IRES relative to readthrough, as can be seen by comparing figure 5.1 and 5.2.

### 5.4 Activity of N-*myc* IRES deletion mutants in neuronal cells

As N-*myc* IRES activity has been shown to vary between cell lines and is greater than that of the c-*myc* IRES in neuronal cells, the effects of N-*myc* IRES deletions were



	Cell line	pRNF/ pRMF
1.	HeLa	1.47
2.	MCF7	1.75
3.	HEK293	3.81
4.	N1E-115	3.87
5.	N2a	4.83
6.	NB2a	5.53
7.	NT2	3.95
8.	SH-SY5Y	6.83

**Figure 5.2 Relative activities of the *c-myc* and *N-myc* IRESs in various cell lines.** The plasmids pRMF and pRNF were introduced into the cell lines indicated above by transfection. IRES activity was determined as a ratio of firefly:*Renilla* luciferase activity for pRMF (black) and pRNF (shaded) in each cell line. Results are an average of three independent experiments and error bars represent standard deviations. The table indicates the ratio of *N-myc*:*c-myc* IRES activity in each cell line.

investigated in a range of cell lines. The pRF-based deletion mutant constructs described in figure 3.15 were introduced into three neuronal cell lines by transfection. IRES activity was determined as a ratio of firefly:*Renilla* luciferase activity and expressed as a percentage of the values obtained on transfection of wild type pRNF (figure 5.3). No significant difference was observed in the effects of deleting portions of the IRES in the three neuronal cell lines tested, NB2a, NT2 and SH-SY5Y, when compared to HeLa cells. This indicates that the same regions of the N-*myc* IRES are crucial for activity in different cellular environments, and supports the theory that internal ribosome entry occurs by the same mechanism in all cell types, but at different efficiency according to the protein factors present.

### 5.5 N-*myc* IRES activity in differentiated neuronal cells

N-*myc* is highly expressed in embryonic neuronal tissue, but its expression is turned off when differentiation to adult neurons occurs (Thiele et al., 1985). It is possible to induce differentiation in some of the neuroblastoma cell lines previously tested using various reagents, so the activity of the N-*myc* IRES was analysed under these circumstances. NT2 cells were treated with 10 $\mu$ M retinoic acid (RA) three times weekly over a period of five weeks, as this results in a large proportion of the cells differentiating completely to hNT neurons (figure 5.4). These neurons were then transfected with pRNF, and the activities of *Renilla* and firefly luciferases were normalised to  $\beta$ -galactosidase activity and expressed relative to the values obtained when pRNF was transfected into untreated NT2 cells (figure 5.5). Cap-dependent *Renilla* luciferase expression declined during differentiation, but IRES-dependent firefly luciferase expression decreased to a greater extent. However, when the same experiments were carried out using pRMF, c-*myc* IRES activity was only slightly lower after differentiation than in untreated cells (figure 5.6). This implies that N-*myc* IRES activity is specifically inhibited during differentiation.

To confirm these findings, the cell lines N2a, NB2a and SH-SY5Y were transfected with pRNF and grown for 24 hours. Differentiation was then induced in a sample of each cell type for a further 24 hours, after which both untreated and treated cells were harvested and luciferase activities assayed, normalised to  $\beta$ -galactosidase activity, and the values obtained from differentiated cells expressed relative to those from untreated cells (figure 5.5). N2a cells were induced to differentiate by the withdrawal of serum, whereas NB2a

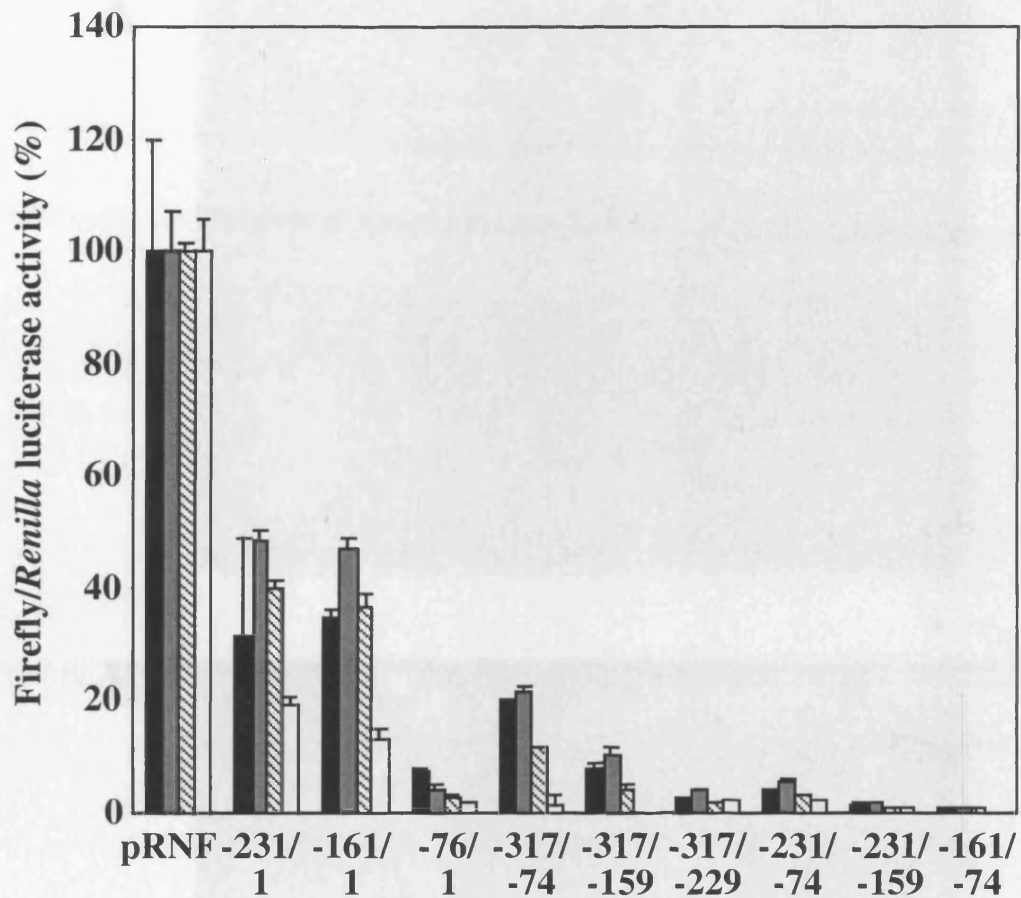
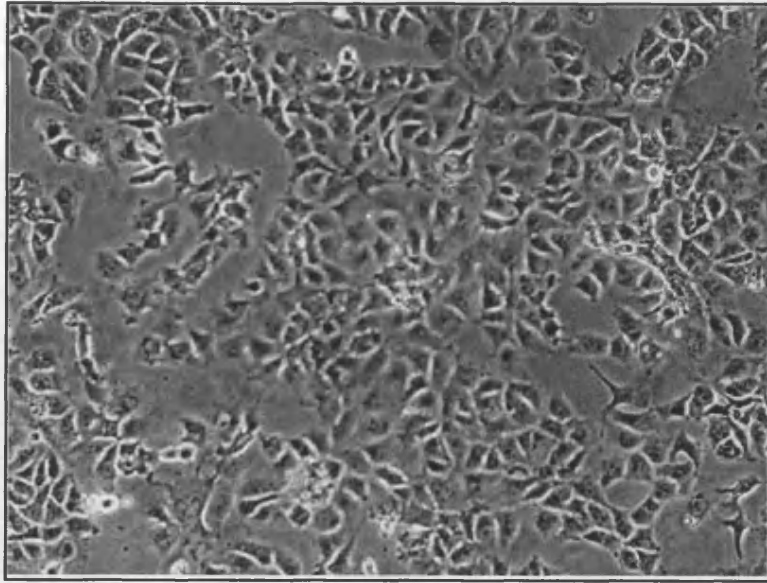


**Figure 5.3 IRES activity of N-myc 5' UTR deletion mutants in various cell lines.** The N-myc IRES fragments shown in figure 3.15 were inserted between the *EcoRI* and *NcoI* sites of the vector pRNF and introduced by transfection into a range of cell lines in parallel with pRNF. IRES activity was determined as a ratio of firefly:*Renilla* luciferase activity, and expressed as a percentage of the values obtained using wild type pRNF. The cell lines used were HeLa (black bars), NB2a (grey), NT2 (shaded) and SH-SY5Y (white). Results are an average of three independent experiments and error bars represent standard deviations.

**A**



**B**

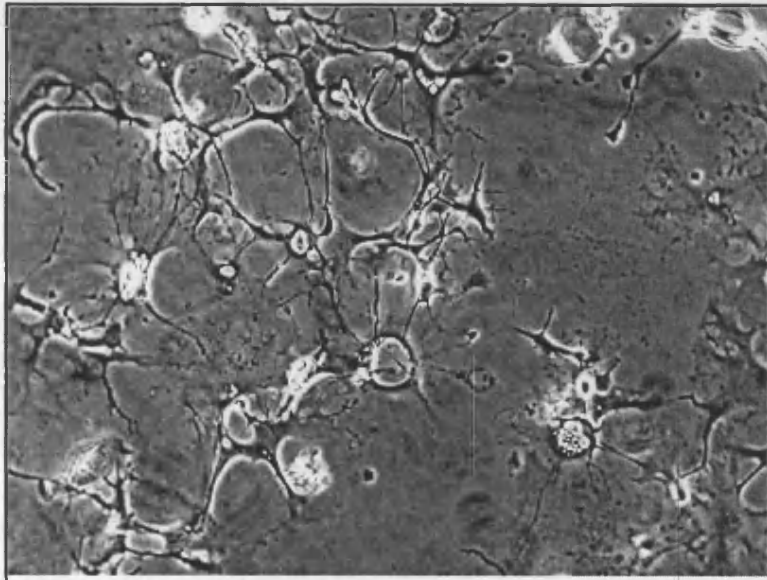
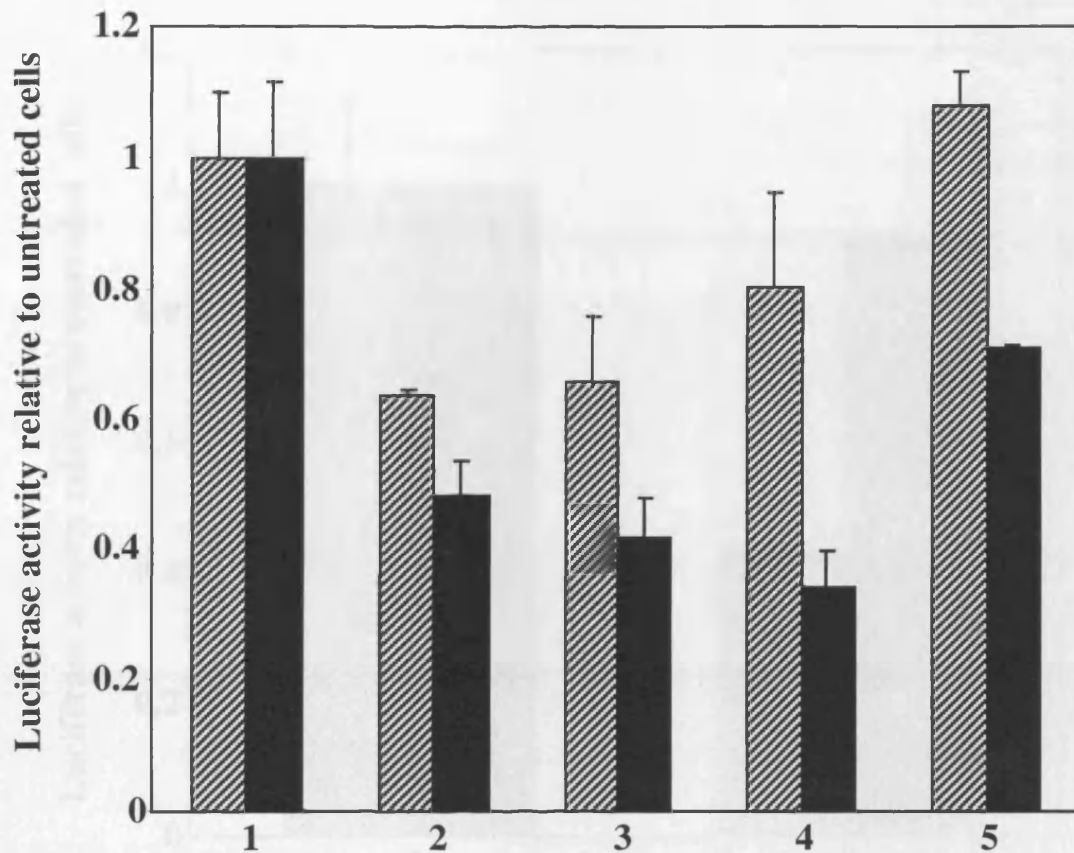


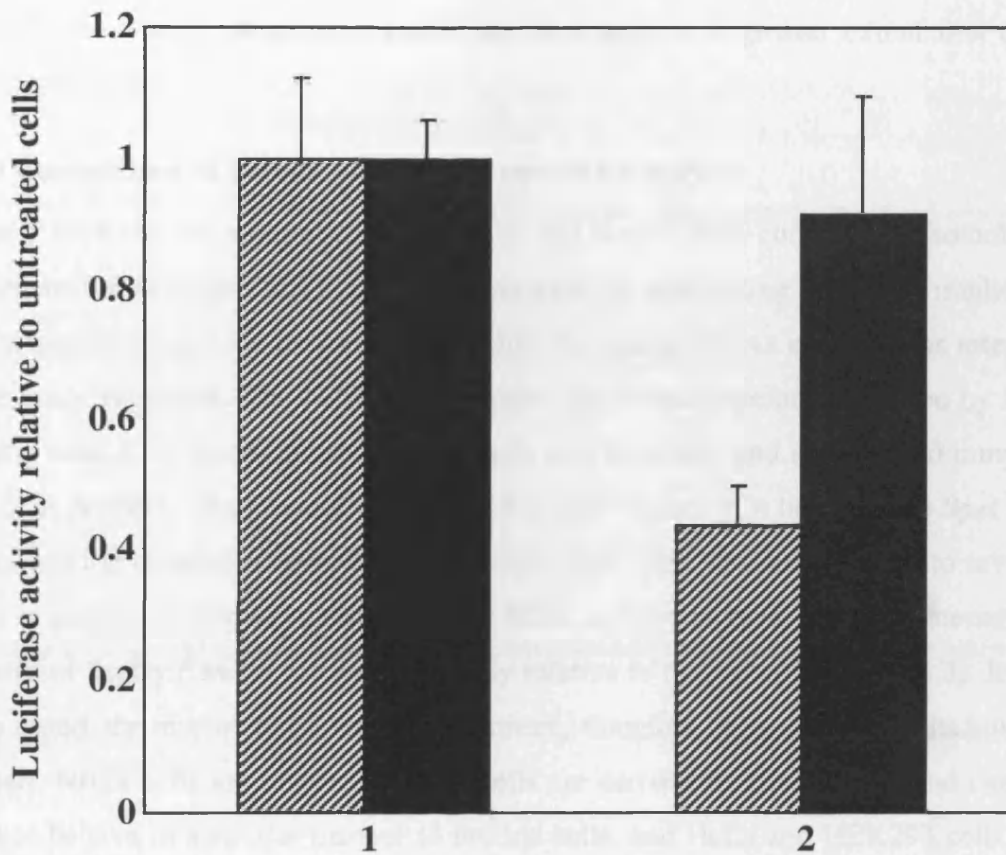
**Figure 5.4 Differentiation of NT2 cells.** (A) Untreated NT2 cells. (B) hNT neurons, produced by a five week programme of 10 $\mu$ M retinoic acid treatment of NT2 cells.



**Cell lines and methods of differentiation**

1. Untreated cells
2. N2a -serum
3. NB2a + dibutyryl cAMP
4. NT2 + RA
5. SY5Y + RA

**Figure 5.5 N-myc IRES activity in differentiated neuronal cells.** The cell lines N2a, NB2a and SY5Y were transfected with pRNF, grown for 24 hours, and half the cells were subjected to differentiation for 24 hours using the reagents indicated. NT2 cells were treated with retinoic acid over a five week period to induce differentiation, after which they were transfected with pRNF and grown for 48 hours. The activities of *Renilla* and firefly luciferases in the cell lysates were normalised to the transfection control of  $\beta$ -galactosidase activity. Results are an average of three independent experiments and error bars represent standard deviations. The values obtained on differentiation are expressed relative to the data from untreated cells of the same line.



1. Untreated NT2 cells
2. NT2 + RA

**Figure 5.6 c-myc IRES activity in differentiated neuronal cells.** NT2 cells were subjected to differentiation by a five week period of retinoic acid treatment and transfected with pRMF.

The activities of *Renilla* (shaded) and firefly (black) luciferases were normalised to the transfection control of  $\beta$ -galactosidase. The data obtained in differentiated cells are expressed relative to the values from untreated NT2 cells. Results are an average of three independent experiments and error bars represent standard deviations.

cells were treated with 1mM dibutyryl cyclic AMP, and SH-SY5Y cells were treated with 4 $\mu$ M retinoic acid (Ammer and Schulz, 1994; Pignatelli et al., 1999; Shea et al., 1991). In each case N-*myc* IRES dependent-translation decreased to a greater extent than cap-dependent translation.

### 5.5 Comparison of human and murine *myc* IRES activity

The 5' UTRs of the murine forms of both c- and N-*myc* show considerable homology to the human forms (figure 5.7). Such conservation of non-coding sequence implies a functional significance, so it appeared likely that the murine RNAs also possess internal ribosome entry segments. The 5' UTR of murine c-*myc* was therefore amplified by RT-PCR, using total RNA extracted from MEL cells as a template, and mmycF and mmycR (table 2.2) as primers. The product was inserted in pRF (figure 3.3) between the *SpeI* and *NcoI* sites and the resultant plasmid was named pRMuF. This was introduced into several cell lines in parallel with pRF and pRMF, and IRES activity in each line was determined by the ratio of firefly:*Renilla* luciferase activity relative to that of pRF (figure 5.8). In all cell lines tested, the murine IRES was approximately threefold more active than its human counterpart. NB2a cells are murine, CHO-T cells are derived from a hamster and can be expected to behave in a similar manner to murine cells, and HeLa and HEK293 cells are human. It therefore appears that c-*myc* IRES activity is not species specific. This is a surprising finding, given the divergence of IRES activity between cells of the same species and therefore its exquisite dependence on cellular environment.

The murine version of the N-*myc* 5' UTR was obtained by RT-PCR of poly(A)<sup>+</sup> RNA from NB2a cells, using the primers NF1 and NGR (table 2.2, figure 3.2, lane 7). This product was used as a template in a further PCR with CJNF and NmycUTRR as primers (table 2.2), and the product of this reaction was digested with *EcoRI* and *NcoI* and inserted into pRF between these sites to create pRMuNF. pRMuNF was introduced into cells by transfection in parallel with pRNF and pRF, and IRES activity was expressed as a ratio of firefly:*Renilla* luciferase activity relative to pRF (figure 5.9). The murine cell line NB2a and the human cell lines HeLa, MCF7 and SH-SY5Y were transfected. In contrast to the c-*myc* IRESs, the murine form of the N-*myc* 5' UTR showed comparable activity to the human form in all cell lines tested. This indicates that murine IRESs are not necessarily more active than the human equivalents, and raises questions as to why the murine c-*myc*

# A

```
human      AGGATCCCCCTAATTCAGCGAGAGGCAGAGGGAGCGAGCGGGCGCCGGCTAGGGTGA 60
murine     --CGTGTAGTAATTCAGCGAGAGACAGAGGGAGTGAGCGGACGGT-----TGGA 49
          *****
human      AGAGCCGGGCGAGCAGAGCTGCGCTGCGGG-CGTCCTGGGAAGGGAGATCCGGAGCGAAT 119
murine     AGAGCCGTGTGTGCAGAGCCGCGCTCCGGGGCGACCTAAGAAGGCAGCTCTGGAGTGAG- 108
          *****
human      AGGGGGCTTCGCCTCTGGCCAGCCCTCCCGCTGATCCC-----CCAGC- 163
murine     -AGGGGCTTTGCCTCCGAGCCTGCCCGCCACTCTCCCAACCCTGCGACTGACCCAACA 167
          *****
human      -CAGCGGTCCGCAACCCTTGCCGCATCCACGAAACTTTGCCCATAGCAGCGGGCGGGCAC 222
murine     TCAGCGG-CCGCAACCCTCGCCCGCGCTGGGAAACTTTGCCCATAGCAGCGGGCAGACAC 226
          *****
human      TTTGCACTGGAACCTACAACACCCGAGCAAGGACGCGACTCTCCCGACGC-GGGGAGGCT 281
murine     TTCTCACTGGAACCTACAATCTGCGAGCCAGGACAGGACTCCCGAGGCTCCGGGGAGGGA 286
          **
human      ATTCT-GCCCATTTGGGGACT--TCCCCGCGCTGCCAG-GACCCGCTTCTCTGAAAG 337
murine     ATTTTGTCTATTTGGGGACAGTGTCTCTGCCTCTGCCCGCATCAGCTCTCCTGAAAA 346
          ***
human      GCTCTCCTTGAGCTGCTTAGACGCTGGATTTTTCGGGTAGTGAAAACCAGCAGCCT 397
murine     GAGCTCCTCG-AGCTGTTTGAAGCTGGATTTCCCTTTGGGCGTTGAAAACCCCGCAGACA 405
          *
human      CCCGCGACCATG 409
murine     GCCACGACCATG 417
          **
```

# B

```
human      -----GACAGTCATCTGTCTGGACGCGCTGGGTGGATGCGGGGGGCTCCTGGGAACTGT 54
murine     GCCAGTGACAGTCATCTGTCTGGACGCGCTGGGTGGATGCGGGGGGCTCCTGGGAACTGG 60
          *****
human      GTTGGAGCCGAGCAAGCGCTAGCCAGGCGCAAGCGCGCACAGACTGTAGCCATCCGAGGA 114
murine     GTTGGAGCCGAACGAGCGCTAGCCAGGCGTAAGCGCGCACACTGCAGCCGCGGAGGA 120
          *****
human      CACCCCC-----GCCCCCGGCCCCACCCGGAGACACCCGCGCAGAATCGCCTC 163
murine     CAACCCCTCCCGCCGCGCTCCCTCAGCCACCCGGAGACCCAGCCCGAGTCGCCTC 180
          **
human      CGGATCCCCTGCAGTCGGCGGGAGTGTGGAGGTCGGCGCGGCCCCCGC--CTTCCGCG 221
murine     CGGATCCCAGGAGTCTGCGGGAGGTAAGAAGCGAGTTGGAGGTTGGCGCGACTCTGCTG 240
          *****
human      CCCCCACGGGAAGGAAGCAC-CCCGGTATTAACGAACGGGGCGGAAAGAAGCCCTC 280
murine     CTCTCCACGGGAAGGAAGCACTCCCCATATTAAGAGCGGAGATATTAAG----- 295
          *
human      AGTCGCGCGCCGGGAGGCGAGCCGATGCCGAGCTGCCACGTCCACCATG----- 331
murine     -----AGAGGCGAACCATGCCAGCTGCACCGCTCCACCATGCCGGGGATG 343
          *****
```

**Figure 5.7 Sequence alignment of *myc* 5' UTRs.** The sequences of the human and murine forms of the (A) *c-myc* and (B) *N-myc* 5' UTR were aligned using the CLUSTALW program.

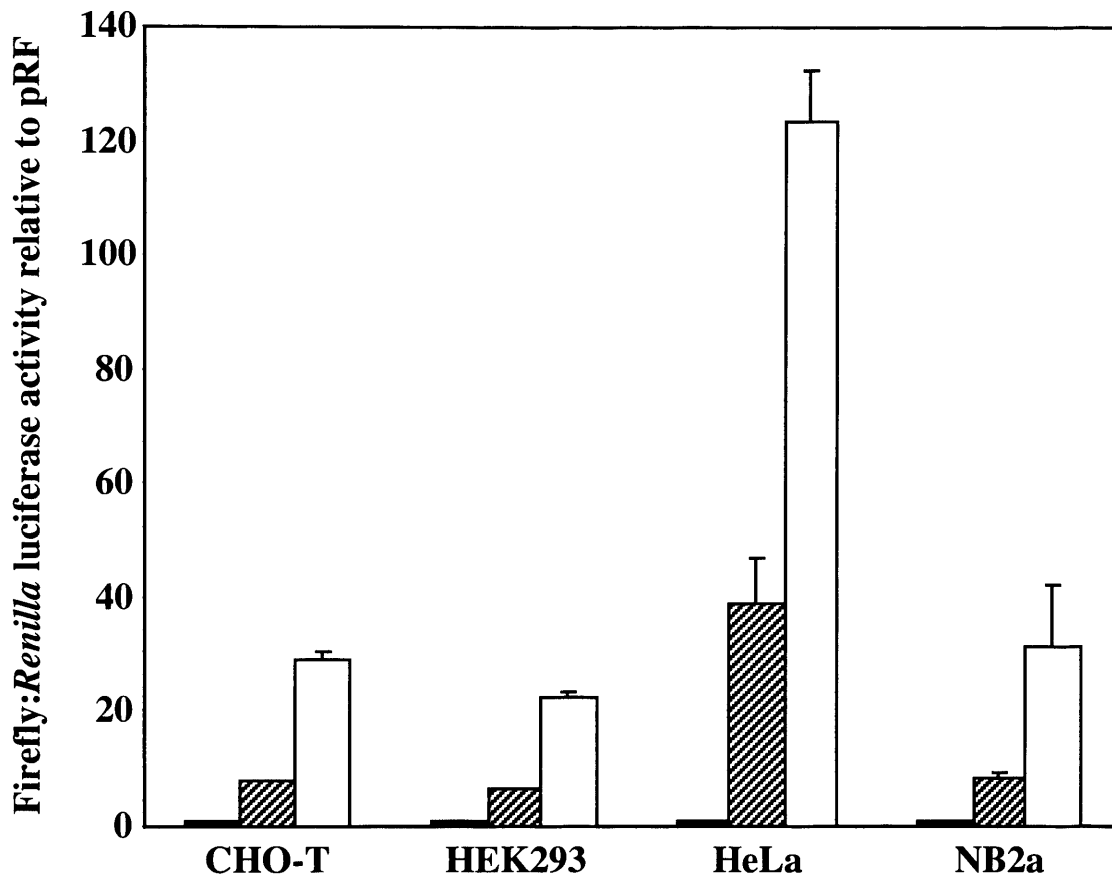


**Figure 5.8 Comparison of the activities of the human and murine *c-myc* IRESs.** The plasmids pRF, pRMF and pRMuF were introduced into the cell lines indicated above by transfection. IRES activity was determined as a ratio of firefly:*Renilla* luciferase activity in lysates. The values obtained on transfection of pRMF (shaded bars) and pRMuF (white bars) are expressed relative to those obtained from pRF (black bars) for each cell line. Results are an average of three independent experiments and error bars represent standard deviations.

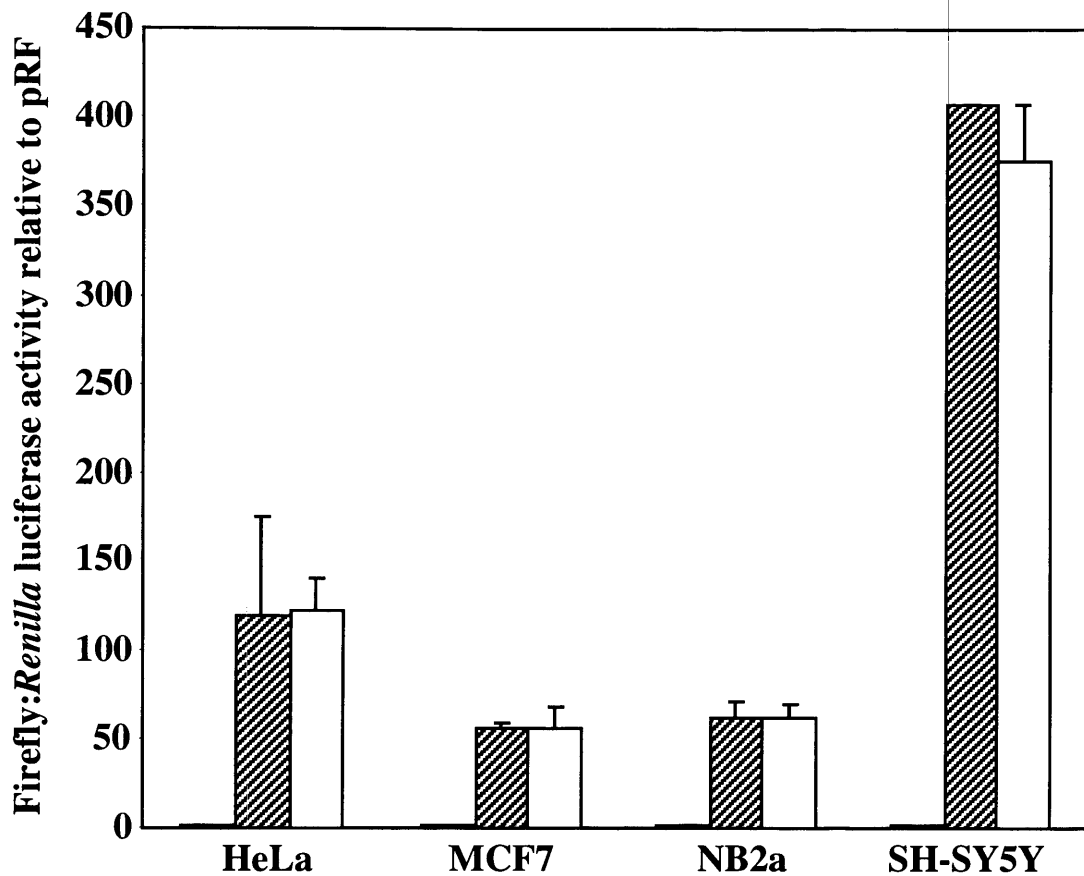


**Figure 5.9 Comparison of the activities of the human and murine N-myc IRESs.** The plasmids pRF, pRNF and pRMuNF were introduced into the cell lines indicated above by transfection. IRES activity was determined as a ratio of firefly:*Renilla* luciferase activity in lysates. The values obtained on transfection of pRNF (shaded bars) and pRMuNF (white bars) are expressed relative to those obtained from pRF (black bars) for each cell line. Results are an average of three independent experiments and error bars represent standard deviations.

IRES is so efficient. However, both c- and N-*myc* IRESs share the property of showing no species specificity.

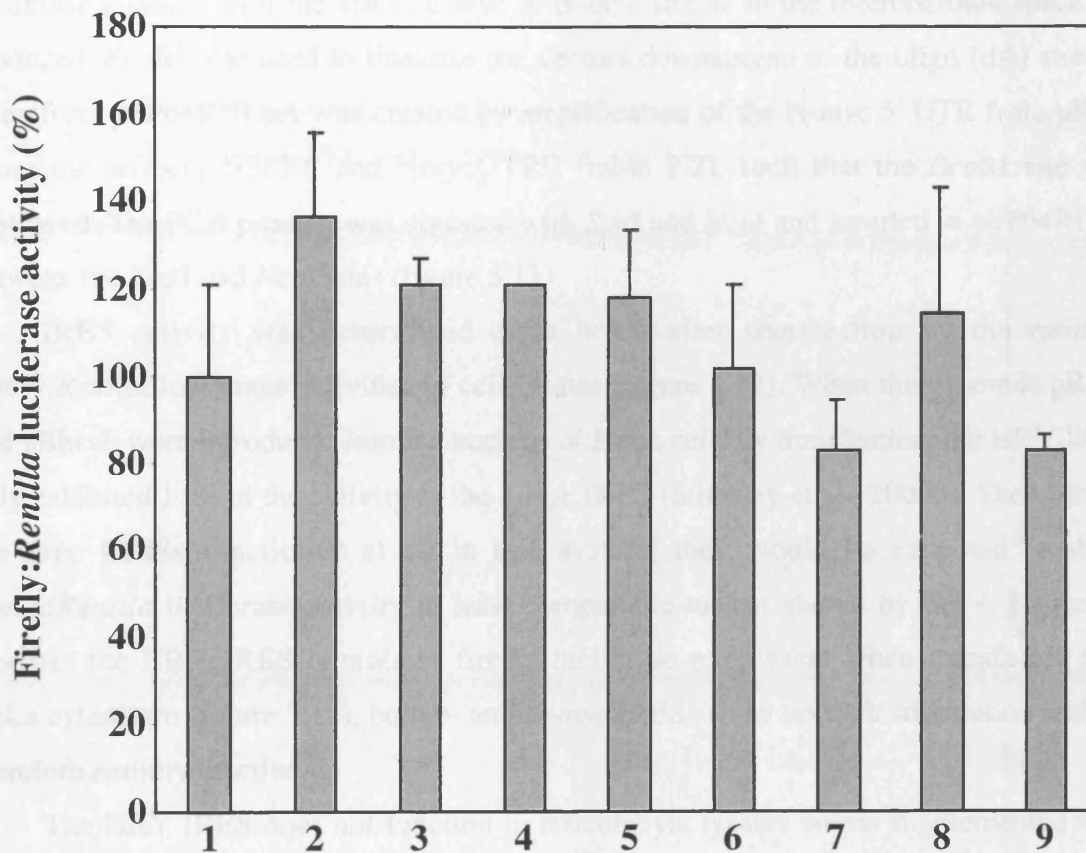
### 5.7 N-*myc* IRES activity in supplemented reticulocyte lysate

The N-*myc* 5' UTR does not support internal ribosome entry in a reticulocyte lysate system (figure 3.4). Similar behaviour of the poliovirus and HRV IRES was due to a deficiency in the *trans*-acting factors unr and PTB in this system, and various other viral IRESs have been found to require proteins that are not part of the canonical translation machinery for activity (section 1.4.5). A number of these factors have been synthesised and purified by the expression of histidine-tagged proteins in a bacterial system (Joanne Evans). Dicistronic RNA was made by *in vitro* transcription using pRNF linearised with *Not*I as a template, and used to programme standard reticulocyte lysate systems to which 2 µg of a protein was also added. After 2 hours of incubation, the activities of firefly and *Renilla* luciferases were assayed and IRES activity expressed as a ratio of firefly:*Renilla* (figure 5.10). The values obtained with supplemented extracts are shown as a percentage of the activity in reticulocyte lysate to which no factors had been added.

The majority of proteins tested had no effect on IRES activity, and PCBP1 and unr caused a slight inhibition. The greatest stimulation was observed when DAP5 was added to the system. However, this only increased IRES activity by 40%. As the N-*myc* 5' UTR is completely inactive as an IRES in reticulocyte lysate, and inhibits downstream cistron activity relative to pRF, a stimulation of this extent is not great enough to indicate that any internal ribosome entry occurs. N-*myc* IRES activity therefore requires a factor that was not tested, or a more complex array of stimulatory factors.

### 5.8 IRES activity in *in vitro* transcribed RNA introduced into cell cytoplasm

Previous data has shown that the c-*myc* IRES requires a "nuclear event" to function; that is, the RNA must be synthesised in the nucleus and transported to the cytoplasm of a cell for internal ribosome entry to occur (Stoneley et al., 2000b). To examine whether this is also true of the N-*myc* IRES, dicistronic RNA was produced by *in vitro* transcription and introduced directly into the cytoplasm of HeLa cells by transfection using lipofectin. Capped and polyadenylated RNA was used and was synthesised by *in vitro* transcription in the presence of cap analogue using the vectors pSP64RhrvLpA, pSP64RMLpA, and pSP64RNLpA as templates. When transcription is carried out from these vectors using



- Supplementary proteins**
1. No added protein
  2. DAP5
  3. eIF4G(613/1090)
  4. ITAF45
  5. La
  6. nPTB
  7. PCBP1
  8. PCBP2
  9. unr

**Figure 5.10 Activity of the N-myc IRES in reticulocyte lysate supplemented with protein factors.** Dicistronic RNA was produced by *in vitro* transcription using pRNF as a template and used to programme reticulocyte lysates. The translation reactions were supplemented with the known IRES *trans*-acting factors detailed above. IRES activity was determined as a ratio of firefly:*Renilla* luciferase activity, and expressed as a percentage of the value obtained in unsupplemented reticulocyte lysate. Results are an average of three independent experiments and error bars represent standard deviations.

SP6 polymerase, polyadenylated dicistronic RNAs containing the *Renilla* and firefly luciferase cistrons with the HRV, *c-myc* or *N-myc* IRESs in the intercistronic space are produced. *EcoRI* was used to linearise the vectors downstream of the oligo (dA) stretch. Therefore, pSP64RNLpA was created by amplification of the *N-myc* 5' UTR from pRNF using the primers NSPEF and NmycUTRR (table 2.2), such that the *EcoRI* site was destroyed. The PCR product was digested with *SpeI* and *NcoI* and inserted in pSP64RLpA between the *XbaI* and *NcoI* sites (figure 5.11).

IRES activity was determined eight hours after transfection by the ratio of firefly:*Renilla* luciferase activities in cell lysates (figure 5.12). When the plasmids pRMF and pRhrvF were introduced into the nucleus of HeLa cells by transfection, the HRV IRES only exhibited 14% of the activity of the *c-myc* IRES (Stoneley et al., 2000b). Therefore, if the *myc* IRESs functioned at all in this system, they would be expected to show firefly/*Renilla* luciferase activity at least comparable to that shown by HRV. However, whereas the HRV IRES stimulates firefly luciferase expression when transfected into HeLa cytoplasm (figure 5.12), both *c-* and *N-myc* IRESs show no such stimulation and are therefore entirely inactive.

The HRV IRES does not function in reticulocyte lysates unless supplemented with the factors unr and PTB, but when introduced into the cytoplasm of cells these factors are available and the IRES is able to function efficiently. The requirements of *myc* IRES activity are clearly more complex. Although it is possible that cytoplasmic proteins stimulate IRES activity, it appears that these IRESs also need to associate with proteins found only in the nucleus or at the nuclear membrane. Alternatively, *c-* and *N-myc* RNA may undergo post-transcriptional modifications when synthesised in the nucleus that render it capable of supporting internal ribosome entry.

### **5.9 Effects of known IRES trans-acting factors on N-myc IRES activity in the context of cultured cells**

As the requirements for *N-myc* IRES function are complex, it is possible that one or more of the protein factors tested in section 5.7 does stimulate this IRES, but is unable to do so in the context of reticulocyte lysate as other necessary factors are absent. To test this hypothesis, cotransfections were carried out in N2a cells in which pRNF was introduced in combination with a pcDNA3-based expression vector encoding a known *trans*-acting

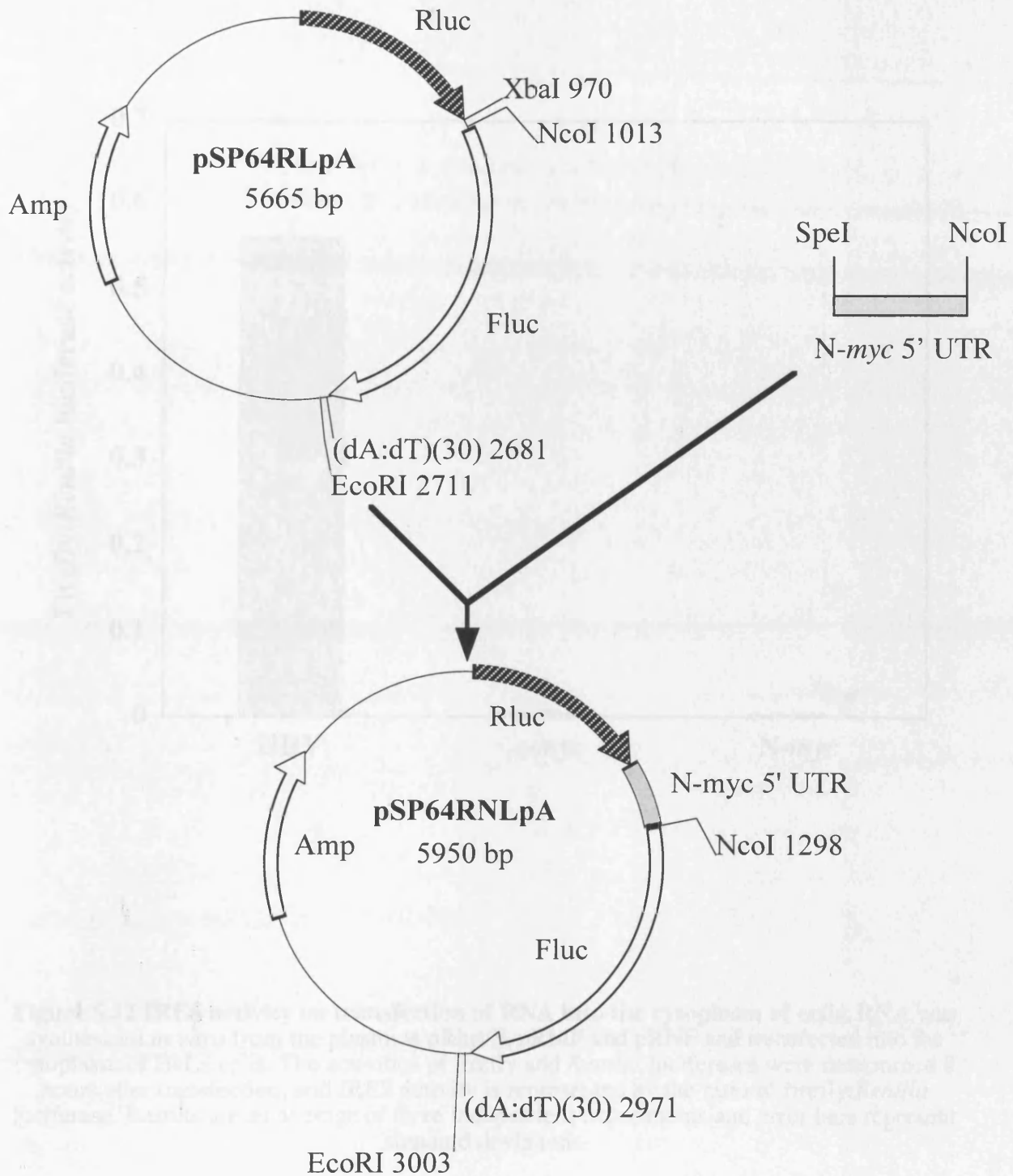


**Figure 5.11 Construction of the vector pSP64RNLpA.** The *N-myc* 5' UTR was amplified by PCR using the primers NSPEF and NmycUTRR, with pRNF as a template, such that the *EcoRI* site was destroyed. The PCR product was digested with *SpeI* and *NcoI* and inserted into pSP64RLpA between the *XbaI* and *NcoI* sites, following restriction digestion and dephosphorylation of the vector.

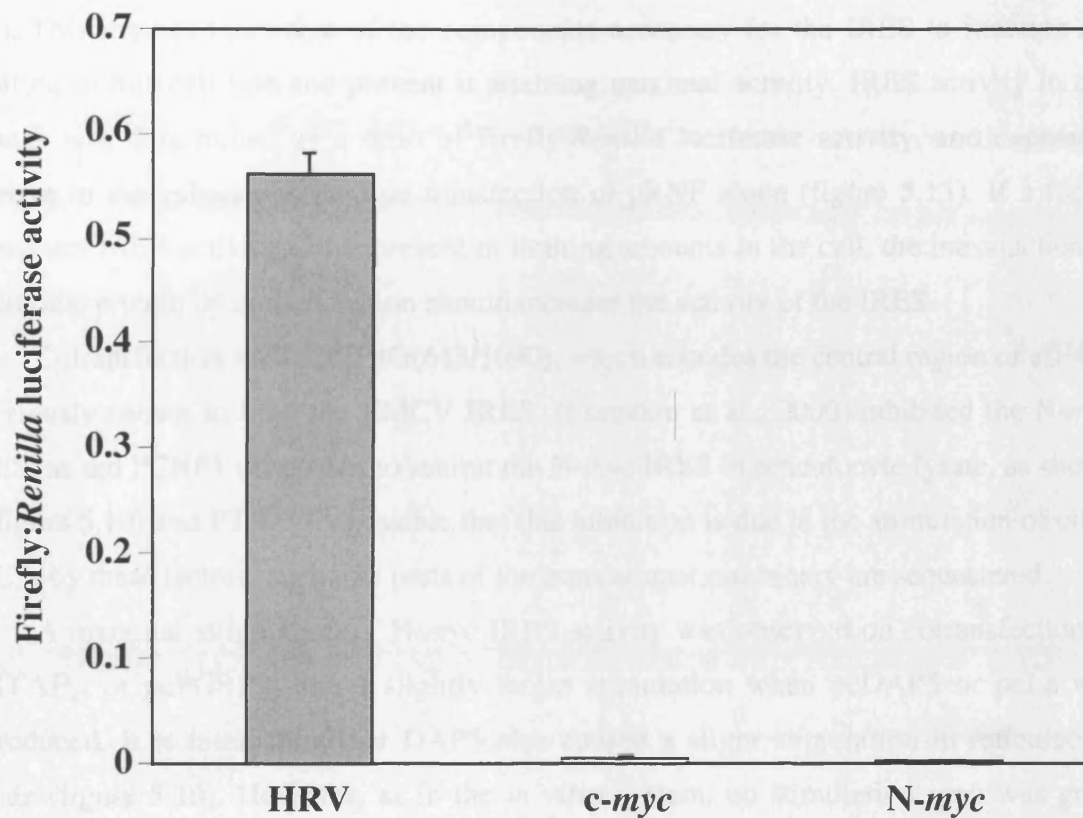


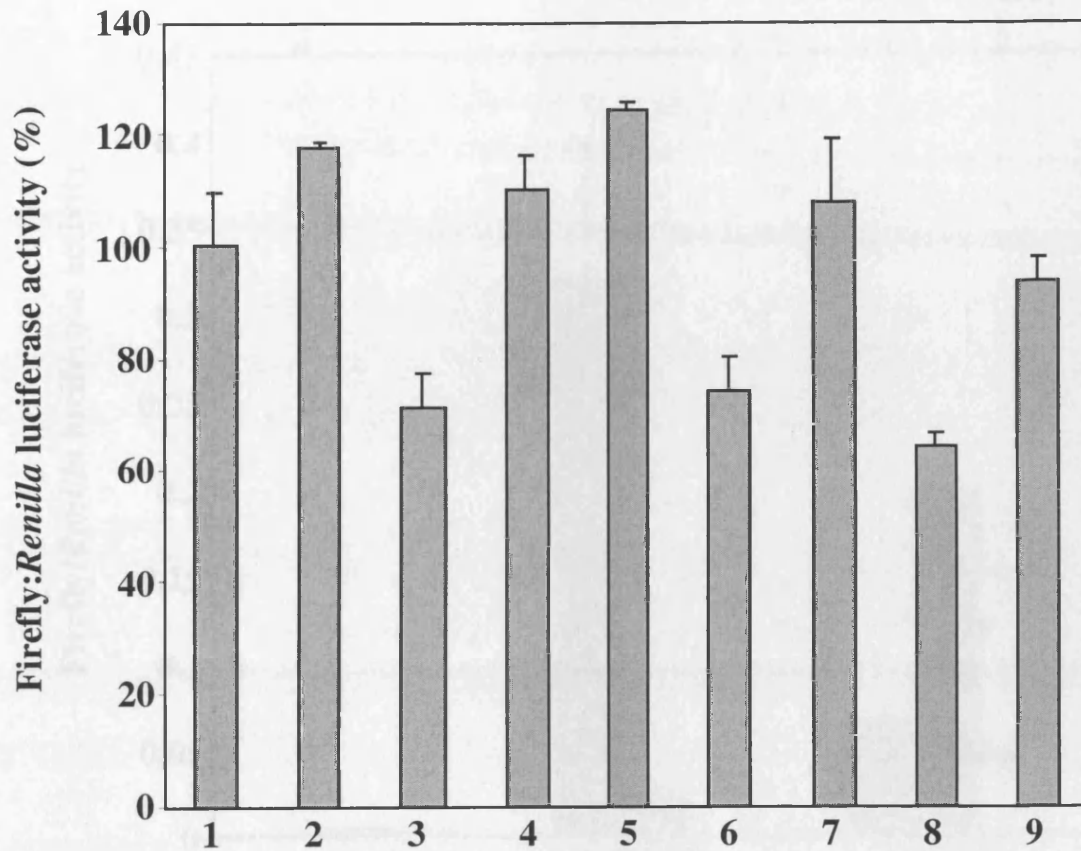
**Figure 5.12 IRES activity on transfection of RNA into the cytoplasm of cells.** RNA was synthesised *in vitro* from the plasmids pRhrvF, pRMF and pRNF and transfected into the cytoplasm of HeLa cells. The activities of firefly and *Renilla* luciferases were determined 8 hours after transfection, and IRES activity is represented by the ratio of firefly:*Renilla* luciferase. Results are an average of three independent experiments and error bars represent standard deviations.

factor (made by Joanne Evans). N2a cells were chosen as the N-*myc* IRES is relatively inactive in these cells when compared to other lines such as NT2 and SH-SY5Y (figure 5.1). This implies that some of the components necessary for the IRES to function are limiting in this cell line and prevent it attaining maximal activity. IRES activity in cell lysates was determined as a ratio of firefly:*Renilla* luciferase activity, and expressed relative to the values obtained on transfection of pRNF alone (figure 5.13). If a factor stimulates IRES activity and is present in limiting amounts in the cell, the introduction of additional protein by cotransfection should increase the activity of the IRES.

Cotransfection with pceIF4G(613/1090), which encodes the central region of eIF4GI previously shown to bind the EMCV IRES, (Lomakin et al., 2000) inhibited the N-*myc* IRES, as did PCBP1 (also seen to inhibit the N-*myc* IRES in reticulocyte lysate, as shown in figure 5.10) and PTB. It is possible that this inhibition is due to the stimulation of other IRESs by these factors, such that parts of the translational machinery are sequestered.

A marginal stimulation of N-*myc* IRES activity was observed on cotransfection of pcITAF<sub>45</sub> or pcPCBP2, and a slightly larger stimulation when pcDAP5 or pcLa was introduced. It is interesting that DAP5 also caused a slight stimulation in reticulocyte lysate (figure 5.10). However, as in the *in vitro* system, no stimulation seen was great enough to indicate a significant effect on IRES activity. This does not prove that none of these proteins is involved in the function of the N-*myc* IRES, as it is possible that a *trans*-acting factor is already present in sufficient quantities in cells such that the expression of additional protein has no effect. However, no positive evidence of stimulation by any of these factors was observed.

A further attempt to implicate or exclude known IRES *trans*-acting factors in the function of the N-*myc* IRES was made using an embryonic stem (ES) cell line in which *unr* has been knocked out (made by Dr H el ene Jacquemin-Sablon, CNRS, Bordeaux). The vectors pRhpF (a control plasmid that contains a hairpin between the *Renilla* and firefly luciferase cistrons, thereby reducing readthrough), pCROL (a CMV-based dicistronic luciferase vector containing the poliovirus IRES) and pRNF were introduced into these cells by transfection. IRES activity in the wildtype ES cell line L, and the *unr* double knockout cell lines A and B, was determined as a ratio of firefly:*Renilla* luciferase activity (figure 5.14). The poliovirus IRES is known to require *unr* to function, and its activity is therefore reduced to 7-11% of its levels in wildtype ES cells when the *unr* gene is knocked



- Cotransfected plasmid**
1. No additional plasmid
  2. pcDAP5
  3. pceIF4G(613/1090)
  4. pcITAF45
  5. pcLa
  6. pcPCBP1
  7. pcPCBP2
  8. pcPTB
  9. pcunr

**Figure 5.13 Effect of cotransfection of expression vectors encoding various *trans*-acting factors on N-myc IRES activity.** N2a cells were transfected with pRNF in combination with pcDNA3-based plasmids encoding the protein factors indicated. IRES activity in cell extracts was determined as a ratio of firefly:*Renilla* luciferase activity and is shown as a percentage of the values obtained on transfection of pRNF alone. Results are an average of three independent experiments and error bars represent standard deviations.

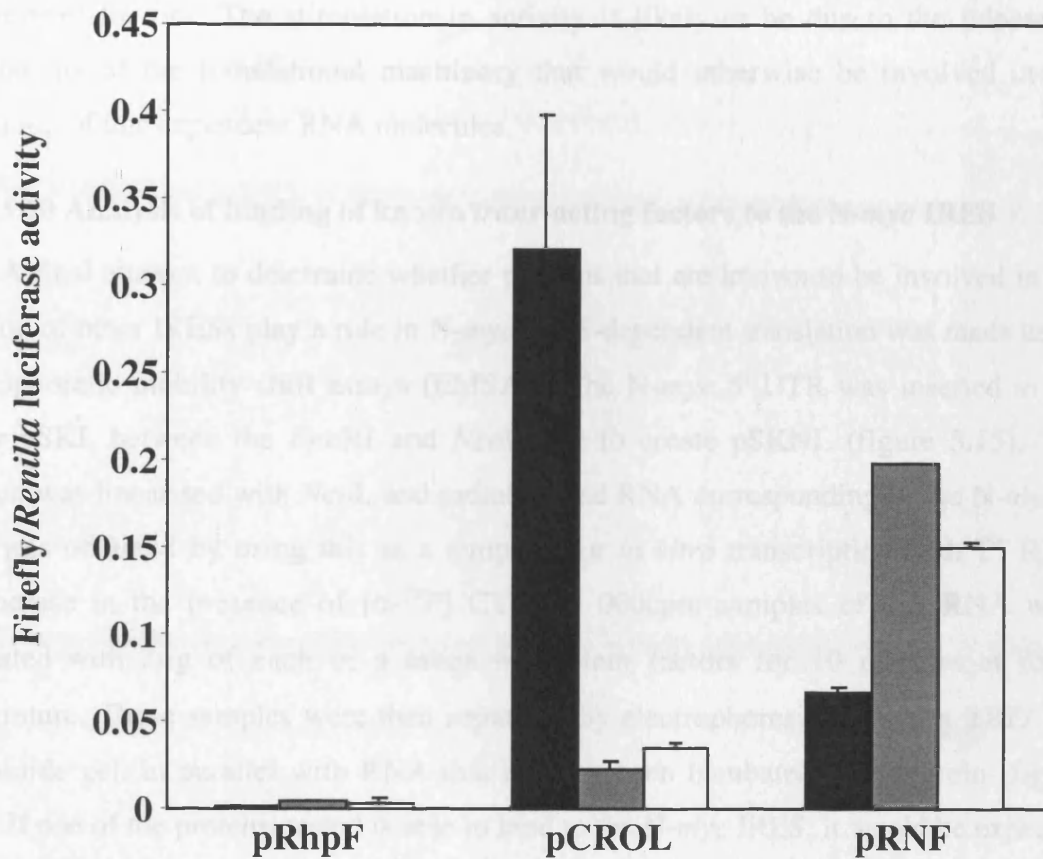


**Figure 5.14 IRES activity in unr knockout cells.** The plasmids pRhpF, pCROL and pRNF were introduced into the wildtype ES cell line L (black bars) and the unr  $-/-$  cell lines A (grey bars) and B (white bars) by transfection. IRES activity was determined as a ratio of firefly:*Renilla* luciferase activity. Results are an average of three independent experiments and error bars represent standard deviations.

out. In contrast, N-*myc* IRES activity is stimulated to 220-290% of its levels in wildtype cells when introduced into the *unr*<sup>-/-</sup> cell lines. This indicates that the N-*myc* IRES has no requirement for *unr*. The stimulation in activity is likely to be due to the release of components of the translational machinery that would otherwise be involved in the translation of *unr*-dependent RNA molecules.

### 5.10 Analysis of binding of known *trans*-acting factors to the N-*myc* IRES

A final attempt to determine whether proteins that are known to be involved in the function of other IRESs play a role in N-*myc* IRES-dependent translation was made using electrophoretic mobility shift assays (EMSAs). The N-*myc* 5' UTR was inserted in the vector pSKL between the *EcoRI* and *NcoI* sites to create pSKNL (figure 5.15). The plasmid was linearised with *NcoI*, and radiolabelled RNA corresponding to the N-*myc* 5' UTR was obtained by using this as a template for *in vitro* transcription with T7 RNA polymerase in the presence of [ $\alpha$ -<sup>32</sup>P] CTP. 25 000cpm samples of this RNA were incubated with 2 $\mu$ g of each of a range of protein factors for 10 minutes at room temperature. These samples were then separated by electrophoresis on a 0.5x TBE/ 5% acrylamide gel, in parallel with RNA that had not been incubated with protein (figure 5.16). If one of the proteins tested is able to bind to the N-*myc* IRES, it would be expected to induce a shift in the position of the radiolabelled RNA band towards a higher molecular weight. However, no alteration in the mobility of the RNA was detected in the presence of PCBP1, PCBP2, ITAF<sub>45</sub>, La, eIF4G(613/1090) or DAP5. This provides further evidence that none of these proteins is required for the N-*myc* IRES to function.

### 5.11 N-*myc* IRES binding to factors in cell extracts

Attempts to replicate the "nuclear event" required for *c-myc* IRES function by *in vitro* transcription and translation in extracts derived from cultured cells have proved unsuccessful (Le Quesne, 2000). Such a course of action was therefore not pursued using the N-*myc* IRES. Instead, total cell extracts were produced from cultured HeLa and NT2 cells and attempts were made to detect IRES-binding factors in these extracts.

Initially, EMSAs were carried out as described in section 5.10. However, instead of adding specific proteins to the RNA, a series of different quantities of the two cell extracts were incubated with radiolabelled N-*myc* IRES RNA. The position of the RNA after electrophoresis of the complexes was visualised by autoradiography (figure 5.17). The

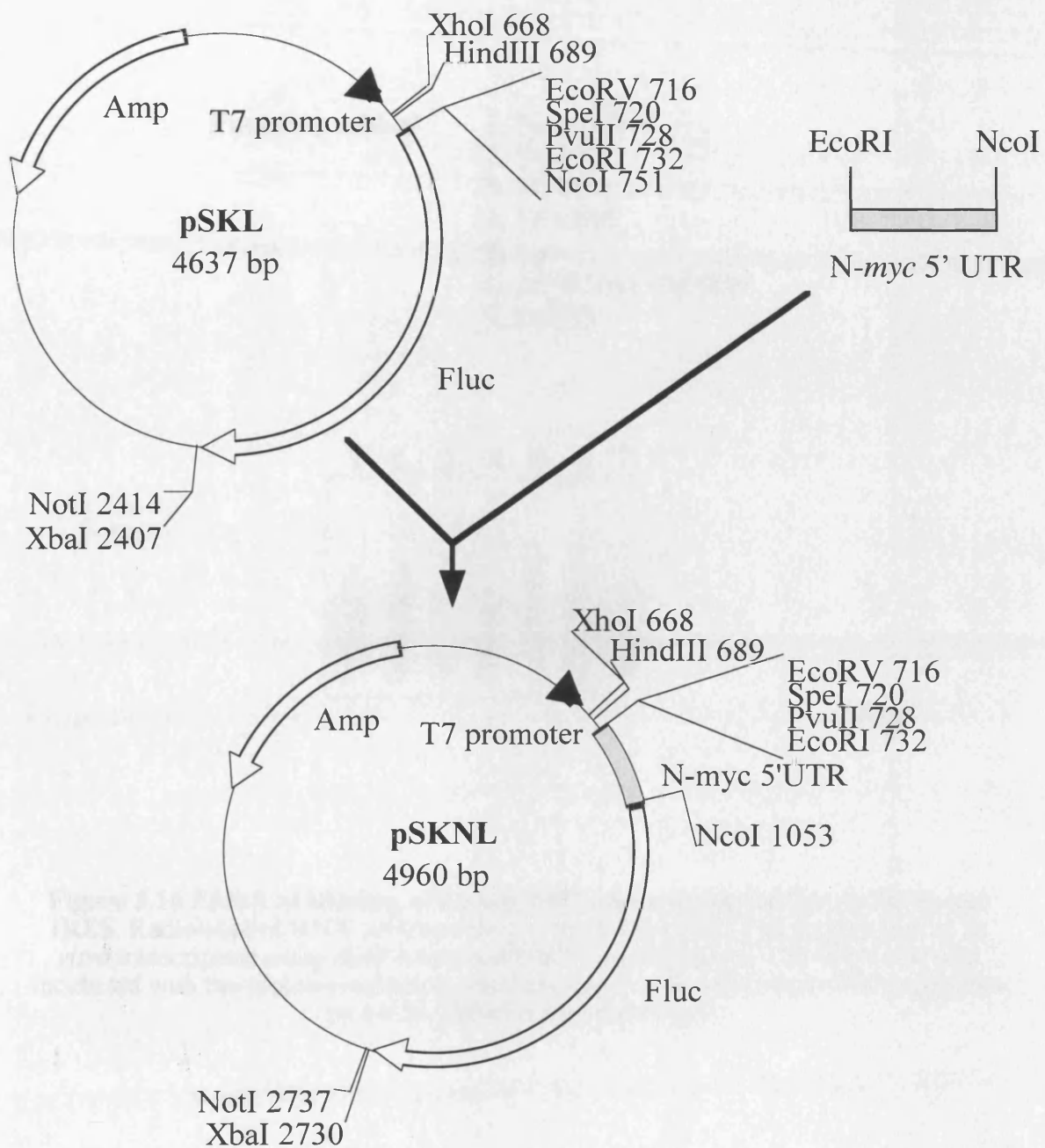


**Figure 5.15 Construction of the vector pSKNL.** An RT-PCR product encoding the N-*myc* 5' UTR was digested with *EcoRI* and *NcoI*. This fragment was inserted between the same sites in the vector pSKL, after restriction digestion and dephosphorylation of the vector. The resultant plasmid was named pSKNL.

**Proteins added**

1. No protein
2. PCBP1
3. PCBP2
4. ITAF45
5. La
6. eIF4G(613/1090)
7. DAP5

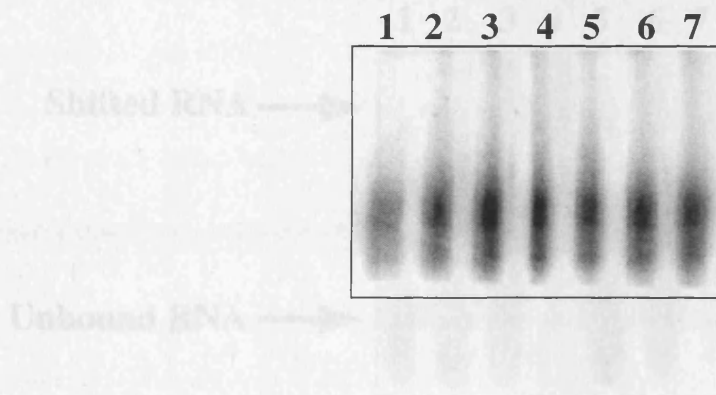


**Figure 5.16 EMSA of binding of known IRES-*trans*-acting factors to the N-*myc* IRES.** Radiolabelled RNA corresponding to the N-*myc* IRES was synthesised by *in vitro* transcription using *Nco*I-linearised pSKNL as a template. The RNA was then incubated with the proteins indicated, and complexes were subjected to electrophoresis on a 0.5x TBE/5% acrylamide gel.

presence of cell extract induces a shift in RNA mobility towards a higher molecular weight, indicating that proteins present in cell extracts are able to bind the RNA with high affinity.

### Cell extracts added

1. No added cell extract
2. 0.008 $\mu$ g HeLa total CE
3. 0.08 $\mu$ g HeLa total CE
4. 0.8 $\mu$ g HeLa total CE
5. 0.008 $\mu$ g NT2 total CE
6. 0.08 $\mu$ g NT2 total CE
7. 0.8 $\mu$ g NT2 total CE

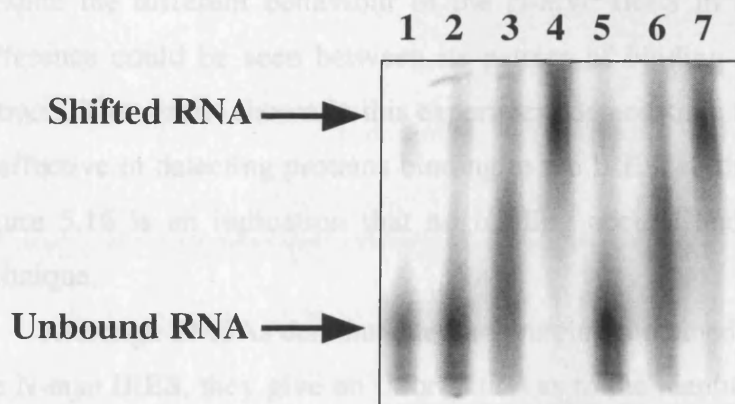


**Figure 5.17 EMSA of protein binding by the *N-myc* IRES in cell extracts.** Radiolabelled *N-myc* IRES RNA, produced by *in vitro* transcription from *Nco*I-linearised pSKNL, was incubated with the quantities of HeLa or NT2 total cell extract indicated. The complexes were separated by electrophoresis on a 0.5x TBE/ 5% acrylamide gel.

presence of cell extract induces a shift in RNA mobility towards a higher molecular weight, indicating that proteins present in the extracts are able to bind the RNA with high enough affinity to remain associated throughout electrophoresis. The extent to which the RNA shifts increases with increasing quantities of cell extract, which implies that several different proteins bind to the RNA. These proteins must either bind with different affinities, or be present at different concentrations within the extracts, to show this variability in shift. Alternatively, it is possible that the N-*myc* IRES is able to bind multiple copies of one protein that is present at low concentration, so that as more cell extract is added more protein molecules are able to bind and the size of the complex increases. Despite the different behaviour of the N-*myc* IRES in HeLa and NT2 cell lines, no difference could be seen between its pattern of binding to proteins from the two cell extracts. The results shown in this experiment demonstrate that the method of EMSA used is effective in detecting proteins binding to the IRES, so that the lack of shift detected in figure 5.16 is an indication that no binding occurs, and is not due to failure of the technique.

Although EMSAs demonstrate that proteins contained within the cell extracts bind to the N-*myc* IRES, they give no information as to the identity of these proteins. UV cross-linking experiments were therefore carried out. <sup>32</sup>P-labelled RNA was synthesised by *in vitro* run-off transcription using pSKNL that had been linearised with *Nco*I as a template. 400 000cpm (2.4pmol) of this RNA was incubated with HeLa or NT2 total cell extract in the presence of increasing quantities of unlabelled competitor RNA. Non-specific GAPDH competitor RNA was synthesised using *Hind*III-linearised pSKGAP:E/H (Paulin, 1997) as template and T3 polymerase, and specific N-*myc* IRES competitor RNA synthesised using the same template as for radiolabelled RNA. The protein-RNA complexes formed were cross-linked using a 312nm UV light source, at 0°C for 30 minutes. After the digestion of unbound RNA, proteins were separated by SDS-PAGE using 10% gels and proteins that were bound to labelled RNA were detected by autoradiography. When N-*myc* IRES RNA was incubated with either HeLa (figure 5.18) or NT2 (figure 5.19) cell extract, a range of proteins of different sizes were bound. However, few proteins were still able to bind in the presence of unlabelled competitor RNA. One protein is of particular interest and is marked by an asterisk in both figures. This protein is approximately 30kDa in molecular weight and remained bound to the IRES even in the presence of the highest concentrations of

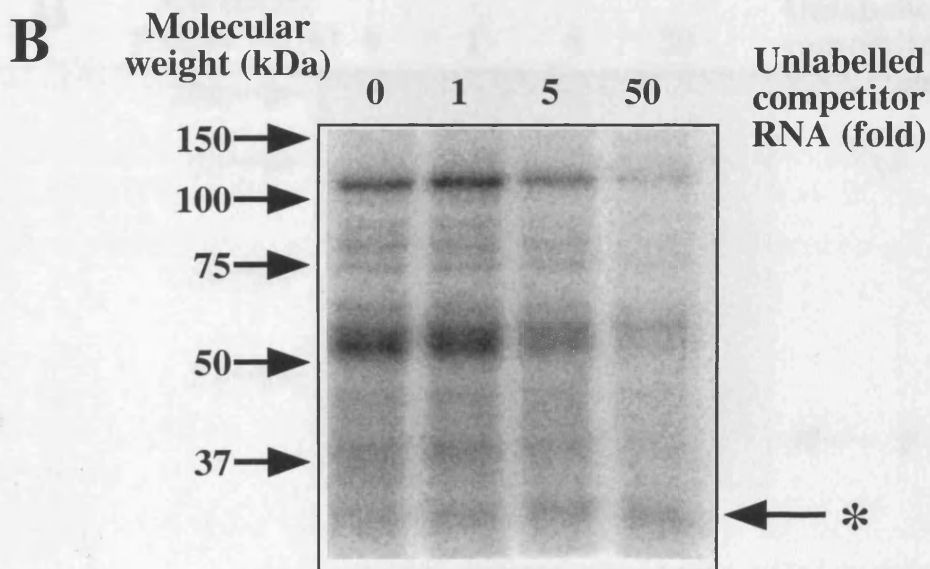
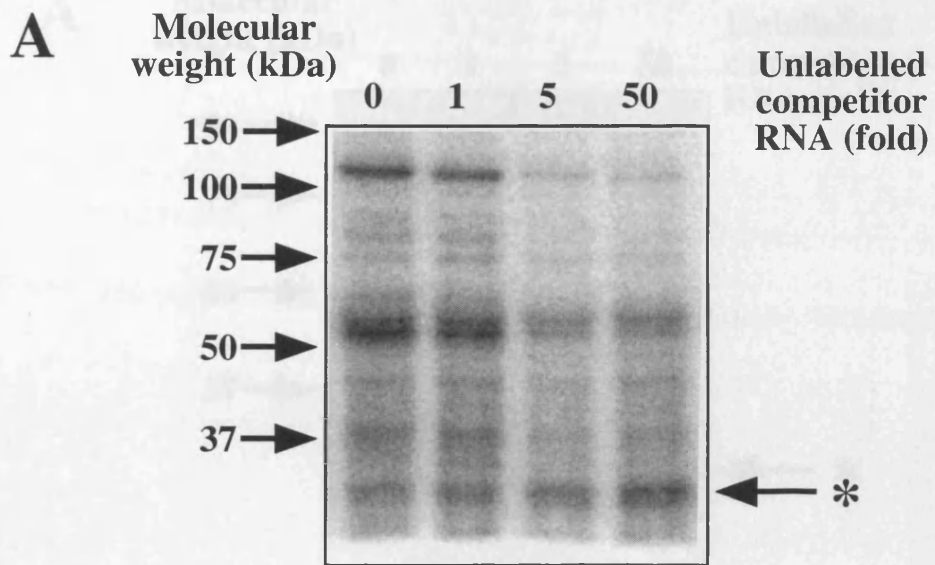


**Figure 5.18 UV cross-linking of HeLa total cell extract to N-myc IRES RNA.** Radiolabelled RNA corresponding to the N-myc IRES was synthesised by *in vitro* transcription using *NcoI*-linearised pSKNL as a template. The RNA was incubated with HeLa total cell extract in the presence of increasing quantities of unlabelled competitor RNA. RNA-protein complexes were linked by UV irradiation, digested with RNase A/ RNase T1, and separated by SDS-PAGE. Protein size markers are indicated to the left of the gel, and the band of interest is marked by an asterisk to the right of the gel. (A) GAPDH competitor RNA. (B) N-myc IRES competitor RNA.

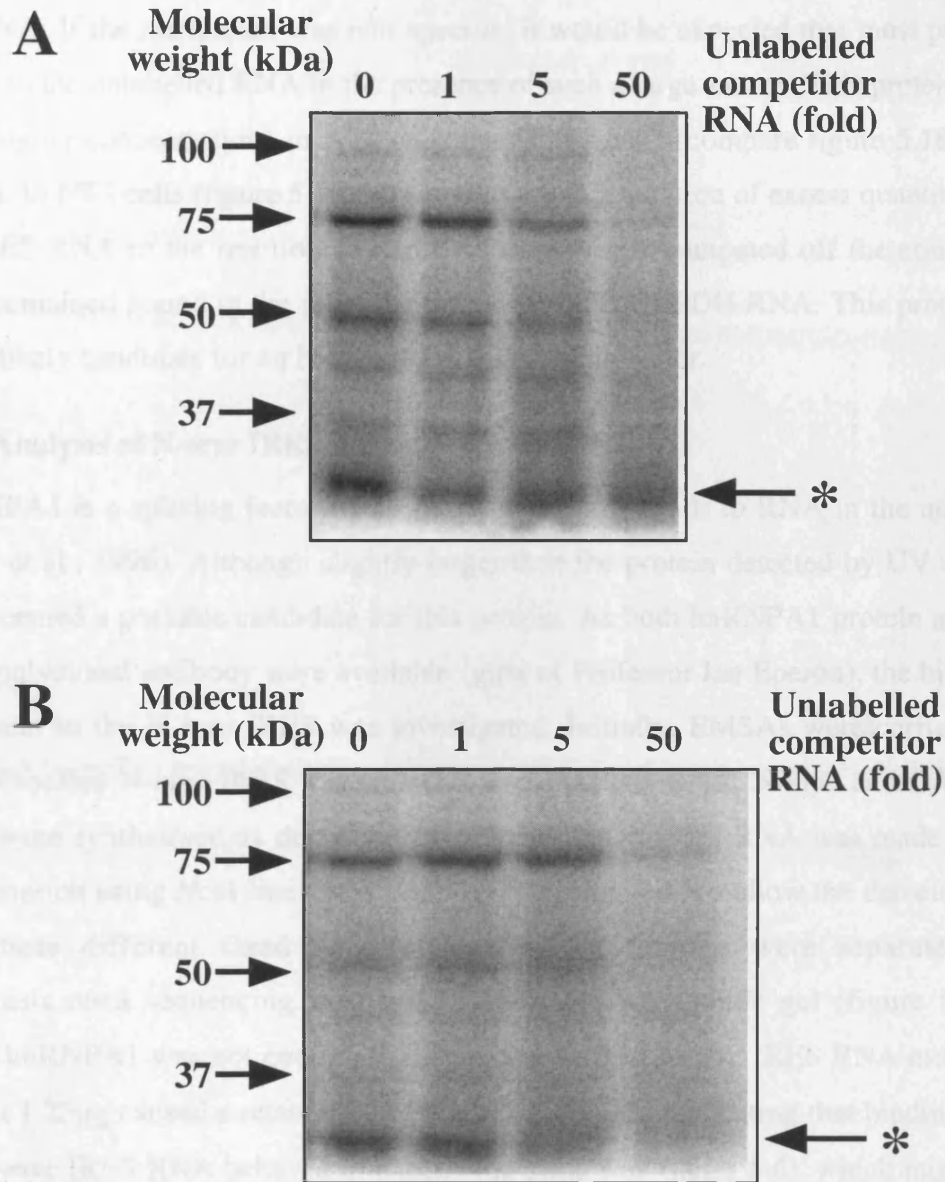


**Figure 5.19 UV cross-linking of NT2 total cell extract to N-myc IRES RNA.**

Radiolabelled RNA corresponding to the N-myc IRES was synthesised by *in vitro* transcription using *NcoI*-linearised pSKNL as a template. UV cross-linking was carried out as described in figure 5.18, but using NT2 total cell extract. Protein size markers are indicated to the left of the gel, and the band of interest is marked by an asterisk to the right of the gel. (A) GAPDH competitor RNA. (B) N-myc IRES competitor RNA.

GAPDH RNA. If the interaction was non-specific, it would be expected that most protein would bind to the unlabelled RNA in the presence of such a large excess. This protein was present at higher concentrations in NT2 cells than HeLa cells (compare figure 5.18 with figure 5.19). In NT2 cells (figure 5.19) it is easy to see that addition of excess quantities of specific IRES RNA to the reaction caused the protein to be competed off the complex, whereas it remained bound in the presence of non-specific GAPDH RNA. This protein is therefore a likely candidate for an N-*myc* IRES *trans*-acting factor.

### 5.12 Analysis of N-*myc* IRES interaction with hnRNPA1

hnRNPA1 is a splicing factor of 38.7kDa in size that binds to RNA in the nucleus (Weighardt et al., 1996). Although slightly larger than the protein detected by UV cross-linking, it seemed a possible candidate for this protein. As both hnRNPA1 protein and an hnRNPA1 polyclonal antibody were available (gifts of Professor Ian Eperon), the binding of this protein to the N-*myc* IRES was investigated. Initially, EMSAs were carried out using radiolabelled N-*myc* IRES, c-*myc* IRES, and GAPDH RNA. N-*myc* and GAPDH transcripts were synthesised as described above, and c-*myc* IRES RNA was made by *in vitro* transcription using *Nco*I linearised pSKML as a template. To allow the detection of shifts in these different sized RNA molecules, the samples were separated by electrophoresis on a sequencing length 0.5x TBE/ 5% acrylamide gel (figure 5.20). 0.125µg of hnRNPA1 was not enough to induce any shift in N-*myc* IRES RNA mobility (lane 2), but 1.25µg caused a retardation of this RNA (lane 3), indicating that binding had occurred. c-*myc* IRES RNA behaved in exactly the same way (lanes 4-6), which might be expected given the similarities between the two IRESs. However, 1.25µg of hnRNPA1 was also enough to induce a shift in mobility of GAPDH RNA (lane 9). As GAPDH RNA shows no IRES characteristics, this led to the conclusion that hnRNPA1 is capable of binding any RNA when present at high enough concentrations, and the binding to the *myc* IRESs observed was non-specific.

A further experiment was carried out in which N-*myc* IRES RNA was incubated with 0.8µg of HeLa total cell extract, as in section 5.11. However, the hnRNPA1 antibody was also added to one of the reactions, with the rationale that if hnRNPA1 was present in the complex of bound proteins, the presence of its antibody would induce a supershift to a higher molecular weight position. The samples were separated on a 0.5x TBE gel in which

the bottom half was 75% acrylamide and the top half was 4% TBE. The RNA and extract complex is visible in lanes 1-3 and 5-6. The N-myc RNA complex is detectable. On addition of 0.125  $\mu$ g of hnRNPA1 to the N-myc RNA complex (lane 4) and 1.25  $\mu$ g of hnRNPA1 (lane 5), the N-myc RNA complex is shifted to a higher position (Figure 5.21). A similar shift was observed for the c-myc RNA complex (lanes 7 and 8) and GAPDH RNA complex (lanes 9 and 10). The N-myc RNA complex that contains hnRNPA1 protein is shifted to a higher position than the unbound N-myc RNA complex and is visible in lanes 4 and 5.

### 5.13 Discussion

The data presented above provide evidence for the ability of hnRNPA1 to bind to N-myc IRES. Whether previous studies have shown that hnRNPA1 binds to IRESs are disputable to some extent. In a study by Wang et al. (1998), the N-myc IRES is considered to be a weak IRES, which the enhanced IRES activity is observed in the presence of hnRNPA1. In a study by Wang et al. (2000), hnRNPA1 is shown to bind to the N-myc IRES and to enhance its activity. In a study by Wang et al. (2001), hnRNPA1 is shown to bind to the N-myc IRES and to enhance its activity. In a study by Wang et al. (2002), hnRNPA1 is shown to bind to the N-myc IRES and to enhance its activity. In a study by Wang et al. (2003), hnRNPA1 is shown to bind to the N-myc IRES and to enhance its activity. In a study by Wang et al. (2004), hnRNPA1 is shown to bind to the N-myc IRES and to enhance its activity. In a study by Wang et al. (2005), hnRNPA1 is shown to bind to the N-myc IRES and to enhance its activity. In a study by Wang et al. (2006), hnRNPA1 is shown to bind to the N-myc IRES and to enhance its activity. In a study by Wang et al. (2007), hnRNPA1 is shown to bind to the N-myc IRES and to enhance its activity. In a study by Wang et al. (2008), hnRNPA1 is shown to bind to the N-myc IRES and to enhance its activity. In a study by Wang et al. (2009), hnRNPA1 is shown to bind to the N-myc IRES and to enhance its activity. In a study by Wang et al. (2010), hnRNPA1 is shown to bind to the N-myc IRES and to enhance its activity. In a study by Wang et al. (2011), hnRNPA1 is shown to bind to the N-myc IRES and to enhance its activity. In a study by Wang et al. (2012), hnRNPA1 is shown to bind to the N-myc IRES and to enhance its activity. In a study by Wang et al. (2013), hnRNPA1 is shown to bind to the N-myc IRES and to enhance its activity. In a study by Wang et al. (2014), hnRNPA1 is shown to bind to the N-myc IRES and to enhance its activity. In a study by Wang et al. (2015), hnRNPA1 is shown to bind to the N-myc IRES and to enhance its activity. In a study by Wang et al. (2016), hnRNPA1 is shown to bind to the N-myc IRES and to enhance its activity. In a study by Wang et al. (2017), hnRNPA1 is shown to bind to the N-myc IRES and to enhance its activity. In a study by Wang et al. (2018), hnRNPA1 is shown to bind to the N-myc IRES and to enhance its activity. In a study by Wang et al. (2019), hnRNPA1 is shown to bind to the N-myc IRES and to enhance its activity. In a study by Wang et al. (2020), hnRNPA1 is shown to bind to the N-myc IRES and to enhance its activity. In a study by Wang et al. (2021), hnRNPA1 is shown to bind to the N-myc IRES and to enhance its activity. In a study by Wang et al. (2022), hnRNPA1 is shown to bind to the N-myc IRES and to enhance its activity. In a study by Wang et al. (2023), hnRNPA1 is shown to bind to the N-myc IRES and to enhance its activity. In a study by Wang et al. (2024), hnRNPA1 is shown to bind to the N-myc IRES and to enhance its activity. In a study by Wang et al. (2025), hnRNPA1 is shown to bind to the N-myc IRES and to enhance its activity.

1 2 3 4 5 6 7 8 9

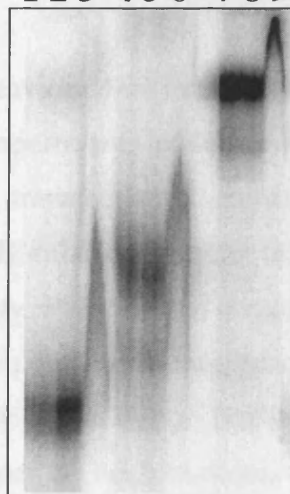


**Figure 5.20 EMSA of hnRNPA1 binding to N-myc, c-myc and GAPDH RNA.** Radiolabelled N-myc, c-myc and GAPDH RNA molecules were synthesised by *in vitro* transcription and incubated with the quantities of hnRNPA1 protein indicated. Bound complexes were separated by electrophoresis on a sequencing length 0.5x TBE/ 5% acrylamide gel.

the bottom half was 5% acrylamide and the top half was 3%. This allowed the RNA-cell extract complex to migrate far enough into the gel to make an additional shift in position detectable. On addition of anti-hnRNPA1 to the reaction, such a supershift was observed (figure 5.21, compare lanes 2 and 3). However, the same reaction was carried out using anti-p70 S6 kinase, as its target would not be expected to bind to an IRES. An identical second shift was observed with this antibody (figure 5.21, lane 4). The supershift observed in the presence of anti-hnRNPA1 must therefore be regarded as non-specific. It is possible that contaminating proteins that do not bind the N-*myc* IRES specifically are present in the retarded RNA-cell extract complex and are detected by antibodies.

### 5.13 Discussion

The data presented above provide some intriguing insights into the behaviour of the N-*myc* IRES. Whereas previous experiments in HeLa cells indicated that the N- and c-*myc* IRESs are comparable in activity, transfection of neuronal cell lines shows the activity of the N-*myc* IRES to be considerably enhanced relative to that of c-*myc*. All the cell lines in which the enhanced IRES activity was detected express N-Myc, whereas activity was comparable in non-neuronal cells in which this gene is not expressed. It should be emphasised that enhanced activity of the N-*myc* IRES relative to that of c-*myc* does not correlate with enhanced activity *per se*; neuroblastoma cell lines such as N2a and NB2a show lower N-*myc* IRES activity than HeLa cells when compared to pRF.

This implies that the cellular requirements of the c- and N-*myc* IRESs are different, although probably only subtly so, and provides a further distinction to add to those already found in chapter 3. Whereas a highly transformed, translationally active cell line such as HeLa is able to support initiation from both *myc* IRESs, and others such as that of Apaf-1 (Coldwell et al., 2000), efficiently, the neuronal cells in which N-Myc protein is expressed provide a specialised environment particularly favourable to the N-*myc* IRES. This is likely to be due to one of two mechanisms; either neuronal cells express a factor that is inhibitory to the c-*myc* IRES but does not affect that of N-*myc*, or, more probably, a neuronal factor stimulates N-*myc* IRES activity to a greater extent than that of c-*myc*. The N-*myc* IRES becomes less active during neuronal differentiation, while the c-*myc* IRES does not. The features that stimulate the N-*myc* IRES relative to that of c-*myc* therefore

appear to be specific to neuronal precursor cells, and to diminish during differentiation, when N-Myc protein expression is also known to increase.

Both *c-myc* and *N-myc* 5' UTRs show considerable homology between human and murine cells, and in fact the murine version also demonstrates IRES activity in all cell lines tested (Table 5.1). The fact that the murine IRES is threefold more active than its human counterpart, although it is likely that the two IRESs function in the same manner, is a parallel that suggests that IRES has assumed an activating function during its evolution.

A range of known IRES factors have been examined for their ability to stimulate the activity of, or interact with, the N-myc IRES. In no case could any such stimulation or interaction be detected. This does not conclusively prove that none of these factors plays any role in N-myc IRES-dependent translation, as it is possible that a multiplicity of indirect interactions are relevant, either a complex of factors is necessary to activate the IRES. Use of the *in vitro* system examined here can definitely be excluded as a site in N-myc IRES function, as IRES activity is maintained in our full cells. On balance, it is unlikely that any of the factors tested is relevant to the N-myc IRES. However, EMSA



**Figure 5.21 EMSA of N-myc RNA with cell extract and hnRNPA1 antibody.**

Radiolabelled N-myc RNA was incubated with HeLa total cell extract, with or without the addition of antibody as indicated. Complexes were separated by electrophoresis on a 0.5x TBE gel of which the bottom half was 5% acrylamide and the top half was 3% acrylamide.

appear to be specific to neuronal precursor cells, and to diminish during differentiation, when N-Myc protein expression is also known to decline.

Both *c-* and *N-myc* 5' UTRs show considerable homology between human and murine cells, and in both cases the murine version also demonstrates IRES activity in all cell lines tested. Interestingly, no species specificity was observed, and the ratio of human:murine IRES activity was the same in all cell lines tested. In the case of the *N-myc* IRES this implies that its function and requirements have been evolutionarily conserved, as the human and murine versions are equally active. However, the murine *c-myc* IRES is threefold more active than its human equivalent. Although it is likely that the two IRESs function in the same manner, it is possible that the murine IRES has acquired an activating mutation during its evolution.

A range of known IRES *trans*-acting factors have been examined for their ability to stimulate the activity of, or interact with, the *N-myc* IRES. In no case could any such stimulation or interaction be detected. This is not conclusive proof that none of these factors plays any role in *N-myc* IRES-dependent translation, as it is possible that a transitory or indirect interaction could be relevant, or that a complex of factors is necessary to activate the IRES. Unr is the only factor examined that can definitely be excluded from a role in *N-myc* IRES function, as IRES activity is stimulated in unr null cells. On balance, it is unlikely that any of the factors tested is relevant to the *N-myc* IRES. However, EMSA and cross-linking data indicate that the IRES does bind specifically to proteins found in HeLa and NT2 cells. The protein identified by cross-linking appears particularly promising as its expression is enhanced in NT2 cells relative to HeLa cells. Despite these encouraging initial results, there has been no success as yet in discovering the identity of this protein and whether it is necessary for *N-myc* IRES activity. Even if so, other factors might be required, and it remains possible that the "nuclear event" is a feature of RNA modification as opposed to protein binding. A further possibility is that one or more essential factors for IRES activity is highly labile and does not survive the process of cell extraction.

## Chapter 6

### Analysis of IRES function

#### 6.1 Introduction

The picornaviral IRESs serve a clear function in allowing efficient translation of the viral genome despite the inhibition of cap-dependent translation that occurs during viral infection (discussed in section 1.4.1). However, it is considerably less clear why certain cellular mRNAs should choose to adapt such a complex strategy for initiation of translation, while most cellular transcripts use the cap-dependent method. An attractive explanation is that it is necessary to maintain translation of certain crucial proteins during physiological situations in which cap-dependent initiation is inhibited. There are numerous situations in which this occurs, such as during heat shock, mitosis, and apoptosis (Sheikh and Fornace, 1999). Prior to these studies, the first suggestions that this might be the case had been provided by the discovery that the VEGF IRES functions during hypoxia (Stein et al., 1998) and the PDGF IRES is activated during differentiation (Bernstein et al., 1997). More recent data has indicated that several other cellular IRESs are active during specific stress situations (Hellen and Sarnow, 2001). It was therefore decided to analyse the function of the *c-myc* IRES during some of these stresses.

#### 6.2 c-Myc protein expression during apoptosis induced by TRAIL and staurosporine

During apoptosis eIF4G is cleaved such that cap-dependent initiation is inhibited (section 1.2.6) (Morley et al., 1998). As it is known that c-Myc expression can contribute to apoptosis (Hoffman and Liebermann, 1998), it was considered to be of particular interest to study the behaviour of the *c-myc* IRES under these conditions. Two different apoptotic stimuli were used in HeLa cells; TRAIL, which acts via a receptor-mediated pathway, and staurosporine, which induces apoptosis in a non-receptor-mediated fashion. Propidium iodide staining and observation of PARP cleavage had previously been used to confirm that these reagents are able to induce apoptosis in these cells, while during treatment eIF4G cleavage was seen to occur and translation to diminish (Stoneley et al., 2000a). HeLa cells were therefore treated with 0.25µg/ml TRAIL or 1µM staurosporine in fresh medium. Protein samples taken during apoptotic timecourses induced by both

reagents were subjected to SDS-PAGE and Western blotting, and the blots were probed with the antibody 9E10 to visualise c-Myc levels (figure 6.1). No change was seen in the levels of protein during an 8 hour time period, even though all the eIF4G had been cleaved in staurosporine-treated cells by 4 hours after treatment (Stoneley et al., 2000a). As the half-life of c-Myc is normally only 20-40 minutes (Hann and Eisenman, 1984), this implied that a transcriptional, translational or mRNA or protein stability mechanism was being used to maintain c-Myc levels during apoptosis.

### 6.3 c-Myc protein stability during apoptosis

Samples taken from HeLa cells during TRAIL-induced apoptosis were subjected to Northern blotting and probed for *c-myc* mRNA, and it was found that levels were unaltered during an 8 hour time period (Stoneley et al., 2000a). This indicates that a change in transcription or stability of the *c-myc* transcript is not responsible for the unaltered protein levels observed during apoptosis, when translation is inhibited. A further possibility to consider is that changes in stability of the c-Myc protein could occur. In accordance with this, HeLa cells were pulse-labelled with <sup>35</sup>S-methionine for 30 minutes, then "chased" with unlabelled methionine, and incorporation of <sup>35</sup>S into c-Myc was determined following immunoprecipitation (figure 6.2). In untreated cells the half-life of c-Myc was approximately 20 minutes, as predicted from the literature (figure 6.2A, closed triangles of figure 6.2B). When cells were subjected to TRAIL treatment for 3 hours before pulse labelling, the half-life of c-Myc was 17 minutes (figure 6.2A, open triangles of figure 6.2B). This demonstrates that TRAIL-induced apoptosis does not lead to stabilisation of c-Myc protein; in fact, it causes a slight reduction in stability. This supports the hypothesis that a translational mechanism is responsible for c-Myc protein maintenance.

### 6.4 *c-myc* IRES activity during apoptosis

To examine the behaviour of the *c-myc* IRES during apoptosis, HeLa cells were transfected with the plasmid pRMF (which contains the *c-myc* IRES between the *Renilla* and firefly luciferase cistrons). 24 hours after transfection, apoptosis was induced using TRAIL, and samples were harvested at fixed time intervals and luciferase activity assayed (figure 6.3). Luciferase activity was normalised to the transfection control of  $\beta$ -galactosidase, as this has a much longer half-life than the two luciferases and should

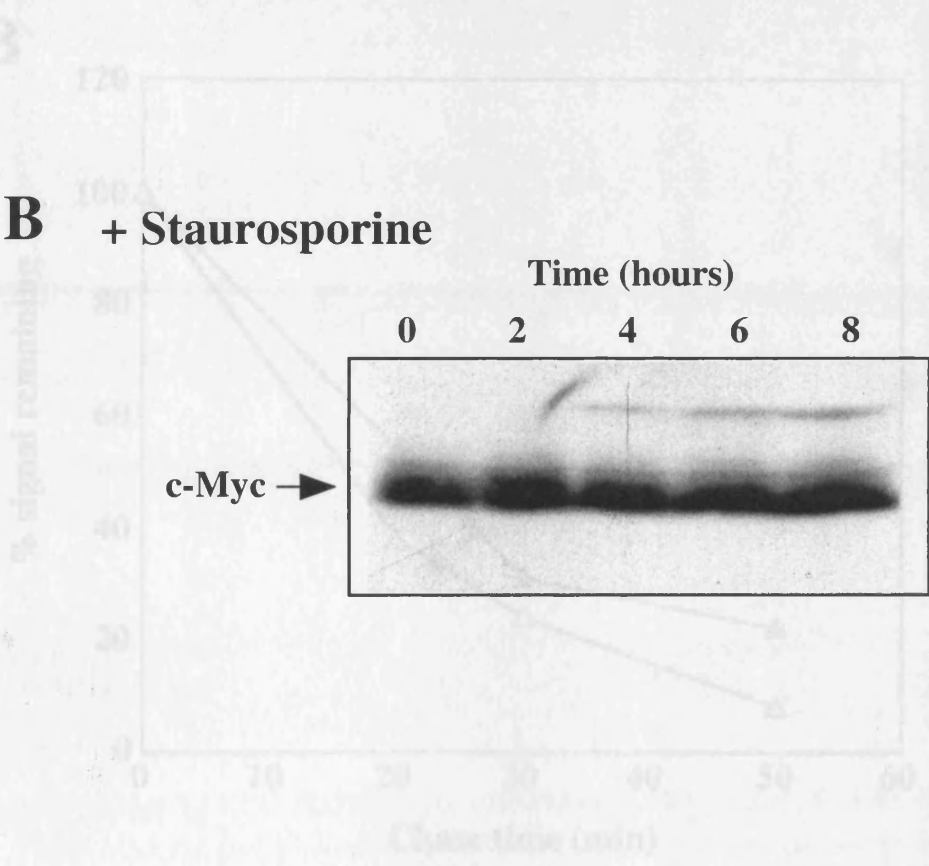
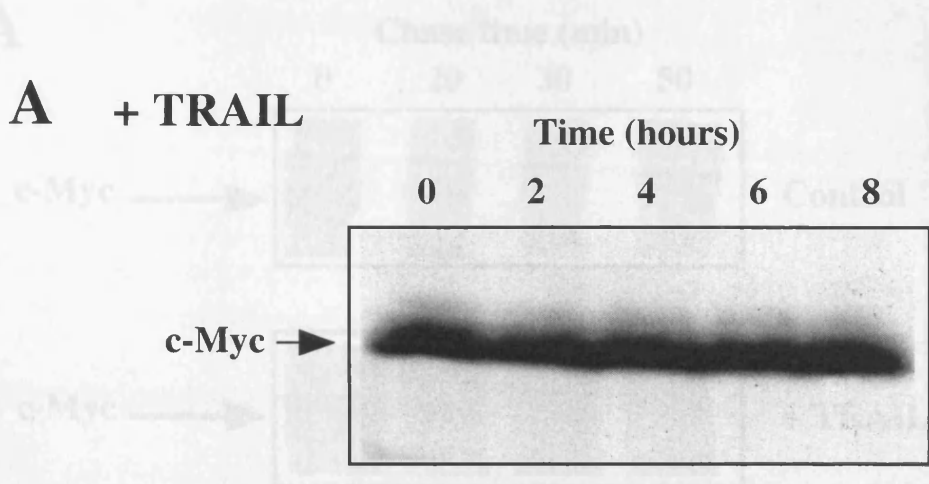


**Figure 6.1 C-Myc protein levels during apoptosis** HeLa cells treated with either TRAIL (A) or staurosporine (B) were harvested at various times after induction of apoptosis, and samples were subjected to SDS-PAGE and Western blotting and probed with the anti-c-Myc antibody 9E10.

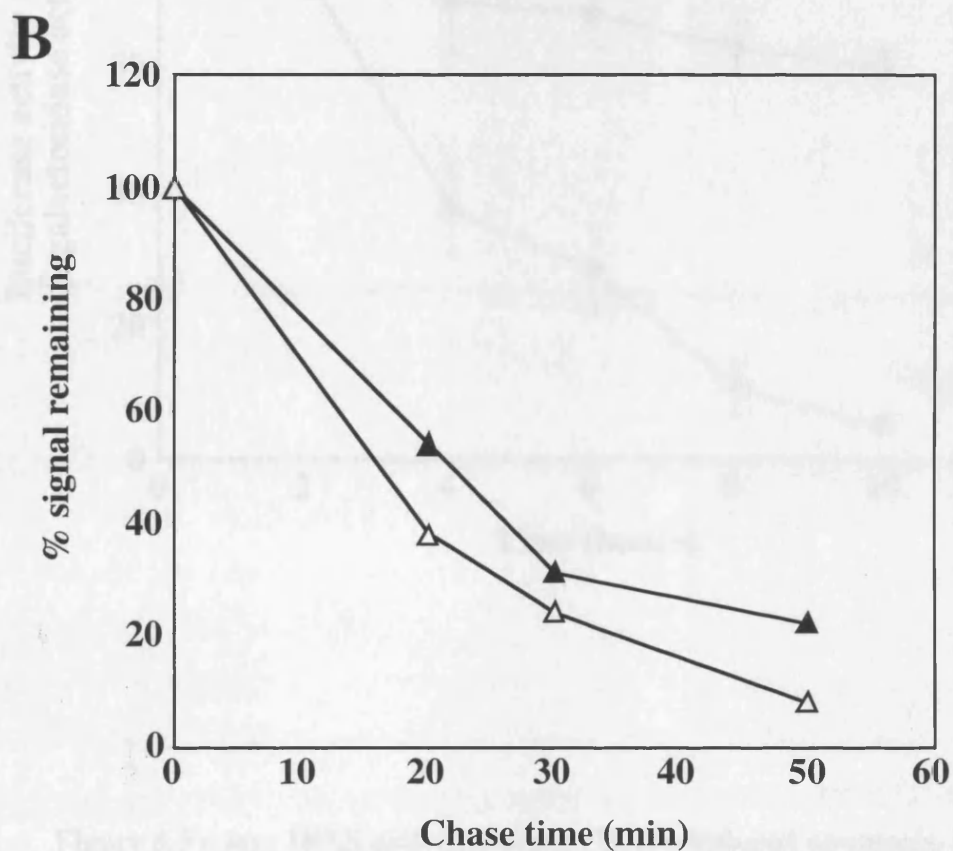
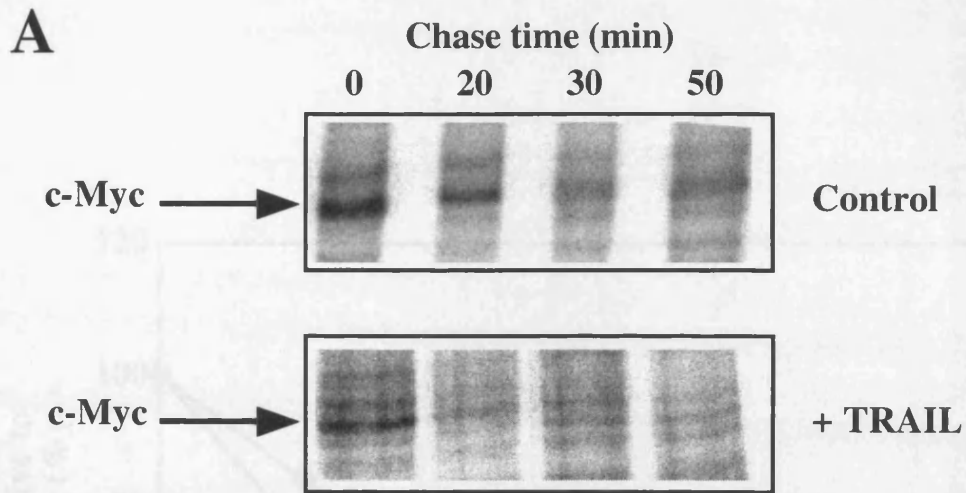


**Figure 6.2 Pulse chase analysis of c-Myc protein half life.** (A) HeLa cells with or without 3 hours preincubation with TRAIL were labelled with  $^{35}\text{S}$  methionine for 30 minutes. The medium was then replaced with fresh complete medium containing unlabelled methionine, and cells were harvested at the times indicated. C-Myc was immunoprecipitated and samples were subjected to SDS-PAGE. (B) The intensity of labeled c-Myc protein in (A) was quantified and expressed as a percentage of values at the start of the chase period. Closed triangles represent control cells, and open triangles represent cells treated with TRAIL.

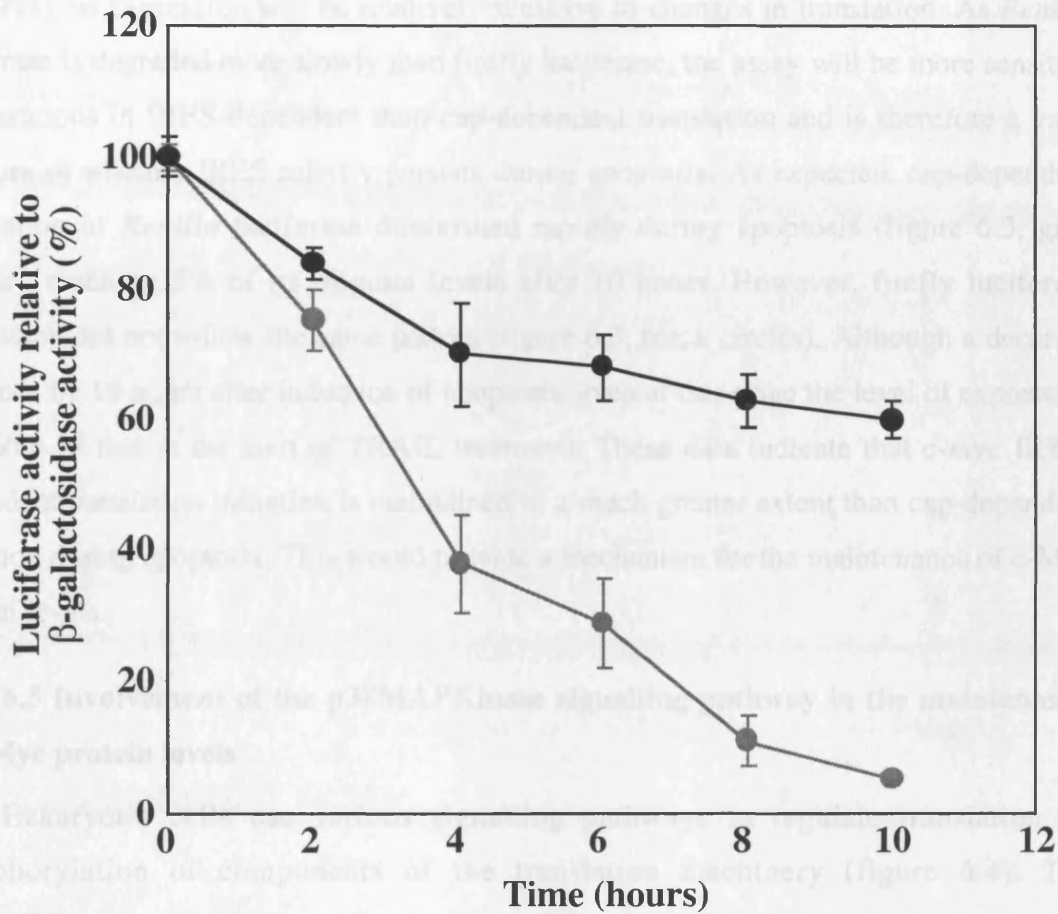


**Figure 6.3 c-myc IRES activity during TRAIL-induced apoptosis.** HeLa cells were transfected with pRMF 24 hours before treatment with 0.25 $\mu$ g/ml TRAIL. Samples were harvested at fixed time intervals and *Renilla* (grey circles) and firefly (black circles) luciferase activities were determined relative to the transfection control of  $\beta$ -galactosidase activity. The results are expressed as a percentage of the values in untreated cells. Results are an average of three independent experiments and error bars represent standard deviations.

therefore be relatively unaffected by apoptosis. In contrast, both *Renilla* and firefly luciferase have short half-lives (5.3 hours for *Renilla* and 3 hours for firefly) (Bronstein et al., 1994), so expression will be relatively sensitive to changes in translation. As *Renilla* luciferase is degraded more slowly than firefly luciferase, the assay will be more sensitive to alterations in IRES-dependent than cap-dependent translation and is therefore a valid measure of whether IRES activity persists during apoptosis. As expected, cap-dependent translation of *Renilla* luciferase diminished rapidly during apoptosis (figure 6.3, grey circles), reaching 5% of its original levels after 10 hours. However, firefly luciferase expression did not follow the same pattern (figure 6.3, black circles). Although a decrease was seen by 10 hours after induction of apoptosis, even at this stage the level of expression was 60% of that at the start of TRAIL treatment. These data indicate that *c-myc* IRES-dependent translation initiation is maintained to a much greater extent than cap-dependent initiation during apoptosis. This would provide a mechanism for the maintenance of *c-Myc* protein levels.

### **6.5 Involvement of the p38MAPKinase signalling pathway in the maintenance of *c-Myc* protein levels**

Eukaryotic cells use various signalling pathways to regulate translation by phosphorylation of components of the translation machinery (figure 6.4). The p38MAPKinase pathway is of particular interest, as it is induced by cellular stress, including apoptosis (Xia et al., 1995). A highly specific inhibitor to the  $\alpha$  and  $\beta$  isoforms of p38MAPK, SB203580, is available. This inhibitor was therefore used to examine whether this signalling pathway is used to maintain *c-Myc* levels during apoptosis. Before doing so it was necessary to confirm that the inhibitor functions effectively during TRAIL-mediated apoptosis in HeLa cells. Cells that were pre-incubated with SB203580 for 1 hour before TRAIL treatment were compared with cells treated with TRAIL in the absence of the inhibitor. In both cases, samples were harvested at fixed time intervals and p38MAPK was isolated from the samples by immunoprecipitation. The kinase activity of the isolated protein was then determined by incubating with the substrate ATF2 in the presence of [ $\gamma$ - $^{32}\text{P}$ ] ATP, and measuring the level of  $^{32}\text{P}$  incorporation following SDS-PAGE (figure 6.5). In cells treated with TRAIL in the absence of inhibitor, apoptosis caused a rapid induction of p38MAPK activity (figure 6.5, open diamonds). However, when cells were

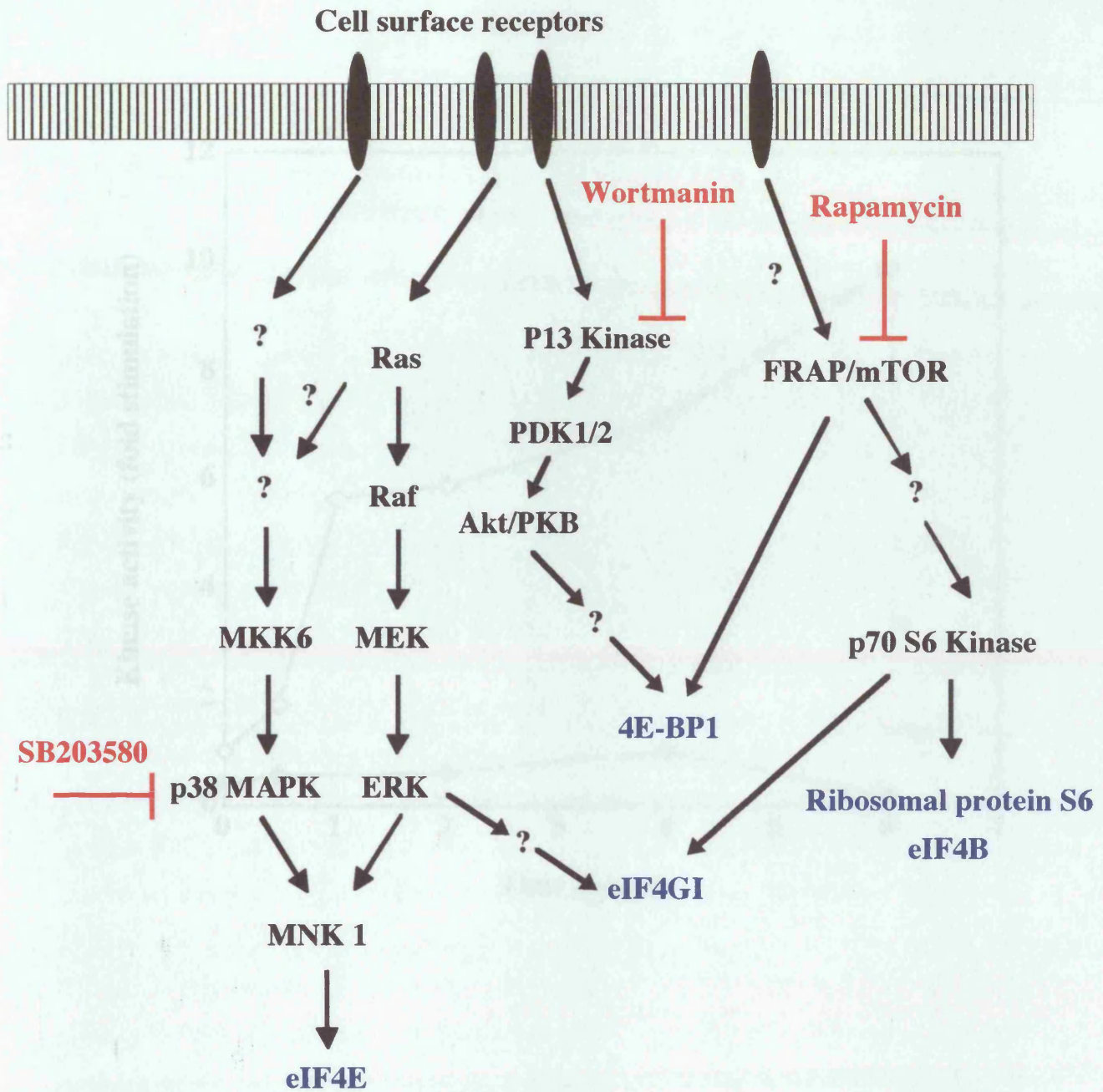


**Figure 6.4 Cell signalling pathways involved in translation.** Some of the signalling pathways implicated in translation are shown, with black arrows indicating phosphorylation targets. Translational targets are shown in blue, and inhibitors of various kinases in red. Question marks are used to indicate uncharacterised components of pathways.

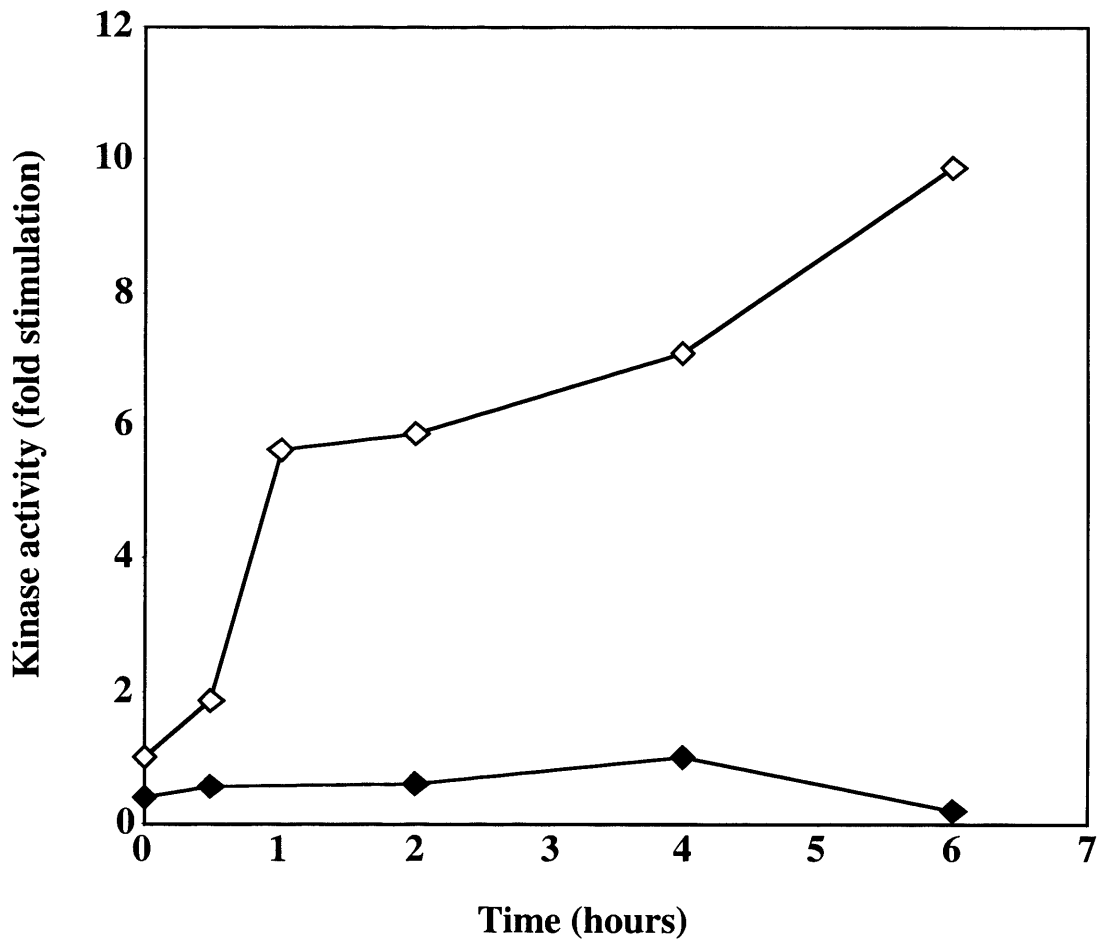


**Figure 6.5 p38MAPKinase activity in apoptotic cells.** TRAIL was used to induce apoptosis in HeLa cells with (closed diamonds) or without (open diamonds) pre-treatment with SB203580. Protein samples were harvested at pre-determined times and p38MAPKinase was isolated by immunoprecipitation. Kinase activity was measured by quantification of the incorporation of radiolabelled ATP into the substrate ATF2.

pre-incubated with SB203580, this induction was prevented completely (closed diamonds). This inhibitor is therefore effective in preventing p38MAPK activity during TRAIL-induced apoptosis.

Samples were then taken from HeLa cells that had been treated with TRAIL with or without pre-incubation with SB203580, and subjected to SDS-PAGE and Western blotting followed by probing with the 9E10 antibody. As before, c-Myc protein levels were maintained over a 6 hour apoptotic timecourse (figure 6.6A). The inhibitor alone has no effect on c-Myc expression or stability, as cells treated with SB203580 and harvested over a time period without TRAIL treatment showed no change in c-Myc levels (figure 6.6B). However, when cells were pre-incubated with SB203580, then subjected to TRAIL treatment, the levels of c-Myc protein were seen to diminish during apoptosis (figure 6.6C). This blot was re-probed for PARP and cleavage was observed, an indicator that apoptosis had occurred (figure 6.6C). This indicates that p38MAPK activity is necessary to maintain c-Myc protein levels during apoptosis.

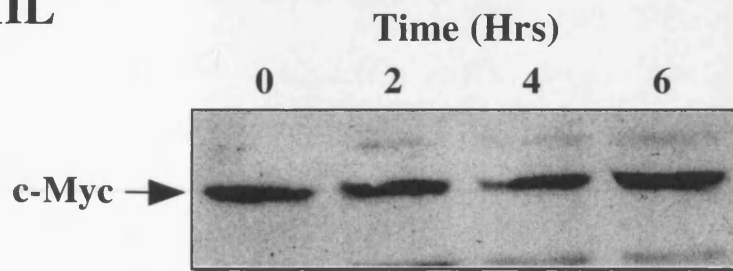
### **6.6 *c-myc* IRES activity in the presence of SB203580**

The effects of this signalling pathway on *c-myc* IRES activity were investigated by transfecting HeLa cells with pRMF. 24 hours after transfection, half the cells were pre-incubated with SB203580 for 1 hour, then all cells were subjected to TRAIL-induced apoptosis. Samples were harvested over a time period and firefly luciferase activity was assayed and normalised to  $\beta$ -galactosidase activity (figure 6.7). In cells treated with TRAIL in the absence of inhibitor (open squares), firefly luciferase levels decreased slightly to 80% of initial levels after 8 hours, as seen in figure 6.3. However, when cells were pre-treated with SB203580, the levels of firefly luciferase dropped rapidly so that by 8 hours after induction of apoptosis, only 15% of the initial activity was seen (closed squares). The maintenance of *c-myc* IRES activity during apoptosis is therefore dependent on signalling via p38MAPK. This provides further support to the hypothesis that the *c-myc* IRES is responsible for the maintenance of c-Myc protein levels during apoptosis, as inhibition of the same signalling pathway negates both these effects.

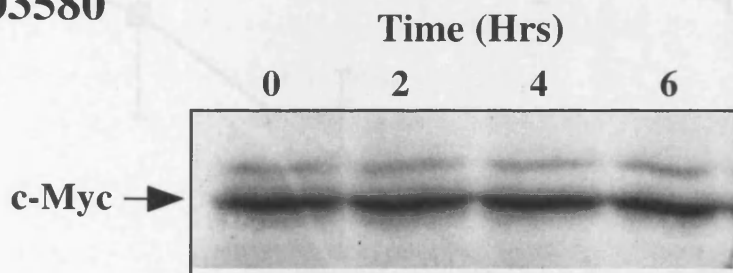
### **6.7 Cotransfection of pRMF with MKK6 expression vectors**

To provide further support to the data presented above, a series of vectors expressing forms of MKK6 were used. MKK6 lies upstream of p38MAPK and activates this kinase,

### A + TRAIL



### B + SB203580



### C + TRAIL and SB203580

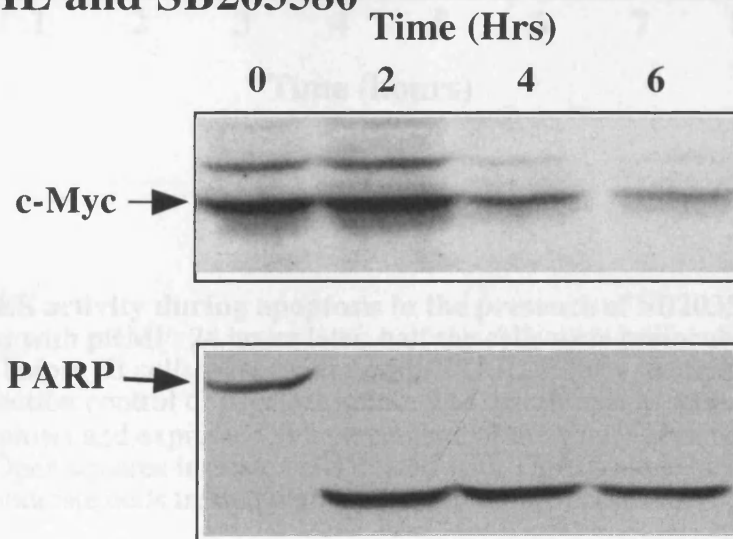


**Figure 6.6 Effects of SB203580 on c-Myc levels during apoptosis.** HeLa cells treated with TRAIL without (A) or with (C) pre-incubation with SB203580, or treated with SB203580 without the induction of apoptosis (B) were harvested at predetermined times. Samples were analysed by SDS-PAGE and Western blotting and probed with the anti-c-Myc antibody 9E10. The blot shown in (C) was stripped and re-probed with an anti-PARP antibody.

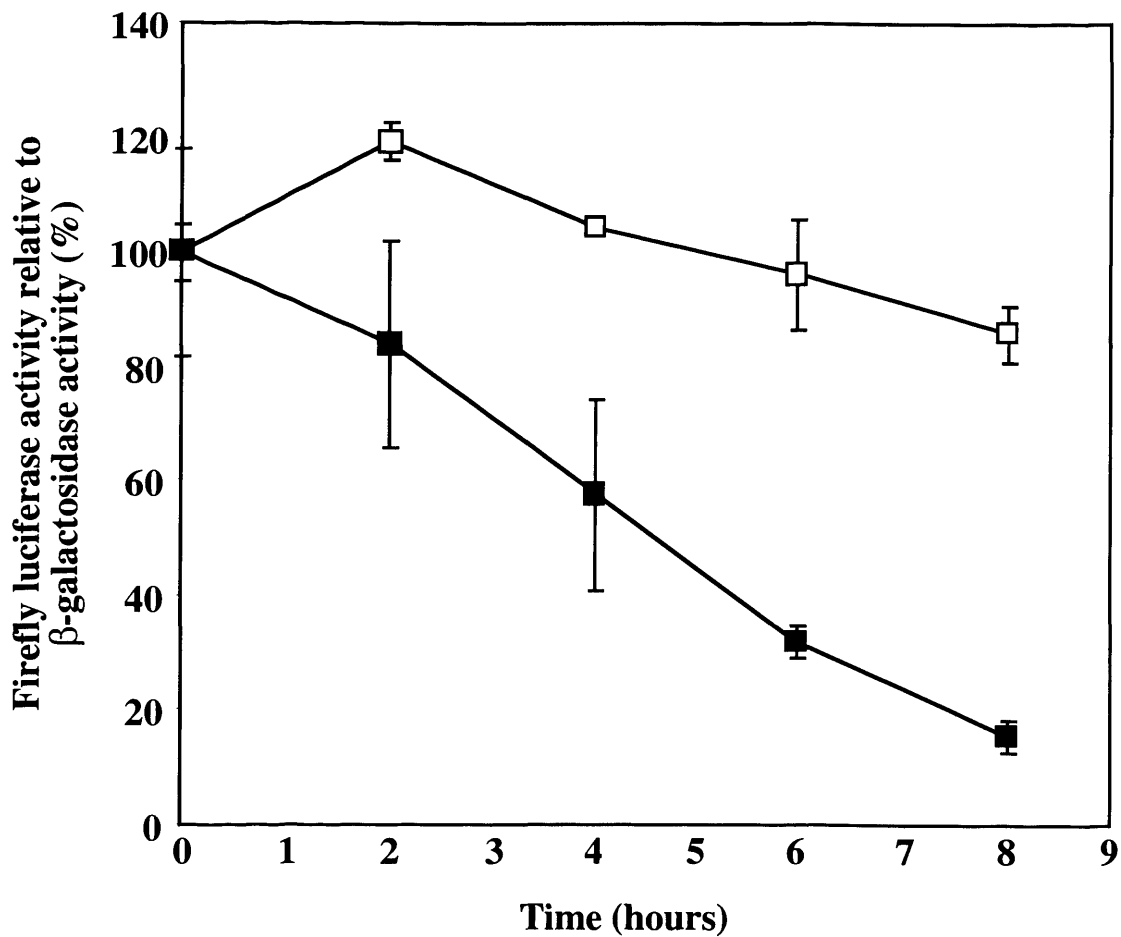


**Figure 6.7 *c-myc* IRES activity during apoptosis in the presence of SB203580.** HeLa cells were transfected with pRMF. 24 hours later, half the cells were preincubated with SB203580 for 1 hour before all cells were treated with TRAIL. Firefly luciferase activity relative to the transfection control of  $\beta$ -galactosidase was determined at set times after the induction of apoptosis and expressed as a percentage of the values obtained before TRAIL treatment. Open squares indicate cells treated with TRAIL alone, and closed squares indicate cells treated with SB203580 before apoptosis.

but not ERK or JNK, by phosphorylation (Han et al., 1996) (figure 6.4). pRMF was introduced into HeLa cells by transfection in combination with the empty vector pcDNA3, a pcDNA3-based vector expressing wild type MKK6, or a similar vector that expresses a constitutively active mutant of MKK6 (MKK6GLU). The activities of *Renilla* and firefly luciferase in lysates of transfected cells were determined, but a  $\beta$ -galactosidase control was not used as MKK6 would be expected to stimulate expression of this reporter as well as the luciferases. It was seen that cotransfection with wild type MKK6 led to an increase in cap-dependent translation of *Renilla* luciferase, as expected (figure 6.8). However, a similar increase in firefly luciferase expression was also observed, indicating that this kinase is able to stimulate *c-myc* IRES-dependent translation. Cotransfection with MKK6GLU increased firefly luciferase expression to approximately the same extent as MKK6WT (figure 6.8). Signalling via MKK6 and p38MAPK is therefore able to activate the *c-myc* IRES.

### 6.8 *c-myc* IRES activity during heat shock

Heat shock is known to result in an inhibition of protein synthesis due to sequestration of eIF4G and changes in the phosphorylation states of other factors (section 1.2.6) (Cuesta et al., 2000; Schneider, 2000). Moreover, *c-Myc* protein levels are maintained during heat shock, and although this is largely due to an increase in protein stability, an increase in protein synthesis was also noted (Lüscher and Eisenman, 1988). To examine whether the *c-myc* IRES is able to function during this translation inhibition, HeLa cells were transfected with either pGL3' or phpML. As the hairpin in phpML impedes ribosome scanning such that firefly luciferase expression is dependent on the *c-myc* IRES, these vectors provide a means of comparing cap-dependent and IRES-dependent initiation. This approach was used due to a lack of success in inhibiting *Renilla* luciferase activity by heat shock in cells transfected with pRMF. 24 hours after transfection, cells were subjected to heat shock at 44°C for a period of 30 minutes, then returned to 37°C to allow recovery. Heat shock was induced by heating media in a waterbath set to 44°C, adding this directly to cells from which the media had previously been removed, and placing the cells in a 44°C oven for the duration of the shock. Cell lysates were harvested at fixed time intervals and firefly luciferase activity was normalised

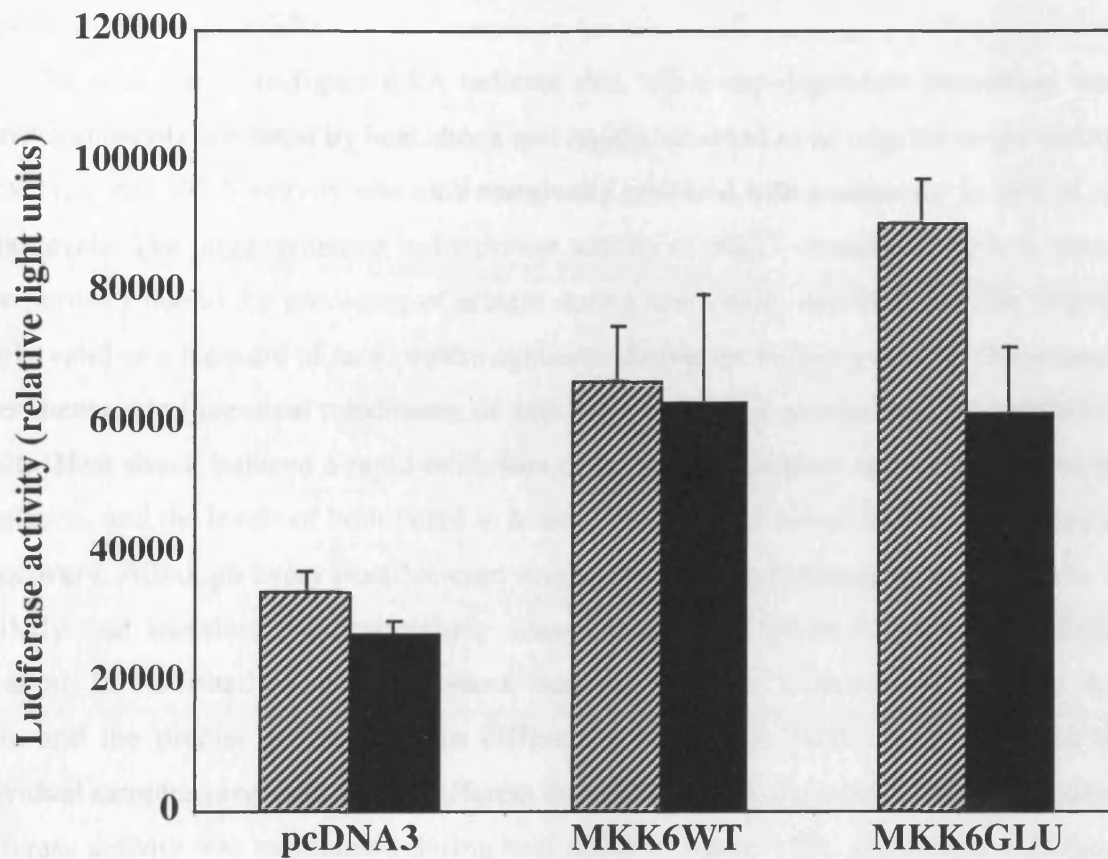


**Figure 6.8 Cotransfection of pRMF with MKK6 expression vectors.** HeLa cells were transfected with pRMF in combination with pcDNA3, MKK6WT or MKK6GLU. The activities of *Renilla* (shaded) and firefly (black) luciferase in lysates of transfected cells were determined and are shown.

to a transfection control of  $\beta$ -galactosidase and expressed as a percentage of activity in unshocked cells (figure 6.9).

The data shown in figure 6.9A indicate that, while cap-dependent translation was almost completely inhibited by heat shock and rapidly returned to its original levels during recovery, *c-myc* IRES activity was only marginally inhibited with a reduction to 70% of its initial levels. The large reduction in luciferase activity in pGL3'-transfected cells is likely to be partially due to the unfolding of protein during heat shock, and therefore this system is only valid as a measure of new protein synthesis during the recovery period. Subsequent experiments using identical conditions, of which figure 6.9B is an example, gave different results. Heat shock induced a rapid inhibition of both cap-dependent and IRES-dependent translation, and the levels of both failed to return to their initial values during a long period of recovery. Although every possible care was taken when performing the experiments, it is likely that translation is exquisitely sensitive to the ambient temperature. Minor variations in the speed of applying heated media to the cells, transfer of the cells to the oven, and the precise temperature in different areas of the oven, could thus lead to individual samples receiving vastly different degrees of shock. As *c-myc* IRES-dependent luciferase activity was maintained during heat shock in figure 6.9A, despite the unfolding of protein that occurs under these circumstances, it is probable that the phpML-transfected cells received a lesser degree of shock than their pGL3'-transfected counterparts. The subsequent failure to replicate these results means that no conclusions can be drawn on the effect of heat shock on the *c-myc* IRES.

### 6.9 *c-myc* IRES activity during G<sub>0</sub>-G<sub>1</sub> transition

Levels of translation initiation vary according to the stage of the cell cycle, and are much greater in cycling cells than during G<sub>0</sub> phase (Pyronnet et al., 2001). MRC5 cells were used to examine the behaviour of the *c-myc* IRES during the transition from G<sub>0</sub> to G<sub>1</sub> phase, as these cells are derived from normal embryonic tissue, and would therefore be expected to enter G<sub>0</sub> phase more readily than a transformed cell line such as HeLa. Cells were transfected with pRMF and grown for 24 hours, after which the medium was removed, the cells were washed several times with PBS to remove all traces of serum, and serum-free medium was added to the cells which were then grown for a further 24 hours. This medium was then replaced with fresh complete medium to induce re-entry into the

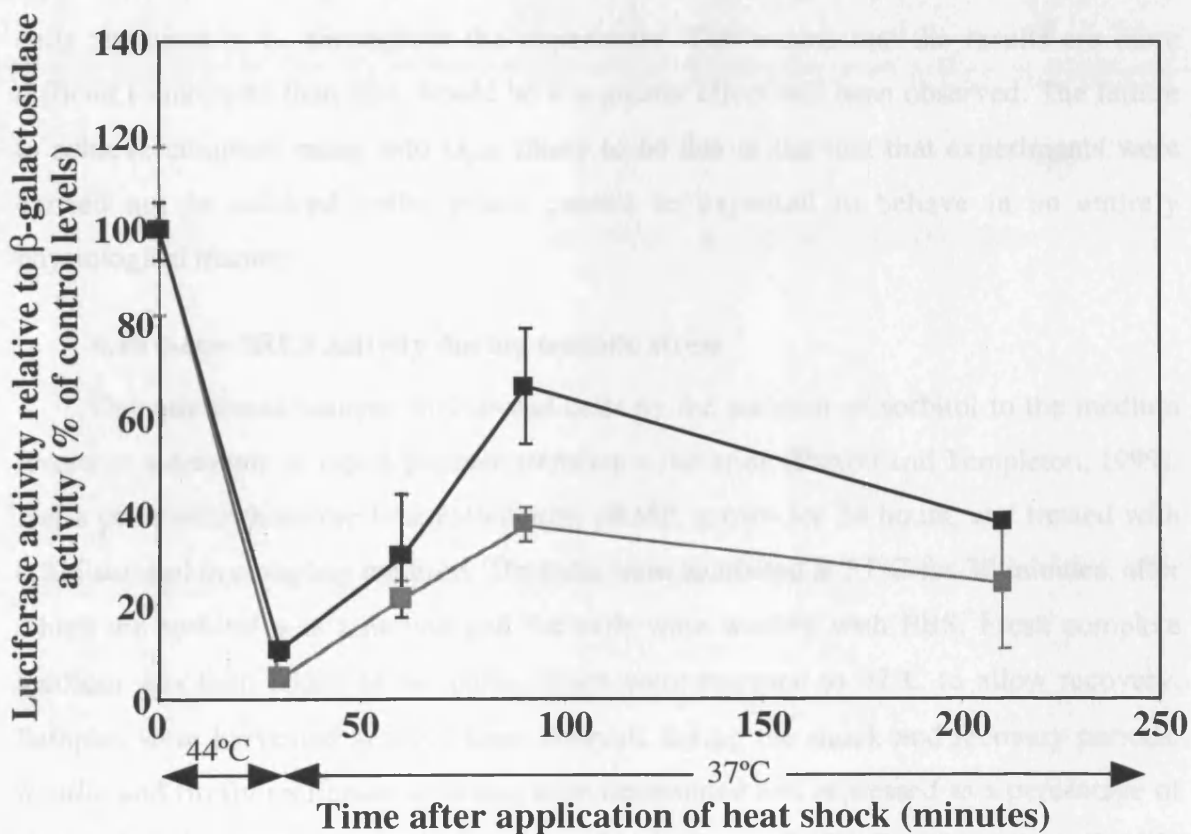
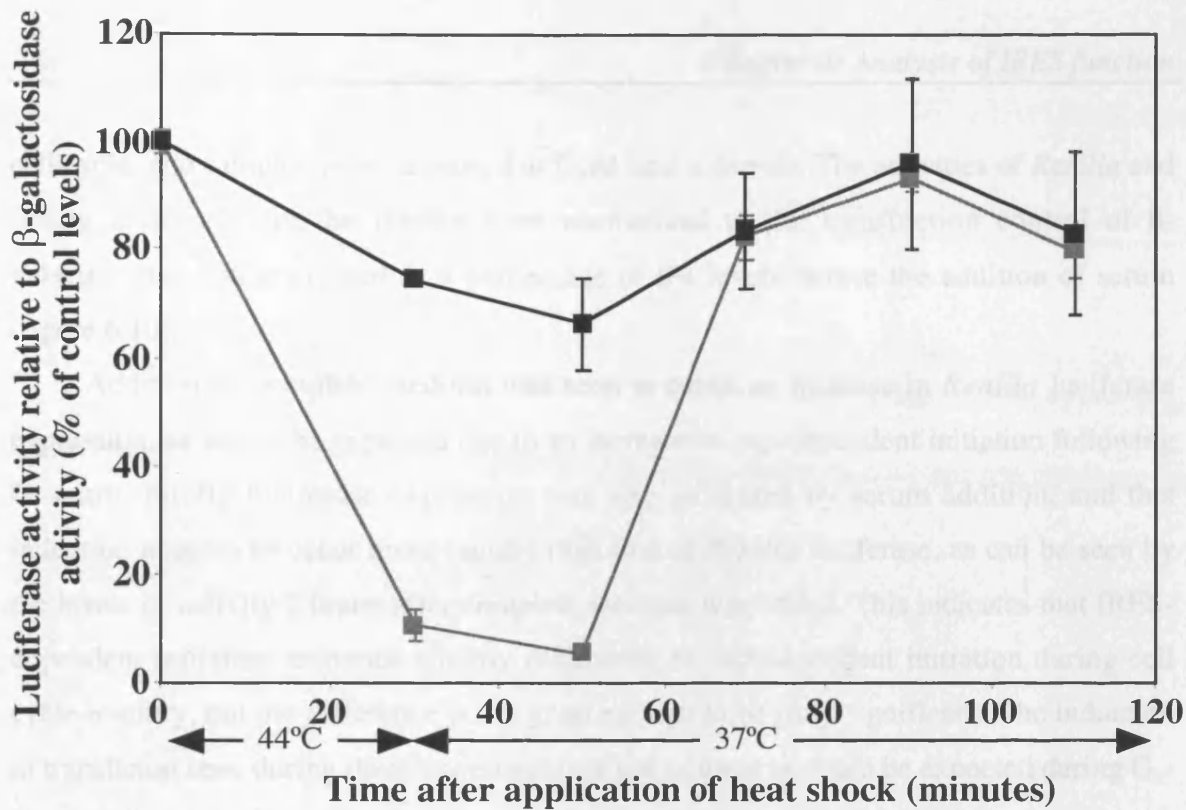


**Figure 6.9 *c-myc* IRES activity during heat shock.** HeLa cells were transfected with pGL3' (grey squares) or phpML (black squares). 24 hours after transfection, the cells were subjected to heat shock by the addition of heated media and incubation in a 44°C oven. After 30 minutes the cells were returned to 37°C and were harvested at fixed time intervals. The activity of firefly luciferase in the lysates was normalised to a transfection control of  $\beta$ -galactosidase activity, and results are expressed relative to the values obtained from unshocked cells. Results are an average of triplicate wells in one experiment, and error bars represent the standard deviation.

cell cycle, and samples were harvested at fixed time intervals. The activities of *Renilla* and firefly luciferases in the lysates were normalised to the transfection control of  $\beta$ -galactosidase and expressed as a percentage of the levels before the addition of serum (figure 6.10).

Addition of complete medium was seen to cause an increase in *Renilla* luciferase expression, as would be expected due to an increase in cap-dependent initiation following  $G_1$  entry. Firefly luciferase expression was also increased by serum addition, and this induction appears to occur more rapidly than that of *Renilla* luciferase, as can be seen by the levels of activity 3 hours after complete medium was added. This indicates that IRES-dependent initiation responds slightly differently to cap-dependent initiation during cell cycle re-entry, but the difference is not great enough to be truly significant. The induction in translation seen during these experiments is not as great as could be expected during  $G_0$ - $G_1$  transition, which implies that the cells had not been completely starved and that many cells remained in  $G_1$  throughout the experiment. This means that the results are more difficult to interpret than they would be if a greater effect had been observed. The failure to achieve complete entry into  $G_0$  is likely to be due to the fact that experiments were carried out in cultured cells, which cannot be expected to behave in an entirely physiological manner.

### 6.10 *c-myc* IRES activity during osmotic stress

Osmotic stress induced in cultured cells by the addition of sorbitol to the medium results in a decrease in cap-dependent translation initiation (Parrott and Templeton, 1999). HeLa cells were therefore transfected with pRMF, grown for 24 hours, and treated with 0.3M sorbitol in complete medium. The cells were incubated at 37°C for 30 minutes, after which the sorbitol was removed and the cells were washed with PBS. Fresh complete medium was then added to the cells, which were returned to 37°C to allow recovery. Samples were harvested at fixed time intervals during the shock and recovery periods. *Renilla* and firefly luciferase activities were determined and expressed as a percentage of the values obtained before addition of sorbitol (figure 6.11). Cap-dependent *Renilla* luciferase expression was reduced to 50% of its original level during osmotic stress, but had recovered fully 90 minutes after removal of the sorbitol. Firefly luciferase expression was seen to follow a similar pattern overall, but did not decline to such a great extent as

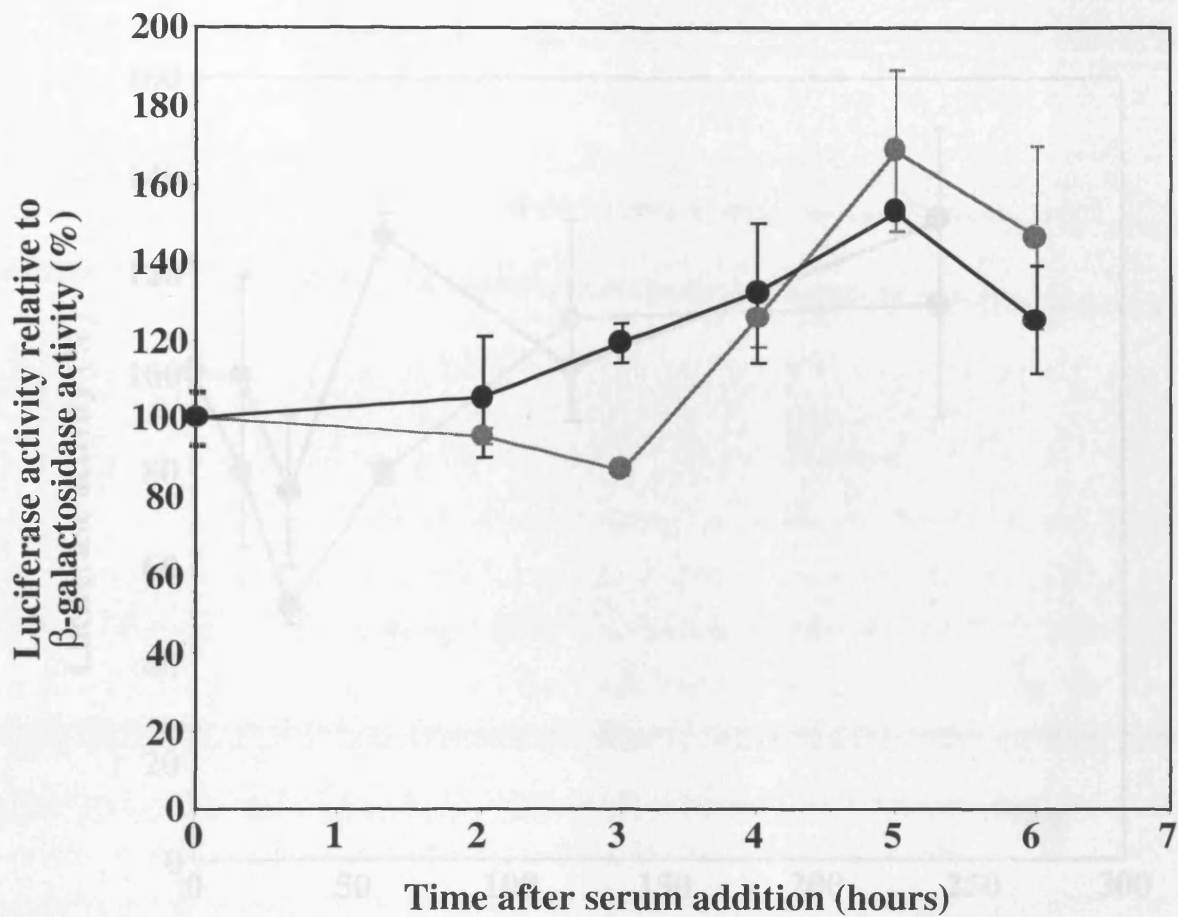


**Figure 6.10 c-myc IRES activity during G0-G1 transition.** MRC5 cells were transfected with pRMF. 24 hours after transfection the cells were grown in serum free medium for a further 24 hours. Complete medium was then added back to the cells and they were harvested at the timepoints indicated. *Renilla* (grey circles) and firefly (black circles) luciferase activities were assayed in cell lysates, and are shown relative to a transfection control of  $\beta$ -galactosidase as a percentage of initial values. Results are an average of three independent experiments and error bars represent standard deviations.

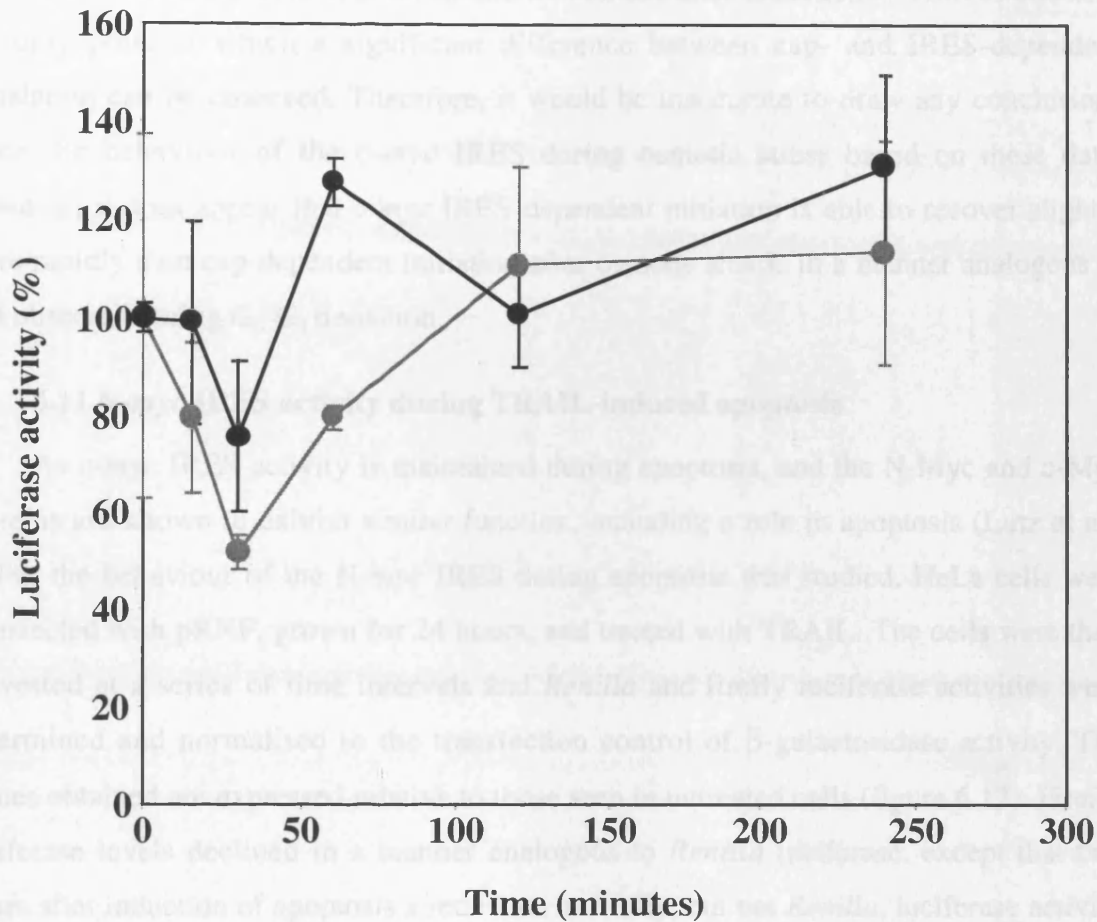


**Figure 6.11 c-myc IRES activity during osmotic stress.** HeLa cells were transfected with pRMF 24 hours before treatment. Osmotic stress was induced by the addition of 0.3M sorbitol to cells for 30 minutes, after which cells were washed with PBS and fresh complete medium was added. Cells were harvested at fixed time intervals after the addition of sorbitol. The activities of *Renilla* (grey circles) and firefly (black circles) luciferases in lysates were determined and are expressed as a percentage of the values obtained from untreated cells. Results are an average of three independent experiments and error bars represent standard deviations.

Previous studies have demonstrated that c-Myc can contribute to apoptosis in cells by targeting the release of cytochrome c from mitochondria (Jung et al., 1999). However,

*Renilla* expression during the shock, and recovered to 130% of its initial levels 30 minutes after removal of the shock. This timepoint, 60 minutes after induction of osmotic stress, is the only point at which a significant difference between cap- and IRES-dependent translation can be observed. Therefore, it would be inaccurate to draw any conclusions about the behaviour of the *c-myc* IRES during osmotic stress based on these data. However, it does appear that *c-myc* IRES-dependent initiation is able to recover slightly more rapidly than cap-dependent initiation after osmotic shock, in a manner analogous to that observed during G<sub>0</sub>-G<sub>1</sub> transition.

### 6.11 N-*myc* IRES activity during TRAIL-induced apoptosis

As *c-myc* IRES activity is maintained during apoptosis, and the N-Myc and c-Myc proteins are known to exhibit similar function, including a role in apoptosis (Lutz et al., 1998), the behaviour of the N-*myc* IRES during apoptosis was studied. HeLa cells were transfected with pRNF, grown for 24 hours, and treated with TRAIL. The cells were then harvested at a series of time intervals and *Renilla* and firefly luciferase activities were determined and normalised to the transfection control of  $\beta$ -galactosidase activity. The values obtained are expressed relative to those seen in untreated cells (figure 6.12). Firefly luciferase levels declined in a manner analogous to *Renilla* luciferase, except that two hours after induction of apoptosis a reduction in firefly, but not *Renilla*, luciferase activity was seen. Therefore, in contrast to the *c-myc* IRES, the N-*myc* IRES is not maintained during apoptosis.

### 6.12 Discussion

The data presented above provide a rationale for the existence of an IRES in *c-myc*. The continued activity of the *c-myc* IRES while cap-dependent initiation is inhibited during apoptosis allows continued synthesis of the labile c-Myc protein. It is also of interest to discover that the *c-myc* IRES lies downstream of a signalling pathway previously implicated in cap-dependent translation, the p38MAPKinase pathway. The requirement for p38MAPK activity to maintain both IRES activity and protein levels during apoptosis provides confirmation that the *c-myc* IRES is responsible for the continued expression of c-Myc under these circumstances.

Previous studies have demonstrated that c-Myc can contribute to apoptosis in cells by triggering the release of cytochrome *c* from mitochondria (Juin et al., 1999). However,

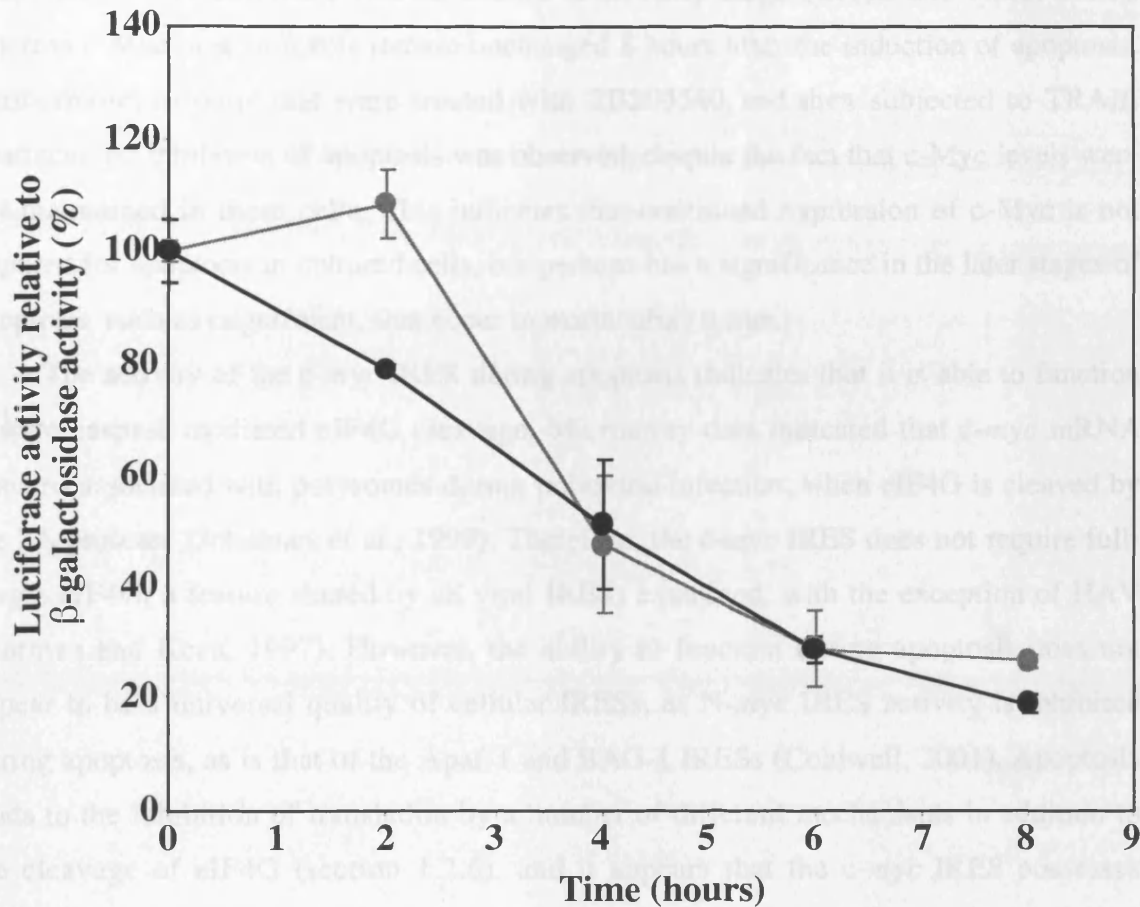


**Figure 6.12 N-myc IRES activity during TRAIL-induced apoptosis.** HeLa cells were transfected with pRNF 24 hours before treatment with TRAIL. Cells were harvested at fixed time intervals after the induction of apoptosis. The activities of *Renilla* (grey circles) and firefly (black circles) luciferases in the lysates were determined and normalised to a transfection control of  $\beta$ -galactosidase. The values obtained are shown as a percentage of the levels of expression in untreated cells. Results are an average of three independent experiments and error bars represent standard deviations.

this does not provide an adequate explanation for the maintenance of c-Myc during apoptosis, as cytochrome *c* release occurs at an early stage (Green and Reed, 1998), whereas c-Myc protein levels remain unchanged 8 hours after the induction of apoptosis. Furthermore, in cells that were treated with SB203580 and then subjected to TRAIL treatment, no inhibition of apoptosis was observed, despite the fact that c-Myc levels were not maintained in these cells. This indicates that continued expression of c-Myc is not required for apoptosis in cultured cells, but perhaps has a significance in the later stages of apoptosis, such as engulfment, that occur in mammalian tissue.

The activity of the *c-myc* IRES during apoptosis indicates that it is able to function despite caspase-mediated eIF4G cleavage. Microarray data indicated that *c-myc* mRNA remains associated with polysomes during polioviral infection, when eIF4G is cleaved by the 2A protease (Johannes et al., 1999). Therefore, the *c-myc* IRES does not require full-length eIF4G, a feature shared by all viral IRESs examined, with the exception of HAV (Borman and Kean, 1997). However, the ability to function during apoptosis does not appear to be a universal quality of cellular IRESs, as *N-myc* IRES activity is inhibited during apoptosis, as is that of the Apaf-1 and BAG-1 IRESs (Coldwell, 2001). Apoptosis leads to the inhibition of translation by a number of different mechanisms in addition to the cleavage of eIF4G (section 1.2.6), and it appears that the *c-myc* IRES possesses specialised features that allow it to function under these conditions. This implies that there is a specific need for c-Myc expression to be maintained during apoptosis, and this requirement is not shared by N-Myc. It seems more likely that the role of the *N-myc* IRES is in neuronal development, as indicated by the data presented in chapter 5. This provides another intriguing example of the differences between the IRESs found in two such closely related genes.

Attempts to determine whether the *c-myc* IRES is active during other stress situations in which cap-dependent initiation is inhibited have proved largely unsuccessful. The difficulties encountered in inducing stress to the correct extent and in a reproducible fashion in a cell culture system have meant that results obtained during the experiments in sections 6.8-6.10 are inconclusive. Previous data indicated an increase in *c-myc* translation in response to heat shock (Lüscher and Eisenman, 1988), and the IRES would seem a likely candidate for this translational response, but this study did not allow any conclusions to be drawn. There are some indications that *c-myc* IRES-dependent translation may

recover more rapidly than cap-dependent translation from osmotic stress and during cell cycle entry, perhaps due to a lower requirement for certain components of the translation machinery. However, IRES-dependent translation does not appear to be maintained during osmotic stress or quiescence. Recent work has shown that the *c-myc* IRES remains active during DNA damage induced by mitomycin C and EMS (Subkhankulova et al., 2001). Therefore, it appears that the *c-myc* IRES is specifically required to maintain production of protein during apoptosis, DNA damage, and possibly heat shock, but is not used during other cell stresses examined, presumably as c-Myc protein is not required in such circumstances.

## Chapter 7

### Discussion

#### 7.1 A comparison of cellular IRESs

Extensive study of viral IRESs has allowed their subdivision into different categories, within which considerable structural and functional similarity is observed. IRESs have now been identified in a number of different cellular genes but as yet no unifying characteristics have emerged. This study has led to the identification of IRESs in the 5' UTRs of *N-myc* and *L-myc*, and thus has allowed a comparison of the features of internal ribosome entry in the three closely related *myc* genes.

#### 7.2 A comparison of *myc* IRES structure

The gene structures of *c-*, *N-* and *L-myc* are extremely similar, consisting of three exons, of which exon 1 is non-coding. Thus, all three transcripts possess a long, structured 5' UTR, although the P2-derived *c-myc* UTR is longer than the *N-myc* UTR, which in turn is longer than the spliced *L-myc* UTR. The unspliced *L-myc* UTR will not be included in these comparisons as the presence of an intron within dicistronic RNA allowed complex splicing events to occur and resulted in loss of integrity of the transcript, such that the data obtained were inconclusive.

Examination of the primary sequence of the *myc* 5' UTRs reveals very little homology. However, little sequence similarity was observed within the families of picornaviral IRES, which instead rely on a common secondary structure to provide conservation of function. It is possible that an evolutionary divergence in sequence between the *myc* IRESs has been constrained by the maintenance of secondary structural motifs, but structural mapping of the *N-* and *L-myc* IRESs is needed to test this hypothesis.

Although the structure of the *N-myc* IRES is not known, mutational analysis has allowed insight into its mechanism. No such analysis has yet been carried out on the *L-myc* IRES and therefore it cannot be included in these comparisons. Deletions from both ends of the *c-myc* IRES induce a gradual decrease in activity, and mutations in individual structural features result in a reduction in activity, but exhibit an additive effect when present in combination (Le Quesne et al., 2001; Stoneley et al., 1998). It was proposed that this IRES is composed of a number of short modules that are able to function

independently but co-operate to direct efficient ribosome entry. The Bip IRES could also be divided into nonoverlapping fragments that demonstrated partial IRES activity (Yang and Sarnow, 1997). The theory that cellular IRESs are modular in nature, and thereby differ from viral IRESs, was supported further by the observation that a short segment of the Gtx IRES shows enhanced activity when present in multiple copies (Chappell et al., 2000a). However, the sensitivity of N-*myc* IRES function to deletions indicated that a modular structure is not a common feature of all cellular IRESs. It is possible that the modular IRESs represent a distinct subset of cellular IRESs, and it is interesting that whereas the *c-myc* IRES falls into this group, the IRES of a gene as closely related as N-*myc* does not. The complementarity to rRNA observed in the Gtx IRES module appears to be a specialised mechanism that is not used by the *myc* genes, and it is likely that the modular nature of the *c-myc* IRES is determined by the co-operation of structural domains.

A further significant difference between *c-* and N-*myc* IRES structure is the importance of the 3' end of the IRES. Whereas *c-myc* IRES activity is refractory to deletion of 56nt from this end (Stoneley et al., 1998), this region is extremely important for efficient N-*myc* IRES function. Activity of the XIAP IRES is strictly dependent on a polypyrimidine tract close to the 3' end (Holcik et al., 1999). However, sequence analysis of this region of the N-*myc* IRES does not reveal a polypyrimidine tract, or any known IRES motifs. Furthermore, the 3' deletions did not allow the definition of a precise essential element within this region. Deletions from the 5' end also result in a considerable reduction in IRES activity. Therefore, the effect of deletion on the N-*myc* IRES appears to be due to a requirement for the entire UTR to assume an appropriate secondary or tertiary structure, rather than the need for a specific motif that is vital for IRES function. Moreover, the requirement for the 3' end of the N-*myc* IRES is not due to an involvement of the coding region in IRES function. Thus, both the *c-* and N-*myc* 5' UTRs appear to demonstrate IRES function independent of the downstream regions. Indeed, it was recently demonstrated that the HCV IRES, which was previously thought to require coding sequences for its function, merely exhibits a requirement for a region of unstructured RNA downstream of the initiation codon (Rijnbrand et al., 2001).

Attempts to map the site of ribosome entry by the insertion of out of frame AUG codons within the 5' UTR reveal similarities between the *c-* and N-*myc* IRESs. In both cases it appears that the ribosome is recruited to a site some distance upstream of the

initiation codon, and traverses the remainder of the IRES by a scanning mechanism. In the case of the *c-myc* IRES the window of entry was well defined (Le Quesne et al., 2001), but analysis of *N-myc* IRES only led to the identification of a broad region in which ribosome entry occurs. The possibility that ribosomes are recruited to multiple sites within this region should not be excluded, and more extensive mutagenic analysis is necessary to examine this theory. The site of ribosome entry in the *c-myc* IRES does not contain the polypyrimidine tract or AUG codon that are features of the ribosome landing site in the viral IRESs, and no such features are present within the region to which the ribosome is recruited in the *N-myc* IRES. Thus, ribosome entry in the two cellular IRESs examined to date occurs by a somewhat different mechanism to that employed by the type I viral IRESs, despite the similarities in function shown by ribosome binding and scanning.

The importance of the 3' end of the *N-myc* 5' UTR for IRES activity remains somewhat undefined in light of the observation that ribosome landing occurs upstream of this region. However, it is possible that tertiary interactions between the 3' end of the UTR and upstream regions are required to direct ribosomes to a central site. The *c-myc* IRES contains a stem-loop structure downstream of the site of ribosome entry, the deletion of which results in an inhibition of IRES activity, and therefore provides a precedent for such a model.

Despite the similarities between the *myc* genes, the IRESs of *c-* and *N-myc* show considerable mechanistic distinctions. This may be due to the cellular milieu in which each IRES is most active, such that optimum activity is provided under the necessary conditions. It is also possible that both genes have developed IRESs independently following evolutionary divergence, and that each has exploited a structured 5' UTR by a different method.

### **7.3 Protein factor requirements of the *myc* IRESs**

All three *myc* IRESs failed to function in an *in vitro* translation system, and the *c-* and *N-myc* IRESs were also inactive when dicistronic RNA was introduced into the cytoplasm of cells, although this experiment has not yet been carried out using the *L-myc* IRES. Thus, it appears that the functional requirements of all three IRESs are complex, and that the *N-myc* IRES requires a "nuclear event" such as that previously postulated for the *c-myc* IRES (Stoneley et al., 2000b). Furthermore, these IRESs show variable activity

according to the cell line transfected, and this implies an exquisite dependence on cellular environment. The c-, N- and L-*myc* IRESs show comparable activity in HeLa cells, but further transfections revealed an important functional distinction in cell type specificity between the c- and N-*myc* IRESs. It is important to emphasise that the c-*myc* IRES was highly active in most of the neuronal cells analysed; however, the N-*myc* IRES was specifically activated relative to it. Thus, a distinction exists between the requirements for efficient c- and N-*myc* IRES function, and it is possible that a differential requirement for protein factors is related to the differences observed in IRES mechanism.

The *trans*-acting factor requirements of the viral IRESs have once again allowed classification into two categories, although differences exist within these classes. The N-*myc* IRES shows significant differences to the viral IRESs both in its requirement for a nuclear event and in its inability to be activated by any of the viral IRES *trans*-acting factors known. However, the possibility of a transient interaction that was not detected by the experimental methods employed, or IRES activation by a combination of these factors, should not be excluded. As yet there is very little data to indicate whether the majority of cellular IRESs share the *trans*-acting factor requirements of the viral IRESs. However, the Apaf-1 IRES is activated by a combination of unr and PTB (Mitchell et al., 2001), so it appears that the same proteins are able to stimulate translation directed by both viral and cellular IRESs.

Attempts to identify specific *trans*-acting factors required for N-*myc* IRES function resulted in one possible candidate, although this is as yet unidentified and has only been shown to bind N-*myc* IRES RNA. An encouraging observation was that the levels of this protein are increased in neuronal cells relative to those in HeLa cells. Thus, if this protein is not required for c-*myc* IRES function, it could provide the neuronal specificity observed with the N-*myc* IRES. It is impossible to draw any firm conclusions on this possibility until the protein has been obtained and tested in functional assays. Therefore, much work is still to be done in elucidating the requirements for N-*myc* IRES function, and the nature of the "nuclear event". It is possible that an extremely labile protein that is not recovered in cell extract preparation is required, or that covalent modification of the IRES RNA takes place in the nucleus. With the exception of neuronal specificity, the functional requirements of the *myc* IRESs appear to be rather similar, although these features are not necessarily shared by other cellular IRESs.

#### 7.4 *myc* IRES function

Both *c-myc* and *N-myc* transcripts are able to direct translation initiation by both cap-dependent and IRES-dependent mechanisms. A rather different situation is observed on analysis of the *L-myc* IRES, as the data obtained from monocistronic hairpin studies indicate that almost all translation occurs by internal ribosome entry in the context of this 5' UTR. This raises the possibility that the *L-myc* IRES exists to allow production of L-Myc protein despite the almost complete inhibition of cap-dependent initiation by UTR structure. In contrast, the *c-* and *N-Myc* proteins could be produced by the cap-dependent method, and therefore their IRESs are likely to serve an alternative purpose. It has been postulated that cellular IRESs exist to allow continued production of essential proteins under conditions in which cap-dependent translation is inhibited, and the observations made with the *c-myc* IRES substantiate this view.

A significant feature of the Myc proteins that contributes to their tightly regulated expression is their short half-lives. This means that levels of these proteins should be extremely sensitive to changes in global translation. *c-Myc* protein levels were unaltered during apoptosis despite the cleavage of eIF4G, and the half-life of the protein and levels of *c-myc* mRNA were unaffected. These observations implied both a specific requirement for this protein late in apoptosis and the use of an alternative mechanism to maintain its translation. The *c-myc* IRES provided such a mechanism and its activity was maintained during apoptosis. The analysis of signalling pathways was important, as the conclusion that p38MAPK activity is required for the apoptotic effects on both *c-myc* IRES activity and protein levels provided further evidence that the IRES is responsible for the continued production of *c-Myc* protein.

The *N-myc* IRES did not remain active under the same circumstances, which implies that this function of the *c-myc* IRES was due to a specific requirement for *c-Myc* and not merely to a reduced need for intact eIF4G in IRES-dependent translation. This represents a further interesting distinction between *c-* and *N-myc* IRES function. It is well established that all three Myc proteins may contribute to apoptosis, but differences between their apoptotic behaviour had been observed, and these data imply that *N-Myc* is not required during apoptosis. It should be emphasised that the *c-myc* IRES allows continued production of protein late in apoptosis, and therefore it appears likely that *c-Myc* is required for as yet uncharacterised late apoptotic events. As the *N-myc* coding region is

able to functionally replace that of *c-myc* (Malynn et al., 2000), it can be assumed that N-Myc would be able to assume the apoptotic function of c-Myc. However, the differences in IRES behaviour mean that only the *c-myc* IRES remains active under these circumstances and therefore c-Myc is the protein produced. It would be interesting to determine what features of the cellular environment allow the specific maintenance of the *c-myc* IRES, but not various other cellular IRESs examined, in the late stages of apoptosis.

The decrease in *N-myc*, but not *c-myc*, IRES activity during neuronal differentiation was particularly interesting as it provides a potential role for the *N-myc* IRES *in vivo*. This is not directly comparable to the apoptotic behaviour of the *c-myc* IRES, as cap-dependent initiation is more active in cycling cells than during differentiation. However, *N-myc* IRES-dependent translation decreased more rapidly than cap-dependent translation during this process. *N-myc* expression is known to be extremely important during differentiation and early development, and it is possible that the *N-myc* IRES exists to provide a particularly sensitive switch mechanism on the induction of differentiation. By this model, the IRES would direct efficient production of N-Myc protein when it is needed during embryogenesis, but would induce an immediate decrease in production when the differentiation process was entered, before cap-dependent translation responded fully.

Since these studies were carried out, a number of other instances have been identified in which an IRES was used to maintain production of a protein under a specific condition in which cap-dependent translation was inhibited. No role was detected for the *c-myc* IRES under other cellular stresses examined in this study, although it is maintained during DNA damage (Subkhankulova et al., 2001). Also, previous studies indicate that c-Myc protein levels increase following heat shock and that, although largely caused by an increase in protein stability, this is partly due to a translational effect (Lüscher and Eisenman, 1988). It is unfortunate that analysis of *c-myc* IRES activity during heat shock was inconclusive. However, it appears that cellular IRESs exist for very specific purposes. This provides a partial explanation for the considerable differences observed in cellular IRES structure and requirements.

These studies indicate that, although three closely related genes contain IRESs, the characteristics of these IRESs show many distinctions. A more extensive comparison of cellular IRESs will be necessary to establish the presence of common structural and functional motifs.

---

**References**

- Adams, J.M., Harris, A.W., Pinkert, C.A., Corcoran, L.M., Alexander, W.S., Cory, S., Palmiter, R.D. and Brinster, R.L. (1985) The *c-myc* oncogene driven by immunoglobulin enhancers induces lymphoid malignancy in transgenic mice. *Nature*, **318**, 533-538.
- Agol, V.I. (1991) The 5' untranslated region of picornaviral genomes. *Adv. Virus Res.*, **40**, 103-180.
- Akiri, G., Nahiri, D., Finkelstein, Y., Le, S.-Y., Elroy-Stein, O. and Levi, B.-Z. (1998) Regulation of vascular endothelial growth factor (VEGF) expression is mediated by internal initiation of translation and alternative initiation of transcription. *Oncogene*, **17**, 227-236.
- Ali, I.K., McKendrick, L., Morley, S.J. and Jackson, R.J. (2001) Activity of the hepatitis A virus IRES requires association between the cap-binding translation initiation factor (eIF4E) and eIF4G. *J. Virol.*, **75**, 7854-7863.
- Ammer, H. and Schulz, R. (1994) Retinoic-acid induced differentiation of human neuroblastoma SH-SY5Y cells is associated with changes in the abundance of G-proteins. *J. Neurochem.*, **62**, 1310-1318.
- Amundson, S.A., Zhan, Q., Penn, L.Z. and Fornace Jr., A.J. (1998) Myc suppresses induction of the growth arrest genes *gadd34*, *gadd45*, and *gadd153* by DNA-damaging agents. *Oncogene*, **17**, 2149-2154.
- Asano, K., Clayton, J., Shalev, A. and Hinnebusch, A.G. (2000) A multifactor complex of eukaryotic initiation factors, eIF1, eIF2, eIF3, eIF5 and initiator tRNA<sup>Met</sup> is an important translation initiation intermediate in vivo. *Genes Dev.*, **14**, 2534-2546.
- Ashkenazi, A. and Dixit, V.M. (1998) Death receptors: Signaling and modulation. *Science*, **281**, 1305-1308.
- Asker, C.E., Magnusson, K.P., Piccoli, S.P., Andersson, K., Klein, G., Cole, M.D. and Wiman, K.G. (1995) Mouse and rat *B-myc* share amino acid sequence homology with the *c-myc* transcriptional activator domain and contain a *B-myc* specific carboxy terminal region. *Oncogene*, **11**, 1963-1969.
- Baudino, T.A. and Cleveland, J.L. (2001) The Max network gene Mad. *Mol. Cell. Biol.*, **21**, 691-702.

- Beales, L.P., Rowlands, D.J. and Holzenburg, A. (2001) The internal ribosome entry site (IRES) of hepatitis C virus visualized by electron microscopy. *RNA*, **7**, 661-670.
- Bello-Fernandez, C., Packham, G. and Cleveland, J.L. (1993) The ornithine decarboxylase gene is a transcriptional target of c-Myc. *Proc. Natl. Acad. Sci. USA*, **90**, 7804-7808.
- Belsham, G.J. (1992) Dual initiation sites of protein synthesis on foot-and-mouth disease virus RNA are selected following internal entry and scanning of ribosomes in vivo. *EMBO J.*, **11**, 1105-1110.
- Bentley, D.L. and Groudine, M. (1986) Novel promoter upstream of the human *c-myc* gene and regulation of *c-myc* expression in B-Cell lymphomas. *Mol. Cell. Biol.*, **6**, 3481-3489.
- Bergamini, G., Preiss, R. and Hentze, M.W. (2000) Picornaviral IRESes and the poly(A) tail jointly promote cap-independent translation in a mammalian cell-free system. *RNA*, **6**, 1781-1790.
- Bernstein, J., Sella, O., Le, S. and Elroy-Stein, O. (1997) PDGF/*c-sis* mRNA leader contains a differentiation-linked internal ribosomal entry site (D-IRES). *J. Biol. Chem.*, **272**, 9356-9362.
- Birrer, M.J., Segal, S., DeGreve, J.S., Kaye, F., Sausville, E.A. and Minna, J.D. (1988) *L-myc* cooperates with *ras* to transform primary rat embryo fibroblasts. *Mol. Cell. Biol.*, **8**, 2668-2673.
- Blyn, L.B., Towner, J.S., Semler, B.L. and Ehrenfeld, E. (1997) Requirement of poly(rC) binding protein 2 for translation of poliovirus RNA. *J. Virol.*, **71**, 6243-6246.
- Bommer, U.A., Lutsch, G., Stahl, J. and Bielka, H. (1991) Eukaryotic initiation factors eIF-2 and eIF-3: Interactions, structure and localization in ribosomal initiation complexes. *Biochimie*, **73**, 1007-1019.
- Bonneau, A.-M. and Sonenberg, N. (1987) Involvement of the 24-kDa cap-binding protein in regulation of protein synthesis in mitosis. *J. Biol. Chem.*, **262**, 11134-11139.
- Boon, K., Caron, H.N., van Asperen, R., Valentijn, L., Hermus, M.-C., van Sluis, P., Roobeek, I., Weis, I., Voûte, P.A., Schwab, M. and Versteeg, R. (2001) N-myc enhances the expression of a large set of genes functioning in ribosome biogenesis and protein synthesis. *EMBO J.*, **20**, 1383-1393.

- Borman, A.M., Bailly, J.-L., Girard, M. and Kean, K.M. (1995) Picornavirus internal ribosome entry segments: comparison of translation efficiency and the requirements for optimal internal initiation of translation *in vitro*. *Nucleic Acids Res.*, **23**, 3656-3663.
- Borman, A.M. and Jackson, R.J. (1992) Initiation of translation of human rhinovirus RNA: Mapping the internal ribosome entry site. *Virology*, **188**, 685-696.
- Borman, A.M. and Kean, K.M. (1997) Intact eukaryotic initiation factor 4G is required for hepatitis A virus internal initiation of translation. *Virology*, **237**, 129-136.
- Brodeur, G.M., Seeger, R.C., Schwab, M., Varmus, H.E. and Bishop, J.M. (1984) Amplification of N-myc in untreated human neuroblastomas correlates with advanced disease stage. *Science*, **224**, 1121-1124.
- Bronstein, I., Fortin, J., Stanley, P.E., Stewart, G.S.A.B. and Kricha, L.J. (1994) Chemiluminescent and bioluminescent reporter gene assays. *Anal. Biochem.*, **219**, 169-181.
- Bushell, M., McKendrick, L., Jänicke, R.U., Clemens, M.J. and Morley, S.J. (1999) Caspase-3 is necessary and sufficient for cleavage of protein synthesis eukaryotic initiation factor 4G during apoptosis. *FEBS Lett.*, **451**, 332-336.
- Bushell, M., Poncet, D., Marissen, W.E., Flotow, H., Lloyd, R.E., Clemens, M.J. and Morley, S.J. (2000a) Cleavage of polypeptide chain initiation factor eIF4GI during apoptosis in lymphoma cells: characterisation of an internal fragment generated by caspase-3-mediated cleavage. *Cell Death Differ.*, **7**, 628-636.
- Bushell, M., Wood, W., Carpenter, G., Pain, V.M., Morley, S.J. and Clemens, M.J. (2001) Disruption of the interaction of mammalian protein synthesis eukaryotic initiation factor 4B with the poly(A)-binding protein by caspase- and viral protease-mediated cleavages. *J. Biol. Chem.*, **276**, 23922-23928.
- Bushell, M., Wood, W., Clemens, M.J. and Morley, S.J. (2000b) Changes in integrity and association of eukaryotic protein synthesis initiation factors during apoptosis. *Eur. J. Biochem.*, **267**, 1083-1091.
- Carter, M.S. and Sarnow, P. (2000) Distinct mRNAs that encode La autoantigen are differentially expressed and contain internal ribosome entry sites. *J. Biol. Chem.*, **275**, 28301-28307.

- Chagnovich, D., Fayos, B.E. and Cohn, S.L. (1996) Differential activity of ELAV-like RNA-binding proteins in human neuroblastoma. *J. Biol. Chem.*, **271**, 33587-33591.
- Chakrabarti, A. and Maitra, U. (1991) Function of eukaryotic initiation factor 5 in the formation of an 80S ribosome polypeptide chain initiation complex. *J. Biol. Chem.*, **266**, 14039-14045.
- Chappell, S.A., Edelman, G.M. and Mauro, V.P. (2000a) A 9-nt segment of a cellular mRNA can function as an internal ribosome entry site (IRES) and when present in linked multiple copies greatly enhances IRES activity. *Proc. Natl. Acad. Sci. USA*, **97**, 1536-1541.
- Chappell, S.A., Le Quesne, J.P.C., Paulin, F.E.M., deSchoolmeester, M.L., Stoneley, M., Soutar, R.L., Ralston, S.H., Helfrich, M.H. and Willis, A.E. (2000b) A mutation in the *c-myc*-IRES leads to enhanced internal ribosome entry in multiple myeloma: A novel mechanism of oncogene de-regulation. *Oncogene*, **19**, 4437-4440.
- Chaudhuri, J., Chowdhury, D. and Maitra, U. (1999) Distinct functions of eukaryotic translation initiation factors eIF1A and eIF3 in the formation of the 40 S ribosomal preinitiation complex. *J. Biol. Chem.*, **274**, 17975-17980.
- Chen, J.-J. (2000) Heme-regulated eIF2 $\alpha$  kinase. In Sonenberg, N., Hershey, J.W.B. and Mathews, M.B. (eds.), *In: Translational Control of Gene Expression*. Cold Spring Harbor Laboratory Press, pp. 529-546.
- Cheng, M., Wang, D. and Roussel, M.F. (1999) Expression of c-Myc in response to colony-stimulating factor-1 requires mitogen-activated protein kinase kinase-1. *J. Biol. Chem.*, **274**, 6553-6568.
- Child, S.J., Miller, M.K. and Geballe, A.P. (1999) Translational control by an upstream open reading frame in the *HER-2/neu* transcript. *J. Biol. Chem.*, **274**, 24335-24341.
- Choi, S.K., Olsen, D.S., Roll-Mecak, A., Martung, A., Remo, K.L., Burley, S.K., Hinnebusch, A.G. and Dever, T.E. (2000) Physical and functional interaction between the eukaryotic orthologs of prokaryotic translation initiation factors IF1 and IF2. *Mol. Cell. Biol.*, **20**, 7183-7191.
- Chung, J., Kuo, C.J., Crabtree, G.R. and Blenis, J. (1992) Rapamycin-FKBP specifically blocks growth-dependent activation of and signaling by the 70 kd S6 protein kinases. *Cell*, **69**, 1227-1236.

- Coldwell, M.J. (2001) Analysis of internal ribosome entry segments in Apaf-1 and BAG-1 mRNAs. *PhD thesis*. University of Leicester.
- Coldwell, M.J., deSchoolmeester, M.L., Fraser, G.A., Pickering, B.M., Packham, G. and Willis, A.E. (2001) The p36 isoform of BAG-1 is translated by internal ribosome entry following heat shock. *Oncogene*, **20**, 4095-4100.
- Coldwell, M.J., Mitchell, S.A., Stoneley, M., MacFarlane, M. and Willis, A.E. (2000) Initiation of Apaf-1 translation by internal ribosome entry. *Oncogene*, **19**, 899-905.
- Cole, M.D. and McMahon, S.B. (1999) The Myc oncoprotein: a critical evaluation of transactivation and target gene regulation. *Oncogene*, **18**, 2916-2924.
- Coller, H.A., Grandori, C., Tamayo, P., Colbert, T., Lander, E.S., Eisenman, R.N. and Golub, T.R. (1999) Expression analysis with oligonucleotide microarrays reveals that MYC regulates genes involved in growth, cell cycle, signaling and adhesion. *Proc. Natl. Acad. Sci. USA*, **97**, 3260-3265.
- Cornelis, S., Bruynooghe, Y., Denecker, G., Van Huffel, S., Tinton, S. and Beyaert, R. (2000) Identification and characterization of a novel cell cycle-regulated internal ribosome entry site. *Mol. Cell*, **5**, 597-605.
- Craig, A.W.B., Haghghat, A., Yu, A.T.K. and Sonenberg, N. (1998) Interaction of polyadenylate-binding protein with the eIF4G homologue PAIP enhances translation. *Nature*, **392**, 520-523.
- Creancier, L., Mercier, P., Prats, A.-C. and Morello, D. (2001) *c-myc* internal ribosome entry site activity is developmentally controlled and subjected to a strong translational repression in adult transgenic mice. *Mol. Cell. Biol.*, **21**, 1833-1840.
- Creancier, L., Morello, D., Mercier, P. and Prats, A.-C. (2000) Fibroblast growth factor 2 internal ribosome entry site (IRES) activity *ex vivo* and in transgenic mice reveals a stringent tissue-specific regulation. *J. Cell Biol.*, **150**, 275-281.
- Cuesta, R., Laroia, G. and Schneider, R.J. (2000) Chaperone Hsp27 inhibits translation during heat shock by binding eIF4G and facilitating dissociation of cap-initiation complexes. *Genes Dev.*, **14**, 1460-1470.
- Dang, C.V. (1999) C-Myc target genes involved in cell growth, apoptosis and metabolism. *Mol. Cell. Biol.*, **19**, 1-11.
- Dang, C.V. and Lee, W.M.F. (1988) Identification of the human *c-myc* protein nuclear translocation signal. *Mol. Cell. Biol.*, **8**, 4048-4054.

- Dani, C., Blanchard, J.M., Piechaczyk, M., El Sabouty, E., Marty, L. and Jeanteur, P. (1984) Extreme instability of myc mRNA in normal and transformed human cells. *Proc. Natl. Acad. Sci. USA*, **81**, 7046-7050.
- Davis, A.C., Wims, M., Spotts, G.D., Hann, S.R. and Bradley, A. (1993) A null c-myc mutation causes lethality before 10.5 days of gestation in homozygotes and reduced fertility in heterozygous female mice. *Genes Dev.*, **7**, 671-682.
- Dean, M., Levine, R.A., Ran, W., Kindy, M.S., Sonenshein, G.E. and Campisi, J. (1986) Regulation of c-myc transcription and mRNA abundance by serum growth factors and cell contact. *J. Biol. Chem.*, **261**, 9161-9166.
- Dmitrovsky, E., Kuehl, W.M., Hollis, G.F., Kirsch, I.R., Bender, T.P. and Segal, S. (1986) Expression of a transfected human c-myc oncogene inhibits differentiation of a mouse erythroleukaemia cell line. *Nature*, **322**, 748-750.
- Dosaka-Akita, H., Rosenberg, R.K., Minna, J.D. and Birrer, M.J. (1991) A complex pattern of translational initiation and phosphorylation in L-myc proteins. *Oncogene*, **6**, 371-378.
- Dufner, A., Andjelkovic, M., Burgering, B.M.T., Hemmings, B.A. and Thomas, G. (1999) Protein kinase B localization and activation differentially affect S6 kinase 1 activity and eukaryotic translation initiation factor 4E-binding protein 1 phosphorylation. *Mol. Cell. Biol.*, **19**, 4525-4534.
- Duncan, R.F., Milburn, S.C. and Hershey, J.W.B. (1987) Regulated phosphorylation and low abundance of HeLa cell initiation factor eIF-4F suggest a role in translational control. *J. Biol. Chem.*, **262**, 380-388.
- Dwarki, V.J., Malone, R.W. and Verma, I.M. (1993) Cationic liposome-mediated RNA transfection. *Meths. in Enzymology*, **217**, 644-654.
- Eilers, M., Schirm, S. and Bishop, J.M. (1991) The MYC protein activates transcription of the  $\alpha$ -prothymosin gene. *EMBO J.*, **10**, 133-141.
- Evan, G.I., Wyllie, A.H., Gilbert, C.S., Littlewood, T.D., Land, H., Brooks, M., Waters, C.M., Penn, L.Z. and Hancock, D.C. (1992) Induction of apoptosis in fibroblasts by c-myc protein. *Cell*, **69**, 119-128.
- Feigenblum, D. and Schneider, R.J. (1993) Modification of eukaryotic initiation factor 4F during infection by influenza virus. *J. Virol.*, **67**, 3027-3035.

- Feigenblum, D. and Schneider, R.J. (1996) Cap-binding protein (eukaryotic initiation factor 4E) and 4E-inactivating protein BP-1 independently regulate cap-dependent translation. *Mol. Cell. Biol.*, **16**, 5450-5457.
- Fernandez, J., Yaman, I., Mishra, R., Merrick, W.C., Snider, M.D., Lamers, W.H. and Hatzoglou, M. (2001) Internal ribosome entry site-mediated translation of a mammalian mRNA is regulated by amino acid availability. *J. Biol. Chem.*, **276**, 12285-12291.
- Flinn, E.M., Busch, C.M.C. and Wright, A.P.H. (1998) myc boxes, which are conserved in myc family proteins, are signals for protein degradation via the proteasome. *Mol. Cell. Biol.*, **18**, 5961-5969.
- Fukunaga, F. and Hunter, T. (1997) MNK1, a new MAP kinase-activated protein kinase, isolated by novel expression screening method for identifying protein kinase substrates. *EMBO J.*, **16**, 1921-1933.
- Futterer, J., Kisslaszlo, Z. and Hohn, T. (1993) Nonlinear ribosome migration on cauliflower mosaic virus-35S RNA. *Cell*, **73**, 789-802.
- Gingras, A.-C., Gygi, S.P., Raught, B., Polakiewicz, R.D., Abraham, R.T., Hoekstra, M.F., Aebersold, R. and Sonenberg, N. (1999a) Regulation of 4E-BP1 phosphorylation: a novel two-step mechanism. *Genes Dev.*, **13**, 1422-1437.
- Gingras, A.-C., Raught, B. and Sonenberg, N. (1999b) eIF4 initiation factors: Effectors of mRNA recruitment to ribosomes and regulators of translation. *Annu. Rev. Biochem.*, **68**, 913-963.
- Gingras, A.-C., Svitkin, Y.V., Belsham, G.J., Pause, A. and Sonenberg, N. (1996) Activation of the translational suppressor 4E-BP1 following infection with encephalomyocarditis virus and poliovirus. *Proc. Natl. Acad. Sci. USA*, **93**, 5578-5583.
- Goossen, B. and Hentze, M.W. (1992) Position is the critical determinant for function of iron-responsive elements as translational regulators. *Mol. Cell. Biol.*, **12**, 1959-1966.
- Gosert, R., Chang, K.H., Rijnbrand, R., Yi, M., Sangar, D.V. and Lemon, S.M. (2000) Transient expression of cellular polypyrimidine-tract binding protein stimulates cap-independent translation directed by both picornaviral and flaviviral internal ribosome entry sites in vivo. *Mol. Cell. Biol.*, **20**, 1583-1595.

- Gradi, A., Imataka, H., Svitkin, Y.V., Rom, E., Raught, B., Morino, S. and Sonenberg, N. (1998) A novel functional human eukaryotic initiation factor 4G. *Mol. Cell Biol.*, **18**, 334-342.
- Gray, N.K. and Hentze, M.W. (1994a) Iron regulatory protein prevents binding of the 43S translation pre-initiation complex to ferritin and eALAS mRNAs. *EMBO J.*, **13**, 3882-3891.
- Gray, N.K. and Hentze, M.W. (1994b) Regulation of protein synthesis by mRNA structure. *Mol. Biol. Rep.*, **19**, 195-200.
- Gray, N.K. and Wickens, M. (1998) Control of translation initiation in animals. *Annu. Rev. Cell Dev. Biol.*, **14**, 399-458.
- Greasley, P.J., Bonnard, C. and Amati, B. (2000) Myc induces the nucleolin and BN51 genes: possible implications in ribosome biogenesis. *Nucleic Acids Res.*, **28**, 446-453.
- Green, D.R. and Reed, J.C. (1998) Mitochondria and apoptosis. *Science*, **281**, 1309-1312.
- Gregory, M.A., Xiao, Q., Cornwall, G.A., Lutterbach, B. and Hann, S.R. (2000) B-Myc is preferentially expressed in hormonally-controlled tissues and inhibits cellular proliferation. *Oncogene*, **19**, 4886-4895.
- Haghighat, A., Mader, S., Pause, A. and Sonenberg, N. (1995) Repression of cap-dependent translation by 4E-binding protein 1: competition with p220 for binding to eukaryotic initiation factor-4E. *EMBO J.*, **14**, 5701-5709.
- Han, J., Lee, J.-D., Jiang, Y., Li, Z., Feng, L. and Ulevitch, R.J. (1996) Characterization of the structure and function of a novel MAP kinase kinase (MKK6). *J. Biol. Chem.*, **271**, 2886-2891.
- Hanahan, D. (1983) Studies on transformation of *Escherichia coli* with plasmids. *Journal of Molecular Biology*, **166**, 557.
- Hann, S.R. and Eisenman, R.N. (1984) Proteins encoded by the human *c-myc* oncogene: differential expression in neoplastic cells. *Mol. Cell Biol.*, **4**, 2486-3497.
- Hann, S.R., King, M.W., Bentley, D.L., Anderson, C.W. and Eisenman, R.N. (1988) A non-AUG translational initiation in *c-myc* exon 1 generates an N-terminally distinct protein whose synthesis is disrupted in Burkitt's lymphomas. *Cell*, **52**, 185-195.
- Harrington, E.A., Bennett, M.R., Fanidi, A. and Evan, G.I. (1994) *c-Myc*-induced apoptosis in fibroblasts is inhibited by specific cytokines. *EMBO J.*, **13**, 3286-3295.

- Hatton, K.S., Mahon, K., Chin, L., Chiu, F.-C., Lee, H.-W., Peng, D., Morgenbesser, S.D., Horner, J. and DePinho, R.A. (1996) Expression and activity of L-Myc in normal mouse development. *Mol. Cell. Biol.*, **16**, 1794-1804.
- Hellen, C.U.T. and Sarnow, P. (2001) Internal ribosome entry sites in eukaryotic mRNA molecules. *Genes Dev.*, **15**, 1593-1612.
- Hemmings-Mieszczak, M. and Hohn, T. (1999) A stable hairpin preceded by a short open reading frame promotes nonlinear ribosome migration on a synthetic mRNA leader. *RNA*, **5**, 1149-1157.
- Henis-Korenblit, S., Levy Strumpf, N., Goldstaub, D. and Kimchi, A. (2000) A novel form of DAP5 protein accumulates in apoptotic cells as a result of caspase cleavage and internal ribosome entry site-mediated translation. *Mol. Cell. Biol.*, **20**, 496-506.
- Henriksson, M. and Luscher, B. (1996) Proteins of the Myc network: Essential regulators of cell growth and differentiation. *Adv. Cancer Res.*, **68**, 109-182.
- Hentze, M.W. (1997) eIF4G: A multipurpose ribosome adapter? *Science*, **275**, 500-501.
- Hentze, M.W., Caughman, S.W., Roualt, T.A., Barriocanal, J.G., Dancis, A., Harford, J.B. and Klausner, R.D. (1987) Identification of the iron-responsive element for the translational regulation of human ferritin mRNA. *Science*, **238**, 1570-1573.
- Hermeking, H. and Eick, D. (1994) Mediation of c-Myc-induced apoptosis by p53. *Science*, **265**, 2091-2093.
- Hershey, J.W.B. and Merrick, W.C. (2000) Pathway and mechanism of initiation of protein synthesis. In Sonenberg, N., Hershey, J.W.B. and Mathews, M.B. (eds.), *Translational Control of Gene Expression*. Cold Spring Harbor Laboratory Press, pp. 33-88.
- Hinnebusch, A.G. (2000) Mechanism and regulation of initiator methionyl-tRNA binding to ribosomes. In Sonenberg, N., Hershey, J.W.B. and Mathews, M.B. (eds.), *In: Translational Control of Gene Expression*. Cold Spring Harbor Laboratory Press, pp. 185-244.
- Hiremath, L.S., Webb, N.R. and Rhoads, R.E. (1985) Immunological detection of the messenger RNA cap-binding protein. *J. Biol. Chem.*, **260**, 7843-7849.
- Hoffman, B. and Liebermann, D.A. (1998) The proto-oncogene *c-myc* and apoptosis. *Oncogene*, **17**, 3351-3357.

- Holcik, M. and Korneluk, R.G. (2000) Functional characterization of the X-linked inhibitor of apoptosis (XIAP) internal ribosome entry site element: Role of La autoantigen in XIAP translation. *Mol. Cell. Biol.*, **20**, 4648-4657.
- Holcik, M., Lefebvre, C., Yeh, C., Chow, T. and Korneluk, R.G. (1999) A new internal-ribosome-entry-site motif potentiates XIAP-mediated cytoprotection. *Nature Cell Biol.*, **1**, 190-192.
- Holcik, M., Yeh, C., Korneluk, R.G. and Chow, T. (2000) Translational upregulation of X-linked inhibitor of apoptosis (XIAP) increases resistance to radiation induced cell death. *Oncogene*, **19**, 4174-4177.
- Hu, M.C.-Y., Tranque, P., Edelman, G.M. and Mauro, V.P. (1999) rRNA-complementarity in the 5' untranslated region of mRNA specifying the Gtx homeodomain protein: Evidence that base-pairing to 18S rRNA affects translational efficiency. *Proc. Natl. Acad. Sci. USA*, **96**, 1339-1344.
- Huang, J. and Schneider, R.J. (1991) Adenovirus inhibition of cellular protein-synthesis involves inactivation of cap-binding protein. *Cell*, **65**, 271-280.
- Hudder, A. and Werner, R. (2000) Analysis of a Charcot-Marie-Tooth disease mutation reveals an essential internal ribosome entry site element in the connexin-32 gene. *J. Biol. Chem.*, **275**, 34586-34591.
- Hunt, S.L., Hsuan, J.J., Totty, N. and Jackson, R.J. (1999) unr, a cellular cytoplasmic RNA-binding protein with five cold-shock domains, is required for internal initiation of human rhinovirus RNA. *Genes Dev.*, **13**, 437-448.
- Hunt, S.L. and Jackson, R.J. (1999) Polypyrimidine-tract binding protein (PTB) is necessary, but not sufficient, for efficient internal initiation of translation of human rhinovirus-2 RNA. *RNA*, **5**, 344-359.
- Hurlin, P.J., Queva, C., Koskinen, P., J., Steingrimsson, E., Ayer, D.E., Copeland, N.G., Jenkins, N.A. and Eisenman, R.N. (1995) Mad3 and Mad4: novel Max-interacting transcriptional repressors that suppress *c-myc* dependent transformation and are expressed during neural and epidermal differentiation. *EMBO J.*, **14**, 5646-5659.
- Ibson, J.M. and Rabbitts, P.H. (1988) Sequence of a germ-line *N-myc* gene and amplification as a mechanism of activation. *Oncogene*, **2**, 399-402.
- Imamura, Y., Iguchi-Arigo, S.M.M. and Ariga, H. (1992) The upstream region of the mouse *N-myc* gene: identification of an enhancer element that functions

- preferentially in neuroblastoma IMR32 cells. *Biochim. Biophys. Acta*, **1132**, 177-187.
- Imataka, H., Olsen, H.S. and Sonenberg, N. (1997) A new translational regulator with homology to eukaryotic translation initiation factor 4G. *EMBO J.*, **16**, 817-825.
- Ioannidis, P., Courtis, N., Havredaki, M., Michailakis, E., Tsiapalis, C.M. and Trangas, T. (1999) The polyadenylation inhibitor cordycepin (3'dA) causes a decline in c-MYC mRNA levels without affecting c-MYC protein levels. *Oncogene*, **18**, 117-125.
- Jackson, R.J. (2000) A comparative view of initiation site selection mechanisms. In Sonenberg, N., Hershey, J.W.B. and Mathews, M.B. (eds.), *Translational Control of Gene Expression*. Cold Spring Harbor Laboratory Press, pp. 127-183.
- Jackson, R.J., Howell, M.T. and Kaminski, A. (1990) The novel mechanism of initiation of picornavirus RNA translation. *Trends Biochem. Sci.*, **15**, 477-483.
- Jackson, R.J., Hunt, S.L., Reynolds, J.E. and Kaminski, A. (1995) Cap-dependent and cap-independent translation: Operational distinctions and mechanistic interpretations. *Current Topics in Microbiol Immunology*, **203**, 1-29.
- Jang, S.K., Kräusslich, H.-G., Nicklin, M.J.H., Duke, G.M., Palmenberg, A.C. and Wimmer, E. (1988) A segment of the 5' nontranslated region of encephalomyocarditis virus RNA directs internal entry of ribosomes during in vitro translation. *J. Virol.*, **62**, 2636-2643.
- Jefferies, H.B., Reinhard, J.C., Kozma, S.C. and Thomas, G. (1994) Rapamycin selectively represses translation of the "polypyrimidine tract" mRNA family. *Proc. Natl. Acad. Sci. USA*, **91**, 4441-4445.
- Johannes, G., Carter, M.S., Eisen, M.B., Brown, P.O. and Sarnow, P. (1999) Identification of eukaryotic mRNAs that are translated at reduced cap-binding complex eIF4F concentrations using a cDNA microarray. *Proc. Natl. Acad. Sci. USA*, **96**, 13118-13123.
- Johnston, L.A., Prober, D.A., Edgar, B.A., Eisenman, R.N. and Gallant, P. (1999) *Drosophila myc* regulates cellular growth during development. *Cell*, **98**, 779-790.
- Jordan, M., Schallhorn, A. and Wurm, F.M. (1996) Transfecting mammalian cells: Optimization of critical parameters affecting calcium-phosphate precipitate formation. *Nucleic Acids Res.*, **24**, 596-601.

- Juin, P., Hueber, A.-O., Littlewood, T. and Evan, G. (1999) c-Myc-induced sensitization to apoptosis is mediated through cytochrome *c* release. *Genes Dev.*, **13**, 1367-1381.
- Kaminski, A., Howell, M.T. and Jackson, R.J. (1990) Initiation of encephalomyocarditis virus RNA translation: the authentic initiation site is not selected by a scanning mechanism. *EMBO J.*, **9**, 3753-3759.
- Kaminski, A. and Jackson, R.J. (1998) The polypyrimidine tract binding protein (PTB) requirement for internal initiation of translation of cardiovirus RNAs is conditional rather than absolute. *RNA*, **4**, 626-628.
- Karn, J., Watson, J.V., Lowe, A.D., Green, S.M. and Vedeckis, W. (1989) Regulation of cell cycle duration by *c-myc* levels. *Oncogene*, **4**, 773-787.
- Kato, G.J., Barrett, J., Villa-Garcia, M. and Dang, C.V. (1990) An amino-terminal c-Myc domain required for neoplastic transformation activates transcription. *Mol. Cell. Biol.*, **10**, 5914-5920.
- Kato, G.J., Lee, W.M.F., Chen, L. and Dang, C.V. (1992) Max: functional domains and interaction with c-Myc. *Genes Dev.*, **6**, 81-92.
- Kato, K., Kanamori, A., Wakamatsu, Y., Sawai, S. and Kondoh, H. (1991) Tissue distribution of N-myc expression in the early organogenesis period of the mouse embryo. *Develop. Growth Differ.*, **33**, 29-36.
- Katoh, K., Sawai, S., Ueno, K. and Kondoh, H. (1988) Complete nucleotide sequence and exon-intron boundaries of the 5' non-coding region of the mouse N-myc gene. *Nucleic Acids Res.*, **16**.
- Kaufman, R.J. (1999) Stress signaling from the lumen of the endoplasmic reticulum: coordination of gene transcriptional and translational controls. *Genes Dev.*, **13**, 1211-1233.
- Kaufman, R.J. (2000) The double-stranded RNA-activated protein kinase PKR. In Sonenberg, N., Hershey, J.W.B. and Mathews, M.B. (eds.), *In: Translational control of gene expression*. Cold Spring Harbor Laboratory Press, pp. 503-527.
- Kaye, F., Battey, J., Nau, M., Brooks, B., Seifter, E., De Greve, J., Birrer, M., Sausville, E. and Minna, J. (1988) Structure and expression of the human L-myc gene reveal a complex pattern of alternative mRNA processing. *Mol. Cell. Biol.*, **8**, 186-195.

- Khaleghpour, K., Svitkin, Y.V., Craig, A.W., DeMaria, C.T., Deo, R.C., Burley, S.K. and Sonenberg, N. (2001) Translational repression by a novel partner of human poly(A) binding protein, Paip2. *Mol. Cell*, **7**, 205-216.
- Kieft, J.S., Zhou, K., Jubin, R. and Doudna, J.A. (2001) Mechanism of ribosome recruitment by hepatitis C IRES RNA. *RNA*, **7**, 194-206.
- Kim, S., Li, Q., Dang, C.V. and Lee, L.A. (2000a) Induction of ribosomal genes and hepatocyte hypertrophy by adenovirus-mediated expression of c-Myc *in vivo*. *Proc. Natl. Acad. Sci. USA*, **97**, 11198-11202.
- Kim, Y.K., Hahm, B. and Jang, S.K. (2000b) Polypyrimidine tract-binding protein inhibits translation of Bip mRNA. *J. Mol. Biol.*, **304**, 119-133.
- Kimball, S.R. (1999) Eukaryotic initiation factor eIF2. *The Int. J. Biochem. Cell Biol.*, **31**, 25-29.
- Kimball, S.R., Fabian, J.R., Pavitt, G.D., Hinnebusch, A.G. and Jefferson, L.S. (1998) Regulation of guanine nucleotide exchange through phosphorylation of eukaryotic initiation factor eIF2 $\alpha$ . *J. Biol. Chem.*, **273**, 12841-12845.
- Kirchweger, R., Ziegler, E., Lamphear, B.J., Waters, D., Liebig, H.-D., Sommergruber, W., Sobrino, F., Hohenadi, C., Blaas, D., Rhoads, R.E. and Skern, T. (1994) Foot-and-mouth disease virus leader proteinase: Purification of the Lb form and determination of its cleavage site on eIF-4 $\gamma$ . *J. Virol.*, **68**, 5677-5684.
- Kohl, N.E., Legouy, E., DePinho, R.A., Nisen, P.D., Smith, R.K., Gee, C.E. and Alt, F.W. (1986) Human N-myc is closely related in organization and nucleotide sequence to c-myc. *Nature*, **319**, 73-77.
- Koromilas, A.E., Lazaris-Karatzas, A. and Sonenberg, N. (1992) mRNAs containing extensive secondary structure in their 5' non-coding region translate efficiently in cells overexpressing initiation factor eIF-4E. *EMBO J.*, **11**, 4153-4158.
- Kozak, M. (1987) An analysis of 5'-noncoding sequences from 699 vertebrate messenger RNAs. *Nucleic Acids Res.*, **15**, 8125-8148.
- Kozak, M. (1989) Context effects and (inefficient) initiation at non-AUG codons in eucaryotic cell-free translation systems. *Mol. Cell. Biol.*, **9**, 5073-5080.
- Kozak, M. (1991) An analysis of vertebrate mRNA sequences: Intimations of translation control. *J. Cell Biol.*, **115**, 887-903.

- Lamphear, B.J. and Panniers, R. (1991) Heat shock impairs the interaction of cap-binding protein complex with 5' mRNA cap. *J. Biol. Chem.*, **266**, 2789-2794.
- Lamphear, B.J., Yan, R., Yang, F., Waters, D., Liebig, H.-D., Klump, H., Kuechler, E., Skern, T. and Rhoads, R.E. (1993) Mapping the cleavage site in protein synthesis initiation factor eIF-4 $\gamma$  of the 2A proteases from human coxsackievirus and rhinovirus. *J. Biol. Chem.*, **268**, 19200-19203.
- Land, H., Parada, L.F. and Weinberg, R.A. (1983) Tumorigenic conversion of primary embryo fibroblasts requires at least two cooperating oncogenes. *Nature*, **304**, 596-602.
- Lazarova, D.L., Spengler, B.A., Biedler, J.L. and Ross, R.A. (1999) HuD, a neuronal-specific RNA-binding protein, is a putative regulator of N-myc pre-mRNA processing/stability in malignant human neuroblasts. *Oncogene*, **18**, 2703-2710.
- Le, H., Tanguay, R.L., Balasta, M.L., Wei, C.-C., Browning, K.S., Metz, A.M., Goss, D.J. and Gallie, D.R. (1997) Translation initiation factors eIF-iso4G and eIF-4B interact with the poly(A)-binding protein and increase its RNA binding activity. *J. Biol. Chem.*, **272**, 16247-16255.
- Le Quesne, J.P.C. (2000) The c-myc IRES: structure and mechanism. *PhD thesis*. University of Leicester.
- Le Quesne, J.P.C., Stoneley, M., Fraser, G.A. and Willis, A.E. (2001) Derivation of a structural model for the c-myc IRES. *J. Mol. Biol.*, **310**, 111-126.
- Le, S.-Y. and Maizel Jr, J.V. (1997) A common RNA structural motif involved in the internal initiation of translation of cellular mRNAs. *Nucleic Acids Res.*, **25**, 362-369.
- Legouy, E., DePinho, R.A., Zimmerman, K., Collum, R., Yancopoulos, G., Mitschke, L., Kriz, R. and Alt, F.W. (1987) Structure and expression of the murine L-myc gene. *EMBO J.*, **6**, 3359-3366.
- Leone, G., Sears, R., Huang, E., Rempel, R., Nuckolls, F., Park, C.-H., Giangrande, P., Wu, L., Saavedra, H.I., Field, S.J., Thompson, M.A., Yang, H., Fujiwara, Y., Greenberg, M.E., Orkin, S., Smith, C. and Nevins, J.R. (2001) Myc requires distinct E2F activities to induce S phase and apoptosis. *Mol. Cell*, **8**, 105-113.

- Li, Q., Imataka, H., Morino, S., Rogers Jr., G.W., Richter-Cook, N.J., Merrick, W.C. and Sonenberg, N. (1999) Eukaryotic translation initiation factor 4AIII (eIF4AIII) is functionally distinct from eIF4AI and eIF4AII. *Mol. Cell. Biol.*, **19**, 7336-7346.
- Lin, C.H. and Patton, J.G. (1995) Regulation of alternative 3' splice site selection by constitutive splicing factors. *RNA*, **1**, 234-245.
- Lomakin, I.B., Hellen, C.U.T. and Pestova, T.V. (2000) Physical association of eukaryotic initiation factor 4G (eIF4G) with eIF4A strongly enhances binding of eIF4G to the internal ribosomal entry site of encephalomyocarditis virus and is required for internal initiation of translation. *Mol. Cell. Biol.*, **20**, 6019-6029.
- Lorsch, J.R. and Herschlag, D. (1998) The DEAD box protein eIF4A. 1. A minimal kinetic and thermodynamic framework reveals coupled binding of RNA and nucleotide. *Biochemistry*, **37**, 2180-2193.
- Lüscher, B. and Eisenman, R.N. (1988) *c-myc* and *c-myb* protein degradation: Effect of metabolic inhibitors and heat shock. *Mol. Cell. Biol.*, **8**, 2504-2512.
- Lutz, W., Fulda, S., Jeremias, I., Debatin, K.-M. and Schwab, M. (1998) MycN and IFN $\gamma$  cooperate in apoptosis of human neuroblastoma cells. *Oncogene*, **17**, 339-346.
- Lutz, W., Stöhr, M., Schürmann, J., Wenzel, A., Löhr, A. and Schwab, M. (1996) Conditional expression of N-*myc* in human neuroblastoma cells increases expression of  $\alpha$ -prothymosin and ornithine decarboxylase and accelerates progression into S-phase early after mitogenic stimulation of quiescent cells. *Oncogene*, **13**, 803-812.
- Ma, A., Moroy, T., Collum, R., Weintraub, H., Alt, F.W. and Blackwell, T.K. (1993) DNA binding by N- and L-Myc proteins. *Oncogene*, **8**, 1093-1098.
- Macejak, D.G. and Sarnow, P. (1991) Internal initiation of translation mediated by the 5' leader of a cellular mRNA. *Nature*, **353**, 90-94.
- Makela, T.P., Saksela, K. and Alitalo, K. (1989) Two N-*myc* polypeptides with distinct amino termini encoded by the second and third exons of the gene. *Mol. Cell. Biol.*, **9**, 1545-1552.
- Malynn, B.A., de Alboran, I.M., O'Hagan, R.C., Bronson, R., Davidson, L., DePinho, R.A. and Alt, F.W. (2000) N-*myc* can functionally replace *c-myc* in murine development, cellular growth, and differentiation. *Genes Dev.*, **14**, 1390-1399.

- Marissen, W.E. and Lloyd, R.E. (1998) Eukaryotic translation initiation factor 4G is targeted for proteolytic cleavage by caspase 3 during inhibition of translation in apoptotic cells. *Mol. Cell. Biol.*, **18**, 7565-7574.
- Matejak, M.K., Obaya, A.J., Adachi, S. and Sedivy, J.M. (1997) Phenotypes of c-Myc-deficient rat fibroblasts isolated by targeted homologous recombination. *Cell Growth Differ.*, **8**, 1039-1048.
- Mathews, M.B., Sonenberg, N. and Hershey, J.W.B. (2000) Origins and Principles of Translational Control. In Sonenberg, N., Hershey, J.W.B. and Mathews, M.B. (eds.), *Translational Control of Gene Expression*. Cold Spring Harbor Laboratory Press, pp. 1-31.
- Meerovitch, K., Svitkin, Y.V., Lee, H.S., Lejbkiewicz, F., Kenan, D.J., Chan, E.K.L., Agol, V.I., Keene, J.D. and Sonenberg, N. (1993) La autoantigen enhances and corrects aberrant translation of poliovirus RNA in reticulocyte lysate. *J. Virol.*, **67**, 3798-3807.
- Meroni, G., Cairo, S., Merla, G., Messali, S., Brent, R., Knickers, D., Ballabio, A. and Raymond, A. (2000) Mlx, a new Max-like bHLHZip family member: the center stage of a novel transcription factors regulatory pathway? *Oncogene*, **19**, 3266-3277.
- Meyuhas, O. and Hornstein, E. (2000) Translational control of TOP mRNAs. In Sonenberg, N., Hershey, J.W.B. and Mathews, M.B. (eds.), *In: Translational Control of Gene Expression*. Cold Spring Harbor Laboratory Press, pp. 671-693.
- Michel, Y., Poncet, D., Piron, M., Kean, K.M. and Borman, A.M. (2000) Cap-poly(A) synergy in mammalian cell-free extracts. *J. Biol. Chem.*, **275**, 32268-32276.
- Michel, Y.M., Borman, A.M., Paulous, S. and Kean, K.M. (2001) Eukaryotic initiation factor 4G-poly(A) binding protein interaction is required for poly(A) tail-mediated stimulation of picornavirus internal ribosome entry segment-driven translation but not for X-mediated stimulation of hepatitis C virus translation. *Mol. Cell. Biol.*, **21**, 4097-4109.
- Minich, W.B., Balasta, M.L., Goss, D.J. and Rhoads, R.E. (1994) Chromatographic resolution of *in vivo* phosphorylated and nonphosphorylated eukaryotic translation initiation factor eIF-4E: Increased cap affinity of the phosphorylated form. *Proc. Natl. Acad. Sci. USA*, **91**, 7668-7672.

- Mitchell, S.A., Brown, E.C., Coldwell, M.J., Jackson, R.J. and Willis, A.E. (2001) Protein factor requirements of the Apaf-1 internal ribosome entry segment: Roles of polypyrimidine tract binding protein and upstream of N-ras. *Mol. Cell. Biol.*, **21**, 3364-3374.
- Miyagi, Y., Sugiyama, A., Asai, A., Okazaki, T., Kuchino, Y. and Kerr, S.J. (1995) Elevated levels of eukaryotic translation initiation factor eIF-4E, messenger RNA in a broad-spectrum of transformed-cell lines. *Cancer Lett.*, **91**, 247-252.
- Morgenbesser, S.D., Schreiber-Agus, N., Bidder, M., Mahon, K.A., Overbeek, P.A., Horner, J. and DePinho, R.A. (1995) Contrasting roles for c-Myc and L-Myc in the regulation of cellular growth and differentiation *in vivo*. *EMBO J.*, **14**, 743-756.
- Morley, S.J., Jeffrey, I., Bushell, M., Pain, V.M. and Clemens, M.J. (2000) Differential requirements for caspase-8 activity in the mechanism of phosphorylation of eIF2 $\alpha$ , cleavage of eIF4GI and signaling events associated with the inhibition of protein synthesis in apoptotic Jurkat T cells. *FEBS Lett.*, **477**, 229-236.
- Morley, S.J., McKendrick, L. and Bushell, M. (1998) Cleavage of translation initiation factor 4G (eIF4G) during anti-Fas IgM-induced apoptosis does not require signalling through the p38 mitogen-activated protein (MAP) kinase. *FEBS Lett.*, **438**, 41-48.
- Morley, S.J. and Traugh, J.A. (1990) Differential stimulation of phosphorylation of initiation factors eIF-4F, eIF-4B, eIF-3, and ribosomal protein S6 by insulin and phorbol esters. *J. Biol. Chem.*, **265**, 10611-10616.
- Morris, D.R. and Geballe, A.P. (2000) Upstream open reading frames as regulators of mRNA translation. *Mol. Cell. Biol.*, **20**, 8635-8642.
- Mount, S.M. (1982) A catalog of splice junction sequences. *Nucleic Acids Res.*, **10**, 459-472.
- Muckenthaler, M., Gray, N.K. and Hentze, M.W. (1998) IRP-1 binding to ferritin mRNA prevents the recruitment of the small ribosomal subunit by the cap-binding complex eIF4F. *Mol. Cell*, **2**, 383-388.
- Muller, A.J. and Witte, O.N. (1989) The 5' noncoding region of the human leukaemia-associated oncogene *BCR/ABL* is a potent inhibitor of *in vitro* translation. *Mol. Cell. Biol.*, **9**, 5234-5238.

- Nadano, D. and Sato, T.-A. (2000) Caspase-3-dependent and -independent degradation of 28 S ribosomal RNA may be involved in the inhibition of protein synthesis during apoptosis initiated by death receptor engagement. *J. Biol. Chem.*, **275**, 13967-13973.
- Nanbru, C., Prats, A.-C., Droogmans, L., Defrance, P., Huez, G. and Kruys, V. (2001) Translation of the human *c-myc* P0 tricistronic mRNA involves two independent internal ribosome entry sites. *Oncogene*, **20**, 4270-4280.
- Nau, M.M., Brooks, B.J., Battey, J., Sausville, E., Gazdar, A.F., Kirsch, I.R., McBride, O.W., Bertness, V., Hollis, G.F. and Minna, J.D. (1985) *L-myc*, a new *myc*-related gene amplified and expressed in human small cell lung cancer. *Nature*, **318**, 69-73.
- Nesbit, C.E., Grove, L.E., Yin, X. and Prochownik, E.V. (1998) Differential apoptotic behaviors of *c-myc*, *N-myc*, and *L-myc* oncoproteins. *Cell Growth Differ.*, **9**, 731-741.
- Nesbit, C.E., Tersak, J.M., Grove, L.E., Drzal, A., Choi, H. and Prochownik, E.V. (2000) Genetic dissection of *c-myc* apoptotic pathways. *Oncogene*, **19**, 3200-3212.
- Nesbit, C.E., Tersak, J.M. and Prochownik, E.V. (1999) *MYC* oncogenes and human neoplastic disease. *Oncogene*, **18**, 3004-3016.
- Nikiforov, M.A., Kotenko, I., Petrenko, O., Beavis, A., Valenick, L., Lemischka, I. and Cole, M.D. (2000) Complementation of *Myc*-dependent cell proliferation by cDNA library screening. *Oncogene*, **18**, 4828-4831.
- Nomoto, A., Kitamura, N., Golini, F. and Wimmer, E. (1977) The 5'-terminal structures of poliovirion RNA and poliovirus mRNA differ only in the genome-linked protein VPg. *Proc. Natl. Acad. Sci. USA*, **74**, 5345-5349.
- Ohlmann, T. and Jackson, R.J. (1999) The properties of chimeric picornavirus IRESes show that discrimination between internal translation initiation sites is influenced by the identity of the IRES and not just the context of the AUG codon. *RNA*, **5**, 764-778.
- Oldfield, S., Jones, B.L., Tanton, D. and Proud, C.G. (1994) Use of monoclonal antibodies to study the structure and function of eukaryotic protein synthesis initiation factor eIF-2B. *Eur. J. Biochem.*, **221**, 399-410.

- Owens, G.C., Chappell, S.A., Mauro, V.P. and Edelman, G.M. (2001) Identification of two short internal ribosome entry sites selected from libraries of random oligonucleotides. *Proc. Natl. Acad. Sci. USA*, **98**, 1471-1476.
- Parrott, L.A. and Templeton, D.J. (1999) Osmotic stress inhibits p70/S6 kinase through activation of a protein phosphatase. *J. Biol. Chem.*, **274**, 24731-24736.
- Paulin, F.E.M. (1997) A study of *c-myc* translational regulation in multiple myeloma. *PhD Thesis*. University of Leicester.
- Paulin, F.E.M., Chappell, S.A. and Willis, A.E. (1998) A single nucleotide change in the *c-myc* internal ribosome entry segment leads to enhanced binding of a group of protein factors. *Nucleic Acids Res.*, **26**, 3097-3103.
- Pause, A., Belsham, G.J., Gingras, A.-C., Donzé, O., Lin, T.-A., Lawrence Jr., J.C. and Sonenberg, N. (1994a) Insulin-dependent stimulation of protein synthesis by phosphorylation of a regulator of 5'-cap function. *Nature*, **371**, 762-767.
- Pause, A., Méthot, N., Svitkin, Y., Merrick, W.C. and Sonenberg, N. (1994b) Dominant negative mutants of mammalian translation initiation factor eIF-4A define a critical role for eIF-4F in cap-dependent and cap-independent initiation of translation. *EMBO J.*, **13**, 1205-1215.
- Pavitt, G.D., Ramaiah, K.V.A., Kimball, S.R. and Hinnebusch, A.G. (1998) eIF2 independently binds two distinct eIF2B subcomplexes that catalyze and regulate guanine-nucleotide exchange. *Genes Dev.*, **12**, 514-526.
- Pelletier, J. and Sonenberg, N. (1988) Internal initiation of translation of eukaryotic mRNA directed by a sequence derived from poliovirus RNA. *Nature*, **334**, 320-325.
- Pestova, T.V., Borukhov, S.I. and C.U.T., H. (1998a) Eukaryotic ribosomes require initiation factors 1 and 1A to locate initiation codons. *Nature*, **394**, 854-859.
- Pestova, T.V., Hellen, C.U.T. and Shatsky, I.N. (1996a) Canonical eukaryotic initiation factors determine initiation of translation by internal ribosome entry. *Mol. Cell. Biol.*, **16**, 6859-6869.
- Pestova, T.V., Hellen, C.U.T. and Wimmer, E. (1994) A conserved AUG triplet in the 5' nontranslated region of poliovirus can function as an initiation codon *in vitro* and *in vivo*. *Virology*, **204**, 729-737.

- Pestova, T.V., Lomakin, I.B., Lee, J.H., Choi, S.K., Dever, T.E. and Hellen, C.U.T. (2000) The joining of ribosomal subunits requires eIF5B. *Nature*, **403**, 332-335.
- Pestova, T.V., Shatsky, I.N., Fletcher, S.P., Jackson, R.J. and Hellen, C.U.T. (1998b) A prokaryotic-like mode of cytoplasmic eukaryotic ribosome binding to the initiation codon during internal translation initiation of hepatitis C and classic swine fever virus RNAs. *Genes Dev.*, **12**, 67-83.
- Pestova, T.V., Shatsky, I.N. and Hellen, C.U.T. (1996b) Functional dissection of eukaryotic initiation factor 4F: the 4A subunit and the central domain of the 4G subunit are sufficient to mediate internal entry of 43S preinitiation complexes. *Mol. Cell. Biol.*, **16**, 6870-6878.
- Pignatelli, M., Cortes-Canteli, M., Santos, A. and Perez-Castillo, A. (1999) Involvement of the NGFI-A gene in the differentiation of neuroblastoma cells. *FEBS Lett.*, **461**, 37-42.
- Pilipenko, E.V., Pestova, T.V., Kolupaeva, V.G., Khitrina, E.V., Poperechnaya, A.N., Agol, V.I. and Hellen, C.U.T. (2000) A cell cycle-dependent protein serves as a template-specific translation initiation factor. *Genes Dev.*, **14**, 2028-2045.
- Poulin, F., Gingras, A.-C., Olsen, H., Chevalier, S. and Sonenberg, N. (1998) 4E-BP3, a new member of the eukaryotic initiation factor 4E-binding protein family. *J. Biol. Chem.*, **273**, 14002-14007.
- Pozner, A., Goldenberg, D., Negreanu, V., Le, S.-Y., Elroy-Stein, O., Levanon, D. and Groner, Y. (2000) Transcription-coupled translation control of AML1/RUNX1 is mediated by cap- and internal ribosome entry site-dependent mechanisms. *Mol. Cell. Biol.*, **20**, 2297-2307.
- Prendergast, G.C. (1999) Mechanisms of apoptosis by c-Myc. *Oncogene*, **18**, 2967-2987.
- Prendergast, G.C. and Ziff, E.B. (1991) Methylation-sensitive sequence-specific DNA binding by the c-Myc basic region. *Science*, **251**, 186-189.
- Prochownik, E.V. and Van Antwerp, M.E. (1993) Differential patterns of DNA binding by myc and max proteins. *Proc. Natl. Acad. Sci. USA*, **90**, 960-964.
- Pyronnet, S., Dostie, J. and Sonenberg, N. (2001) Suppression of cap-dependent translation in mitosis. *Genes Dev.*, **15**, 2083-2093.

- Pyronnet, S., Imataka, H., Gingras, A.-C., Fukunaga, R., Hunter, T. and Sonenberg, N. (1999) Human eukaryotic translation initiation factor 4G (eIF4G) recruits Mnk1 to phosphorylate eIF4E. *EMBO J.*, **18**, 270-279.
- Pyronnet, S., Pradayrol, L. and Sonenberg, N. (2000) A cell cycle-dependent internal ribosome entry site. *Mol. Cell*, **5**, 607-616.
- Rabbitts, P.H., Watson, J.V., Lamond, A., Forster, A., Stinson, M.A., Evan, G., Fischer, W., Atherton, E., Sheppard, R. and Rabbitts, T.H. (1985) Metabolism of *c-myc* gene products: *c-myc* mRNA and protein expression in the cell cycle. *EMBO J.*, **4**, 2009-2015.
- Rau, M., Ohlmann, T., Morley, S.J. and Pain, V.M. (1996) A reevaluation of the cap-binding protein, eIF4E, as a rate-limiting factor for initiation of translation in reticulocyte lysate. *J. Biol. Chem.*, **271**, 8983-8990.
- Reitsma, P.H., Rothberg, P.G., Astrin, S.M., Trial, J., Bar-Shavit, Z., Hall, A., Teitelbaum, S.L. and Kahn, A.J. (1983) Regulation of *myc* gene expression in HL-60 leukaemia cells by a vitamin D metabolite. *Nature*, **306**, 492-494.
- Reynolds, J.E., Kaminski, A., Kettinen, H.J., Grace, K., Clarke, B.E., Carroll, A.R., Rowlands, D.J. and Jackson, R.J. (1995) Unique features of internal initiation of hepatitis C virus RNA translation. *EMBO J.*, **14**, 6010-6020.
- Rijnbrand, R., Bredenbeek, P.J., Haasnoot, P.C., Kieft, J.S., Spaan, W.J.M. and Lemon, S.M. (2001) The influence of downstream protein-coding sequence on internal ribosome entry on hepatitis C virus and other flavivirus RNAs. *RNA*, **7**, 585-597.
- Rijnbrand, R., van der Straaten, T., van Rijin, P.A., Spaan, W.J.M. and Bredenbeek, P.J. (1997) Internal ribosome entry of ribosomes is directed by the 5' non-coding region of classical swine fever virus and is dependent on the presence of an RNA pseudoknot upstream of the initiation codon. *J. Virol.*, **71**, 451-457.
- Robertson, M.E.M., Seamons, R.A. and Belsham, G.J. (1999) A selection system for functional internal ribosome entry site (IRES) elements: Analysis of the requirement for a conserved GNRA tetraloop in the encephalomyocarditis virus IRES. *RNA*, **5**, 1167-1179.
- Rogers Jr., G.W., Richter, N.J. and Merrick, W.C. (1999) Biochemical and kinetic characterization of the RNA helicase activity of eukaryotic initiation factor 4A. *J. Biol. Chem.*, **274**, 12236-12244.

- Ron, D. and Harding, H.P. (2000) PERK and translational control by stress in the endoplasmic reticulum. In Sonenberg, N., Hershey, J.W.B. and Mathews, M.B. (eds.), *In: Translational Control of Gene Expression*. Cold Spring Harbor Laboratory Press, pp. 547-560.
- Rosenwald, I.B., Rhoads, D.B., Callanan, L.D., Isselbacher, K.J. and Schmidt, E.V. (1993) Increased expression of eukaryotic translation initiation factors eIF-4E and eIF-2 $\alpha$  in response to growth induction by *c-myc*. *Proc. Natl. Acad. Sci. USA*, **90**, 6175-6178.
- Sachs, A.B., Sarnow, P. and Hentze, M.W. (1997) Starting at the beginning, middle, and end: Translation initiation in eukaryotes. *Cell*, **89**, 831-838.
- Sadee, W., Yu, V.C., Richard, M.L., Preis, P.N., Schwab, M.R., Brodsky, F.M. and Biedler, J.L. (1987) Expression of neurotransmitter receptors and *myc* proto-oncogenes in subclones of a human neuroblastoma cell-line. *Cancer Res.*, **47**, 5207-5212.
- Saito, H., Hayday, A.C., Wiman, K., Hayward, W.S. and Tonegawa, S. (1983) Activation of the *c-myc* gene by translocation: A model for translational control. *Proc. Natl. Acad. Sci. USA*, **80**, 7476-7480.
- Sasaki, J. and Nakashima, N. (1999) Translation initiation at the CUU codon is mediated by the internal ribosome entry site of an insect picorna-like virus in vitro. *J. Virol.*, **73**, 1219-1226.
- Sasaki, J. and Nakashima, N. (2000) Methionine-independent initiation of translation in the capsid protein of an insect RNA virus. *Proc. Natl. Acad. Sci. USA*, **97**, 1512-1515.
- Scheper, G.C., Morrice, N.A., Kleijn, M. and Proud, C.G. (2001) The mitogen-activated protein kinase signal-integrating kinase Mnk2 is a eukaryotic initiation factor 4E kinase with high levels of basal activity in mammalian cells. *Mol. Cell. Biol.*, **21**, 743-754.
- Schneider, R.J. (2000) Translational control during heat shock. In Sonenberg, N., Hershey, J.W.B. and Mathews, M.B. (eds.), *Translational Control of Gene Expression*. Cold Spring Harbor Laboratory Press, pp. 581-593.
- Schwab, M., Alitalo, K., Klempnauer, K.-H., Varmus, H.E., Bishop, J.M., Gilbert, F., Brodeur, G., Goldstein, M. and Trent, J. (1983) Amplified DNA with limited

- homology to *myc* cellular oncogene is shared by human neuroblastoma cell lines and a neuroblastoma tumour. *Nature*, **305**, 245-248.
- Schwab, M., Varmus, H.E. and Bishop, J.M. (1985) Human N-*myc* gene contributes to neoplastic transformation of mammalian cells in culture. *Nature*, **316**, 160-162.
- Sella, O., Gerlitz, G., S.-Y., L. and Elroy-Stein, O. (1999) Differentiation-induced internal translation of c-*sis* mRNA: Analysis of the *cis* elements and their differentiation-linked binding to the hnRNP C protein. *Mol. Cell. Biol.*, **19**, 5429-5440.
- Shatkin, A.J. (1976) Capping of eucaryotic mRNAs. *Cell*, **9**, 645-653.
- Shea, T.B., Beermann, M.L. and Nixon, R.A. (1991) Multiple proteases regulate neurite outgrowth in NB2a/DL neuroblastoma cells. *J. Neurochem.*, **56**, 842-851.
- Sheikh, M.S. and Fornace, A.J. (1999) Regulation of translation initiation following stress. *Oncogene*, **18**, 6121-6128.
- Shen-Li, H., O'Hagan, R.C., Hou Jr., H., Horner II, J.W., Lee, H.-W. and DePinho, R.A. (2000) Essential role for Max in early embryonic growth and development. *Genes Dev.*, **14**, 17-22.
- Sivak, L.E., Pont-Kingdon, G., Le, K., Mayr, G., Tai, K.-F., Stevens, B.T. and Carroll, W.L. (1999) A novel intron element operates posttranscriptionally to regulate human N-*myc* expression. *Mol. Cell. Biol.*, **19**, 155-163.
- Sood, R., Porter, A.C., Olsen, D., Cavener, D.R. and Wek, R.C. (2000) A mammalian homologue of GCN2 protein kinase important for translational control by phosphorylation of eukaryotic initiation factor-2 $\alpha$ . *Genetics*, **154**, 787-801.
- Soucie, E.L., Annis, M.G., Sedivy, J., Filmus, J., Leber, B., Andrews, D.W. and Penn, L.Z. (2001) Myc potentiates apoptosis by stimulating Bax activity at the mitochondria. *Mol. Cell. Biol.*, **21**, 4725-4736.
- Spahn, C.M.T., Kieft, J.S., Grassucci, R.A., Penczek, P.A., Zhou, K., Doudna, J.A. and Frank, J. (2001) Hepatitis C virus IRES RNA-induced changes in the conformation of the 40S ribosomal subunit. *Science*, **291**, 1959-1962.
- Spotts, G.D., Patel, S.V., Xiao, Q. and Hann, S.R. (1997) Identification of downstream-initiated c-Myc proteins which are dominant-negative inhibitors of transactivation by full-length c-Myc proteins. *Mol. Cell. Biol.*, **17**, 1459-1468.

- Stanton, B.R., Perkins, A.S., Tessarollo, L., Sassoon, D. and Parada, L.F. (1992) Loss of N-*myc* function results in embryonic lethality and failure of the epithelial component of the embryo to develop. *Genes Dev.*, **6**, 2235-2257.
- Stanton, L.W., Schwab, M. and Bishop, J.M. (1986) Nucleotide sequence of the human N-*myc* gene. *Proc. Natl. Acad. Sci. USA*, **83**, 1772-1776.
- Stein, I., Itin, A., Einat, P., Skaliter, R., Grossman, Z. and Keshet, E. (1998) Translation of vascular endothelial growth factor mRNA by internal ribosome entry: Implications for translation under hypoxia. *Mol. Cell. Biol.*, **18**, 3112-3119.
- Stoneley, M. (1998) Functional Analysis of the 5' untranslated region of the *c-myc* proto-oncogene. *PhD Thesis*. University of Leicester.
- Stoneley, M., Chappell, S.A., Jopling, C.L., Dickens, M., MacFarlane, M. and Willis, A.E. (2000a) c-Myc protein synthesis is initiated from the internal ribosome entry segment during apoptosis. *Mol. Cell. Biol.*, **20**, 1162-1169.
- Stoneley, M., Paulin, F.E.M., Le Quesne, J.P.C., Chappell, S.A. and Willis, A.E. (1998) C-Myc 5' untranslated region contains an internal ribosome entry segment. *Oncogene*, **16**, 423-428.
- Stoneley, M., Spencer, J.P. and Wright, S.C. (2001) An internal ribosome entry segment in the 5' untranslated region of the *mnt* gene. *Oncogene*, **20**, 893-897.
- Stoneley, M., Subkhankulova, T., Le Quesne, J.P.C., Coldwell, M.J., Jopling, C.L., Belsham, G.J. and Willis, A.E. (2000b) Analysis of the *c-myc* IRES; a potential role for cell-type specific trans-acting factors and the nuclear compartment. *Nucleic Acids Res.*, **28**, 687-694.
- Subkhankulova, T., Mitchell, S.A. and Willis, A.E. (2001) Internal ribosome entry segment-mediated initiation of c-Myc protein synthesis following genotoxic stress. *Biochem. J.*, **359**, 183-192.
- Sugiyama, A., Kume, A., Nemoto, K., Lee, S.Y., Asami, Y., Nemoto, F., Nishimura, S. and Kuchino, Y. (1989) Isolation and characterization of s-*myc*, a member of the rat *myc* gene family. *Proc. Natl. Acad. Sci. USA*, **86**, 9144-9148.
- Sugiyama, A., Miyagi, Y., Shirasawa, Y. and Kuchino, Y. (1991) Different usage of two polyadenylation signals in transcription of the N-*myc* gene in rat tumor cells. *Oncogene*, **6**, 2027-2032.

- Svitkin, Y.V., Pause, A., Haghghat, A., Pyronnet, S., Witherell, G., Belsham, G.J. and Sonenberg, N. (2001) The requirement for eukaryotic initiation factor 4A (eIF4A) in translation is in direct proportion to the degree of mRNA 5' secondary structure. *RNA*, **7**, 382-394.
- Thiele, C.J., Reynolds, C.P. and Israel, M.A. (1985) Decreased expression of N-Myc precedes retinoic acid-induced morphological -differentiation of human neuroblastoma. *Nature*, **313**, 404-406.
- Thornberry, N.A. and Lazebnik, Y. (1998) Caspases: Enemies within. *Science*, **281**, 1312-1316.
- Timme, T.L., Goltsov, A., Tahir, S., Li, L., Wang, J., Ren, C., Johnston, R.N. and Thompson, T.C. (2000) Caveolin-1 is regulated by *c-myc* and suppresses *c-myc*-induced apoptosis. *Oncogene*, **19**, 3256-3265.
- Tsukiyama-Kohara, K., Iizuka, N., Kohara, M. and Nomoto, A. (1992) Internal ribosome entry site within hepatitis C virus RNA. *J. Virol.*, **66**, 1476-1483.
- Vagner, S., Gensac, M.-C., Maret, A., Bayard, F., Amalric, F., Prats, H. and Prats, A.-C. (1995) Alternative translation of human fibroblast growth factor 2 mRNA occurs by internal entry of ribosomes. *Mol. Cell. Biol.*, **15**, 35-44.
- Vennstrom, B., Sheiness, D., Zabielski, J. and Bishop, J.M. (1982) Isolation and characterization of *c-myc*, a cellular homolog of the oncogene (*v-myc*) of avian myelocytomatosis virus strain 29. *J. Virol.*, **42**, 773-779.
- Wagner, A.J., Small, M.B. and Hay, N. (1993) Myc-mediated apoptosis is blocked by ectopic expression of Bcl-2. *Mol. Cell. Biol.*, **13**, 2432-2440.
- Walter, B.L., Nguyen, J.H.C., Ehrenfeld, E. and Semler, B.L. (1999) Differential utilization of poly(rC) binding protein 2 in translation directed by picornavirus IRES elements. *RNA*, **5**, 1570-1585.
- Wang, C.Y., Le, S.Y., Ali, N. and Siddiqui, A. (1995) An RNA pseudoknot is an essential structural element of the internal ribosome entry site located within the hepatitis C virus 5' noncoding region. *RNA*, **1**, 526-537.
- Waskiewicz, A.J., Johnson, J.C., Penn, B., Mahalingam, M., Kimball, S.R. and Cooper, J.A. (1999) Phosphorylation of the cap-binding protein eukaryotic translation initiation factor 4E by protein kinase Mnk1 in vivo. *Mol. Cell. Biol.*, **19**, 1871-1880.

- Wei, C.-C., Balasta, M.L., Ren, J. and Goss, D.J. (1998) Wheat germ poly(A) binding protein enhances the binding affinity of eukaryotic initiation factor 4F and (iso)4F for cap analogues. *Biochemistry*, **37**, 1910-1916.
- Weighardt, F., Biamanti, G. and Riva, S. (1996) The role of heterogeneous nuclear ribonucleoproteins (hnRNP) in RNA metabolism. *Bioessays*, **18**, 747-756.
- Wells, S.E., Hillner, P.E., Vale, R.D. and Sachs, A.B. (1998) Circularisation of mRNA by eukaryotic translation initiation factors. *Mol. Cell*, **2**, 135-140.
- West, M.J., Stoneley, M. and Willis, A.E. (1998) Translational induction of the *c-myc* oncogene via activation of the FRAP/TOR signalling pathway. *Oncogene*, **17**, 769-780.
- Willis, A.E. (1999) Translational control of growth factor and proto-oncogene expression. *Int. J. Biochem. Cell Biol.*, **31**, 73-86.
- Wilson, J.E., Pestova, T.V., Hellen, C.U.T. and Sarnow, P. (2000a) Initiation of protein synthesis from the A site of the ribosome. *Cell*, **102**, 511-520.
- Wilson, J.E., Powell, M.J., Hoover, S.E. and Sarnow, P. (2000b) Naturally occurring dicistronic cricket paralysis virus RNA is regulated by two internal ribosome entry sites. *Mol. Cell. Biol.*, **20**, 4990-4999.
- Xia, Z., Dickens, M., Raingeaud, J., Davis, R.J. and Greenberg, M.E. (1995) Opposing effects of ERK and JNK-p38 MAP kinases on apoptosis. *Science*, **270**, 1326-1331.
- Yang, G. and Sarnow, P. (1997) Location of the internal ribosome entry site in the 5' non-coding region of the immunoglobulin heavy-chain binding protein (BiP) mRNA: Evidence for specific RNA-protein interactions. *Nucleic Acids Res.*, **25**, 2800-2807.
- Yanisch-Perron, L., Vieira, J. and Messing, J. (1985) Improved M13 phage cloning vectors and host strains: Nucleotide sequences of the M13mp18 and pUC19 vectors. *Gene*, **33**, 103.
- Yueh, A. and Schneider, R.J. (1996) Selective translation initiation by ribosome jumping in adenovirus-infected and heat-shocked cells. *Genes Dev.*, **10**, 1557-1567.
- Yueh, A. and Schneider, R.J. (2000) Translation by ribosome shunting on adenovirus and *hsp70* mRNAs facilitated by complementarity to 18S rRNA. *Genes Dev.*, **14**, 414-421.
- Ziegler, E., Borman, A.M., Kirchweger, R., Skern, T. and Kean, K.M. (1995) Foot-and-mouth disease virus Lb proteinase can stimulate rhinovirus and enterovirus IRES-

driven translation and cleave several proteins of cellular and viral origin. *J. Virol.*, **69**, 3465-3474.

Zimmerman, K.A., Yancopoulos, G.D., Collum, R.G., Smith, R.K., Kohl, N.E., Denis, K.A., Nau, M.M., Witte, O.N., Toran-Allerand, D., Gee, C.E., Minna, J.D. and Alt, F.W. (1986) Differential expression of *myc* family genes during murine development. *Nature*, **319**, 780-783.

## Publications

Jopling, C.L. and Willis, A.E. (2001) N-myc translation is initiated via an internal ribosome entry segment that displays enhanced activity in neuronal cells. *Oncogene*, **20**, 2664-2670

Stoneley, M., Chappell, S.A., Jopling, C.L., Dickens, M., MacFarlane, M. and Willis, A.E. (2000) c-Myc protein synthesis is initiated from the internal ribosome entry segment during apoptosis. *Mol. Cell. Biol.*, **20**, 1162-1169.

Stoneley, M., Subkhankulova, T., Le Quesne, J.P.C., Coldwell, M.J., Jopling, C.L., Belsham, G.J. and Willis, A.E. (2000) Analysis of the c-myc IRES; a potential role for cell-type specific trans-acting factors and the nuclear compartment. *Nucleic Acids Res.*, **28**, 687-694.

## N-myc translation is initiated via an internal ribosome entry segment that displays enhanced activity in neuronal cells

Catherine L Jopling<sup>1</sup> and Anne E Willis<sup>\*1</sup>

<sup>1</sup>Department of Biochemistry, University of Leicester, University Road, Leicester LE1 7RH, UK

Eukaryotic translation can be initiated either by a cap-dependent mechanism or by internal ribosome entry, a process by which ribosomes are directly recruited to structured regions of mRNA upstream of the initiation codon. We analysed the 5' untranslated region (UTR) of the proto-oncogene *N-myc*, and demonstrated by transfections in a dicistronic vector system that it contains a potent internal ribosome entry segment (IRES). The IRES is similar in length to the *c-myc* IRES and the activities of these IRESs are comparable in non-neuronal cells. Transfections were also carried out in cell lines derived from neuroblastomas, in which *N-myc* is expressed, and in a neuronal precursor cell line. In these cells the *N-myc* IRES is up to seven times more active than that of *c-myc*, suggesting that neuronal-specific non-canonical *trans*-acting factors are used by the *N-myc* but not the *c-myc* IRES. *N-myc* expression is increased by gene amplification in many neuroblastomas, but this is the first example of a translational mechanism by which *N-myc* expression could be further increased. The discovery of an IRES that displays enhanced activity in neuronal cell lines has important potential as a tool for protein expression in neural tissue. *Oncogene* (2001) 20, 2664–2670.

**Keywords:** *N-myc*; translation initiation; IRES; neuronal

### Introduction

The *myc* family of genes comprises *c-*, *N-*, and *L-myc*. All three genes give rise to nuclear phosphoproteins that function as transcription factors. The Myc proteins are known to perform this role by binding to target E-box DNA sequences as heterodimers with the protein Max (Blackwood and Eisenman, 1991; Dang, 1999). Myc proteins are important in the control of cell growth, differentiation, and apoptosis (Lutz *et al.*, 1996, 1998; Dang, 1999), although the identity of Myc target genes has proved to be elusive. In accordance with the stimulatory effect of the Myc proteins on cell growth, their overexpression is

associated with a number of different cancers. *N-myc* was originally identified as a gene amplified in neuroblastoma (Schwab *et al.*, 1983) and further work has shown that overexpression of *N-myc* occurs in almost all neuroblastomas; high levels of N-Myc correlate with a poor prognosis (Brodeur *et al.*, 1984). *N-myc* overexpression has also been documented in some small cell lung carcinomas and occasionally in other tumours (Nesbit *et al.*, 1999).

The physiological expression of *N-myc* is restricted to early stages of development. For example, during embryogenesis *N-myc* is expressed in the gut, kidney and lung, and at highest levels in the central nervous system (Zimmerman *et al.*, 1986). Knockout studies show that N-Myc is essential for embryonic survival (Stanton *et al.*, 1992) and a recent study has shown that the *N-myc* gene can functionally replace *c-myc* in transgenic mice (Malynn *et al.*, 2000). *C-myc* has a different expression pattern to that of *N-myc* and is almost ubiquitous. However, the organization of the *N-myc* gene is very similar to that of *c-myc*, comprising three exons, exon 1 of which is entirely non-coding (Kohl *et al.*, 1986). Hence, both genes give rise to mRNAs that have long 5' untranslated regions (UTR) with a high degree of predicted secondary structure. The *c-myc* 5' UTR is involved in translational regulation (Saito *et al.*, 1983) and recently we and others have shown that the 5' UTR of the *c-myc* mRNA contains an internal ribosome entry segment (IRES) (Stoneley *et al.*, 1998; Nanbru *et al.*, 1997).

IRESs are highly structured regions of RNA that are able to recruit the 40S subunit independently of a cap structure and, in most cases, in the absence of intact eukaryotic initiation factor 4G (eIF4G) (Jackson *et al.*, 1995; Stoneley *et al.*, 2000a). IRESs were first identified in the picornaviral family but a number of cellular IRESs have been identified. A high proportion of cellular IRESs have been located in genes involved in cell growth or death, for example fibroblast growth factor-2 (FGF-2) (Vagner *et al.*, 1995), vascular endothelial growth factor (Akiri *et al.*, 1998; Huez *et al.*, 1998; Miller *et al.*, 1998; Stein *et al.*, 1998), platelet derived growth factor (PDGF) (Bernstein *et al.*, 1997), the apoptotic protease activating factor-1 (Coldwell *et al.*, 2000), the X-linked inhibitor of apoptosis (Holcik *et al.*, 1999), and death-associated protein 5 (Henis-Korenblit *et al.*, 2000). It is becoming apparent that

\*Correspondence: AE Willis  
Received 21 November 2000; revised 15 February 2001; accepted 19 February 2001

# **BEST COPY NOTE**

**THE FOLLOWING PAGES  
ARE STUCK IN SUCH A  
MANNER THAT  
FILMING IS IMPEDED**

## N-*myc* translation is initiated via an internal ribosome entry segment that displays enhanced activity in neuronal cells

Catherine L Jopling<sup>1</sup> and Anne E Willis<sup>\*,1</sup>

<sup>1</sup>Department of Biochemistry, University of Leicester, University Road, Leicester LE1 7RH, UK

Eukaryotic translation can be initiated either by a cap-dependent mechanism or by internal ribosome entry, a process by which ribosomes are directly recruited to structured regions of mRNA upstream of the initiation codon. We analysed the 5' untranslated region (UTR) of the proto-oncogene N-*myc*, and demonstrated by transfections in a dicistronic vector system that it contains a potent internal ribosome entry segment (IRES). The IRES is similar in length to the c-*myc* IRES and the activities of these IRESs are comparable in non-neuronal cells. Transfections were also carried out in cell lines derived from neuroblastomas, in which N-*myc* is expressed, and in a neuronal precursor cell line. In these cells the N-*myc* IRES is up to seven times more active than that of c-*myc*, suggesting that neuronal-specific non-canonical *trans*-acting factors are used by the N-*myc* but not the c-*myc* IRES. N-*myc* expression is increased by gene amplification in many neuroblastomas, but this is the first example of a translational mechanism by which N-*myc* expression could be further increased. The discovery of an IRES that displays enhanced activity in neuronal cell lines has important potential as a tool for protein expression in neural tissue. *Oncogene* (2001) 20, 2664–2670.

**Keywords:** N-*myc*; translation initiation; IRES; neuronal

### Introduction

The *myc* family of genes comprises c-, N-, and L-*myc*. All three genes give rise to nuclear phosphoproteins that function as transcription factors. The Myc proteins are known to perform this role by binding to target E-box DNA sequences as heterodimers with the protein Max (Blackwood and Eisenman, 1991; Dang, 1999). Myc proteins are important in the control of cell growth, differentiation, and apoptosis (Lutz *et al.*, 1996, 1998; Dang, 1999), although the identity of Myc target genes has proved to be elusive. In accordance with the stimulatory effect of the Myc proteins on cell growth, their overexpression is

associated with a number of different cancers. N-*myc* was originally identified as a gene amplified in neuroblastoma (Schwab *et al.*, 1983) and further work has shown that overexpression of N-*myc* occurs in almost all neuroblastomas; high levels of N-Myc correlate with a poor prognosis (Brodeur *et al.*, 1984). N-*myc* overexpression has also been documented in some small cell lung carcinomas and occasionally in other tumours (Nesbit *et al.*, 1999).

The physiological expression of N-*myc* is restricted to early stages of development. For example, during embryogenesis N-*myc* is expressed in the gut, kidney and lung, and at highest levels in the central nervous system (Zimmerman *et al.*, 1986). Knockout studies show that N-Myc is essential for embryonic survival (Stanton *et al.*, 1992) and a recent study has shown that the N-*myc* gene can functionally replace c-*myc* in transgenic mice (Malynn *et al.*, 2000). C-*myc* has a different expression pattern to that of N-*myc* and is almost ubiquitous. However, the organization of the N-*myc* gene is very similar to that of c-*myc*, comprising three exons, exon 1 of which is entirely non-coding (Kohl *et al.*, 1986). Hence, both genes give rise to mRNAs that have long 5' untranslated regions (UTR) with a high degree of predicted secondary structure. The c-*myc* 5' UTR is involved in translational regulation (Saito *et al.*, 1983) and recently we and others have shown that the 5' UTR of the c-*myc* mRNA contains an internal ribosome entry segment (IRES) (Stoneley *et al.*, 1998; Nanbru *et al.*, 1997).

IRESs are highly structured regions of RNA that are able to recruit the 40S subunit independently of a cap structure and, in most cases, in the absence of intact eukaryotic initiation factor 4G (eIF4G) (Jackson *et al.*, 1995; Stoneley *et al.*, 2000a). IRESs were first identified in the picornaviral family but a number of cellular IRESs have been identified. A high proportion of cellular IRESs have been located in genes involved in cell growth or death, for example fibroblast growth factor-2 (FGF-2) (Vagner *et al.*, 1995), vascular endothelial growth factor (Akiri *et al.*, 1998; Huez *et al.*, 1998; Miller *et al.*, 1998; Stein *et al.*, 1998), platelet derived growth factor (PDGF) (Bernstein *et al.*, 1997), the apoptotic protease activating factor-1 (Coldwell *et al.*, 2000), the X-linked inhibitor of apoptosis (Holcik *et al.*, 1999), and death-associated protein 5 (Henis-Korenblit *et al.*, 2000). It is becoming apparent that

\*Correspondence: AE Willis

Received 21 November 2000; revised 15 February 2001; accepted 19 February 2001

certain cellular IRESs are utilised during physiological situations in which cap-dependent translation is reduced. For example, *c-myc* IRES-dependent translation is maintained during apoptosis when eIF4G is cleaved by caspases (Stoneley *et al.*, 2000a), while the PDGF and AML1 IRESs are induced during cellular differentiation (Bernstein *et al.*, 1997; Pozner *et al.*, 2000) and ornithine decarboxylase and the p58<sup>PITSLRE</sup> protein kinase possess IRESs that function during mitosis (Pyronnet *et al.*, 2000; Cornelis *et al.*, 2000). There is very little sequence similarity between the *c-myc* and *N-myc* 5' UTRs, but as the *N-myc* 5' UTR is long and GC-rich, with a high degree of predicted secondary structure, we decided to investigate the possibility that *N-myc* could contain an IRES.

## Results

*The published N-myc 5' UTR sequence contains an incorrectly assigned splice site*

To investigate whether the *N-myc* 5' UTR is translationally regulated, we obtained the DNA corresponding to this region by RT-PCR of RNA from five human neuroblastoma-derived cell lines. The PCR products were all 327 bp in size, whereas the predicted size was 637 bp (Ibson and Rabbitts, 1988). Sequencing indicated that the size disparity was due to the incorrect prediction of the position of the donor splice site of intron 1. No larger PCR product compatible with the published splice site was detected, confirming that the exon1/intron 1 boundary is upstream of the published position, and the donor splice site we obtained is in good context. Furthermore, the murine (Kato *et al.*, 1988) and rat (Sugiyama *et al.*, 1991) *N-myc* 5' UTRs are similar in length to that obtained from human cells and show high levels of homology (74.2 and 77.7% identical, respectively) with exon 1/intron 1 boundaries in a similar position.

*The N-myc 5' UTR contains an internal ribosome entry segment*

The cDNA encoding the human *N-myc* 5' UTR was inserted into the dicistronic vector pRF (Figure 1a; previously known as pGL3R2, Stoneley *et al.*, 1998) to create the construct pRNF. This was transfected into HeLa cells in parallel with pRF, pRMF and pRemcvF (in which the *c-myc* and EMCV IRESs have been inserted between the two cistrons of pRF). The activities of *Renilla* and firefly luciferases were determined and normalized to a transfection control of  $\beta$ -galactosidase. Translation of the upstream *Renilla* luciferase cistron is cap-dependent, whereas the downstream firefly luciferase cistron is translated at a very low rate unless internal ribosome entry can occur between the two cistrons. In HeLa cells the *N-myc* 5' UTR was seen to stimulate downstream cistron expression to a considerable extent (87-fold) relative to that seen in the control vector (Figure 1b). This

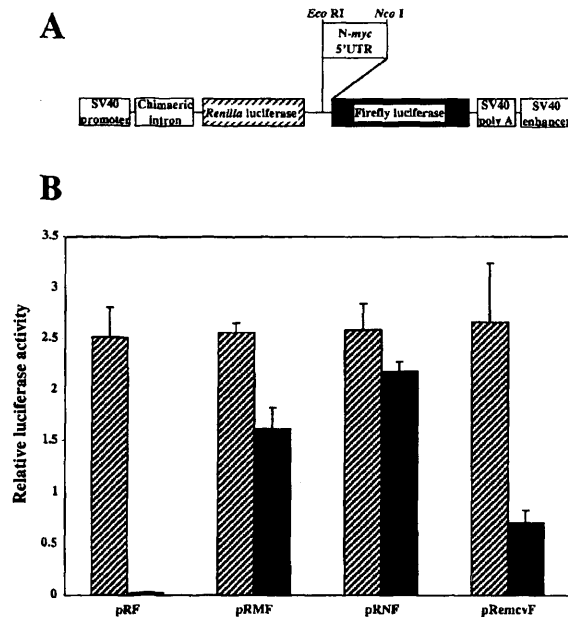


**Figure 1** The *N-myc* 5' UTR stimulates downstream cistron expression in a dicistronic system. (a) The dicistronic vector pRF. The cDNA encoding the *N-myc* 5' UTR was inserted between the *Renilla* and firefly luciferase cistrons to create pRNF. (b) HeLa cells were transfected with pRF, pRMF (containing the *c-myc* IRES), pRNF and pRemcvF. *Renilla* (shaded) and firefly (black) luciferase activities were determined and are expressed relative to the transfection control of  $\beta$ -galactosidase. The results represent an average of three independent experiments

suggests that the *N-myc* 5' UTR contains an element capable of stimulating internal ribosome entry. The stimulation of downstream cistron expression observed is approximately threefold greater than that seen with the highly active EMCV IRES, and marginally higher than that seen with the *c-myc* IRES (Figure 1b).

To ensure that internal ribosome entry rather than enhanced ribosomal readthrough or reinitiation was responsible for the stimulation observed, the DNA encoding the *N-myc* 5' UTR was inserted into the vector pRF to create the construct pRNF (Figure 2a). This harbours a palindromic sequence upstream of the *Renilla* luciferase coding region that, when transcribed, forms a stable RNA hairpin ( $-55$  kcal/mol). This is sufficient to impede scanning ribosomes, leading to an 80% reduction in expression of the cap-dependent *Renilla* luciferase cistron on transfection into NB2a cells. Expression of firefly luciferase induced by the *N-myc* 5' UTR did not show a concomitant decrease in the presence of the hairpin (Figure 2b). The small induction seen is likely to be due to the increased availability of limiting initiation factors when translation of *Renilla* luciferase is reduced. This demonstrates that the *N-myc* 5' UTR does not induce downstream cistron activity by a stimulation of ribosomal readthrough or reinitiation.

It is possible that a cryptic promoter or splice site or an RNA cleavage site is present in the *N-myc* 5' UTR,

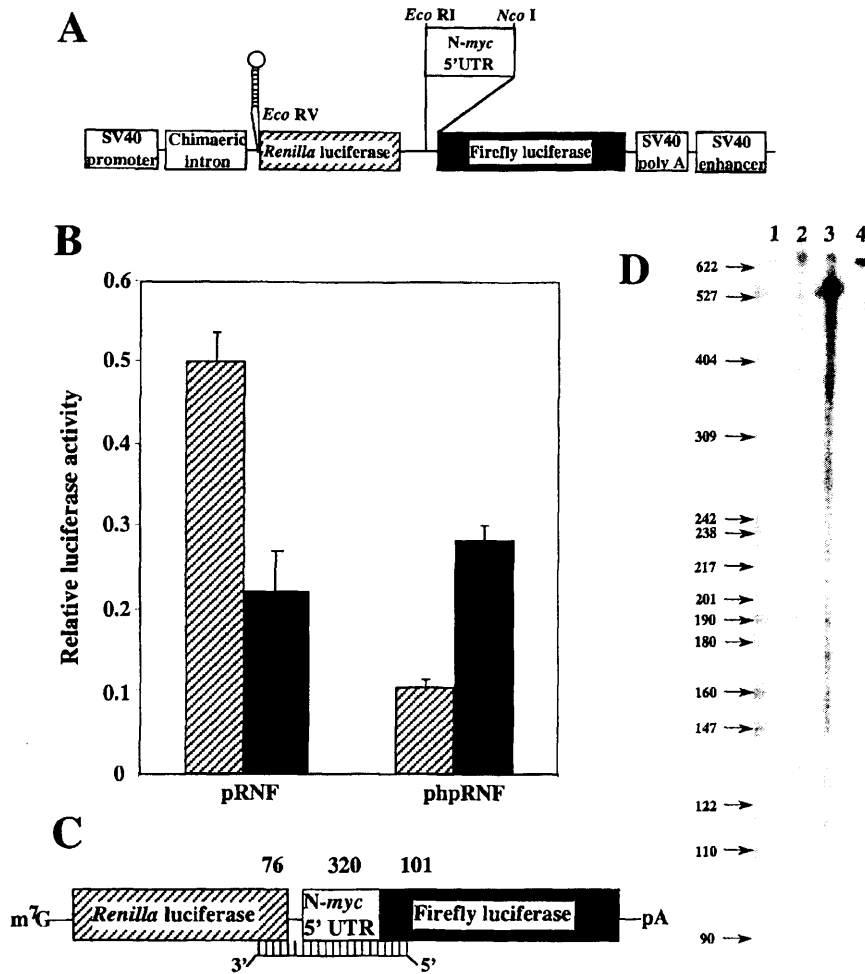


**Figure 2** Downstream cistron expression is not due to enhanced ribosomal readthrough or the production of truncated RNAs. (a) A palindromic sequence was inserted upstream of the *Renilla* luciferase cistron in pRNF to create the vector phpRNF. (b) NB2a cells were transfected with pRNF and phpRNF. *Renilla* (shaded) and firefly (black) luciferase activities were determined and are expressed relative to the transfection control of  $\beta$ -galactosidase. (c) The 647 nucleotide probe used for RNase protection hybridized to a dicistronic RNA molecule containing the N-myc 5' UTR. (d) RNase protection. The radiolabelled probe indicated in (c) was hybridized to (1) yeast tRNA (2) RNA extracted from mock-transfected HeLa cells and (3) RNA extracted from pRNF-transfected HeLa cells. Lane 4, undigested probe. Corresponding RNA sizes are indicated to the left of the gel

leading to the production of monocistronic mRNAs from which firefly luciferase can be expressed on transfection of pRNF. RNase protection assays were carried out using RNA extracted from HeLa cells 48 h after transient transfection with pRNF. This RNA was hybridized to a radiolabelled probe complementary to a region of pRNF encompassing the 3' end of the *Renilla* luciferase cistron, the N-myc 5' UTR, and the 5' end of the firefly luciferase cistron (Figure 2c). A band of the expected size for a full length dicistronic RNA was protected from RNase one digestion (Figure 2d, lane 3). If a monocistronic firefly luciferase RNA were present, to be functional it would have to be at least 101 nucleotides in length. No bands of this size were detected. No protected products were detected when RNA was extracted from mock-transfected HeLa cells (Figure 2d, lane 2). The N-myc 5' UTR is therefore

able to stimulate expression of the downstream cistron in the context of a dicistronic RNA, and we conclude that it contains an IRES.

#### *The N-myc IRES has enhanced activity in neuronal cell types*

The N-myc IRES was compared to the c-myc IRES by transfection of pRNF into various cell lines in parallel with the vector pRNF (previously known as pGL3R2utr, Stoneley *et al.*, 1998), which harbours the c-myc 5' UTR. The activities of *Renilla* and firefly luciferases were calculated and IRES activity in each cell line was determined by the ratio of firefly:*Renilla* (Figure 3). The ratio of N-myc:c-myc IRES activity for each cell line is indicated in a table (Figure 3). We observed that in the cell lines HeLa and MCF7, which

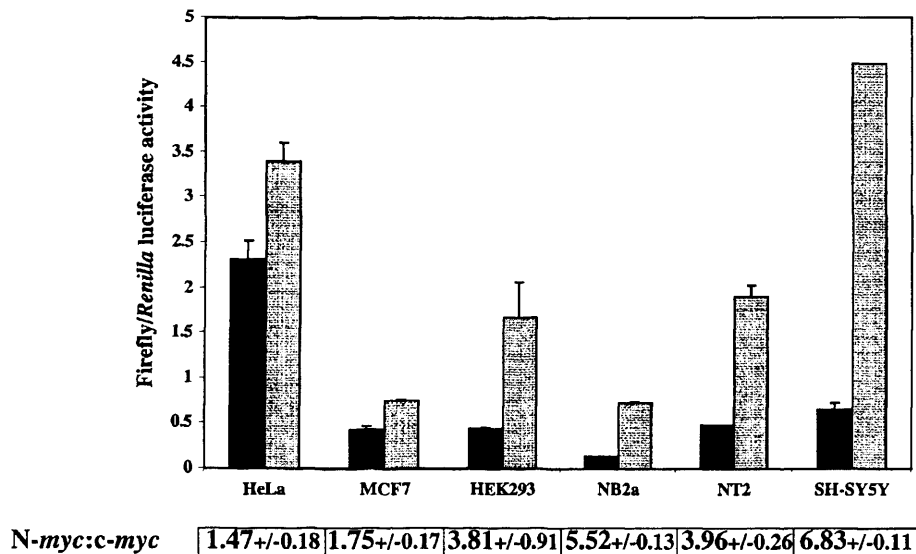


**Figure 3** The N-myc IRES is enhanced relative to c-myc in neuronal cell lines. The cell lines indicated were transfected with the vectors pRMF (black) and pRNF (grey). *Renilla* and firefly luciferase activities were determined and IRES activity shown by firefly luciferase expressed relative to *Renilla* luciferase. The ratio of N-myc:c-myc IRES activity for each cell line is indicated in the table. The results represent an average of three independent experiments

do not express N-myc mRNA, the N-myc IRES induced downstream cistron expression at a level only slightly greater than that induced by the c-myc IRES. The neuronal precursor cell line NT2, the neuroblastoma cell lines NB2a and SH-SY5Y, and the embryonic kidney cell line HEK293 were also transfected. In all these cell lines the N-myc IRES induced downstream cistron expression to a much greater extent than c-myc, with a maximum relative activation of 6.83-fold seen in the human neuroblastoma cell line SH-SY5Y. It therefore appears that the N-myc IRES is specifically activated relative to that of c-myc in cells in which N-myc is expressed. Both the hairpin vector and RNase protection control experiments were carried out in neuronal cell types with the same results as in HeLa cells (data not shown). We observe no correlation between the absolute activity of the N-myc IRES as determined by firefly:*Renilla* ratios and its activity relative to the c-myc IRES (Figure 3) in the different cell lines tested.

#### The complete N-myc IRES is necessary for full activity

To map the N-myc IRES in greater detail a deletion series was constructed. Fragments of approximately 80 nucleotides in length were deleted sequentially from both the 5' and 3' ends of the N-myc 5' UTR and the truncated products obtained were inserted into the vector pRF between the *Renilla* and firefly luciferase cistrons. The resultant plasmids were analysed by transfection into HeLa, NB2a and NT2 cells. *Renilla* and firefly luciferase activities were determined and the ratio of firefly:*Renilla* was compared to that obtained from the parent vector pRNF (Figure 4). The deletions had similar effects in all three cell lines. A 50–60%

decrease in IRES activity was observed on deletion of the most 5' 86 nucleotides, although deletion of the next 70 nucleotides had no further effect. However, further deletion of 85 nucleotides from the 5' end led to an almost complete abolition of IRES activity, with a reduction to 3–10% of full activity. All deletions from the 3' end of the IRES had a drastic effect on IRES activity, with reductions of 80–90%, 88–96% and 96–98% observed on deletion of 74, 159 and 229 nucleotides respectively. These data imply that the entire 5' UTR is necessary for full IRES activity and that the 3' end in particular is crucial.

#### N-myc IRES activity decreases during neuronal differentiation

It is known that the expression of N-myc decreases during the differentiation of neuronal cells (Thiele *et al.*, 1985). We therefore examined the behaviour of the N-myc IRES during this process in three different cell lines, NB2a, NT2, and SH-SY5Y. NB2a and SH-SY5Y cells were subjected to a 24-h induction of differentiation following transfection with pRNF, using the agents dibutyryl cyclic AMP (dibutyryl cAMP) (Shea, 1994) and retinoic acid (RA) (Strickland and Mahdavi, 1978) respectively. NT2 cells were subjected to a 5-week period of differentiation induced by RA before transfection with pRNF. *Renilla* and firefly luciferase activities were determined and normalized to  $\beta$ -galactosidase. In all cells tested the induction of differentiation caused a decrease in the activity of the N-myc IRES (Figure 5). A small decrease in c-myc IRES activity was also seen in cells subjected to the same conditions (data not shown), but the decrease observed for N-myc was much greater.

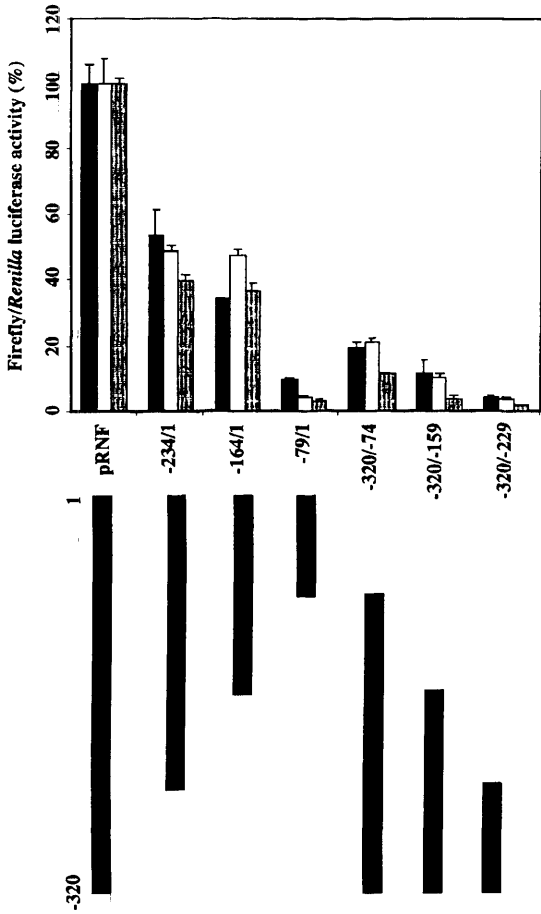


**Figure 4** The entire *N-myc* IRES is necessary for full activity. The truncated versions of the *N-myc* 5' UTR indicated were inserted into the vector pRNF and compared to the full UTR by transfection into HeLa (black), NB2a (white) and NT2 (grey) cells. Firefly luciferase activity relative to *Renilla* luciferase activity was calculated for each deletion mutant and is shown as a percentage of full IRES activity. The results represent an average of three independent experiments

## Discussion

In conclusion, the *N-myc* 5' UTR contains a highly active IRES. It is of similar size to that of *c-myc* and these IRESs share certain other features. Both show comparable activity in non-neuronal cell types and both are inactive in *in vitro* reticulocyte lysate translation systems (data not shown), implying the need for non-canonical *trans*-acting factors for activity (Stoneley *et al.*, 2000b). However, there is very little sequence homology between the *c-myc* and *N-myc* IRESs, and the enhanced activity of the *N-myc* IRES in neuronal cell types suggests a differential requirement for *trans*-acting protein factors. This is further supported by the fact that truncation of the *N-myc* IRES has a far more dramatic effect than that of the *c-myc* IRES, in which deletions from either the 5' or 3' ends lead to a gradual loss of activity and the most 3' 56 nucleotides can be removed with no reduction of

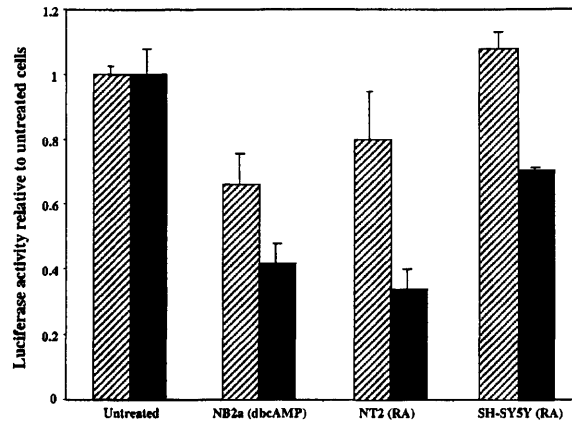


**Figure 5** *N-myc* IRES activity decreases during differentiation of neuronal cells. The cell lines NB2a and SH-SY5Y were transfected with pRNF and treated with 1 mM dibutyryl cAMP and 4  $\mu$ M retinoic acid respectively for 24 h prior to harvesting. NT2 cells were subjected to a 5-week period of 10  $\mu$ M retinoic acid treatment before transfection with pRNF. *Renilla* (shaded) and firefly (black) luciferase activities are expressed relative to a  $\beta$ -galactosidase control and normalized to the activities obtained on transfection of pRNF into untreated cells of the same type. The results represent an average of three independent experiments

activity (Stoneley *et al.*, 1998). We posit that the effect of deletions of the *N-myc* IRES is due to a requirement for the complete UTR to fold into an appropriate secondary structure for the binding of factors necessary for internal ribosome entry. The deletion mutants had the same effect in all cell lines tested, indicating that this is not a neuronal-specific observation. We were therefore unable to map the disparity between *c-myc* and *N-myc* IRES activity to a particular region of the *N-myc* IRES.

It is probable that a factor, or factors, present in neuronal precursor cells is able to specifically activate the *N-myc* IRES but has no effect on that of *c-myc*. Alternatively, factors present only in non-neuronal cells may inhibit the *N-myc*, but not the *c-myc* IRES. It was recently shown that a factor that is not expressed in neuronal cells, ITAF<sub>45</sub>, is required for the activity of the foot-and-mouth disease virus (FMDV) IRES, but is not needed by the Theiler's murine encephalomyelitis virus (TMEV) IRES, thereby allowing neurovirulence of TMEV but not FMDV (Pilipenko *et al.*, 2000). It is possible that a similar mechanism could contribute to the activity of the *c-myc* and *N-myc* IRESs, and protein factor requirements will now be investigated.

The reduction of IRES activity during neuronal differentiation implies that levels of an activating factor are reduced during this process. This observation is in contrast to the IRESs that have previously been shown to be implicated in differentiation, PDGF and AML1. Both these IRESs are activated during haematopoietic differentiation (Bernstein *et al.*, 1997; Pozner *et al.*, 2000). However, in both cases the protein produced by the IRES is upregulated during this differentiation programme. In addition, the FGF-2 IRES was shown

to be active in brain tissue in transgenic mice as well as in neuroblastoma cells (Créancier *et al.*, 2000). For N-myc the IRES would provide an attractive means of maintaining high protein levels in undifferentiated neuronal cells but reducing these levels during differentiation. The activity of the N-myc IRES did not decline to a level comparable to that of c-myc during the differentiation processes initiated (data not shown). Even so, the decline in IRES activity we observed during differentiation is great enough to make a partial contribution to the abolition of N-myc expression in differentiated neurons.

The expression of N-myc has previously been shown to be regulated at a post-transcriptional level by the binding of a neuronal RNA stabilizing factor to elements in the 3' UTR (Chagnovich and Cohn, 1996), and by the presence of a tissue-specific element that is inhibitory to gene expression in intron 1 (Sivak *et al.*, 1999). We have identified a method by which the translation of N-myc RNA is regulated in a neuronal-specific manner, thereby emphasising the complexity of the control of N-myc expression in neuronal and non-neuronal cells. The stimulation of the activity of this IRES in neuroblastoma cells provides a novel method by which N-Myc protein expression is upregulated in these cell types. It is therefore likely that translation initiation mediated by the N-myc IRES plays a contributory role in the high expression of N-Myc in neuroblastomas. Finally, we found the N-myc IRES to be considerably more active (between three- and sevenfold, depending on the cell line) than even the highly active EMCV IRES in all neuronal cell lines tested (data not shown). In this respect it could be of great value as a tool for expressing proteins in the central nervous system. This could be advantageous relative to viral IRESs that have already been tested for this purpose (Derrington *et al.*, 1999).

## Materials and methods

### Cell culture

All cell lines were grown at 37°C in a humidified atmosphere containing 5% CO<sub>2</sub>. The cell lines HeLa (human cervical epitheloid carcinoma), MCF7 (human breast carcinoma) and HEK293 (human embryonic kidney) were grown in Dulbecco's modified Eagle's medium with Glutamax (Gibco BRL) supplemented with 10% foetal calf serum (Helena Biosciences). The cell lines SH-SY5Y (human neuroblastoma) and NT2 (neuronal precursor cells derived from a human teratocarcinoma) were grown in 50% DMEM and 50% Ham F12 (Gibco BRL), supplemented with 10% foetal calf serum and 2 mM L-glutamine. The cell line NB2a (murine neuroblastoma) was grown in DMEM supplemented with 5% foetal calf serum and 5% horse serum. MCF7 cells were a gift from Dr M MacFarlane (MRC-Human Toxicology Unit, Leicester, UK), NB2a cells were a gift from Dr WG McLean (University of Liverpool, UK) and NT2 cells were a gift from Dr K Young (University of Leicester, UK). All other cell lines were purchased from the American type culture collection.

### Plasmid constructs

The plasmids pRF (formerly pGL3R2), pRMF (formerly pGL3R2utr) and phpRMF (formerly pGL3R2utrH) have been described previously (Stoneley *et al.*, 1998). A cDNA encoding the N-myc 5'UTR was obtained by RT-PCR of RNA extracted from SH-SY5Y cells using TRI Reagent (Sigma) and poly(A)<sup>+</sup> selected using oligo(dT) Dynabeads (Dynal). The oligonucleotides used were 5'-AAGAATTCGCTCTGGACGCGCTGGGTGGATGCGGG-3' and 5'-TTTCCATGGTGGACGTGGAGCAGC-3'. The PCR product was inserted into pRF between the EcoRI and NcoI sites to create the vector pRNF. The DNA encoding the N-myc 5'UTR was excised from pRNF between the SpeI and NcoI sites and inserted into the vector phpRF between these sites to create the vector phpRNF.

The 5' deletion mutants -234/1, -164/1 and -79/1 were created by PCR using pRNF as a template and the reverse primer used to amplify the N-myc 5' UTR. The forward primers used were 5'-GCGGAATTCCTGTAGCCATCCGAG-3', 5'-GCCGAATTCCTCCCTGCAGTCGGC-3' and 5'-CCCGAATTCAAAACGAAACGGGGCG-3' respectively. The 3' deletion mutants -320/-74, -320/-159 and -320/-229 were created by PCR using pRNF as a template and the forward primer used to amplify the N-myc 5' UTR. The reverse primers used were 5'-GTTCCATGGAA-TACCGGGGGTGTCT-3', 5'-TGCCCATGGTCCGGATTCTGATTCT-3' and 5'-TGGCCATGGTCTGTGCGCGCT-TGC-3' respectively. All PCR products were inserted into the vector pRF between the EcoRI and NcoI sites.

### DNA transfections

All cells were transfected using FuGENE6 (Roche) according to the manufacturer's protocols.

### Reporter gene analysis

The activity of both firefly and Renilla luciferase in lysates prepared from transfected cells was measured using the Dual-luciferase reporter assay system (Promega), according to the manufacturer's instructions. The activity of β-galactosidase in lysates prepared from cells transfected with pcDNA3.1/HisB/lacZ was measured using the Galactolight plus assay system (Tropix). Light emission was measured over 10 s using an Opticomp-1 Luminometer (MGM instruments).

### RNase protection

A DNA fragment was amplified from pRNF using the primers 5'-GCAAGAAGATGCACCTGATG-3' and 5'-ATAAGCTTGCATCTCTTCATAGCCTT-3' and ligated into the plasmid pSK<sup>+</sup> Bluescript (Stratagene) between the EcoRV and HindIII sites so as to be in an antisense orientation relative to the T7 promoter. The resultant plasmid was linearized using NotI and used as a template to generate a <sup>32</sup>P-UTP (800 Ci/mmol) labelled riboprobe by run-off transcription using T7 RNA polymerase. RNase protection was then performed using poly(A)<sup>+</sup> mRNA from HeLa cells transfected with pRNF, poly(A)<sup>+</sup> mRNA from mock-transfected HeLa cells, and 10 μg tRNA as described previously (Stoneley *et al.*, 1998).

### Differentiation of neuronal cells

Differentiation was initiated in SH-SY5Y cells by the application of 4 μM retinoic acid (Sigma) for 24 h, and in

NB2a cells by the application of 1 mM dibutyryl cyclic AMP (Sigma) for 24 h. NT2 cells were treated with 10  $\mu$ M retinoic acid three times weekly over a 5-week period to induce differentiation to hNT neurons.

## References

- Akiri G, Nahari D, Finkelstein Y, Le SY, Elroy-Stein O and Levi BZ. (1998). *Oncogene*, **17**, 227–236.
- Bernstein J, Sella O, Le S and Elroy-Stein O. (1997). *J. Biol. Chem.*, **272**, 9356–9362.
- Blackwood EM and Eisenman RN. (1991). *Science*, **251**, 1211–1217.
- Brodeur GM, Segar RC, Schwab M, Varmus HE and Bishop JM. (1984). *Science*, **224**, 1121–1124.
- Chagnovich D and Cohn SL. (1996). *J. Biol. Chem.*, **271**, 33580–33586.
- Coldwell MJ, Mitchell SA, Stoneley M, MacFarlane M and Willis AE. (2000). *Oncogene*, **19**, 899–905.
- Cornelis S, Bruynooghe Y, Denecker G, Van Huffel S, Tinton S and Beyaert R. (2000). *Mol. Cell*, **5**, 597–605.
- Créancier L, Morello D, Mercier P and Prats A-C. (2000). *J. Cell Biol.*, **150**, 275–281.
- Dang CV. (1999). *Mol. Cell Biol.*, **19**, 1–11.
- Derrington EA, Lopez-Lastra M, Chapel-Fernandez S, Cosset FL, Belin MF, Rudkin BB and Darlix JL. (1999). *Hum. Gene Ther.*, **10**, 1129–1138.
- Henis-Korenblit S, Levy Strumpf N, Goldstaub D and Kimchi A. (2000). *Mol. Cell Biol.*, **20**, 496–506.
- Holcik M, Lefebvre C, Yeh C, Chow T and Korneluk RG. (1999). *Nat. Cell Biol.*, **1**, 190–192.
- Huez I, Créancier L, Audigier S, Gensac MC, Prats AC and Prats H. (1998). *Mol. Cell Biol.*, **18**, 6178–6190.
- Ibson JM and Rabbitts PH. (1988). *Oncogene*, **2**, 399–402.
- Jackson RJ, Hunt SL, Reynolds JE and Kaminski A. (1995). *Curr. Top. Microbiol. Immunol.*, **203**, 1–29.
- Katoh K, Sawai S, Ueno K and Kondoh H. (1988). *Nuc. Acids Res.*, **16**, 3589.
- Kohl NE, Legouy E, DePinho RA, Nisen PD, Smith RK, Gee CE and Alt FW. (1986). *Nature*, **319**, 73–77.
- Lutz W, Stohr M, Schurmann J, Wenzel A, Lohr A and Schwab M. (1996). *Oncogene*, **13**, 803–812.
- Lutz W, Fulda S, Jeremias I, Debatin KM and Schwab M. (1998). *Oncogene*, **17**, 339–346.
- Malynn BA, de Alboran IM, O'Hagan RC, Bronson R, Davidson L, DePinho RA and Alt FW. (2000). *Genes Dev.*, **14**, 1390–1399.
- Miller D, Dibbens J, Damert A, Risau W, Vadas M and Goodall G. (1998). *FEBS Lett.*, **434**, 417–420.
- Nanbru C, Lafon I, Audigier S, Gensac MC, Vagner S, Guez G and Prats AC. (1997). *J. Biol. Chem.*, **272**, 32061–32066.
- Nesbit CE, Tersak JM and Prochownik EV. (1999). *Oncogene*, **18**, 3004–3016.
- Pilipenko EV, Pestova TV, Kolupaeva VG, Khitrina EV, Poperechnaya AN, Agol VI and Hellen CUT. (2000). *Genes Dev.*, **14**, 2028–2045.
- Pozner A, Goldenberg D, Negreanu V, Le SY, Elroy-Stein O, Levanon D and Groner Y. (2000). *Mol. Cell Biol.*, **20**, 2297–2307.
- Pyronnet S, Pradayrol L and Sonenberg N. (2000). *Mol. Cell*, **5**, 607–616.
- Saito H, Hayday AC, Wiman K, Hayward WS and Tonegawa S. (1983). *Proc. Natl. Acad. Sci. USA*, **80**, 7476–7460.
- Schwab M, Alitalo K, Klempnauer KH, Varmus HE, Bishop JM, Gilbert F, Brodeur G, Goldstein M and Trent J. (1983). *Nature*, **305**, 245–248.
- Shea TB. (1994). *Neuroreport*, **5**, 797–800.
- Sivak LE, Pont-Kingdon G, Le K, Mayr G, Tai KF, Stevens BT and Carroll WL. (1999). *Mol. Cell Biol.*, **19**, 155–163.
- Stanton BR, Perkins AS, Tessarollo L, Sassoon DA and Parada LF. (1992). *Genes Dev.*, **6**, 2235–2247.
- Stein L, Itin A, Einat P, Skaliter R, Grossman Z and Keshet E. (1998). *Mol. Cell Biol.*, **18**, 3112–3119.
- Stoneley M, Paulin FEM, Le Quesne JPC, Chappell SA and Willis AE. (1998). *Oncogene*, **16**, 423–428.
- Stoneley M, Chappell SA, Jopling CL, Dickens M, MacFarlane M and Willis AE. (2000a). *Mol. Cell Biol.*, **20**, 1162–1169.
- Stoneley M, Subkhankulova T, Le Quesne JPC, Coldwell MJ, Jopling CL, Belsham GJ and Willis AE. (2000b). *Nuc. Acids Res.*, **28**, 687–694.
- Strickland S and Mahdavi V. (1978). *Cell*, **15**, 393–403.
- Sugiyama A, Miyagi Y, Shirasawa Y and Kuchino Y. (1991). *Oncogene*, **6**, 2027–2032.
- Thiele CJ, Reynolds CP and Israel MA. (1985). *Nature*, **313**, 404–406.
- Vagner S, Gensac MC, Maret A, Bayard F, Amalric F, Prats H and Prats AC. (1995). *Mol. Cell Biol.*, **15**, 35–44.
- Zimmerman KA, Yancopoulos GD, Collum RG, Smith RK, Kohl NE, Denis KA, Nau MM, Witte ON, Toran-Allerand D, Gee CE, Minna JD and Alt FW. (1986). *Nature*, **319**, 780–783.

## Acknowledgments

This work was funded by the BBSRC (advanced fellowship to AE Willis). CL Jopling holds an MRC studentship.

## c-Myc Protein Synthesis Is Initiated from the Internal Ribosome Entry Segment during Apoptosis

MARK STONELEY,<sup>1†</sup> STEPHEN A. CHAPPELL,<sup>1‡</sup> CATHERINE L. JOPLING,<sup>1</sup> MARTIN DICKENS,<sup>1</sup>  
MARION MACFARLANE,<sup>2</sup> AND ANNE E. WILLIS<sup>1\*</sup>

*Department of Biochemistry, University of Leicester, Leicester LE1 7RH,<sup>1</sup> and MRC Toxicology Unit,  
University of Leicester, Leicester LE1 9HN,<sup>2</sup> United Kingdom*

Received 14 July 1999/Returned for modification 8 September 1999/Accepted 9 November 1999

Recent studies have shown that during apoptosis protein synthesis is inhibited and that this is in part due to the proteolytic cleavage of eukaryotic initiation factor 4G (eIF4G). Initiation of translation can occur either by a cap-dependent mechanism or by internal ribosome entry. The latter mechanism is dependent on a complex structural element located in the 5' untranslated region of the mRNA which is termed an internal ribosome entry segment (IRES). In general, IRES-mediated translation does not require eIF4E or full-length eIF4G. In order to investigate whether cap-dependent and cap-independent translation are reduced during apoptosis, we examined the expression of c-Myc during this process, since we have shown previously that the 5' untranslated region of the *c-myc* proto-oncogene contains an IRES. c-Myc expression was determined in HeLa cells during apoptosis induced by tumor necrosis factor-related apoptosis-inducing ligand. We have demonstrated that the c-Myc protein is still expressed when more than 90% of the cells are apoptotic. The presence of the protein in apoptotic cells does not result from either an increase in protein stability or an increase in expression of *c-myc* mRNA. Furthermore, we show that during apoptosis initiation of *c-myc* translation occurs by internal ribosome entry. We have investigated the signaling pathways that are involved in this response, and cotransfection with plasmids which harbor either wild-type or constitutively active MKK6, a specific immediate upstream activator of p38 mitogen-activated protein kinase (MAPK), increases IRES-mediated translation. In addition, the *c-myc* IRES is inhibited by SB203580, a specific inhibitor of p38 MAPK. Our data, therefore, strongly suggest that the initiation of translation via the *c-myc* IRES during apoptosis is mediated by the p38 MAPK pathway.

The cellular proto-oncogene *c-myc* is involved in very disparate cellular processes including proliferation, transformation, and cell death (apoptosis) (17, 22). It encodes a transcription factor of the helix-loop-helix/leucine zipper class and binds, in conjunction with its partner Max, to E-box sequences (7, 8, 9). Myc-Max heterodimers are potent activators of transcription, and it has been suggested elsewhere that Myc acts by activating a critical set of target genes (1, 2, 13). The regulation of *c-myc* expression is complex and occurs at multiple levels, including control of transcription (38), stability of both the mRNA and the protein (8, 35, 36, 51, 56), and by control of translation (11, 43, 46, 53, 59).

In eukaryotic cells, the majority of the control of translation occurs at the initiation stage by a scanning mechanism. This involves the binding of eukaryotic initiation factor 4F (eIF4F), a complex of proteins which includes eIF4E (the cap binding protein), eIF4G [a large protein which acts as a scaffold for the proteins in the complex and has binding sites for eIF4E, eIF4A, eIF3, and poly(A) binding protein], and eIF4A (RNA helicase) to the m<sup>7</sup>GpppN cap structure, recruitment of a 40S ribosomal subunit, and scanning to the first AUG codon in the correct context (45). Much of the control of translation initiation is mediated by changes in the phosphorylation states of proteins in the eIF4F complex and their binding partners, e.g.,

4EBP1 and 4EBP2 (49). Messages that have large structured 5' untranslated regions (UTRs) such as *c-myc* are, under normal cellular circumstances, only poorly translated, and it has been suggested elsewhere that this is because the levels of eIF4E are normally limiting and so restrict the formation of the active eIF4F complexes which are required for translation initiation (15, 33). In agreement with this, in cells overexpressing eIF4E there is an increase in the expression of *c-myc* (14, 15). We have shown that the control of cap-dependent translational regulation of *c-myc* is mediated by changes in the phosphorylation of 4EBP1 via the FRAP/mTOR signaling pathway (62).

Translation initiation can also occur by a mechanism that does not require the cap structure, and in this case, ribosomes enter at a region termed an internal ribosome entry segment (IRES), which can be up to 1,000 nucleotides from the 5' end of the RNA (24–26). IRESs were originally identified in picornaviral RNAs, and upon picornaviral infection, there is often a switch of translation from host-encoded cellular mRNAs to viral transcripts. In some picornaviruses, this is in part mediated by the proteolytic cleavage of eIF4G into an N-terminal and a C-terminal domain serving to bifurcate the eIF4E and eIF4A binding functions (34). This C-terminal domain has been shown to be sufficient to support cap-independent translation, in the absence of eIF4E, providing a rationale for the preferential translation of viral mRNAs due to their internal mechanism of ribosome entry (44, 47). There are now several examples of mammalian mRNAs which contain IRESs, and interestingly, many of them are associated with proteins that are involved in the control of cell growth. These include fibroblast growth factor 2, platelet-derived growth factor, vascular endothelial growth factor, and *c-myc* (6, 41, 43, 58–60).

One of the main areas of interest in the study of eukaryotic

\* Corresponding author. Mailing address: Department of Biochemistry, University of Leicester, University Rd., Leicester LE1 7RH, United Kingdom. Phone: 0116 2523363. Fax: 0116 2523369. E-mail: aew5@le.ac.uk.

† Present address: School of Biochemistry and Molecular Biology, The University of Leeds, Leeds LS2 9JT, United Kingdom.

‡ Present address: Department of Neurobiology, The Scripps Research Institute, La Jolla, CA 92037.

IRESs is the situations in which they are required, especially since initiation of translation of certain IRES-containing mRNAs, e.g., *c-myc* and fibroblast growth factor 2, can also be cap dependent (14, 31). Given that many viral IRESs function when the host cell cap-dependent translation is severely compromised, one hypothesis is that eukaryotic IRESs will also be used by a cell where the normal scanning cap-dependent mechanism of translation is inactive. In agreement with this, the vascular endothelial growth factor IRES is active during hypoxia when protein synthesis is inhibited (58) and the platelet-derived growth factor IRES is more active during cell differentiation, where protein synthesis rates are also reduced (6).

During apoptosis induced by Fas/CD95L, cap-dependent translation is decreased due to the cleavage of eIF4G by caspase 3 (39, 42). Induction of apoptosis by members of the tumor necrosis factor (TNF) transmembrane receptor family (which includes Fas/CD95) which results from binding to their cognate ligands, e.g., TNF and CD95L, has been well studied (44, 55). Apoptosis induced by TNF-related apoptosis-inducing ligand (TRAIL) has only recently been investigated and is more complex due to the existence of multiple TRAIL receptors (20, 37). The intracellular domains of this family of proteins contain highly conserved "death domains" which aggregate upon induction of apoptosis and recruit a group of proteins which form the death-inducing signaling complex (40, 55). Recruitment of the initiator caspase, caspase 8, into the death-inducing signaling complex results in its activation and in turn leads to activation of downstream effector caspases that are responsible for many of the morphological and biochemical changes associated with apoptosis. Overexpression of *c-myc* in the absence of the correct survival factors leads to apoptosis (18), and it has been shown previously that this mechanism of apoptotic induction is downstream of CD95 (23). It has been therefore proposed that *c-myc* could promote the efficacy with which CD95 and its ligand engage the apoptotic machinery of the cell (23). More recently, it has been shown that activation of *c-myc* triggers the release of cytochrome *c* from the mitochondria (28).

The role of *c-Myc* during apoptosis, the short half-life of this protein, and the two alternative mechanisms of *c-myc* mRNA translation initiation led us to investigate the synthesis of this protein in apoptotic cells. In this paper, we show that *c-Myc* protein expression in apoptotic HeLa cells, initiated with TRAIL, remains constant for up to 8 h. We demonstrate that *c-Myc* protein synthesis under these circumstances is initiated from the *c-myc* IRES, and this is the first example of a specific function which has been ascribed to this region of RNA. We investigated events that lie upstream of IRES-mediated *c-Myc* protein synthesis and show that signaling through the p38 mitogen-activated protein kinase (MAPK) pathway is required. Hence, *c-myc* internal initiation was stimulated by overexpression of MKK6, whereas the p38 kinase inhibitor SB203580 inhibited both *c-Myc* protein expression and internal ribosome entry on dicistronic mRNAs containing the *c-myc* IRES in apoptotic cells.

## MATERIALS AND METHODS

**Cell culture.** HeLa cells were maintained on 90-mm-diameter plates in culture at 37°C and 5% CO<sub>2</sub> in Dulbecco's modified Eagle's medium (GIBCO-BRL) and 10% fetal calf serum (Advanced Protein Products). To induce apoptosis, cells were treated with 0.25 µg of recombinant human TRAIL (37) per ml or 1 µM staurosporine. For treatment with signaling inhibitors, cells were preincubated with medium containing rapamycin (20 nM), SB203580 (40 µM), or an equivalent dilution of solvent (dimethyl sulfoxide) for 1 h before the addition of TRAIL.

**Immunoprecipitation.** Cells were labeled and immunoprecipitations were performed as described previously (36). Briefly, 2 × 10<sup>6</sup> cells, either untreated or

used 4 h after the addition of 0.25 µg of TRAIL per ml, were labeled with 250 µCi of [<sup>35</sup>S]methionine in 1 ml of methionine-free medium for 30 min. After addition of fresh complete medium, cell samples were harvested at 0, 20, 30, and 50 min. Cells were solubilized in antibody buffer (36) and disrupted by passage through a syringe attached to a 21-gauge needle. The samples were precleared by incubation for 1 h at 4°C with mouse immunoglobulin G and protein A/G-agarose (Santa Cruz Biotechnology, Inc.). Myc proteins were immunoprecipitated overnight at 4°C using Myc monoclonal antibody C-33 (Santa Cruz Biotechnology, Inc.). Samples were subjected to sodium dodecyl sulfate-polyacrylamide gel electrophoresis (SDS-PAGE), and the amount of radiolabel incorporated was visualized on a PhosphorImager (Molecular Dynamics). Experiments were performed on three independent occasions.

**DNA transfections and reporter gene analysis.** HeLa cells were transfected using the calcium phosphate DNA coprecipitation method as described previously (3). Cells (2 × 10<sup>5</sup>) were transfected with 2 µg of pGL3RutR (59), 0.5 µg of the MKK6 vectors (50), and 0.2 µg of β-galactosidase construct pDNA3.1/HisB/LacZ (Invitrogen) as a transfection control. Cells were harvested after 48 h, luciferase expression was determined using the dual-luciferase assay system (Promega), and β-galactosidase expression was determined using a Galactolight Plus system (Tropix). Both activities were measured in an Opticom-1 luminometer (MGM Instruments). Variations in transfection efficiency were corrected by normalizing luciferase activity to β-galactosidase activity. All assays were performed in triplicate on three independent occasions.

**p38 kinase assays.** HeLa cells with or without preincubation with 40 µM SB203580 for 1 h were then treated with 0.25 µg of TRAIL per ml. Cells were harvested at predetermined times, washed in ice-cold phosphate-buffered saline (PBS), and lysed in 250 µl of Triton lysis buffer (20 mM HEPES [pH 7.5]; 137 mM NaCl; 25 mM β-glycerolphosphate; 2 mM NaPPi; 2 mM EDTA; 10% glycerol; 1% Triton X-100; 1 mM phenylmethylsulfonyl fluoride; 2.5 µg of pepstatin, antipain, and leupeptin per ml; 2 mM benzamide; 0.5 mM dithiothreitol; 1 mM Na<sub>3</sub>VO<sub>4</sub>). After centrifugation, the supernatants were incubated with anti-p38 antibody and 4 mg of protein A-Sepharose for 3 h. After this period, the pellets were washed three times with Triton lysis buffer and one time with kinase buffer (25 mM HEPES [pH 7.4], 25 mM β-glycerolphosphate, 25 mM MgCl<sub>2</sub>, 0.5 mM Na<sub>3</sub>VO<sub>4</sub>, 0.5 mM EDTA, 0.5 mM dithiothreitol). Pellets were then resuspended in 30 µl of kinase assay buffer–5 µg of glutathione *S*-transferase-ATF2 (1–109)–50 µM [γ-<sup>32</sup>P]ATP (2,000 cpm/pmol) for 30 min at 30°C. Samples were electrophoresed on an SDS–10% polyacrylamide gel, and incorporation of <sup>32</sup>P into glutathione *S*-transferase-ATF2 protein was determined by phosphorimager analysis.

**Determination of protein synthesis rates.** For determination of protein synthesis rates in the presence of TRAIL, the method used was that described previously (62).

**Cell viability.** Apoptosis was determined using propidium iodide staining of nuclei. Cells (2 × 10<sup>5</sup> per time point) were washed three times in PBS and then fixed in a solution of 1:1 methanol-acetone for 10 min. Following five washes in PBS, the cells were incubated with 900 µl of PBS–100 µl of propidium iodide (50 µg/ml) at 37°C for 30 min before fluorescence analysis. Apoptosis was assessed by determining the percentage of cells with condensed nuclei relative to the total population of nuclei counted.

**SDS-PAGE and Western blotting.** For analysis of *c-Myc*, eIF4G, and poly-(ADP-ribose) polymerase (PARP), cell pellets were solubilized in electrophoresis buffer (50 mM Tris-HCl [pH 6.8], 4% SDS, 10% 2-mercaptoethanol, 1 mM EDTA, 10% glycerol, and 0.01% bromophenol blue) by sonication. Cell extracts (10<sup>6</sup> cells per lane) were then analyzed by SDS-PAGE on 7.5 or 10% polyacrylamide 16-cm gels (Bio-Rad), and proteins were transferred to nitrocellulose (Schleicher and Schuell) by electroblotting in transfer buffer (0.2 M glycine, 20 mM Tris, 20% [vol/vol] methanol) for 1.5 h at 85 V. Equal loading of protein was determined on all blots by staining with Ponceau S. Blots were blocked by incubation in 5% skimmed milk in Tris-buffered saline–Tween for 1 to 2 h and then probed with the relevant antibodies for 1 h at room temperature. *c-Myc* protein was detected using the mouse monoclonal antibody 9E10 (generated by T. Harrison) at a 1:400 dilution, and α-tubulin proteins were detected using a mouse monoclonal antibody (Sigma) at a 1:10,000 dilution. Rabbit polyclonal antibodies used to detect eIF4G were kindly provided by S. Morley (Sussex University) at dilutions of 1:7,000. A mouse monoclonal antibody which was used to detect PARP was obtained from G. Poirier, Laval University, Quebec, Canada. Blots were then incubated with peroxidase-conjugated secondary antibodies raised against mouse or rabbit immunoglobulins and developed using the chemiluminescence reagent Illumin 8 (generated by M. Murray, Department of Genetics, Leicester University).

**Northern blot analysis.** Total cellular RNA and poly(A)<sup>+</sup>-selected (using DynaBeads) mRNA were prepared and analyzed by Northern blotting exactly as described previously (63). DNA probes used for the detection of *c-myc* and glyceraldehyde-3-phosphate dehydrogenase (GAPDH) mRNA species were also as described previously (63).

## RESULTS

***c-Myc* protein levels remain constant during apoptosis when protein synthesis is inhibited. In HeLa cells in which apoptosis**

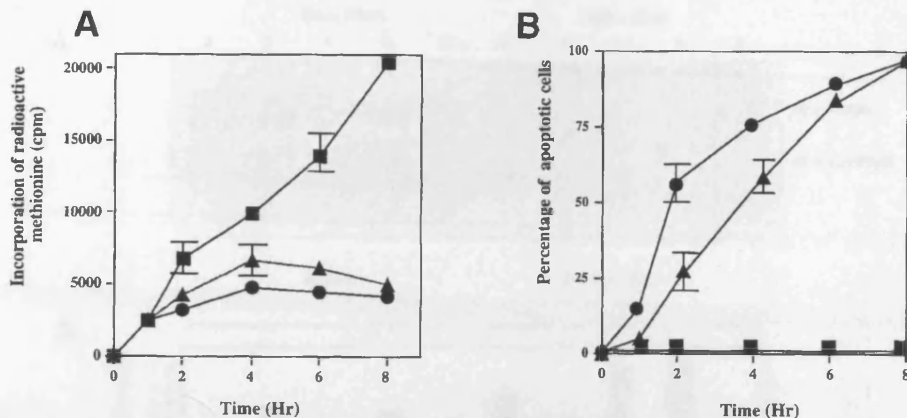


FIG. 1. Treatment of HeLa cells with either TRAIL or staurosporine causes a general inhibition of translation and a decrease in cell viability. HeLa cells, in triplicate, were incubated in either the absence (closed squares) or the presence of 0.25  $\mu$ g of TRAIL (closed triangles) per ml or 1  $\mu$ M staurosporine (closed circles). (A) Protein synthesis was estimated by labeling the cells with [ $^{35}$ S]methionine before harvesting at the times indicated. (B) Parallel cultures were used to determine apoptosis by staining with propidium iodide.

has been triggered with either staurosporine or TRAIL, protein synthesis is inhibited within 2 h (Fig. 1). This inhibition of protein synthesis correlates with the cleavage of eIF4G (Fig. 2A and B) that occurs at the same time as cleavage of PARP (Fig. 2D), known to be cleaved by effector caspases. Thus, there is a rapid cleavage of eIF4G into fragments of 150 and 76 kDa and a corresponding appearance of the specific 89-kDa

cleavage fragment of PARP (Fig. 2D). The degradation of eIF4G appears to be a general phenomenon during the onset of apoptosis and has also been shown to occur in Jurkat cells treated with anti-CD95 (42), in BJAB cells during serum starvation (12), and in HeLa cells treated with etoposide or cisplatin (39). Since protein synthesis rates are very much decreased during apoptosis, it would be expected that the abundance of proteins that have a short half-life would be greatly reduced a few hours after the onset of apoptosis. The initiation of synthesis of the c-Myc protein (which has a relatively short half-life of between 20 and 40 min [21]) can occur both in a cap-dependent manner and by internal ribosome entry (43, 59, 62). Thus, to determine the steady-state levels of c-Myc protein in HeLa cells undergoing apoptosis, when cap-dependent translation is compromised, Western blots were probed with anti-c-Myc antibodies (Fig. 2C). Interestingly, we found that the levels of this protein remained constant during apoptosis (Fig. 2C). Thus, even 8 h after the onset of apoptosis, when 95% of cells were apoptotic as assessed by propidium iodide staining of condensed nuclei, c-Myc protein levels were unaltered (Fig. 1B and 2C). Consistent with the intimate role of the *c-myc* gene product in the regulation of cellular proliferation and differentiation, the expression of this proto-oncogene is controlled at multiple levels (38). Thus, there are a number of possible explanations for these data: firstly, levels of *c-myc* RNA are increased during apoptosis; secondly, there is a change in the stability of c-Myc protein during this process; and finally, the c-Myc protein is translated by an alternative mechanism during apoptosis which does not require full-length eIF4G. To distinguish between these possibilities, the following series of experiments were carried out.

**During apoptosis in HeLa cells, there is no increase in the level of *c-myc* mRNA.** An increase in the levels of *c-myc* mRNA could occur either by an increase in the transcription of *c-myc* or by an increase in the stability of the message. To investigate these possibilities, the steady-state level of *c-myc* mRNA was analyzed during apoptosis. HeLa cells were incubated with TRAIL, total and poly(A)<sup>+</sup> mRNA was isolated over 8 h, and Northern blot analysis was performed. There was no change in the ratio of *c-myc* to GAPDH during apoptosis (Fig. 3), and in the absence of a large induction of mRNA expression, it is evident that increased transcription rates and/or increased mRNA stability is not the key mechanism involved in the

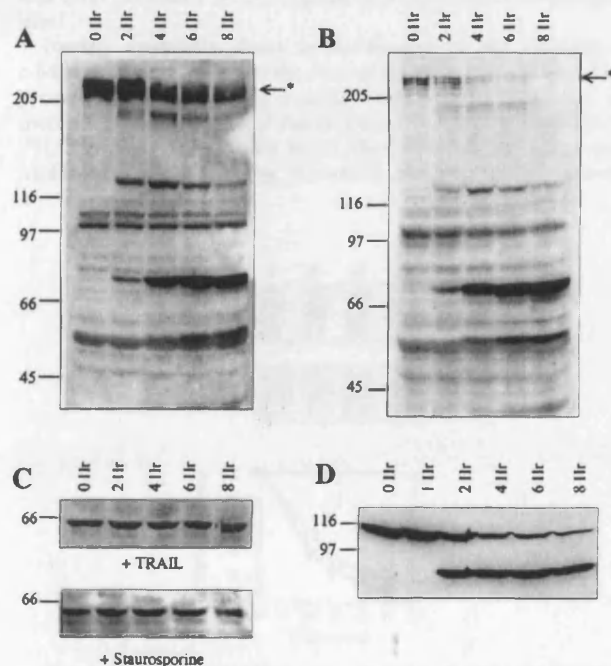


FIG. 2. Inhibition of translation correlates with cleavage of eIF4G and PARP. Cells were incubated with 0.25  $\mu$ g of TRAIL (A) per ml or 1  $\mu$ M staurosporine (B) and harvested at the time points shown. Cell extracts ( $10^6$  cells) were separated by SDS-PAGE, Western blotted, and probed with antibodies to eIF4G and then with the c-Myc antibody 9E10 (C). Samples from the blot shown in panel A were rerun on an SDS-7.5% polyacrylamide gel and then probed with antibodies to PARP (D). Results are representative of at least three independent experiments. The asterisk marks the full-length eIF4G. Numbers to the left of each panel indicate molecular masses in kilodaltons.

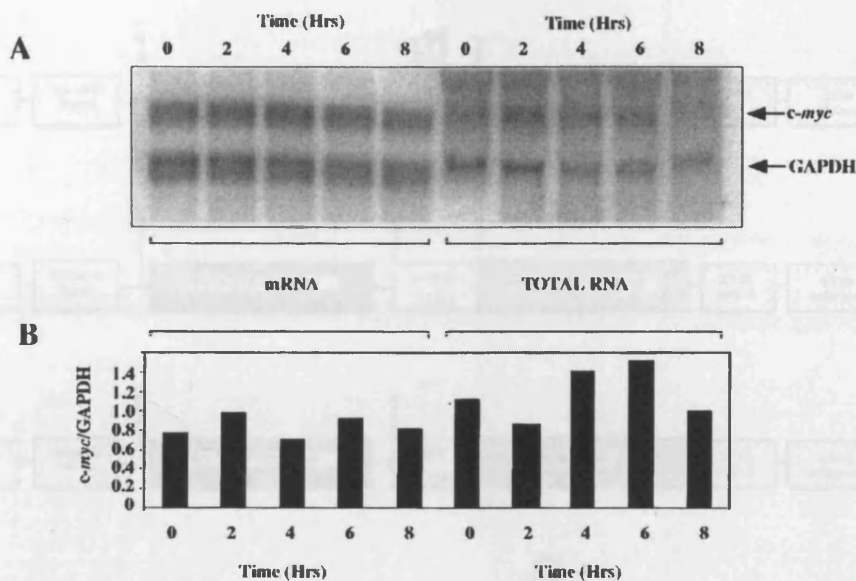


FIG. 3. *c-myc* mRNA levels are unchanged during apoptosis. Poly(A)<sup>+</sup> mRNA or total cellular RNA was prepared from samples taken over an 8-h period after the addition of TRAIL and then analyzed by Northern blotting for levels of *c-myc* mRNA, and levels of the control message GAPDH were determined using specific probes (A). The Northern blot was analyzed using a Molecular Dynamics PhosphorImager, and *c-myc* mRNA levels were normalized to those of GAPDH (B).

expression of c-Myc protein described here. Since c-Myc protein expression has been shown to be subject to regulation at the level of both protein stability and translation (36, 56, 57), it was then necessary to distinguish between these two possibilities.

**During apoptosis, there is no change in the half-life of c-Myc protein.** Studies of the rate of degradation of the c-Myc protein using pulse-chase analysis revealed that there was no increase in the stability of the protein 4 h after the addition of TRAIL, a point at which more than 65% of the cells were undergoing apoptosis (Fig. 1C and 4). Indeed, the Myc protein

appeared to be slightly less stable during apoptosis, with a half-life of approximately 17 min, compared to the control samples, which had a half-life of approximately 23 min, a value consistent with published data (21, 62). In addition, the amounts of c-Myc protein synthesized during the 30-min labeling time ( $t = 0$ ) were also similar, demonstrating that Myc is still synthesized from the endogenous message during apoptosis.

Further experiments performed were aimed at determining the mechanism of *c-myc* translation initiation in apoptosis.

**The *c-myc* IRES is functional during apoptosis.** We and others have shown that the *c-myc* 5' UTR contains an IRES and that translation initiation of this message can therefore occur in a cap-independent manner (43, 59). In addition, it has been shown that *c-myc* is still translated in cells which have been infected with polio virus (27). In this situation, cap-dependent translation of most host cell mRNAs is blocked due to the specific cleavage of eIF4G.

To determine whether the *c-myc* IRES was active during apoptosis, HeLa cells were transiently transfected with either the control dicistronic plasmid containing the *Renilla* luciferase gene upstream and the firefly luciferase gene downstream (pGL3R [Fig. 5A]), the dicistronic construct containing the *c-myc* IRES fused in frame with the firefly luciferase gene (pGL3Rutr [Fig. 5A]) (59), or a plasmid construct containing the human rhinovirus IRES (HRV-IRES, pGL3RHRV [Fig. 5A]). This was used to determine whether a similar effect was observed using an IRES of viral origin (Fig. 5A) (59). Apoptosis was initiated with TRAIL, and the amount of luciferase produced from each cistron was measured over 10 h (Fig. 5B and C). When firefly luciferase activity was normalized to *Renilla* luciferase activity, there was an apparent increase in firefly luciferase activity following stimulation with TRAIL (Fig. 5B). This suggests that, during apoptosis, cap-dependent translation from the *Renilla* luciferase cistron was down modulated whereas initiation of translation by internal ribosome entry was maintained. The difference between the synthesis of these pro-

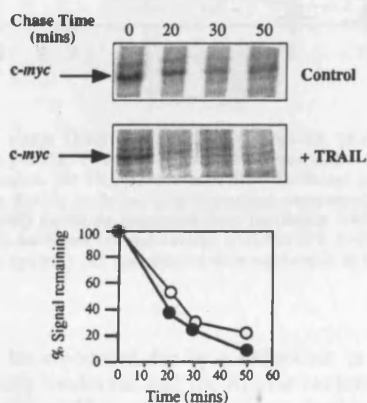


FIG. 4. c-Myc protein stability is unaltered during apoptosis. Determination of the half-life of the c-Myc protein in control HeLa cells and at 4 h post-addition of TRAIL is shown. Pulse-chase analysis and immunoprecipitation were performed as described in Materials and Methods. Cells were labeled for 30 min and then harvested following the chase times indicated. Samples were subjected to PAGE, and the amount of radiolabel incorporated into each band was determined by using a phosphorimager. (A) Representative gels of pulse-chase immunoprecipitations. (B) Phosphorimager analysis of the gels shown in panel A. Open circles, untreated HeLa cells; closed circles, HeLa cells incubated with TRAIL for 4 h.

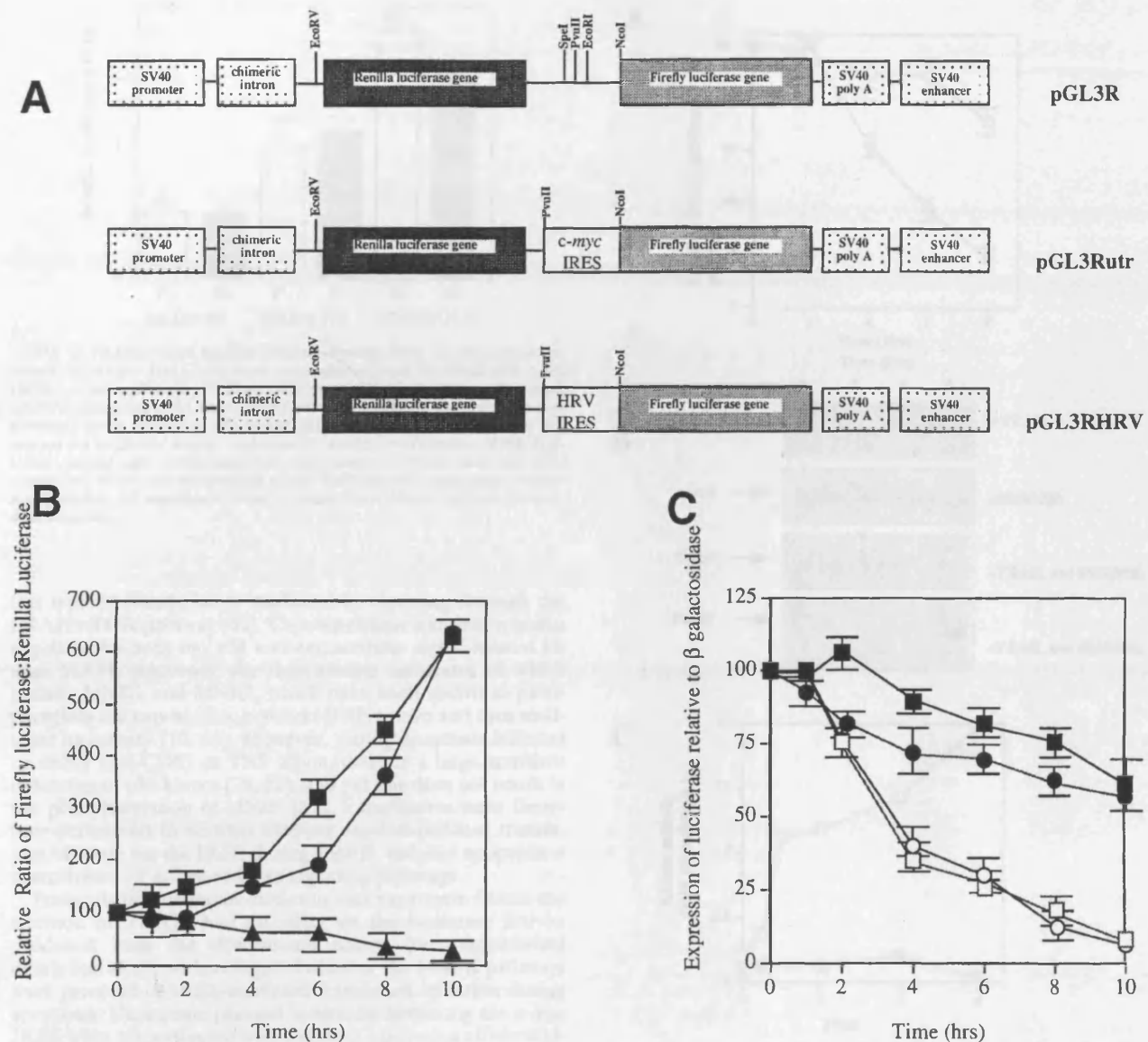


FIG. 5. The c-Myc IRES is active during apoptosis. (A) HeLa cells were cotransfected (in triplicate) with pcDNA3.1/HisB/LacZ and either pGL3Rutr, pGL3RHRV, or pGL3R. Twenty-four hours after transfection, apoptosis was induced by the addition of 0.25  $\mu$ g of TRAIL per ml, and samples were harvested at the time points indicated. (B) The expression of firefly luciferase generated from the IRES (by a cap-independent mechanism) was calculated relative to the expression of the upstream *Renilla* luciferase (cap-dependent expression), pGL3Rutr (closed circles), pGL3RHRV (closed squares), or pGL3R (closed triangles). (C) The expression of firefly luciferase generated from translation initiation of the IRES was also determined relative to that of the transfection control  $\beta$ -galactosidase, pGL3Rutr firefly luciferase (closed circles), pGL3RHRV firefly luciferase (closed squares), pGL3Rutr *Renilla* luciferase (open circles), and pGL3RHRV *Renilla* luciferase (open squares). All experiments were performed in triplicate on three independent occasions. SV40, simian virus 40; HRV, human rhinovirus.

teins cannot be accounted for by a difference in half-life between the firefly luciferase and the *Renilla* luciferase, since we have found that in HeLa cells they have similar half-lives of approximately 2.5 h, in agreement with previously published data (data not shown and reference 10). Indeed, this interpretation was confirmed when the firefly luciferase activity (IRES mediated) was calculated relative to that of  $\beta$ -galactosidase, which is a more stable protein with a half-life of approximately 20 h (Fig. 5C). In this case, the firefly luciferase actually decreased to approximately 70% 10 h after apoptosis had been triggered, whereas the *Renilla* luciferase activity decreased to

11%. These data are consistent with the IRES sustaining c-Myc protein expression, as opposed to inducing it, during apoptosis when cap-dependent translation is compromised.

To gain further information about the cellular consequences of *c-myc* expression during apoptosis, the effects of compounds which have been shown to specifically inhibit translation were investigated.

**Proteins required for initiation of protein synthesis by the c-myc IRES are downstream of the MAPK pathway.** We have shown recently that cap-dependent translational regulation of *c-myc* is blocked by rapamycin, suggesting that regulation of

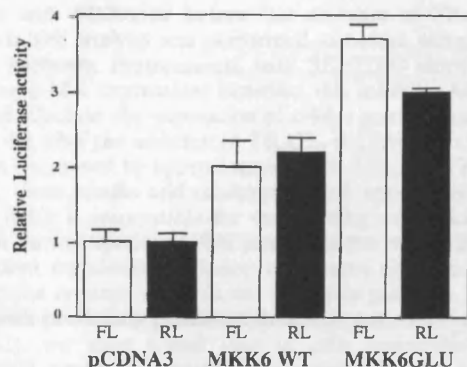


FIG. 6. Proteins which mediate internal ribosome entry of *c-myc* are downstream of MKK6. HeLa cells were cotransfected with the dicistronic *c-myc* IRES-containing plasmid pGL3Rutr and either pcDNA3 (control empty vector), pcDNA3 containing DNA encoding MKK6WT, or pcDNA3 containing the constitutively active version of this kinase, MKK6Glu. Cells were harvested and assayed for luciferase activity to determine whether coexpression of the dicistronic plasmid with MKK6 increased cap-dependent (*Renilla* luciferase [RL] expression) and/or cap-independent (firefly luciferase [FL] expression) translation initiation. All experiments were performed in triplicate on three independent occasions.

this type of translation is mediated by signaling through the FRAP/mTOR pathway (62). Cap-dependent translation is also regulated by both the p38 and extracellular signal-related kinase MAPK pathways, the downstream substrates of which include MNK1 and MNK2, which have been shown to phosphorylate the cap-binding protein eIF4E in vivo and thus modulate its activity (19, 61). However, during apoptosis initiated by either anti-CD95 or TNF alpha, there is a large transient induction of p38 kinase (29, 52), and yet this does not result in the phosphorylation of eIF4E (42). Experiments were therefore performed to address whether cap-independent translation of *c-myc* via the IRES during TRAIL-induced apoptosis is downstream of either of these signaling pathways.

Preincubation of transfected cells with rapamycin before the addition of TRAIL had no effect on the luciferase activity produced from the downstream cistron (our unpublished data); therefore, we investigated whether the MAPK pathways were involved in IRES-mediated translation initiation during apoptosis. Dicistronic plasmid constructs harboring the *c-myc* IRES were cotransfected with plasmids expressing either wild-type MKK6 (MKK6WT), an immediate upstream activator of p38 MAPK, or a constitutively active form, MKK6Glu (50). Both the wild-type and the constitutively active version of MKK6 cause an increase in the activity of both the *Renilla* luciferase (cap dependent) and the firefly luciferase (cap independent) (Fig. 6). For the *Renilla* luciferase, this is not surprising, since downstream substrates in this pathway include MNK1 and MNK2, which phosphorylate the cap-binding protein of eIF4E. However, these data also suggest that the p38 MAPK pathway activates a protein(s) which is required for cap-independent translation.

To investigate these observations further, cells (pGL3Rutr) were transfected with the dicistronic plasmid construct incubated with TRAIL either with or without pretreatment with SB203580, and harvested over an 8-h period. As before, (Fig. 5C), relative to the expression of  $\beta$ -galactosidase, the level of firefly luciferase decreased to approximately 70% of the original value by 8 h (Fig. 7A). However, in cells pretreated with SB203580 (which inhibits p38 MAPK [Fig. 7C]), the expression of firefly luciferase derived from the *c-myc* IRES is very much

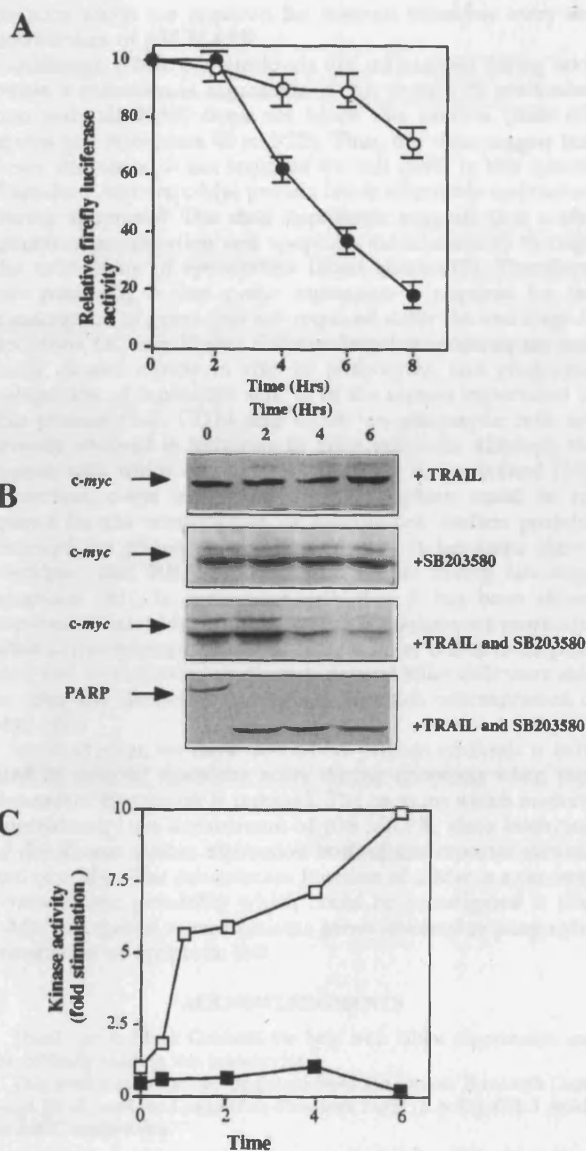


FIG. 7. The *c-myc* IRES is downstream of p38 MAPK. (A) cells were cotransfected with dicistronic reporter plasmids containing the *c-myc* IRES (pGL3Rutr) and  $\beta$ -galactosidase (pcDNA3.1/HisB/LacZ), and half the samples were preincubated for 1 h with 40  $\mu$ M SB203580. Open circles, absence of inhibitor; closed circles, presence of inhibitor. Cells were then treated with 0.25  $\mu$ g of TRAIL per ml, and samples were harvested at the time points shown and assayed for firefly luciferase and  $\beta$ -galactosidase activity. The relative ratio of firefly luciferase to  $\beta$ -galactosidase is shown. (B) Cells ( $10^6$ ) were incubated with TRAIL with or without a 1-h preincubation with 40  $\mu$ M SB203580. Samples were harvested at the time points shown, analyzed by PAGE and Western blotting with an anti-*c-Myc* antibody, and then stripped and reprobed with an anti-PARP antibody. (C) p38 MAPK activity was assayed in the presence (closed squares) or absence (open squares) of SB203580 (preincubation for 1 h) followed by the addition of 0.25  $\mu$ g of TRAIL per ml. As expected, the activity of this enzyme is induced up to 10-fold during apoptosis, and this induction is inhibited by the presence of the inhibitor.

reduced (Fig. 7A). Hence, after 4 h the expression is decreased to 60%, compared to 93% in the untreated control cells, and by 8 h, the levels of firefly luciferase are reduced to 18% of their original value. To determine whether a similar effect was observed with *c-Myc* protein expression, HeLa cells were pre-

treated with SB203580 before the addition of TRAIL and Western blot analysis was performed as before using an anti-c-Myc antibody. Pretreatment with SB203580 alone had no effect on c-Myc expression; however, this inhibitor had a very marked effect on the expression of c-Myc protein during apoptosis; 4 h after the addition of TRAIL, the levels of the c-Myc protein decreased by approximately 70% (Fig. 7B). Taken together, these results add credence to our hypothesis that the c-myc IRES is responsible for maintaining expression of this protein during apoptosis. We posit that the switch from cap-dependent translation initiation to internal ribosome entry is likely to be an early event in the apoptotic pathway. In agreement with previously published data with anti-CD95 and TNF (42, 52), we have found that in cells preincubated with SB203580 apoptosis occurs slightly more rapidly (data not shown). Therefore, the decrease in c-myc expression does not appear to affect the efficiency with which cells initiate apoptosis.

These data strongly suggest that proteins which are responsible for IRES-mediated translation initiation during apoptosis are downstream of p38 MAPK.

## DISCUSSION

Protein synthesis of the proto-oncogene *c-myc* can be initiated by two mechanisms. Evidence for a cap-dependent scanning mechanism of translation initiation comes from the observations that the translation of *c-myc* mRNA is increased in cells which overexpress eIF4E (14) and that an increase in the degree of phosphorylation of 4EBP1 (which causes the dissociation of eIF4E from this binding partner) results in an increase in c-Myc expression (62). More recently, we and others have shown that the *c-myc* 5'-UTR contains an IRES and that therefore *c-myc* mRNA can be translated in a manner which is independent of the cap structure (43, 59). The *c-myc* gene encodes four different transcripts, P0, P1, P2, and P3, of approximately 3.1, 2.4, 2.25, and 2.0 kb, respectively (4, 5, 64), and most of this heterogeneity is in the length of the 5' UTR. The IRES is contained within the 5' UTR of mRNAs which initiate from P2 (59); thus (as these transcripts represent 75 to 90% of the *c-myc* mRNA, in most cells), the majority of *c-myc* mRNA in a cell has the potential to initiate translation via internal ribosome entry.

We have investigated the circumstances in which the *c-myc* IRES is utilized and have found that it is active during apoptosis (Fig. 3 and 6) when the levels of cap-dependent translation are reduced due to cleavage of eIF4G (Fig. 2) (12, 39, 42). Our data suggest that cleaved eIF4G is sufficient to allow initiation of translation by internal ribosome entry by the *c-myc* IRES, since 8 h after the induction of apoptosis with staurosporine there is no remaining full-length eIF4G and yet c-Myc protein is still expressed (Fig. 2C). In addition, it has been shown recently that *c-myc* mRNA is still associated with the translational machinery in cells that have been infected with poliovirus, whereby eIF4G is cleaved subsequent to viral infection (25, 27).

p38 MAPK is activated during apoptosis (29, 52), and yet this is not accompanied by phosphorylation of eIF4E (42), which has been shown to be a downstream target *in vivo* (19, 61). Our data demonstrate that cotransfection of wild-type and constitutively active MKK6 increases the activity of IRES-mediated translation, suggesting that the *c-myc* IRES is also downstream of p38 MAPK (Fig. 6). The p38 inhibitor SB203580 blocks both the activity of the firefly luciferase downstream of the *c-myc* IRES and the expression of c-Myc during apoptosis (Fig. 6 and 7), again strongly suggesting that

proteins which are required for internal ribosome entry are downstream of p38 MAPK.

Although c-Myc protein levels are maintained during apoptosis, a reduction in expression of this protein by preincubation with SB203580 does not block this process (data not shown and references 42 and 52). Thus, our data suggest that *c-myc* expression is not required for cell death in this system. Therefore, why are c-Myc protein levels selectively maintained during apoptosis? The dual hypothesis suggests that c-Myc promotes proliferation and apoptosis simultaneously through the modulation of appropriate target genes (17). Therefore, one possibility is that *c-myc* expression is required for the transcription of genes that are required at/for the end stage of apoptosis, i.e., engulfment. Cells undergoing apoptosis are normally cleared rapidly *in vivo* by phagocytes, and phagocytic recognition of "apoptotic self" is of the utmost importance to this process (54). CD14 and CD36 on phagocytic cells are directly involved in tethering to apoptotic cells, although the ligands with which they interact have yet to be defined (16). Therefore, *c-myc* expression during apoptosis could be required for the transcription of specific cell surface proteins required for phagocyte recognition, and it has been shown elsewhere that RNA synthesis still occurs during late-stage apoptosis (30). In agreement with this, it has been shown previously that c-Myc-overexpressing fibroblasts are more sensitive to the cytotoxic effects of natural killer cell-derived granules, and in coculture experiments natural killer cells were able to efficiently destroy only target cells which overexpressed c-Myc (32).

In conclusion, we show that c-Myc protein synthesis is initiated by internal ribosome entry during apoptosis when cap-dependent translation is reduced. The proteins which mediate internal entry are downstream of p38 MAPK, since inhibition of this kinase ablates expression both of the reporter enzyme and of c-Myc. The downstream function of c-Myc is unknown; however, one possibility which could be investigated is that c-Myc is required to transactivate genes involved in phagocytic recognition of apoptotic self.

## ACKNOWLEDGMENTS

Thanks go to Mark Coldwell for help with initial experiments and for critically reading the manuscript.

This work was supported by grants from the Cancer Research Campaign (M.S.) and the Leukaemia Research Fund (S.A.C.). C.L.J. holds an MRC studentship.

## REFERENCES

- Amati, B., M. W. Brooks, N. Levy, T. D. Littlewood, G. I. Evan, and H. Land. 1993. Oncogenic activity of the c-Myc protein requires dimerization with Max. *Cell* 72:233-245.
- Amati, B., T. D. Littlewood, G. I. Evan, and H. Land. 1993. The c-Myc protein induces cell cycle progression and apoptosis through dimerization with Max. *EMBO J.* 12:5083-5087.
- Ausubel, R. M., et al. 1987. *Current protocols in molecular biology*, p. 9.11-9.17. Wiley-Interscience, New York, N.Y.
- Batley, J., C. Moulding, R. Taub, W. Murphy, T. Stewart, H. Potter, G. Lenoir, and P. Leder. 1983. The human *c-myc* oncogene: structural consequences of translocation into the IgH locus in Burkitt lymphoma. *Cell* 34:779-787.
- Bentley, D. L., and M. Groudine. 1986. Novel promoter upstream of the human *c-myc* gene and regulation of *c-myc* expression in B-cell lymphomas. *Mol. Cell. Biol.* 6:3481-3489.
- Bernstein, J., O. Sella, S. Le, and O. Elroy-Stein. 1997. PDGF/c-sis mRNA leader contains a differentiation-linked internal ribosomal entry site. *J. Biol. Chem.* 272:9356-9362.
- Blackwell, T. K., L. Kretzner, E. M. Blackwood, R. N. Eisenman, and H. Weintraub. 1990. Sequence-specific DNA binding by the c-Myc protein. *Science* 250:1149-1151.
- Blackwood, E. M., and R. N. Eisenman. 1991. Max: a helix-loop-helix zipper protein that forms a sequence-specific DNA-binding complex with Myc. *Science* 251:1211-1217.

9. Blackwood, E. M., B. Luscher, and R. N. Eisenman. 1992. Myc and Max associate in vivo. *Genes Dev.* 6:71–80.
10. Bronstein, I., J. Fortin, P. E. Stanley, G. S. Stewart, and L. J. Kricka. 1994. Chemiluminescent and bioluminescent reporter gene assays. *Anal. Biochem.* 219:169–181.
11. Butnick, N. Z., C. Miyamoto, R. Chizzonite, B. R. Cullen, G. Ju, and A. M. Skalka. 1985. Regulation of the human *c-myc* gene: 5' noncoding sequences do not affect translation. *Mol. Cell. Biol.* 5:3009–3016.
12. Clemens, M. J., M. Bushell, and S. J. Morley. 1998. Degradation of eIF4G in response to induction of apoptosis in human lymphoma cell lines. *Oncogene* 17:2921–2931.
13. Dang, C. V. 1999. *c-Myc* target genes involved in cell growth, apoptosis, and metabolism. *Mol. Cell. Biol.* 19:1–11.
14. De Benedetti, A., B. Joshi, J. R. Graff, and S. G. Zimmer. 1994. CHO cells are transformed by the translation initiation factor eIF-4E display increased levels of *c-myc* expression, but require concomitant overexpression of Max for tumorigenicity. *Mol. Cell. Differ.* 2:347–371.
15. De Benedetti, A., and R. E. Rhoads. 1990. Overexpression of eukaryotic protein synthesis initiation factor 4E in HeLa cells results in aberrant growth and morphology. *Proc. Natl. Acad. Sci. USA* 87:8212–8216.
16. Devitt, A., O. C. Moffatt, C. Raykundalia, J. D. Capra, D. L. Simmons, and C. D. Gregory. 1998. Human CD14 mediates recognition and phagocytosis of apoptotic cells. *Nature* 392:505–509.
17. Evan, G. I., and T. D. Littlewood. 1993. The role of *c-myc* in cell growth. *Curr. Opin. Genet. Dev.* 3:44–49.
18. Evan, G. I., A. H. Wyllie, C. S. Gilbert, T. D. Littlewood, H. Land, M. Brooks, C. M. Waters, L. Z. Penn, and D. C. Hancock. 1992. Induction of apoptosis in fibroblasts by *c-myc* protein. *Cell* 69:119–128.
19. Fukunaga, F., and T. Hunter. 1997. Mnk1, a new map kinase-activated protein kinase, isolated by novel expression screening method for identifying protein kinase substrates. *EMBO J.* 16:1921–1933.
20. Goodwin, R., and C. A. Smith. 1998. The TRAIL of death. *Apoptosis* 3:83–88.
21. Hann, S. R., and R. N. Eisenman. 1984. Proteins encoded by the human *c-myc* oncogene: differential expression in neoplastic cells. *Mol. Cell. Biol.* 4:2486–2497.
22. Hueber, A. O., and G. I. Evan. 1998. Traps to catch unwary oncogenes. *Trends Genet.* 14:364–367.
23. Hueber, A. O., M. Zornig, D. Lyon, T. Suda, S. Nagata, and G. I. Evan. 1997. Requirement for the CD95 receptor-ligand pathway in *c-myc*-induced apoptosis. *Science* 278:1305–1309.
24. Jackson, R. J., S. L. Hunt, C. L. Gibbs, and A. Kaminski. 1994. Internal initiation of translation of picornavirus RNAs. *Mol. Biol. Rep.* 19:147–159.
25. Jackson, R. J., S. L. Hunt, J. E. Reynolds, and A. Kaminski. 1995. Cap-dependent and cap-independent translation: operational distinctions and mechanistic interpretations. *Curr. Top. Microbiol. Immunol.* 203:1–29.
26. Jackson, R. J., and A. Kaminski. 1995. Internal initiation of translation in eukaryotes: the picornavirus paradigm and beyond. *RNA* 1:985–1000.
27. Johannes, G., and P. Sarnow. 1998. Cap-independent polysomal association of natural mRNAs encoding *c-myc*, Bip, and eIF4F conferred by internal ribosome entry sites. *RNA* 4:1500–1513.
28. Juin, P., A. Hueber, T. Littlewood, and G. Evan. 1999. *c-Myc*-induced sensitization to apoptosis is mediated through cytochrome C release. *Genes Dev.* 13:1367–1381.
29. Juo, P., C. J. Kuo, S. E. Reynolds, R. F. Konz, J. Raingeaud, R. J. Davis, H.-P. Biemann, and J. Blenis. 1997. Fas activation of the p38 mitogen-activated protein kinase signalling pathway requires ICE/CED-3 family proteases. *Mol. Cell. Biol.* 17:24–35.
30. Kerkhoff, E., and E. B. Ziff. 1995. Deregulated messenger RNA expression during T cell apoptosis. *Nucleic Acids Res.* 23:4857–4863.
31. Kevil, C., P. Carter, B. Hu, and A. DeBenedetti. 1995. Translational enhancement of FGF-2 by eIF-4 factors and alternate utilization of CUG and AUG codons for translation initiation. *Oncogene* 11:2339–2348.
32. Klefstrom, J., P. E. Kovanen, K. Somersalo, A.-O. Hueber, T. Littlewood, G. I. Evan, A. H. Greenberg, E. Saksela, T. Timonen, and K. Alitalo. 1999. *c-Myc* and E1A induced cellular sensitivity to activated NK cells involves cytosolic granules as death effectors. *Oncogene* 18:2181–2188.
33. Koromilas, A. E., A. Lazaris-Karatzas, and N. Sonenberg. 1991. mRNAs containing extensive secondary structure in their 5' non-coding region translate efficiently in cells overexpressing initiation factor eIF4E. *EMBO J.* 11:4153–4158.
34. Lamphear, B. J., R. Kirchweger, T. Skern, and R. E. Rhoads. 1995. Mapping of functional domains in eukaryotic protein synthesis initiation factor 4G (eIF4G) with picornaviral proteases. *J. Biol. Chem.* 270:21975–21983.
35. Lee, C. H., P. Leeds, and R. J. Ross. 1998. Purification and characterization of a polysome-associated endoribonuclease that degrades *c-myc* mRNA in vitro. *J. Biol. Chem.* 273:25261–25271.
36. Luscher, B., and R. N. Eisenman. 1988. *c-myc* and *c-myb* protein degradation: effect of metabolic inhibitors and heat shock. *Mol. Cell. Biol.* 8:2504–2512.
37. MacFarlane, M., M. Ahmad, M. Srinivasula, T. Fernandes-Alnemri, G. M. Cohen, and E. S. Alnemri. 1997. Identification and molecular cloning of two novel receptors for the cytotoxic ligand TRAIL. *J. Biol. Chem.* 272:25417–25420.
38. Marcu, K. B., S. A. Bossone, and A. J. Patel. 1992. *myc* function and regulation. *Annu. Rev. Biochem.* 61:809–860.
39. Marissen, W., and R. E. Lloyd. 1998. Eukaryotic translation initiation factor 4G is targeted for proteolytic cleavage by caspase 3 during inhibition of translation in apoptotic cells. *Mol. Cell. Biol.* 18:7565–7574.
40. Medema, J. P., C. Scaffidi, F. C. Kischkel, A. Shevchenko, M. Mann, P. H. Kramer, and M. E. Peter. 1997. FLICE is activated by association with the CD95 death-inducing signaling complex (DISC). *EMBO J.* 16:2794–2804.
41. Miller, D., J. Dibbens, A. Damert, W. Risau, M. Vadas, and G. Goodall. 1998. The vascular endothelial growth factor mRNA contains an internal ribosome entry site. *FEBS Lett.* 434:417–420.
42. Morley, S. J., L. McKendrick, and M. Bushell. 1998. Cleavage of translation initiation factor 4G during anti-Fas IgM-induced apoptosis does not require signalling through the p38 mitogen-activated protein kinase. *FEBS Lett.* 438:41–48.
43. Nanbru, C., I. Lafon, S. Audiger, G. Gensac, S. Vagner, G. Huez, and A.-C. Prats. 1997. Alternative translation of the proto-oncogene *c-myc* by an internal ribosome entry site. *J. Biol. Chem.* 272:32061–32066.
44. Ohlmann, T., M. Rau, V. M. Pain, and S. J. Morley. 1996. The C-terminal domain of eukaryotic protein synthesis initiation factor (eIF) 4G is sufficient to support cap-independent translation in the absence of eIF-4E. *EMBO J.* 15:1371–1382.
45. Pain, V. M. 1996. Initiation of protein synthesis in eukaryotic cells. *Eur. J. Biochem.* 236:747–771.
46. Parkin, N., A. Darveau, R. Nicholson, and N. Sonenberg. 1988. *cis*-acting translational effects of the 5' noncoding region of *c-myc* mRNA. *Mol. Cell. Biol.* 8:2875–2883.
47. Pestova, T., I. N. Shatsky, and C. U. T. Hellen. 1996. Functional dissection of eukaryotic initiation factor 4F: the 4A subunit and the central domain of the 4G subunit are sufficient to mediate internal entry of 43S preinitiation complexes. *Mol. Cell. Biol.* 16:6870–6878.
48. Peter, M. E., and P. H. Kramer. 1998. Mechanisms of CD95 (APO-1/Fas)-mediated apoptosis. *Curr. Opin. Immunol.* 10:545–551.
49. Proud, C. G., and R. M. Denton. 1997. Molecular mechanisms for the control of translation by insulin. *Biochem. J.* 328:329–341.
50. Raingeaud, J., A. J. Whitmarsh, B. Barrett, Y. Derjard, and R. J. Davis. 1996. MKK3- and MKK6-regulated gene expression is mediated by the p38 mitogen-activated protein kinase signal transduction pathway. *Mol. Cell. Biol.* 16:1247–1255.
51. Ross, J. 1995. mRNA stability in mammalian cells. *Microbiol. Rev.* 59:423–450.
52. Roulston, A., C. Reinhard, P. Amiri, and L. T. Williams. 1997. Early activation of c-jun N-terminal kinase and p38 kinase regulate cell survival response to tumour necrosis factor  $\alpha$ . *J. Biol. Chem.* 273:10232–10239.
53. Saito, H., A. C. Hayday, K. Wiman, W. S. Hayward, and S. Toneyawa. 1983. Activation of the *c-myc* gene by translocation: a model for translational control. *Proc. Natl. Acad. Sci. USA* 80:7476–7460.
54. Savill, J., V. Fadok, P. Henson, and C. Haslett. 1993. Phagocyte recognition of cells undergoing apoptosis. *Immunol. Today* 14:131–136.
55. Schulze-Osthoff, K., D. Ferrari, M. Los, S. Wesselborg, and M. E. Peter. 1998. Apoptosis signaling by death receptors. *Eur. J. Biochem.* 254:439–459.
56. Shindo, H., E. Tani, T. Matsumoto, T. Hashimoto, and J. Furuyama. 1993. Stabilization of *c-myc* protein in human glioma-cells. *Acta Neuropathol.* 86:345–352.
57. Spotts, G. D., and S. R. Hann. 1990. Enhanced translation and increased turnover of *c-myc* proteins occur during differentiation of murine erythroleukemia cells. *Mol. Cell. Biol.* 10:3952–3964.
58. Stein, I., A. Itin, P. Einat, R. Skaliter, Z. Grossman, and E. Keshet. 1998. Translation of vascular endothelial growth factor mRNA by internal ribosome entry: implications for translation under hypoxia. *Mol. Cell. Biol.* 18:3112–3119.
59. Stoneley, M., F. E. M. Paulin, J. P. C. Le Quesne, S. A. Chappell, and A. E. Willis. 1998. *c-Myc* 5' untranslated region contains an internal ribosome entry segment. *Oncogene* 16:423–428.
60. Vagner, S., M.-C. Gensac, A. Maret, F. Bayard, F. Amalric, H. Prats, and A.-C. Prats. 1995. Alternative translation of human fibroblast growth factor 2 mRNA occurs by internal entry of ribosomes. *Mol. Cell. Biol.* 15:35–44.
61. Waskiewicz, A. J., A. Flynn, C. G. Proud, and J. A. Cooper. 1997. Mitogen-activated protein kinases activate the serine/threonine kinases Mnk1 and Mnk2. *EMBO J.* 16:1909–1920.
62. West, M. J., M. Stoneley, and A. E. Willis. 1998. Translational induction of the *c-myc* oncogene via activation of the FRAP/TOR signalling pathway. *Oncogene* 17:769–780.
63. West, M. J., N. F. Sullivan, and A. E. Willis. 1995. Translational upregulation of the *c-myc* oncogene in Bloom's syndrome cell lines. *Oncogene* 13:2515–2524.
64. Yang, J.-Q., S. R. Bauer, J. F. Mushinski, and K. B. Marcu. 1985. Chromosome translocations clustered 5' of the murine *c-myc* gene qualitatively affect promoter usage: implications for the site of normal *c-myc* regulation. *EMBO J.* 4:1441–1447.

# Analysis of the *c-myc* IRES; a potential role for cell-type specific trans-acting factors and the nuclear compartment

Mark Stoneley, Tatyana Subkhankulova, John P. C. Le Quesne, Mark J. Coldwell, Catherine L. Jopling, Graham J. Belsham and Anne E. Willis\*

Department of Biochemistry, University of Leicester, University Road, Leicester LE1 7RH, UK

Received October 21, 1999; Revised and Accepted December 8, 1999

## ABSTRACT

The 5' UTR of *c-myc* mRNA contains an internal ribosome entry segment (IRES) and consequently, *c-myc* mRNAs can be translated by the alternative mechanism of internal ribosome entry. However, there is also some evidence suggesting that *c-myc* mRNA translation can occur via the conventional cap-dependent scanning mechanism. Using both bicistronic and monocistronic mRNAs containing the *c-myc* 5' UTR, we demonstrate that both mechanisms can contribute to *c-myc* protein synthesis. A wide range of cell types are capable of initiating translation of *c-myc* by internal ribosome entry, albeit with different efficiencies. Moreover, our data suggest that the spectrum of efficiencies observed in these cell types is likely to be due to variation in the cellular concentration of non-canonical translation factors. Interestingly, the *c-myc* IRES is 7-fold more active than the human rhinovirus 2 (HRV2) IRES and 5-fold more active than the encephalomyocarditis virus (EMCV) IRES. However, the protein requirements for the *c-myc* IRES must differ significantly from these viral IRESs, since an unidentified nuclear event appears to be a pre-requisite for efficient *c-myc* IRES-driven initiation.

## INTRODUCTION

The proto-oncogene *c-myc* is required for both cell proliferation and programmed cell death (apoptosis), and de-regulated *c-myc* expression is associated with a wide range of cancers (1,2). It is therefore not surprising that *c-myc* gene expression is tightly controlled at multiple levels (3). The post-transcriptional regulation of *c-myc* involves alterations in the stability of both the mRNA and the protein (4–7), and the control of *c-myc* translation (8–12).

In common with many other genes involved in the regulation of cell growth, the *c-myc* mRNA has a long and potentially highly structured 5' untranslated region (UTR, located in exon 1). Multiple transcription start sites exist within the gene, giving rise to four transcripts (P0, P1, P2 and P3, with sizes of ~3.1, 2.4, 2.25 and 2.0 kb respectively; 13–15), with the

predominant mRNA (P2) having a 5' UTR of ~400 nt. It has been suggested that mRNAs with structured 5' UTRs, such as *c-myc*, are poorly translated due to their reduced ability to associate with the cap-binding complex, the eukaryotic initiation factor 4F (eIF4F). Indeed, over-expression of the cap-binding protein eIF4E, which is believed to be a limiting component of this complex, causes an increase in the translation of mRNAs with structured 5' UTRs such as *c-myc* (16–18). Furthermore, in certain circumstances the translational regulation of *c-myc* is mediated by phosphorylation and inactivation of the eIF4E inhibitor protein 4EBP1 (19).

It has also been shown that the 5' UTR of *c-myc* contains an internal ribosome entry segment (IRES) (11,12). IRESs were originally identified in the 5' UTRs of picornaviral RNAs and these complex structural elements allow ribosomes to enter at a considerable distance (often >1000 nt) from the 5' end of the mRNA (20–22). Several eukaryotic mRNAs have the potential to initiate translation by an internal ribosome entry mechanism and interestingly many of the mammalian IRESs identified to date have been found in genes whose protein products are associated with the control of cell growth, e.g. *c-myc*, fibroblast growth factor -2 (FGF-2), platelet derived growth factor (PDGF) and vascular endothelial growth factor (VEGF) (11,12,23–26).

The region of *c-myc* mRNA that contains the IRES is located downstream of the P2 promoter (12). Approximately 75–90% of *c-myc* transcripts are synthesised from this promoter (3). Therefore, the majority of *c-myc* mRNAs have the potential to initiate translation via internal ribosome entry. The *c-myc* IRES appears to function under conditions where cap-dependent translation is compromised. Indeed, we have recently shown that the *c-myc* IRES is utilised during apoptosis when cap-dependent translation is reduced due to cleavage of eIF4G (27). Furthermore, in poliovirus-infected HeLa cells, in which there is a substantial reduction in cap-dependent protein synthesis due to the proteolysis of eIF4G and sequestration of eIF4E, *c-myc* mRNAs remain associated with heavy polysomes (28). However, since there is some evidence that *c-myc* mRNA can also be translated by a cap-dependent mechanism, to date it has not been possible to assess the contribution that either mechanism makes to the synthesis of c-Myc polypeptides (12,19).

In this study we present further evidence for the existence of an IRES in the *c-myc* 5' UTR. In addition our data confirm that

\*To whom correspondence should be addressed. Tel: +44 116 2523363; Fax: +44 116 2523369; Email: aew5@le.ac.uk

Present addresses:

Mark Stoneley, Department of Biochemistry and Molecular Biology, The University of Leeds, Leeds LS2 9JT, UK  
Graham J. Belsham, BBSRC, Institute for Animal Health, Pirbright, Woking GU4 0NF, UK

*c-myc* mRNAs can also be translated by a cap-dependent mechanism. This has led us to propose that both mechanisms operate *in vivo*. We demonstrate that the *c-myc* IRES is active (with one exception) in all cell lines of human origin tested, although there is a wide variation in its efficiency, whereas the IRES is not active in cell lines of murine origin. When compared to IRESs of picornaviral origin, the *c-myc* IRES is 7- and 5-fold more active than the IRESs derived from HRV and EMCV, respectively. Finally we provide evidence that the *c-myc* IRES depends on a prior nuclear event for efficient initiation of translation.

## MATERIALS AND METHODS

### Cell culture

All cell lines were grown at 37°C in Dulbecco's modified Eagle's medium supplemented with 10% foetal calf serum, in a humidified atmosphere containing 5% CO<sub>2</sub>. The cell lines HeLa (Human cervical epitheloid carcinoma), HepG2 (Human hepatocyte carcinoma), HK293 (Human embryonic kidney cell line immortalised with adenovirus DNA), Balb/c-3T3 (Murine embryonic fibroblast cell line), MCF7 (Human breast carcinoma), Cos-7 [Monkey epithelial cell line (CV-1) immortalised with SV40 DNA] and MEL cells (murine erythroleukaemic cells) were purchased from the American type culture collection. The cell line MRC5 (human lung fibroblast) was a kind gift from Dr M. MacFarlane (MRC-Human Toxicology Unit, Leicester, UK). The human SV40 immortalised fibroblast cell line GM637 was obtained from NIGMS.

### Plasmid constructs

The plasmids pGL3, pGML (formerly pGL3utr), pRF and pRMF (formerly pGL3R and pGL3Rutr) have been described previously (12). cDNA encoding the HRV2 IRES was obtained from the plasmid pXLJ(10-605) (a gift from Dr R. Jackson, University of Cambridge) and inserted into pRF between the *PvuII* and *NcoI* sites, thus creating pRhrvF. To obtain the sequence encoding the EMCV IRES, a polymerase chain reaction (PCR) was performed using the oligonucleotides 5'-GATGACTAGTCCGCCCTCTCCCTCCCCC-3' and 5'-GATGCCATGGC-CATATTATCATCGTGTT-3', with pCAGSIP (an expression vector that contains the EMCV-IRES; a gift from Dr S. Monkley, University of Leicester, UK) as a template. Subsequently, the PCR product was inserted into pRF between the *SpeI* and *NcoI* sites to generate pRemcvF.

A DNA fragment containing a 60 bp palindromic sequence was amplified from pGL3RutrH (12) in a PCR using the oligonucleotides 5'-ACCTCGAGAGATATCTGGTACCGAGCTC-3' and 5'-ACAAGCTTAGATCTGGTACCGAGCTC-3'. This fragment was inserted into pGL3 and pGML at the *SpeI* site, thus creating pHpL and pHpML, respectively.

The *c-myc* P2 cDNA was obtained by reverse transcription and PCR amplification of HeLa cell total RNA, using Super-script reverse transcriptase and *Taq* DNA polymerase (Life Technologies Inc). The fragments encoding the P2 *c-myc* cDNA from -396 to +6 and +7 to +1320 were amplified using the primer sets 5'-TAATTCAGCGAGAGGCAGA-3' with 5'-GGGCATCGTCGCGGGAGGCTG-3', and 5'-CTCAAC-GTTAGCTTACCAAC-3' with 5'-CGGAATTCTTACGCA-CAAGAGTTGCCGAT-3', respectively. These sequences

were inserted sequentially into pSK+-bluescript (Stratagene) using the *SmaI* and *EcoRI* sites thus recreating the entire P2 cDNA in the plasmid pSKMyc. The construct pSKMycΔ1 containing the P2 sequence from -56 to +1320 bp, was obtained by inserting a 1381 bp *PvuII*-*EcoRI* fragment derived from pSKMyc into pSK+ bluescript between the *SmaI* and *EcoRI* sites. Both constructs were linearised with *HindIII* prior to performing *in vitro* transcription reactions.

To create the bicistronic plasmids, pCRF and pCRMF, DNA fragments containing the Firefly luciferase (*luc*) coding region or a 5' UTR-*luc* fusion were excised from pSKL and pSKutrL, respectively. These sequences were inserted into pRL-CMV (Promega) downstream of the *Renilla* luciferase coding region at the *XbaI* site.

The constructs in the pSP64R(x)L Poly A series were generated in two stages. Initially, the *Renilla* luciferase coding region was obtained from pRL-CMV and inserted into pSP64 Poly A (Promega) at the *XbaI* site. Subsequently, DNA fragments containing the luciferase coding region, a *c-myc* 5' UTR-*luc* fusion and a HRV2 IRES-*luc* fusion were excised from pGL3, pGML and pRhrvF, respectively, and blunt-end ligated into the *SmaI* site of pSP64RPoly A downstream of the *Renilla* luciferase sequence. Constructs in this series were digested with *EcoRI* prior to inclusion in an *in vitro* transcription reaction. The resulting transcripts have a 3' terminal polyadenylate tail of 30 residues.

### DNA transfections

Calcium phosphate-mediated DNA transfection of mammalian cells, with the exception of MRC5, MEL and GM637 cells, was performed essentially as described by Jordan *et al.* (29). The remaining cell lines were transfected with FuGene6 (Roche) according to the manufacturer's protocols.

### *In vitro* run-off transcription and *in vitro* translation reactions

Plasmid constructs were linearised and *in vitro* transcriptions were performed using either SP6 (pSP6R(x)L series) or T3 (pSKMyc and pSKMycΔ1) polymerase as previously described. Capped transcripts were synthesised in a reaction containing 2 mM m<sup>7</sup>(5')ppp(5')G, 0.5 mM GTP and 1 mM of the remaining nucleotides. All RNAs were purified using size exclusion chromatography and quantified using the absorbance at 260 nm. In addition, the integrity of each transcript was verified using agarose gel electrophoresis and ethidium bromide staining.

*In vitro* translation reactions were performed using rabbit reticulocyte lysate (Promega) according to the manufacturer's recommendations. The translation products were fractionated by SDS-polyacrylamide gel electrophoresis and visualised using phosphorimager analysis (Molecular Dynamics).

### Cationic liposome-mediated RNA transfection

Cationic liposome-mediated RNA transfection of mammalian cells was performed as described previously (30). Capped and polyadenylated transcripts were synthesised using *in vitro* run-off transcription on an *EcoRI* linearised pSP64R(x)L poly(A) template. Approximately 2 × 10<sup>5</sup> HeLa cells were transfected with 5 μg of RNA previously incubated with 12.5 μg of Lipofectin (Life Technologies Inc.). After 8 h of transfection, cells were harvested and processed for reporter gene analysis.

### Reporter gene analysis

The activity of Firefly luciferase in lysates prepared from cells transfected with pGL3, pGML, pHpML and pHpL was measured using a luciferase reporter assay system (Promega). Light emission was measured either over 1 s using a 1253 luminometer (Bio-Orbit) or over 10 s using an Optocomp-1 Luminometer (MGM instruments). The activity of both Firefly and *Renilla* luciferase in cell lysates with bicistronic luciferase plasmids was measured using the Dual-luciferase reporter assay system (Promega). Assays were performed according to the manufacturer's recommendations. The activity of  $\beta$ -galactosidase in lysates prepared from cells transfected with pcDNA3.1/HisB/*lacZ* was measured using a Galactolight plus assay system (Tropix).

## RESULTS

### *c-myc* translation initiation can occur by internal ribosome entry and the conventional cap-dependent mechanism

We and others have shown that *c-Myc* protein synthesis can occur in a cap-dependent manner and by internal ribosome entry (11,12,17,19). To assess the contribution that these two disparate mechanisms make to *c-myc* expression, a palindromic sequence capable of forming a stable RNA hairpin ( $-55$  kcal/mol) was introduced into the control luciferase reporter construct, (pGL3) and the 5' UTR containing construct (pGML, previously known as pGL3utr) at the *SpeI* site (Fig. 1A). As a consequence, ribosome scanning from the cap structure of the transcripts produced by the new constructs (pHpL and pHpML) should be severely impeded, whereas ribosomes entering at a site distal to the hairpin will be unaffected. HeLa cells were transfected with pGL3, pGML, pHpL or pHpML and in agreement with our previously published data, the *c-myc* IRES does not inhibit translation of the downstream Firefly luciferase reporter gene. Moreover, we consistently observe that there is a slight elevation in expression of this enzyme in the presence of the IRES (Fig. 1B). In cells transfected with the construct pHpL there is a 200-fold reduction in the amount of luciferase produced when compared to the control vector pGL3 (Fig. 1B). Hence, as expected the RNA hairpin structure inhibits cap-dependent translation initiation. However, in cells transfected with pHpML, in which the *c-myc* IRES lies downstream of the RNA hairpin, luciferase expression is stimulated by  $\sim 67$ -fold when compared to pHpL. These data demonstrate that the 5' UTR can promote efficient translation initiation despite the presence of an RNA structure which blocks ribosome scanning from the 5' end and thus provide further support for the presence of an IRES within this leader sequence. Nevertheless, it is notable that the RNA hairpin does reduce luciferase expression from a transcript containing the *c-myc* 5' UTR by 3-fold. This observation would indicate that mRNAs originating from the P2 promoter must also support a cap-dependent scanning mechanism in addition to internal initiation.

### Comparison of *c-myc* IRES-mediated internal initiation in a range of cell types

We have shown previously that the *c-myc* IRES is capable of promoting translation of the downstream cistron on a bicistronic mRNA in both HeLa and HepG2 cells. To investigate how

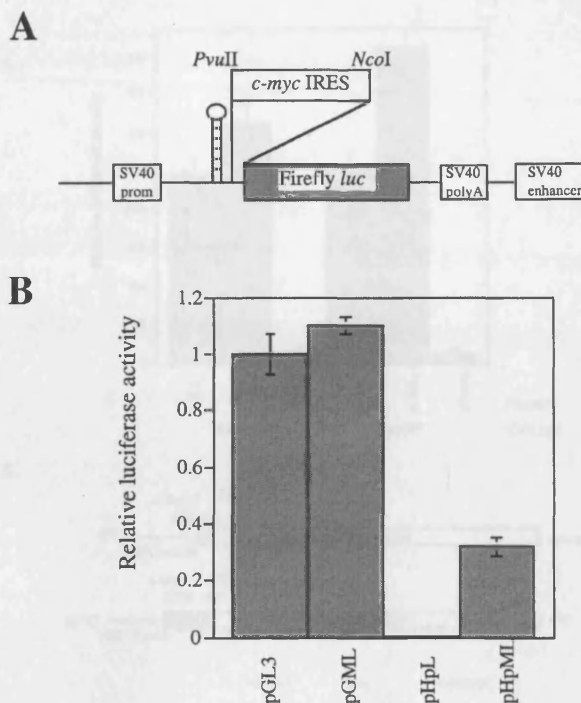


**Figure 1.** A comparison between the efficiency of IRES-mediated translation and scanning. (A) A diagrammatic representation of the monocistronic hairpin containing plasmids pHpL and pHpML. The hairpin was inserted into the *SpeI* site upstream of the *PvuII* site. (B) HeLa cells were transfected (in triplicate) with the plasmids shown and Firefly luciferase activity is expressed relative to the transfection control  $\beta$ -galactosidase. All experiments were performed on three independent occasions.

widely the IRES is utilised, a range of cell types derived from different tissues, including Cos-7, MCF7, Balb/c-3T3, MEL, MRC5, HK293, GM637, HeLa and HepG2 were co-transfected with either pRF or pRMF and pcDNA3.1/HisB/*lacZ* (Fig. 2A). The expression from both *Renilla* and Firefly luciferase cistrons was assayed and normalised to the transfection control  $\beta$ -galactosidase. Between cell types, significant variation in the level of readthrough re-initiation was observed on the control bicistronic plasmid (data not shown). Accordingly, the efficiency of the IRES is represented as a ratio of FL to RL expressed from pRMF. In each cell line, the presence of the *c-myc* IRES in the mRNA did not significantly alter *Renilla* luciferase expression and indeed, the largest difference was observed in HeLa cells, in which the *c-myc* IRES reduced *Renilla* luciferase activity by  $\sim 11\%$  (data not shown; 12). However, it is clear that the efficiency of *c-myc* IRES-driven translation varies widely between cell lines (Fig. 2B). Hence the IRES is most active in HeLa cells, followed by MRC5, HepG2, GM637, HK293 and Cos-7. Interestingly, the IRES is almost inactive in the MCF7 cells suggesting that these cells may lack a factor which is essential for IRES-mediated translation. Alternatively, these cells could express a higher level of a specific inhibitor of internal initiation. One possible explanation for the inactivity of the human *c-myc* IRES in cell lines of murine origin, Balb/c-3T3

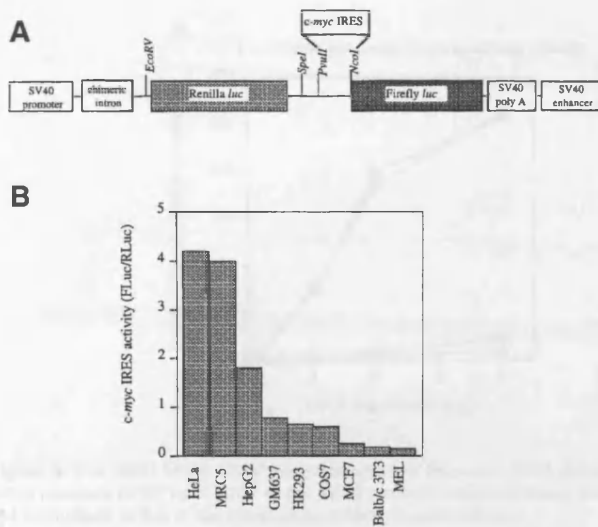


**Figure 2.** A comparison of the efficiency of *c-myc* IRES initiated translation in cell lines of different origin. (A) A schematic representation of the bicistronic reporter plasmids pRF and pRMF. (B) IRES activity is expressed using the ratio of downstream cistron expression to upstream cistron expression (Fluc/RLuc) with any differences in transfection efficiencies corrected for using the  $\beta$ -galactosidase transfection control. All experiments were performed in triplicate on three independent occasions.

and MEL cells, is that the function of the IRES displays species specificity. However, we have recently shown that this is not the case, since the *c-myc* IRES isolated from murine cells is active in HeLa cells and yet also relatively inactive in Balb/c-3T3 cells (data not shown).

#### *c-myc* P2 transcripts can be translated by a cap-dependent mechanism in Balb/c 3T3 cells, MCF-7 cells and in reticulocyte lysates

The relative inactivity of the *c-myc* IRES in Balb/c 3T3 and MCF7 cells enabled us to analyse the effect of the P2 5' UTR on cap-dependent translation initiation. To this end, these cell lines were transfected with the monocistronic control construct, the 5' UTR-containing constructs, pGL3 and pGML, and the *c-myc* 5' UTR construct containing the hairpin pHpML respectively. The P2 5' UTR does not inhibit cap-dependent translation initiation, at least in these cell lines (Fig. 3A). However, the additional presence of the hairpin structure was sufficient to prevent scanning demonstrating that the *c-myc* IRES is relatively inactive in these cell types and consequently *c-myc* is translated by a cap-dependent mechanism (Fig. 3A).

To further investigate the impact of the P2 5' UTR on cap-dependent translation initiation we turned to reticulocyte lysate. This system cannot support internal ribosome entry on the *c-myc* leader sequence (our unpublished data; 31), therefore the contribution of the 5' cap structure can be assessed directly. Thus, rabbit reticulocyte lysate was primed with capped or uncapped *c-myc* transcripts, either bearing the P2 5' UTR sequence (*myc*) or lacking this element (*myc $\Delta$ 1) (Fig. 3B). Two species of *c-myc* protein can arise from the P2 transcripts by use of alternate translation initiation codon (CUG or AUG), which give rise to protein products with apparent molecular*

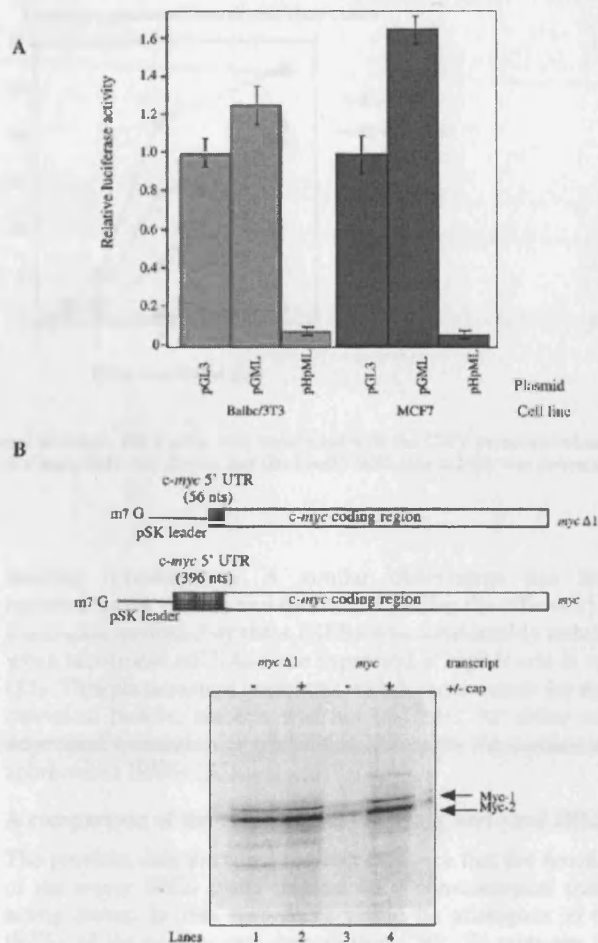


**Figure 3.** Cap-dependent translation of *c-myc* P2 transcripts in Balb/c 3T3, MCF7 cells and in rabbit reticulocyte lysates. (A) MCF7 and Balb/c cells were transfected with the plasmids pGL3, pGML or pHpML and the Firefly luciferase activity measured as described previously. (B) *c-myc* transcripts bearing 56 nt (*myc $\Delta$ 1) or 396 nt (*myc*) of the *c-myc* 5' UTR were synthesised *in vitro* using linearised plasmids pSKM $\Delta$ 1 or pSKM respectively. Rabbit reticulocyte lysate was programmed with 5 ng/ $\mu$ l of either capped (+) or uncapped (-) *myc* or *myc $\Delta$ 1 transcripts. Radiolabelled polypeptides synthesised in the reaction were then fractionated by SDS-PAGE and detected using phosphorimager analysis.**

weights of 67 and 64 kDa respectively (32). As expected, capping the *myc $\Delta$ 1 RNA stimulated the synthesis of both Myc-1 and 2 polypeptides (Fig. 3B, lanes 1 and 2). This modest effect of 2–2.5-fold is consistent with the previously reported values for relatively unstructured RNAs using this system (33). In the absence of a cap structure, the *c-myc* 5' UTR reduced the synthesis of both the AUG and CUG-initiated polypeptides by ~90% (Fig. 3B, lanes 1 and 3). It is likely that structural elements within the 5' UTR are responsible for this effect since this element is GC-rich. However, the synthesis of both proteins was enhanced by 14–16-fold on capping of the *myc* transcript (Fig. 3B, lanes 3 and 4), with the result that the*

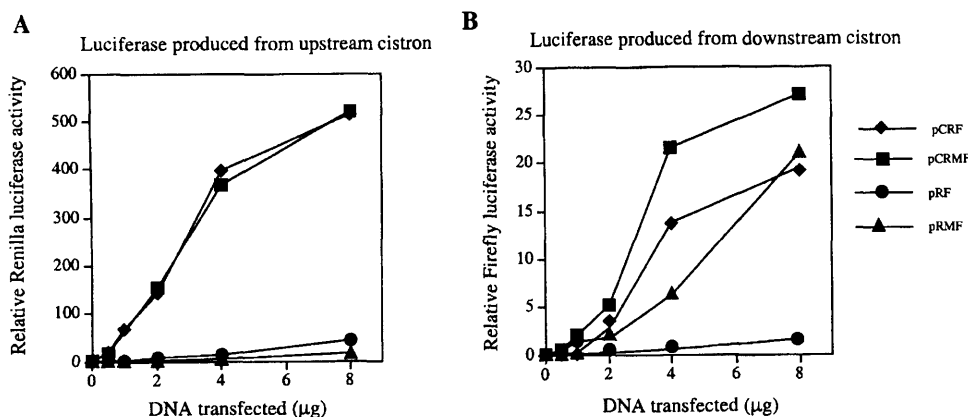


**Figure 4.** The effect of the CMV promoter/enhancer on *c-myc* IRES directed internal initiation. HeLa cells were transfected with the CMV promoter/enhancer based plasmids pCRF or pCRMF or the SV40 promoter/enhanced based plasmids, pRF and pRMF. (A) *Renilla* and (B) Firefly luciferase activity was determined and normalised to that of the transfection control,  $\beta$ -galactosidase.

5' UTR inhibits translation initiation by only 50%. Hence, the P2 5' UTR strongly attenuates the translational efficiency of uncapped *c-myc* transcripts. Nevertheless, much of this repression is relieved by the presence of a 5' cap. Therefore, translation initiation on the P2 transcript is strongly cap-dependent in the reticulocyte lysate system.

#### Overexpression of bicistronic mRNAs inhibits the function of the *c-myc* IRES

Thus far, we have demonstrated that in many cell lines *c-myc* translation can occur by the alternative mechanism of internal ribosome entry. However, *c-myc* can also be translated by the conventional cap-dependent mechanism in certain backgrounds. One model that would explain the cell-type specific variation in the efficiency of *c-myc* IRES-driven translation posits that non-canonical *trans*-acting factors are required for the recruitment of the 40S ribosome to this element. In this scenario, the activity of one or more of these factors is considerably reduced in the Balb/c-3T3 and MCF7 cell lines. Further evidence in support of this model was provided by experiments in which the bicistronic mRNAs were overexpressed using the powerful cytomegalovirus (CMV) promoter/enhancer region; this transcriptional element has been shown to result in significantly higher levels of expression than the SV40 promoter/enhancer (34). The *Renilla* luciferase activity measured in cells transfected with a CMV-based control bicistronic plasmid pCRF was significantly greater than that achieved with the analogous plasmid, pRF (~27-fold, Fig. 4A, compare pCRF *Renilla* luciferase to pRF *Renilla* luciferase). However, in cells transfected with the 5' UTR-containing construct, pCRMF, there was not a corresponding increase in Firefly luciferase activity when compared to pRMF. Transfection with 4 or 8 µg of pCRMF produced only 4- or 1.25-fold more Firefly luciferase than pRMF, respectively (Fig. 4B). Consequently, using the CMV promoter/enhancer, the apparent activity of the *c-myc* IRES when calculated relative to readthrough is only 1.5–2 fold compared to 50-fold for the SV40 based constructs (Fig. 4B). These data suggest that a *trans*-acting factor, which is required for initiation of translation via the *c-myc* IRES, is present at a

limiting concentration. A similar observation has been reported for the entero- and rhinovirus IRESs; the efficiency of translation mediated by these IRESs was considerably reduced when bicistronic mRNAs were expressed at high levels *in vivo* (35). This phenomenon correlates with a requirement for non-canonical factors, since it was not observed for either cap-dependent translation or translation driven by the cardio- and aphthovirus IRESs (35).

#### A comparison of the efficiency of the *c-myc* and viral IRESs

The previous data provided indirect evidence that the function of the *c-myc* IRES could depend on a non-canonical *trans*-acting factor. In this respect, it would be analogous to the IRESs of the entero- and rhinoviruses (36). To compare the efficiency of the *c-myc*, HRV and EMCV IRESs, HeLa cells were transfected with the plasmids pRF, pRMF, pRhrvF, pRemcvF. The activities of *Renilla* and Firefly luciferase were determined and normalised to that of the transfection control,  $\beta$ -galactosidase (Fig. 5). Expression of the upstream cistron, *Renilla* luciferase, was not greatly affected by the presence of the EMCV, HRV or the *c-myc* IRES in the intercistronic region (data not shown). A comparison of the downstream cistron activities revealed that all of these elements stimulated Firefly luciferase expression (Fig. 5). However, the extent to which expression from the downstream cistron was enhanced differed widely between these IRESs. In fact, the *c-myc* IRES elevated Firefly luciferase activity by 70.8-fold, whilst the HRV and EMCV IRESs caused a lesser stimulation of 9.6- and 14-fold, respectively. Thus, these data suggest that both of these IRESs are less efficient in this system at promoting internal ribosome entry than the *c-myc* IRES.

#### *c-myc* IRES-driven translation requires a nuclear event

It has been suggested previously that efficient translation driven by the IRES located in the 5' UTR of the immunoglobulin heavy chain binding protein (Bip) requires a nuclear event (37). Moreover, two specific nuclear protein factors have been identified which interact with the Bip IRES (38). To test whether the *c-myc* IRES also has such a requirement for

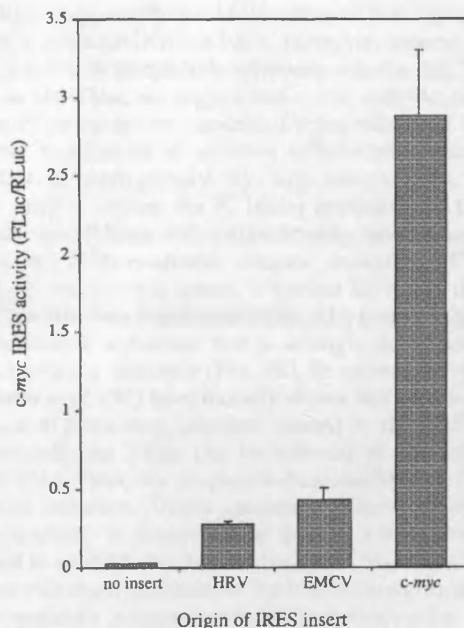


**Figure 5.** A comparison of the efficiency of HRV, EMCV and *c-myc* IRES-initiated internal ribosome entry on bicistronic mRNAs transcribed in the nucleus. HeLa cells were transfected in triplicate with either the control plasmid pRF, the *c-myc* IRES containing plasmid pRMF, the HRV IRES containing plasmid pRhrvF or the EMCV IRES containing plasmid pRemcvF. Upstream cistron (*Renilla* luciferase) and downstream cistron (Firefly luciferase) activities were determined and normalised to that of the transfection control,

nuclear factors, the plasmid constructs pSP64RL poly(A), pSP64R(*c-myc*)L poly(A) and pSP64R(hrv)L poly(A) were generated. Bicistronic transcripts containing an m<sup>7</sup>GpppG cap structure and a polyadenylated tail at the 5' and 3' termini, respectively, were synthesised from each of the plasmids in the pSP64RL(x)Lpoly(A) series by *in vitro* run-off transcription (Fig. 6A). Cationic liposomes were used to encapsulate equimolar quantities of each transcript and introduce them into the cytoplasm of HeLa cells. After a period of 8 h, the expression from the upstream and downstream cistrons was monitored (Fig. 6B and C). In cells transfected with the control bicistronic transcript, Rluc, the *Renilla* luciferase cistron was translated efficiently, whilst little expression of the downstream cistron was observed (Fig. 6B and C). Insertion of the HRV IRES between the two cistrons resulted in a 52-fold stimulation of Firefly luciferase activity when compared to the expression due to readthrough-re-initiation (Fig. 6C). In contrast, the expression of the downstream cistron was only enhanced by 1.4-fold on the *Rc-mycL* transcript (Fig. 6B). Thus, the *c-myc* IRES cannot stimulate the translation of the downstream cistron on a bicistronic mRNA introduced directly into the cytoplasm. To confirm these data, the plasmids pRF and pRMF were transfected into human TK143 cells previously infected with a recombinant vaccinia virus that expresses the T7 RNA polymerase (vTF7-3) (39). The presence of a T7 RNA polymerase promoter upstream of the *Renilla* luciferase cistron in pRF and pRMF results in the transcription of bicistronic mRNAs in the cytoplasmic compartment. However, the *c-myc* 5' UTR did not promote

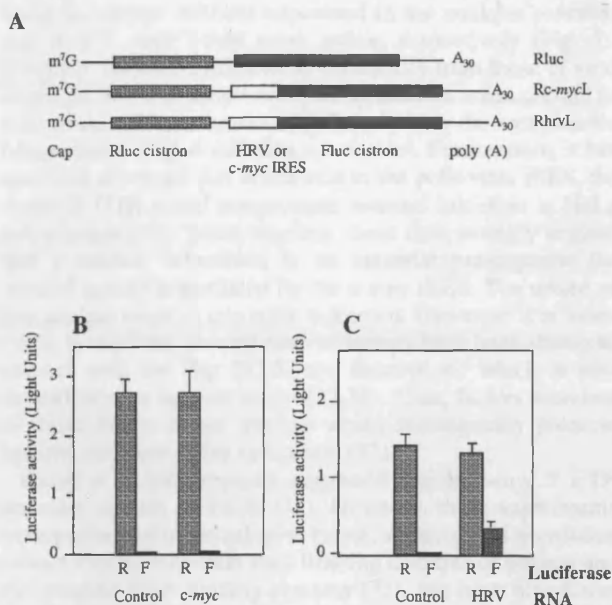


**Figure 6.** A comparison of the efficiency of the *c-myc* IRES and HRV-IRES directed internal initiation on mRNAs introduced directly into the cytoplasm. (A) A diagrammatic representation of the control (Rluc), *c-myc* 5' UTR containing (*Rc-mycL*) and HRV IRES containing (*RhrvL*) bicistronic RNAs. Transcripts were synthesised *in vitro* and possess both a 5' cap structure and a 3' terminal polyadenylate tail of 30 residues. (B) HeLa cells were transfected with Rluc (control) or *Rc-mycL* (*c-myc*) by lipofection. After 8 h *Renilla* (R) and Firefly (F) luciferase expression was determined. (C) Similarly, HeLa cells were transfected with Rluc (control) or *RhrvL* (HRV IRES) and *Renilla* and Firefly luciferase activities determined.

internal initiation on mRNAs transcribed in the cytoplasm using the T7/vaccinia system (data not shown). In contrast, the IRESs of the entero- and rhinoviruses have been shown to function efficiently using bicistronic mRNAs expressed in this manner (35,40). These data appear to suggest a fundamental difference between the function of the entero- and rhinovirus IRESs and that of *c-myc*. The *c-myc* IRES is only able to promote internal initiation on transcripts expressed in the nucleus, however the HRV element is capable of performing this task on mRNAs that do not originate in this compartment. Therefore, we propose that a nuclear event is a pre-requisite for efficient *c-myc* internal initiation.

## DISCUSSION

We and others have shown previously that the 5' UTR of *c-myc* contains an IRES (11,12). We have investigated several features of the *c-myc* IRES and compared its activity in a range of cell lines and to IRESs of viral origin.

First, using a stable RNA structure to substantially impede ribosome scanning from the 5' cap, we have demonstrated that efficient translation initiation can be restored by positioning the *c-myc* 5' UTR downstream of this inhibitory element (Fig. 1). This observation provides further evidence that the P2 leader sequence can support internal entry of ribosomes via an IRES. In these experiments, internal initiation directed by the

*c-myc* IRES is apparently 3-fold less efficient than cap-dependent translation initiation (but see later). However, reporter mRNAs are translated with comparable efficiency whether the 5' UTR is present or not. Thus, we suggest that *c-myc* mRNAs originating from the P2 promoter are capable of being translated via a cap-dependent mechanism in addition to internal initiation. This hypothesis is strengthened by two observations. First, a reporter mRNA bearing the P2 leader sequence was translated efficiently in cell lines with a significantly reduced capacity to promote 5' UTR-mediated internal initiation (Fig. 3A). Second, in reticulocyte lysate, a system in which the *c-myc* IRES is inactive (our unpublished data; 31), *c-myc* P2 transcripts are translated in a manner that is strongly dependent on the presence of a cap structure (Fig. 3B). In agreement with these data, Carter *et al.* (31) have recently shown that the considerable repression of translation initiation caused by the P1 5' UTR in rabbit reticulocyte lysate can be relieved by the addition of eIF4F/E (31). Thus, we propose a dual mechanism for *c-myc* translation initiation. Under conditions where cap-dependent protein synthesis is compromised there is a shift from a cap-dependent to an IRES-directed mechanism of translation initiation. In accord with this hypothesis, we have recently shown that *c-myc* protein synthesis is maintained during apoptosis by virtue of the IRES, whereas overall cap-dependent translation is significantly inhibited (27).

We have also identified several factors that influence the efficacy of the *c-myc* IRES. Expression of bicistronic mRNAs containing the *c-myc* IRES in a panel of cell lines demonstrated that the activity of this element is critically dependent on cellular origin (Fig. 2). Although the IRES stimulated protein synthesis from the downstream cistron in all the cell lines tested, there was a 20-fold disparity between HeLa and MCF7 cells, the lines in which the IRES is most and least active, respectively. This cell-type specific variation in IRES activity implies that the function of this element could be modulated by non-canonical *trans*-acting factors. In this regard, we have recently demonstrated that ribonuclear protein complexes assembled on the *c-myc* 5' UTR *in vitro* using cell extracts from different cell lines vary distinctly in composition (41). Furthermore, overexpression of bicistronic mRNAs using the powerful CMV promoter/enhancer drastically reduced the apparent efficiency of the *c-myc* IRES (Fig. 4). We speculate that the concentration of a *trans*-acting factor essential for *c-myc* IRES-driven translation initiation is limiting under these conditions. The low concentration of this factor could also explain why *c-myc* internal initiation appears to be 3-fold less efficient than cap-dependent translation (Fig. 1) since transcripts expressed from the monocistronic constructs (pGL3, pGML, pHpL and pHpML) accumulate to a level approximately an order of magnitude higher than those produced from the bicistronic constructs (pRF and pRMF) (our unpublished observations). Significantly, the characteristics described above are not unique to the *c-myc* IRES. Both cell-type specific variations in IRES activity and saturation of IRES function have also been described for the better defined IRESs of the entero- and rhinoviruses (35,40). The activity of these elements is known to be dependent on host-specific *trans*-acting factors suggesting that the *c-myc* IRES has similar requirements.

A comparison of the *c-myc* IRES to those of the human rhinovirus (HRV) and encephalomyocarditis virus (EMCV),

using bicistronic mRNAs expressed in the nucleus, revealed that it is 7- and 5-fold more active, respectively (Fig. 5). However, the *c-myc* IRES differs markedly from those of viral origin, in that it is almost completely inactive when present in bicistronic mRNAs introduced directly into the cytoplasmic compartment (Fig. 6 and data not shown). Furthermore, it has also been observed that in contrast to the poliovirus IRES, the *c-myc* 5' UTR could not promote internal initiation in HeLa cell extracts (42). Taken together, these data strongly suggest that a nuclear experience is an essential pre-requisite for internal initiation mediated by the *c-myc* IRES. The nature of this nuclear event is currently unknown. However, it is interesting to note that several nuclear factors have been shown to interact with the Bip IRES, the function of which is also dependent on a nuclear origin (37,38). Thus, factors recruited to these IRESs in the nucleus could subsequently promote internal initiation in the cytoplasm (37).

Carter *et al.* have recently suggested that the *c-myc* 5' UTR does not contain an IRES (31). However, these experiments were performed in reticulocyte lysate, a specialised translation extract known to contain very limiting amounts of nuclear and cytoplasmic RNA binding proteins (33). We have also found that the *c-myc* IRES cannot function in reticulocyte lysate (data not shown). In this respect it is similar to the IRESs of the entero- and rhinoviruses, which function inefficiently or not at all in this system. Indeed, reticulocyte lysate must be supplemented with cytoplasmic extracts to support efficient entero/rhinovirus internal initiation (36). Most importantly, to our knowledge no eukaryotic cellular IRES has been shown to promote internal initiation in this system. Using bicistronic mRNAs expressed in the nucleus of cell lines, we and others identified an IRES in the *c-myc* 5' UTR (11,12). This finding has been supported by the observation that *c-myc* mRNAs are efficiently translated in poliovirus-infected HeLa cells and in cells undergoing apoptosis (27,28). Here we present further evidence that *c-myc* mRNAs can be translated by internal initiation and we provide additional mechanistic insights. Our data support a model in which both non-canonical *trans*-acting factors and a nuclear experience participate in *c-myc* internal ribosome entry. In the light of these results, it is hardly surprising that the *c-myc* IRES does not function in the reticulocyte lysate system. Finally, we are currently attempting to identify the cytoplasmic and nuclear factors involved in the formation of ribonuclear protein complexes with the *c-myc* 5' UTR. The effect of these factors on *c-myc* internal initiation can then be rigorously tested in cell-free extracts.

## ACKNOWLEDGEMENTS

This work was funded by a grant from the Cancer Research Campaign (M.S. and T.S.). J.P.C.L.Q., M.J.C. and C.L.J. hold MRC studentships.

## REFERENCES

- Henriksson, M. and Lüscher, B. (1996) *Adv. Cancer Res.*, **68**, 109–182.
- Prengergast, G.C. (1999) *Oncogene*, **18**, 2967–2987.
- Marcu, K.B., Bossone, S.A. and Patel, A.J. (1992) *Ann. Rev. Biochem.*, **61**, 809–860.
- Ross, J. (1995) *Microbiol. Rev.*, **59**, 16–95.
- Lee, C.H., Leeds, P. and Ross, J. (1998) *J. Biol. Chem.*, **273**, 25261–25271.
- Lüscher, B. and Eisenmann, R.N. (1988) *Mol. Cell. Biol.*, **8**, 2504–2512.

7. Shindo, H., Tani, E., Matsumoto, T., Hashimoto, T. and Furuyama, J. (1993) *Acta Neuropathol.*, **86**, 345–352.
8. Saito, H., Hayday, A.C., Wiman, K., Hayward, W.S. and Tonegawa, S. (1983) *Proc. Natl Acad. Sci. USA*, **80**, 7476–7460.
9. Butnick, N.Z., Miyamoto, C., Chizzonite, R., Cullen, B.R., Ju, G. and Skalka, A.M. (1985) *Mol. Cell. Biol.*, **5**, 3009–3016.
10. Parkin, N.T., Darveau, A., Nicholson, R. and Sonenberg, N. (1988) *Mol. Cell. Biol.*, **8**, 2875–2883.
11. Nanbru, C., Lafon, I., Audigier, S., Gensac, M.-G., Vagner, S., Huez, G. and Prats, A.-C. (1997) *J. Biol. Chem.*, **272**, 32061–32066.
12. Stoneley, M., Paulin, F.E.M., Le Quesne, J.P.C., Chappell, S.A. and Willis, A.E. (1998) *Oncogene*, **16**, 423–428.
13. Battey, J., Moulding, C., Taub, R., Murphy, W., Stewart, T., Potter, H., Lenoir, G. and Leder, P. (1983) *Cell*, **34**, 779–787.
14. Bentley, D.L. and Groudine, M. (1986) *Mol. Cell. Biol.*, **6**, 3481–3489.
15. Yang, J.-Q., Bauer, S.R., Mushinski, J.F. and Marcu, K.B. (1985) *EMBO J.*, **4**, 1441–1447.
16. Koromilas, A.E., Lazaris-Karatzas, A. and Sonenberg, N. (1992) *EMBO J.*, **11**, 4153–4158.
17. De Benedetti, A., Joshi, B., Graff, J.R. and Zimmer, S.G. (1994) *Mol. Cell. Differ.*, **2**, 347–371.
18. De Benedetti, A. and Rhoads, R.E. (1990) *Proc. Natl Acad. Sci. USA*, **87**, 8212–8216.
19. West, M.J., Stoneley, M. and Willis, A.E. (1998) *Oncogene*, **17**, 769–780.
20. Jackson, R.J., Hunt, S.L., Reynolds, J.E. and Kaminski, A. (1995) *Curr. Top. Microbiol. Immunol.*, **203**, 1–29.
21. Jackson, R.J. and Kaminski, A. (1995) *RNA*, **1**, 985–1000.
22. Jackson, R.J., Hunt, S.L., Gibbs, C.L. and Kaminski, A. (1994) *Mol. Biol. Reports*, **19**, 147–159.
23. Vagner, S., Gensac, M.-C., Maret, A., Bayard, F., Amalric, F., Prats, H. and Prats, A.-C. (1995) *Mol. Cell. Biol.*, **15**, 35–44.
24. Bernstein, J., Sella, O., Le, S. and Elroy-Stein, O. (1997) *J. Biol. Chem.*, **272**, 9356–9362.
25. Stein, I., Itin, A., Einat, P., Skaliter, R., Grossman, Z. and Keshet, E. (1998) *Mol. Cell. Biol.*, **18**, 3112–3119.
26. Miller, D., Dibbens, J., Damert, A., Risau, W., Vadas, M. and Goodall, G. (1998) *FEBS Lett.*, **434**, 417–420.
27. Stoneley, M., Chappell, S.A., Jopling, C.L., Dickens, M., MacFarlane, M. and Willis, A.E. (2000) *Mol. Cell. Biol.*, **20**, in press.
28. Johannes, G. and Sarnow, P. (1998) *RNA*, **4**, 1500–1513.
29. Jordan, M., Schallhorn, A. and Wurm, F.M. (1996) *Nucleic Acids Res.*, **24**, 596–601.
30. Dwarki, V.J., Malone, R.W. and Verma, I.M. (1993) *Methods Enzymol.*, **217**, 644–654.
31. Carter, P.S., Pardo-Jarquin, M. and DeBenedetti, A. (1999) *Oncogene*, **18**, 4326–4335.
32. Hann, S.R., King, M.W., Bentley, D.L., Anderson, C.W. and Eisenman, R.N. (1988) *Cell*, **52**, 185–195.
33. Svitkin, Y.V., Ovchinnikov, L.P., Dreyfuss, G. and Sonenberg, N. (1996) *EMBO J.*, **15**, 7147–7155.
34. Sutherland, L.C. and Williams, G.T. (1997) *J. Immunol. Meth.*, **207**, 179–183.
35. Borman, A.M., LeMercier, P., Girard, M. and Kean, K.M. (1997) *Nucleic Acids Res.*, **25**, 925–932.
36. Belsham, G.J. and Sonenberg, N. (1996) *Microbiol. Rev.*, **60**, 499–513.
37. Iizuka, N., Chen, C., Yang, Q., Johannes, G. and Sarnow, P. (1995) *Curr. Top. Microbiol. Immunol.*, **203**, 156–177.
38. Yang, Q. and Sarnow, P. (1997) *Nucleic Acids Res.*, **25**, 2800–2807.
39. Fuerst, T.R., Niles, E.G., Studier, F.W. and Moss, B. (1986) *Proc. Natl Acad. Sci. USA*, **83**, 8122–8126.
40. Roberts, L.O., Seamons, R.A. and Belsham, G.J. (1998) *RNA*, **4**, 520–529.
41. Paulin, F.E.M., Chappell, S.A. and Willis, A.E. (1998) *Nucleic Acids Res.*, **26**, 3097–3103.
42. Pelletier, J. and Sonenberg, N. (1988) *Nature*, **334**, 320–325.